Die approbierte gedruckte Originalversion dieser Dissertation ist an der TU Wien Bibliothek verfügbar.
The approved original version of this doctoral thesis is available in print at TU Wien Bibliothek.

TECHNISCHE UNIVERSITÄT WIEN
Vienna University of Technology

Dissertation

SYNTHESIS AND APPLICATION OF DOUBLE-CLICK AZOBENZENES IN THE DEVELOPMENT OF LIGHT-RESPONSIVE SURFACES FOR BIOLOGICAL APPLICATIONS

ausgeführt zum Zwecke der Erlangung des akademischen Grades eines Doktors der technischen Wissenschaften unter der Leitung von

Prof. Dr. Marko D. Mihovilovic

Prof. Dr. Helmuth Hoffmann

Institute of Applied Synthetic Chemistry, TU Wien

eingereicht an der Technischen Universität Wien
Fakultät für Technische Chemie

von

MSc. Rafaela Carina Oliveira Conceição
[redacted]

Vienna, September 2021

TU Bibliothek Your knowledge hub WIEN

Die approbierte gedruckte Originalversion dieser Dissertation ist an der TU Wien Bibliothek verfügbar.
The approved original version of this doctoral thesis is available in print at TU Wien Bibliothek.

Die approbierte gedruckte Originalversion dieser Dissertation ist an der TU Wien Bibliothek verfügbar.
The approved original version of this doctoral thesis is available in print at TU Wien Bibliothek.

"Success is walking from failure to failure
with no loss of enthusiasm."
Winston Churchill

Declaration

Jakob Raffler contributed to the synthetic work presented in Section C.1.2 as well as in the determination of the photophysical properties of some azobenzenes in Section C.1.4. More details can be found in his bachelor thesis.

The scanning electron microscopy images were recorded by ARätin Elisabeth Eitenberger from the Institute of Chemical Technologies and Analytics of the Faculty of Technology of Vienna.

Die approbierte gedruckte Originalversion dieser Dissertation ist an der TU Wien Bibliothek verfügbar.
The approved original version of this doctoral thesis is available in print at TU Wien Bibliothek.
TU Bibliothek Your knowledge hub WIEN

Table of contents

Declaration i

Table of contents ii

Ackowledgments v

Abstract vii

Kurzfassung ix

A Synthetic schemes 13
- A.1 Preparation of the *trans*-cyclooctene building blocks . . . 14
- A.2 Preparation of CuAAc-tetrazine ligation azobenzenes . . . 15
- A.3 Preparation of SPAAC-tetrazine ligation azobenzene . . . 17
- A.4 Preparation of CuAAc-thiol azobenzene . . . 18
- A.5 Preparation of a model azobenzene for surface functionalization and test of click reactions . . . 19
- A.6 Surface preparation . . . 21
- A.7 Biotin modifications . . . 22

B Introduction 25
- B.1 Photoswitches and photopharmacology . . . 25
- B.2 Smart light-responsive surfaces . . . 35
- B.3 Click chemistry . . . 45
- B.4 Project overview . . . 50
- B.5 Objective . . . 52

C Results and discussion 53
- C.1 Synthesis of double-click azobenzenes . . . 53
  - C.1.1 CuAAC-tetrazine ligation . . . 53
  - C.1.2 SPAAC-tetrazine ligation . . . 56
  - C.1.3 CuAAC-thiol azobenzene . . . 61
  - C.1.4 Photoswitching and thermal half-life time of the double-click azobenzenes 62
- C.2 Preparation of photoswitchable azobenzene functionalized surfaces . . . 65
  - C.2.1 Synthesis of a model azobenzene for surface functionalization . . . 66
  - C.2.2 Test in solution of the click reactions . . . 67

Die approbierte gedruckte Originalversion dieser Dissertation ist an der TU Wien Bibliothek verfügbar.
The approved original version of this doctoral thesis is available in print at TU Wien Bibliothek.
TU Bibliothek Your knowledge hub WIEN

C.2.3 Preparation of an azide coated flat silicon surface . . . 71
C.2.4 *Trans* immobilization on flat silicon . . . 72
C.2.5 Preventing surface overcrowding - *cis* immobilization . . . 77
C.2.6 Aiming for an increased difference in the WCA - immobilization on rough surfaces . . . 82
C.3 Towards a photoswitchable DNA origami platform for T-cell activation . . . 95
C.3.1 Functionalization of double-click azobenzenes with biotin . . . 99
C.3.2 Testing the binding to the DNA origami platform . . . 106
C.3.3 Determining the force generated by the photoswitching of a single azobenzene . . . 109

D Summary and outlook **114**

E Experimental part **117**
E.1 Materials and methods - chemical synthesis . . . 117
E.1.1 NMR spectroscopy . . . 117
E.1.2 Chromatographic methods . . . 118
E.1.3 Melting points . . . 119
E.1.4 HR-MS . . . 119
E.2 Chemical synthesis . . . 119
E.2.1 CuAAC-tetrazine ligation azobenzene . . . 119
E.2.2 SPAAC-tetrazine ligation azobenzene . . . 136
E.2.3 CuAAC-thiol azobenzene . . . 148
E.2.4 Compounds for surface immobilization . . . 152
E.2.5 Biotin modifications . . . 162
E.2.6 AFM click reactions . . . 172
E.3 UV-Vis spectroscopy . . . 175
E.3.1 Azobenzene photoswitching and thermal half-life time determination . . . 175
E.3.2 HABA assay . . . 175
E.4 Preparation of the silicon and aluminum samples . . . 176
E.4.1 Cutting and cleaning of the substrates . . . 176
E.4.2 Etching of silicon nanowires . . . 176
E.4.3 Bohemite preparation on aluminum . . . 177
E.4.4 Surface modifications . . . 177
E.4.5 Azobenene immobilization . . . 178
E.4.6 Surface analysis . . . 180

F Bibliography **183**

G Appendix **192**
G.1 Half-life time calculations - linear regressions . . . 192
G.2 WCA photoswitchable surfaces - raw data . . . 195
G.2.1 *Trans* immobilization . . . 195
G.2.2 *Cis* immobilization . . . 196
G.3 Publications and conference activities resulting from this thesis . . . 197
G.4 List of abbreviations . . . 199

Die approbierte gedruckte Originalversion dieser Dissertation ist an der TU Wien Bibliothek verfügbar.
The approved original version of this doctoral thesis is available in print at TU Wien Bibliothek.
TU Bibliothek Your knowledge hub WIEN

G.5 Reference list of compounds 200
G.6 Curriculum vitae 201

Die approbierte gedruckte Originalversion dieser Dissertation ist an der TU Wien Bibliothek verfügbar.
The approved original version of this doctoral thesis is available in print at TU Wien Bibliothek.

Ackowledgments

With the end of this exciting journey approaching, it is time to thank everyone that one way or other took part on this journey with me.

Dear Marko I would like in the first place to thank you for giving me the opportunity to come to Vienna to do my PhD under your supervision. This has been an experience that I have utterly enjoyed. Thank you very much for all the guidance, mentoring and support that you have always provided.

Dear Helmuth thank you very much for all the scientific input and support, even when I would appear unannounced at your office. I really appreciate your effort to always make the time to give me valuable advice.

Working in the FGMDM group has been without any doubt a wonderful experience, both scientifically and personally. Michael, Florian and Christian, your advice and feedback in the seminars has without any doubt proven valuable for the completion of this work. To the members of the "Girl's lab", my scientific "home" of the last 3 years, a special thank you is in order. Blanca, Dani and Resi thank you very much for creating such an enjoyable working environment. This environment is one of the things that made possible to deal with the frustrating days that research always brings. Blanca thank you for such a warm reception to the lab and for making adaptation to Vienna so much easier. Erna and Letícia, I am really grateful that you always made me fell like a "honorary" member of the biolab. I have really had a great time with you inside and outside the lab. To all the group a big thank you!

Being a member of the doctoral school "BioInterface" was an amazing opportunity that has allowed me to work in a challenging interdisciplinary environment. Not only have I met

Die approbierte gedruckte Originalversion dieser Dissertation ist an der TU Wien Bibliothek verfügbar.
The approved original version of this doctoral thesis is available in print at TU Wien Bibliothek.
TU Bibliothek Your knowledge hub WIEN

several enthusiastic and talented colleagues but I also really enjoyed to take part in our seminars and retreats.

Á minha família e amigos que ficaram em Portugal, não tenho palavras suficientes para expressar quanta falta me fazem. Vir para Viena foi simultaneamente excitante e assustador, mas saber que mesmo longe podia contar convosco deu-me a força necessária para prosseguir.

Muito obrigada Telma e Sarah por continuarem a serem presenças frequentes, mesmo quando as nossas vidas tanto têm mudado! Rita e Renato obrigada por todas as "águas das pedras" e Gin tónicos e por sempre proporcionarem a vossa casa como um ponto de encontro. Carla, HD, Rita e Soraia, agredeço o tempo que tiram quando vou a Portugal, mesmo sendo complicado. É sempre um prazer saber o que se passa convosco e rever os nossos tempos em Braga, dos quais tanta falta sinto.

Aos meus pais, irmãs e avós um muito obrigado por sempre acreditarem em mim e me darem sempre o apoio necessário para atingir os meus objetivos. Sem vocês isto nunca teria sido possível! Também tenho de agradecer todo o miminho que recebo sempre que vos visito, e que tão feliz me faz. Não posso deixar de agradecer o bom cuidado que os meus pais e irmãs dão ao meu Pantera, a minha "máquina de ronroms" preferida.

Finalmente tenho de agradecer ao Bruno, o meu companheiro há quase 10 anos, por todo o apoio e compreensão. Muito obrigada por me acompanhares nesta mudança para Viena e por todas a vezes em que me lembraste que tudo ia correr bem.

To all of you, a heartfelt thank you very much!

A todos vós, um sincero muito obrigada!

Die approbierte gedruckte Originalversion dieser Dissertation ist an der TU Wien Bibliothek verfügbar.
The approved original version of this doctoral thesis is available in print at TU Wien Bibliothek.

Die approbierte gedruckte Originalversion dieser Dissertation ist an der TU Wien Bibliothek verfügbar.
The approved original version of this doctoral thesis is available in print at TU Wien Bibliothek.

Abstract

Photoswitches have become an incredibly useful tool in the fields of biology, pharmacology and medicine due to their ability to control the activity of biological compounds with light, an external stimulus with a high spacial and temporal resolution, orthogonal towards most components of living systems, non-toxic and with adjustable intensity and wavelength. Upon irradiation, photoswitches undergo a reversible configuration change and when a biomolecule is covalently bound to it, this change is expected to lead to a difference in the affinity to its target.

Among all photoswitches, azobenzenes that switch between *trans* and *cis* have a privileged position thanks to their high isomerization quantum yields, fast photoisomerization, resistance to optical fatigue, synthetic versatility and difference in the dipole moment after isomerization. As a consequence, azobenzenes have been applied to control the activity of several biomolecules such as ion channels, drugs and enzymes.

Another attractive use of azobenzenes is in the preparation of smart light-responsive surfaces, meaning surfaces that can change their physical and chemical properties in response to light. When a biomolecule is immobilized on top of an azobenzene coated surface, the activity of this biological compounds can also be controlled and systems that mimic biological processes (cell adhesion for example) can be developed. In addition to control the activity of biomolecules, azobenzene coated surfaces are promising for the development of smart self-cleaning materials or microfluid devices since upon irradiation the surface's polarity changes.

In this thesis, we have synthesized several azobenzenes functionalized with two different click chemistry moieties in the *para* positions aiming for an easy, fast and selective binding to biomolecules. Afterwards, we have focused on the application of these azobenzenes in the

development of light-responsive surfaces for biological applications.

One of the double-click azobenzenes was chosen to prepare a light responsive silicon surface that can be used for the immobilization of biomolecules by mild and selective chemistry and to develop a platform for the control of a biological process in the future. Another of these double-click azobenzenes has also been clicked to biotin in order to develop a photoswitchable DNA origami platform for the study of T-cell activation.

One fundamental problem of this work related with the preparation of azobenzene photoswitchable surfaces turned out to be surface overcrowding. This issue occurs when the concentration of azobenzene on the surface is too high and therefore there is no space for the switching from *trans* to *cis*. We have addressed this problem by immobilizing the azobenzene while on the most spatially demanding configuration, the *cis* isomer.

We have also tried to use rough surfaces to obtain an azobenzene coated surface that could switch between superhydrophobic and superhydrophilic so that the switching of azobenzenes could be undoubtedly followed by the difference in the water contact angle upon irradiation. Such a system would also be useful in the development of a smart self-cleaning surface. This effort, however, turned out to be more complex than expected and strongly dependent on the particular surface morphology of the rough substrate. Silicon nanowires, porous silicon and rough aluminum were tested in this respect, but none of them showed, as hoped, a superhydrophobic/superhydrophilic switching upon *trans*/*cis* photoisomerization. More work is needed here focusing on systematic surface structure variation and wetting transition studies, which exceeded the scope of this thesis.

Die approbierte gedruckte Originalversion dieser Dissertation ist an der TU Wien Bibliothek verfügbar.
The approved original version of this doctoral thesis is available in print at TU Wien Bibliothek.
TU Bibliothek Your knowledge hub WIEN

Kurzfassung

Moleküle, die unter Einfluss von Licht unterschiedliche Konfiguration einnehmen können, sogenannte Photoswitches, sind im letzten Jahrzehnt im Bereich der Biologie, Pharmazie und Medizin ein nützliches Instrument geworden. Ihre Stärke zeigt sich durch ihre Fähigkeit die Aktivität von biologischen Verbindungen durch Licht zu kontrollieren. Denn Licht ist ein externer Stimulus mit einer hohen räumlichen und zeitlichen Auflösung, besitzt keine Interaktionen mit den meisten lebenden Systemen, ist nicht toxisch und seine Wechselwirkung kann über Intensität und Wellenlänge reguliert werden. Bei der Bestrahlung gehen die Photoswitches eine reversible Konformationsänderung ein und durch die kovalente Bindung eines Biomoleküls daran kann davon ausgegangen werden, dass das Biomolekül dadurch seine Affinität verändert.

Unter all den zurzeit bekannten Photoswitches nehmen Azobenzene, die zwischen der *trans*- und *cis*-Konfiguration schalten können, eine besondere Position ein und das dank ihrer Isomerisierungs-Quantenausbeute, ihrer schnellen Photoisomerisierung, ihrer Resistenz gegenüber optischer Ermüdung, ihrer synthetischen Vielseitigkeit und dem Unterschied in ihrem Dipolmoment nach der Isomerisierung. Als direkte Konsequenz daraus werden Azobenzene dafür genutzt, die Aktivität von diversen Biomolekülen zu kontrollieren, wie beispielsweise Ionenkanäle, Medikamente und Enzyme. Eine andere attraktive Nutzung von Azobenzenen ist die Herstellung von sogenannten smart light-responsive surfaces. Diese "schlauen" Oberflächen können auf Lichtstrahlung reagieren, indem sie ihre physikalischen und chemischen Eigenschaften verändern. Wenn Biomoleküle auf einer Azobenzen-belegten Oberfläche immobilisiert sind, könnte die Aktivität dieser Biomoleküle durch Licht kontrolliert werden und Systeme, welche biologische Prozesse nachahmen, könnten entwickelt werden, wie bspw. in der Zelladhäsion. Um die Aktivität von Biomolekülen zu kontrollieren eignen sich daher auch

Die approbierte gedruckte Originalversion dieser Dissertation ist an der TU Wien Bibliothek verfügbar.
The approved original version of this doctoral thesis is available in print at TU Wien Bibliothek.
TU Bibliothek Your knowledge hub WIEN

Oberflächen, die mit Azobezenen besetzt sind. Dieses System scheint vielversprechend für die Entwicklung von sogenannten selbstreinigenden Materialien oder Mikrofluid-Systeme zu sein, da nach der Einstrahlung die Polarität der Oberfläche verändert wird.

In dieser Arbeit wurden mehrere Azobenzene synthetisiert und mit zwei unterschiedlichen Click-Chemie Substituenten in *para* - Position funktionalisiert. Wodurch eine einfache, schnelle und selektive Bindung an Biomolekülen ermöglicht wird. Des Weiteren haben wir uns auf die Anwendung dieser Azobenzene für die Entwicklung von lichtsensitiven Oberflächen für biologische Applikationen konzentriert. Eine dieser double-click Azobenzene wurde auserwählt, um lichtsensitive Siliziumoberflächen zu erzeugen, welche in der Zukunft für die milde und selektive chemische Immobilisierung von Biomolekülen und als Plattform zur Kontrolle biologischer Prozesse genutzt werden könnte.

Ein anderes der synthetisierten Azobenzene wurde an ein Biotin "geklickt", um eine photoschaltbare DNA-Origami Plattform für die Studie an T-cell Aktivierung zu entwickeln.

Im Zuge dieser Arbeiten sind wir auf ein fundamentales Problem von photoschaltbaren Oberflächen, genannt "Surface overcrowding", gestossen, dessen Ursache im unterschiedlichen Platzbedarf der beiden photoisomeren Moleküle liegt. Dieses Problem taucht dann auf, wenn die Konzentration des Azobenzens auf der Oberfläche zu hoch ist, sodass der Übergang von der *trans*- zur *cis*-Konfiguration nicht mehr möglich ist. Wir haben dieses Problem lösen können, indem wir das Azobenzen in in seiner räumlich anspruchsvolleren *cis*-Konfiguration adsorbierten, indem die Adsorption unter kontinuierlicher UV-Bestrahlung der Adsorptionslösung durchgeführt wurde.

Wir nutzten auch raue Oberflächen, um die Oberflächenkonzentration von Azobenzen und damit die Empfindlichkeit darauf basierender, photoschaltbarer Sensoren zu erhöhen sowie andererseits eine mit Azobenzen besetzte Oberfläche zu erzeugen, die mit Licht zwischen superhydrophilen und superhydrophoben Eigenschaften geschalten werden kann und dieser Wechsel über den Wasser-Kontaktwinkel hochempfindlich detektiert werden kann. Solche Systeme könnten etwa in der Entwicklung von sogenannten selbstreinigenden Oberflächen nützlich sein. Dieses Vorhaben erwies sich jedoch als wesentlich komplexer als erwartet aufgrund des grossen Einflusses der speziellen Oberflächenmorphologie des rauen Substrats. Sili-

Die approbierte gedruckte Originalversion dieser Dissertation ist an der TU Wien Bibliothek verfügbar.
The approved original version of this doctoral thesis is available in print at TU Wien Bibliothek.
TU Bibliothek Your knowledge hub WIEN

zium-Nanodrähte, poröses Silizium und raue Aluminium-Substrate wurden in diesem Zusammenhang untersucht, jedoch konnte in keinem Fall der erhoffte, schaltbare superhydrophil/superhydrophob Wechsel als Folge der *trans*/*cis* Photoisomerisation festgestellt werden. Systematische Untersuchungen sowie eine gezielte Steuerung der Oberflächenmorphologie und Porenstruktur des Substrats sind hier erforderlich, welche jedoch den Umfang der vorliegenden Arbeit hier überstiegen.

Die approbierte gedruckte Originalversion dieser Dissertation ist an der TU Wien Bibliothek verfügbar.
The approved original version of this doctoral thesis is available in print at TU Wien Bibliothek.
TU Bibliothek Your knowledge hub WIEN

Chapter A

Synthetic schemes

The compounds prepared or used as starting materials in this thesis are numbered in bold arabic numerals. Compounds unknown to the literature are additionally underlined. Surfaces were named according to the material (Silicon-Si, Aluminum-Al), surface morphology (F-flat, NW-nanowires, P-porous), the immobilization method (*trans* or *cis*) and the immobilized compound.

Die approbierte gedruckte Originalversion dieser Dissertation ist an der TU Wien Bibliothek verfügbar.
The approved original version of this doctoral thesis is available in print at TU Wien Bibliothek.
TU Bibliothek Your knowledge hub WIEN

A.1 Preparation of the *trans*-cyclooctene building blocks

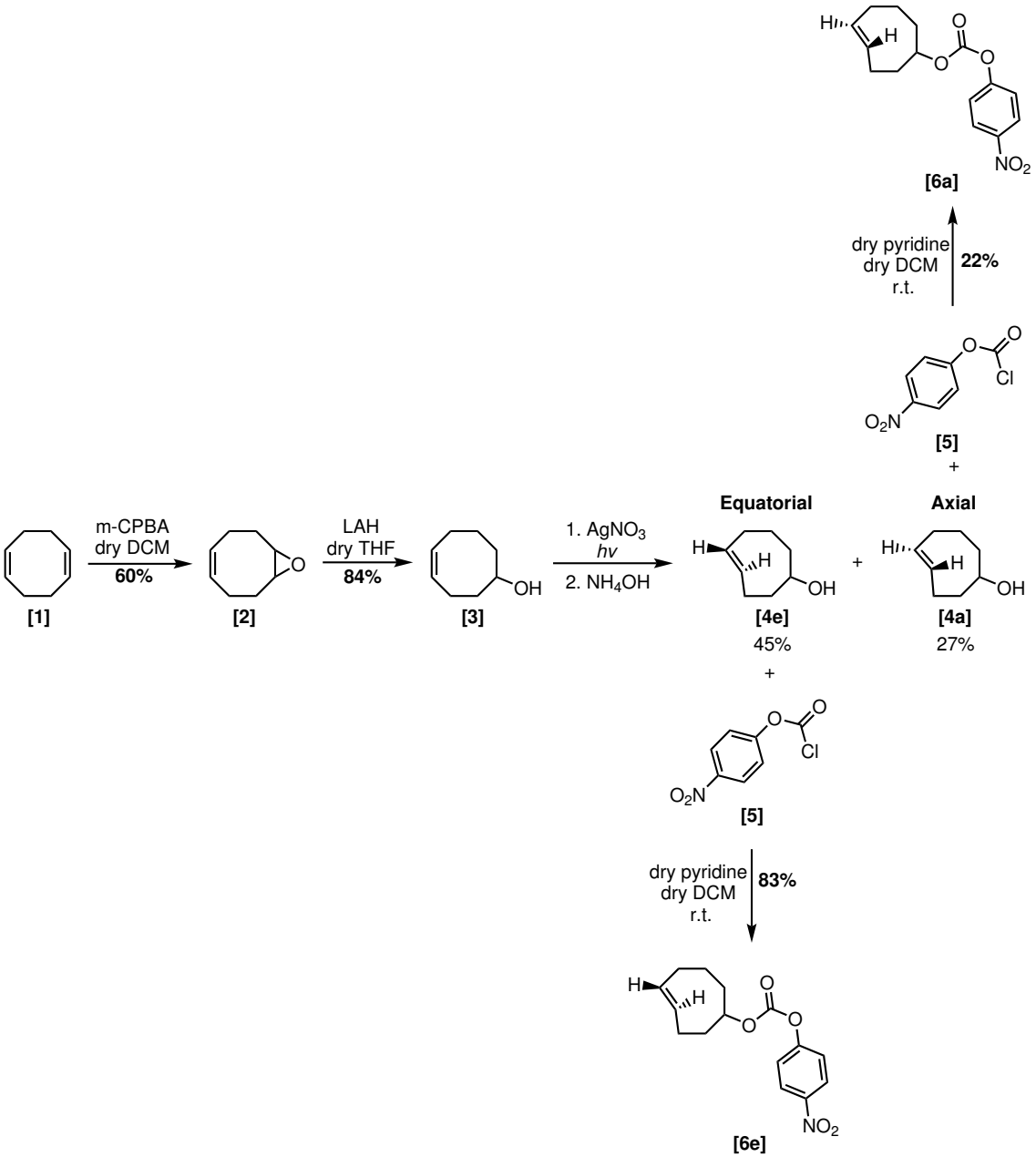

Die approbierte gedruckte Originalversion dieser Dissertation ist an der TU Wien Bibliothek verfügbar.
The approved original version of this doctoral thesis is available in print at TU Wien Bibliothek.

A.2 Preparation of CuAAc-tetrazine ligation azobenzenes

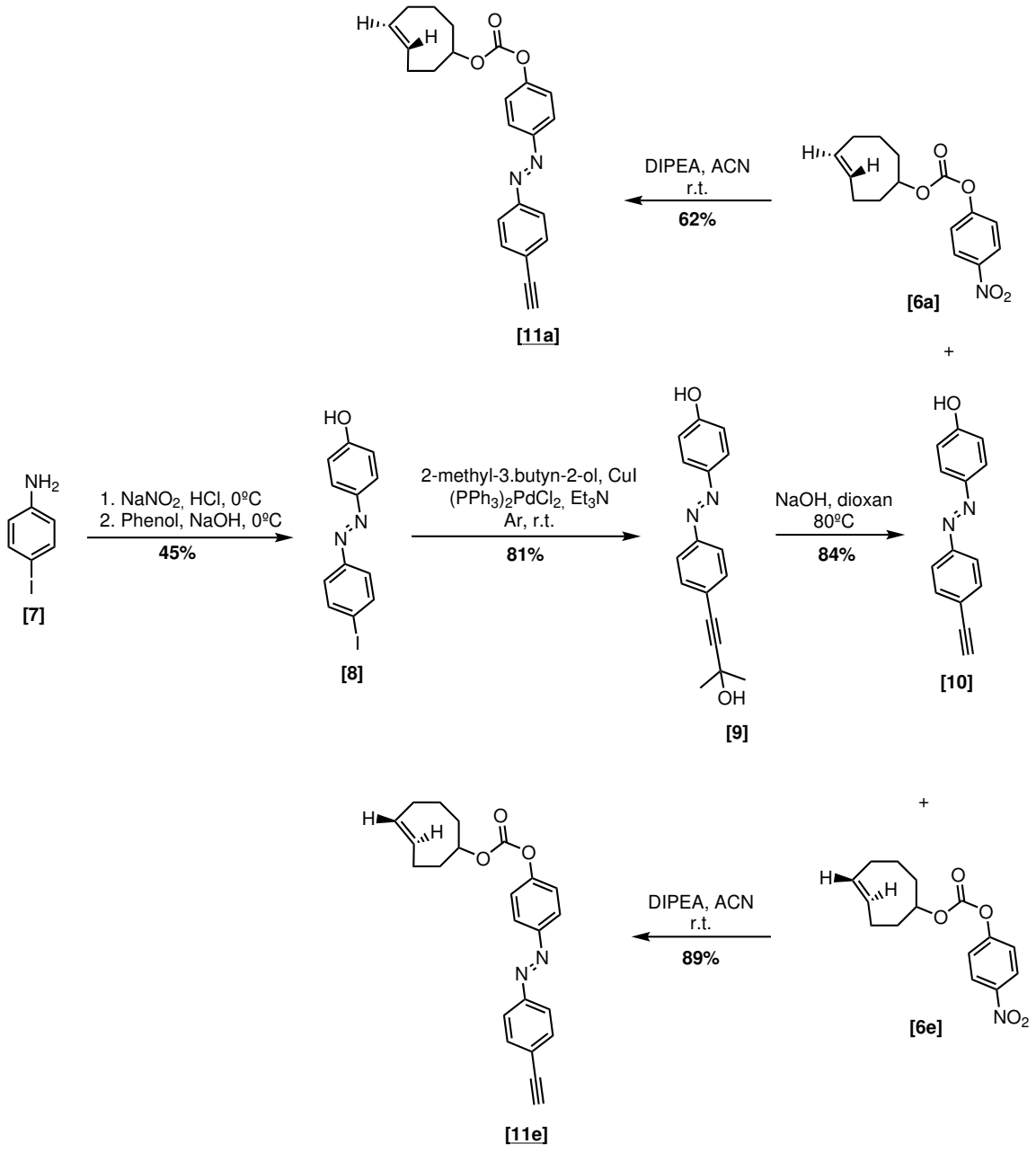

Die approbierte gedruckte Originalversion dieser Dissertation ist an der TU Wien Bibliothek verfügbar.
The approved original version of this doctoral thesis is available in print at TU Wien Bibliothek.

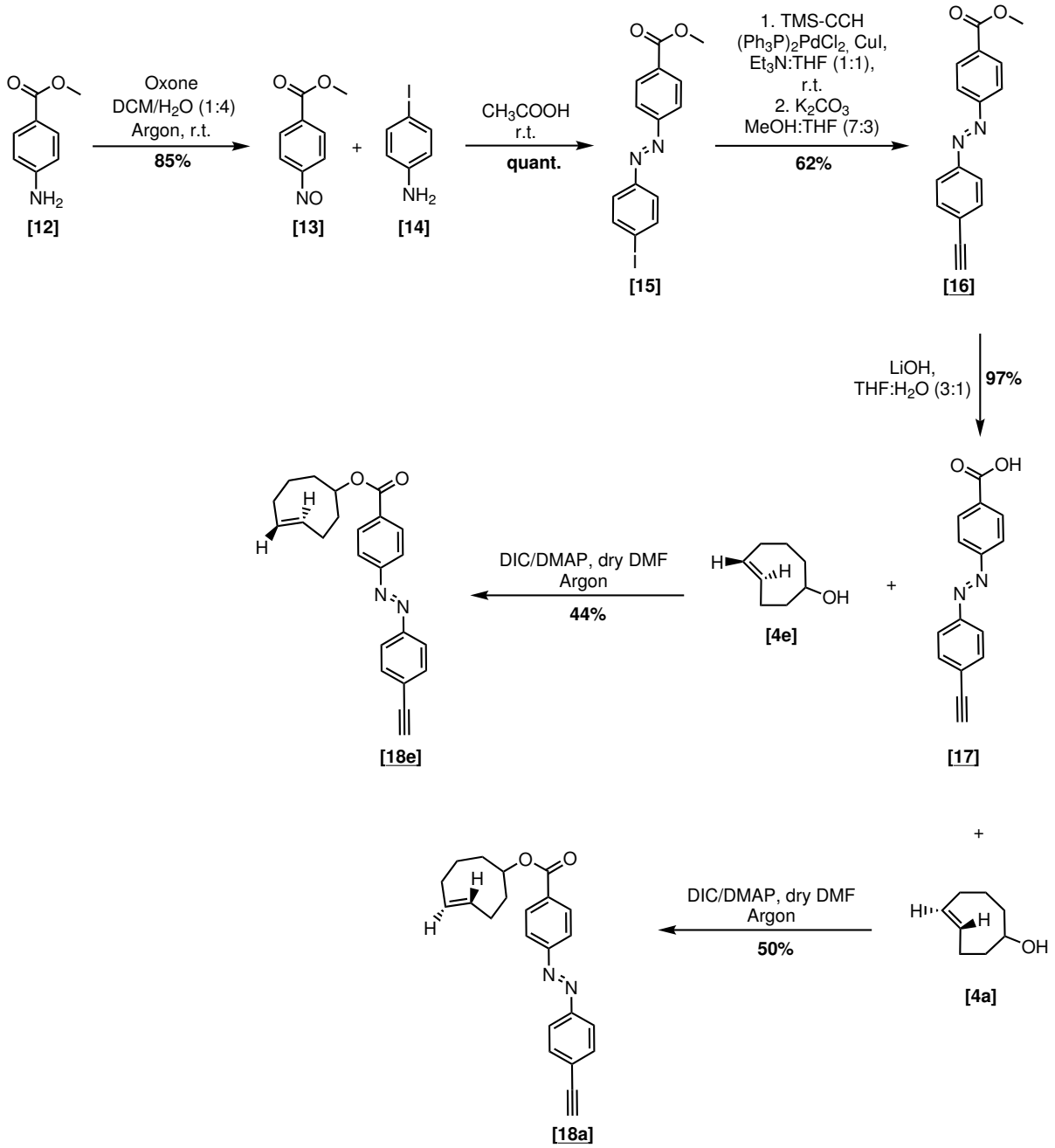

Die approbierte gedruckte Originalversion dieser Dissertation ist an der TU Wien Bibliothek verfügbar.
The approved original version of this doctoral thesis is available in print at TU Wien Bibliothek.

A.3 Preparation of SPAAC-tetrazine ligation azobenzene

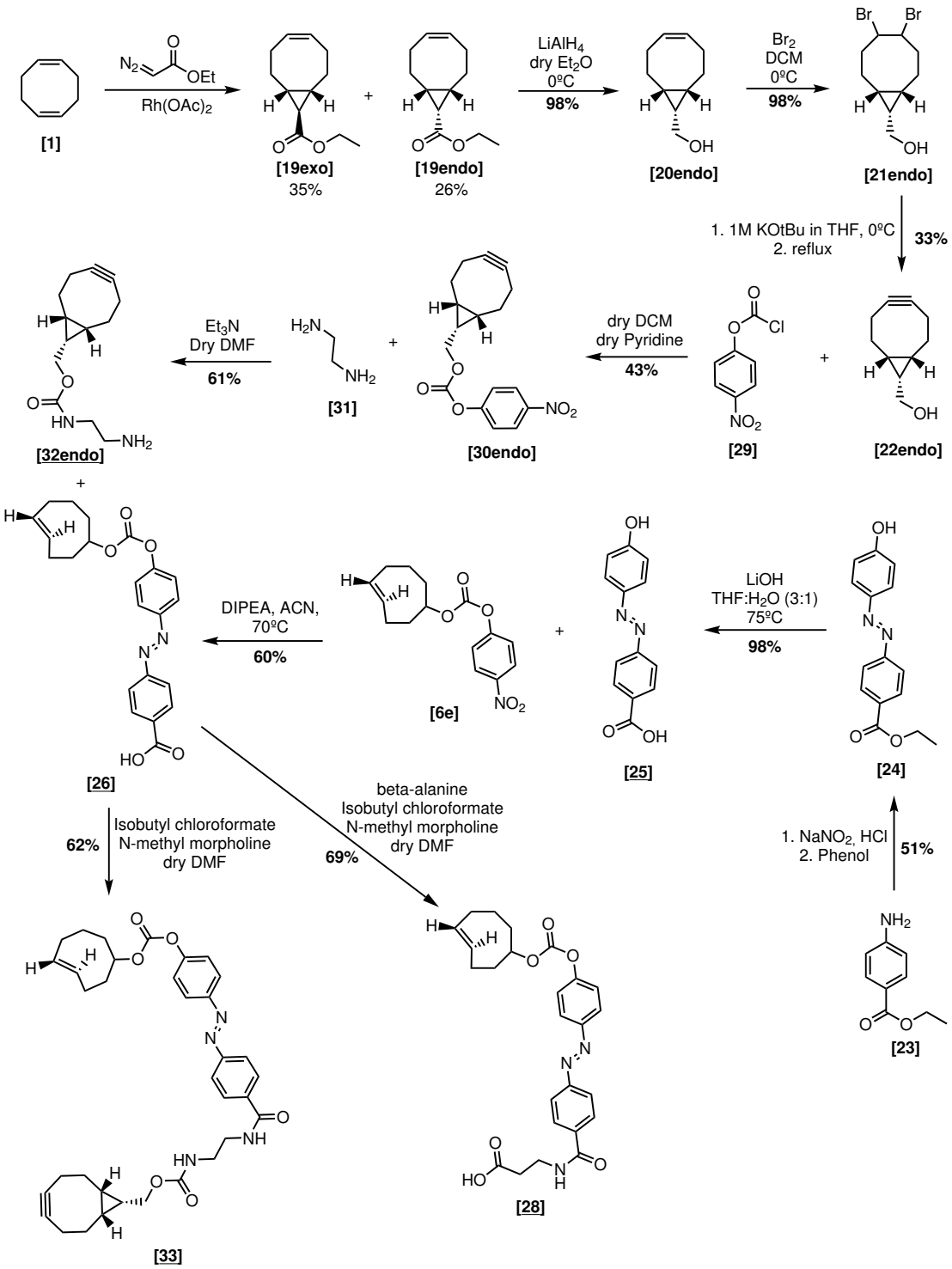

Die approbierte gedruckte Originalversion dieser Dissertation ist an der TU Wien Bibliothek verfügbar.
The approved original version of this doctoral thesis is available in print at TU Wien Bibliothek.

A.4 Preparation of CuAAc-thiol azobenzene

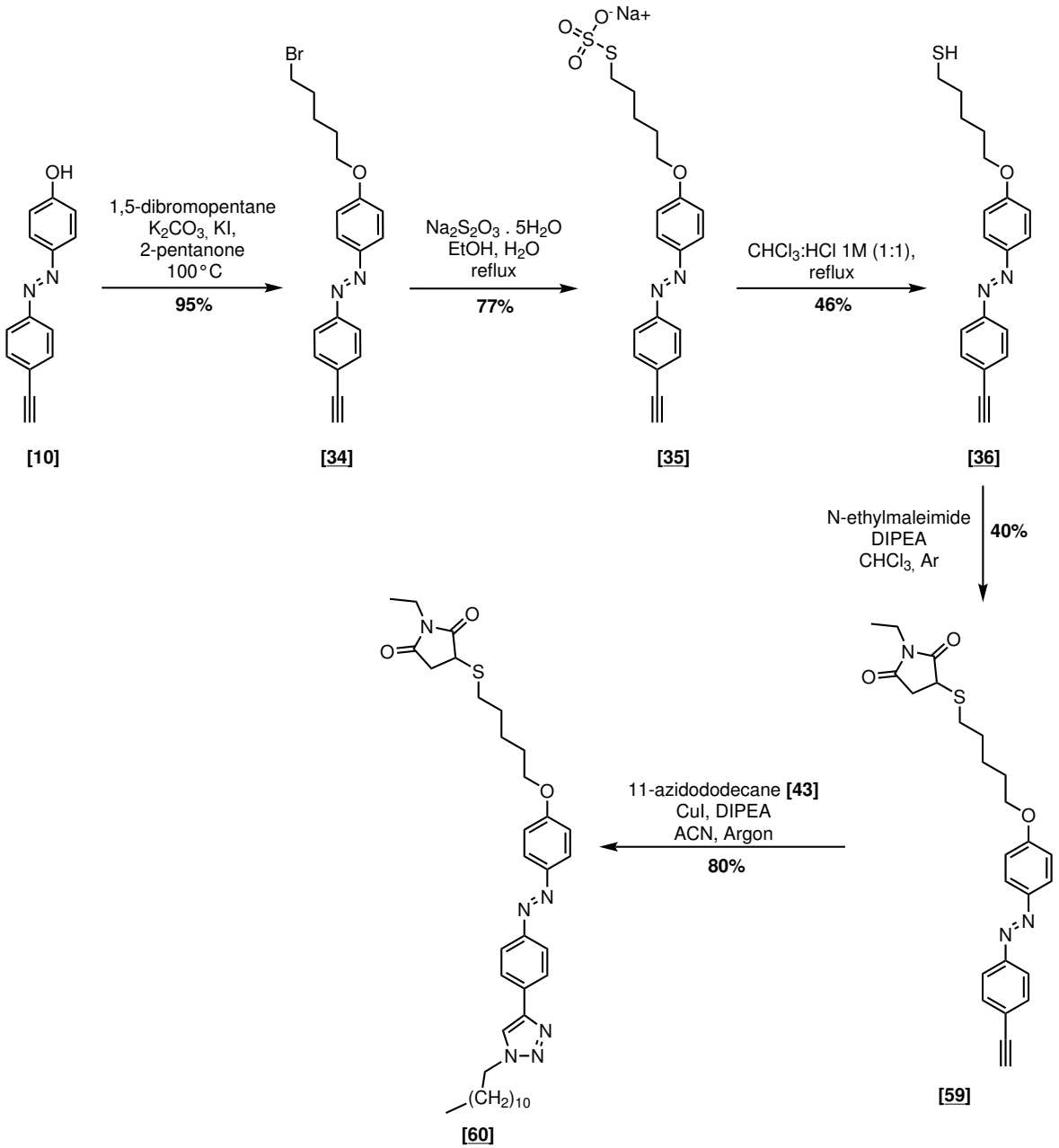

Die approbierte gedruckte Originalversion dieser Dissertation ist an der TU Wien Bibliothek verfügbar.
The approved original version of this doctoral thesis is available in print at TU Wien Bibliothek.

A.5 Preparation of a model azobenzene for surface functionalization and test of click reactions

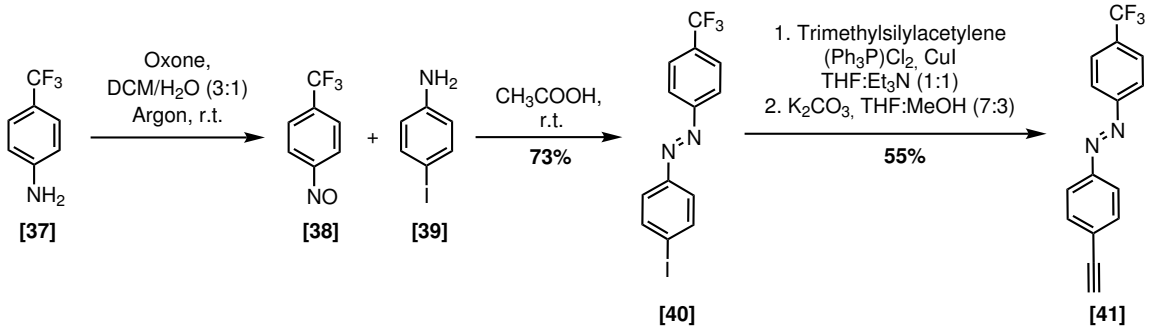

Die approbierte gedruckte Originalversion dieser Dissertation ist an der TU Wien Bibliothek verfügbar.
The approved original version of this doctoral thesis is available in print at TU Wien Bibliothek.

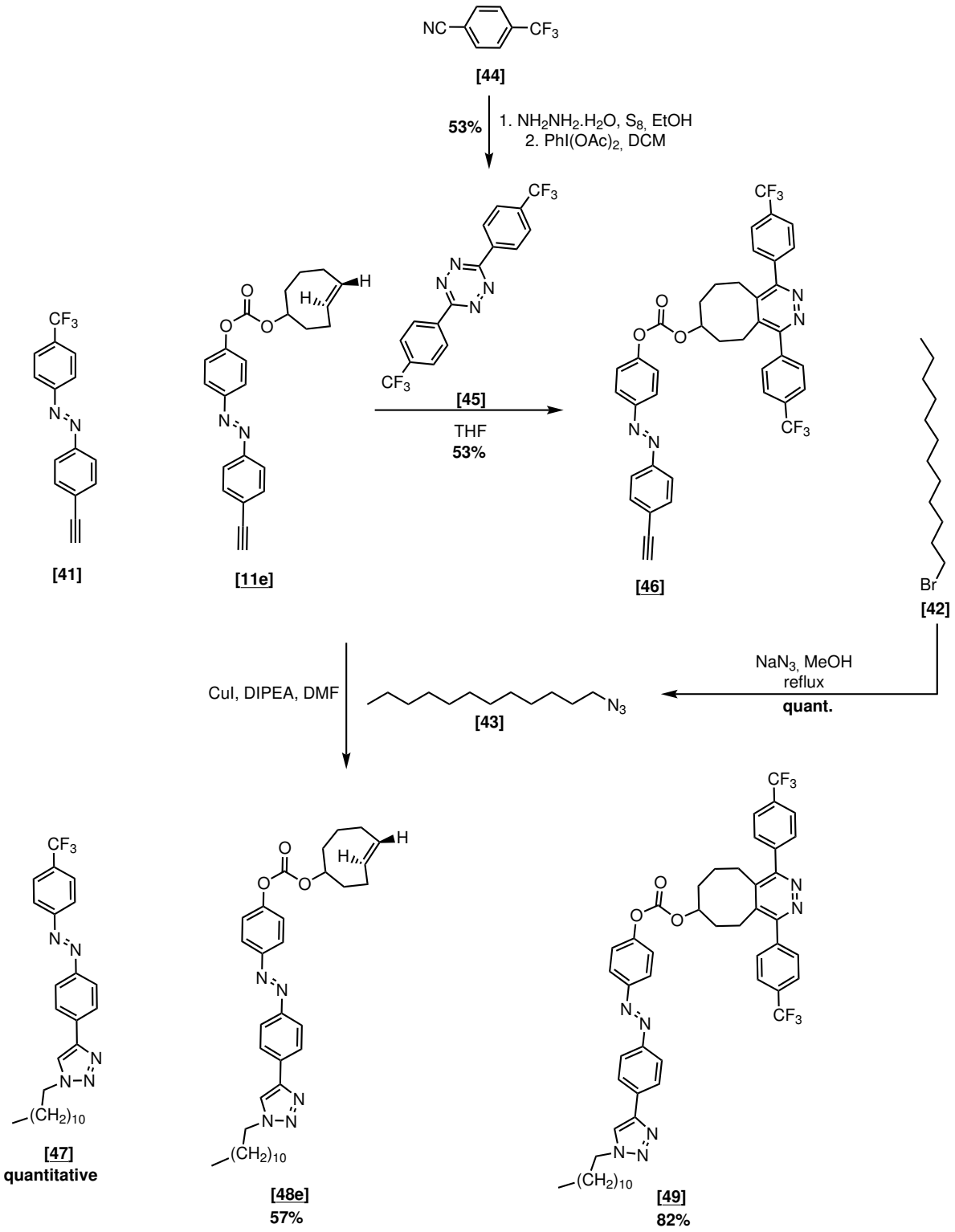

Die approbierte gedruckte Originalversion dieser Dissertation ist an der TU Wien Bibliothek verfügbar.
The approved original version of this doctoral thesis is available in print at TU Wien Bibliothek.

A.6 Surface preparation

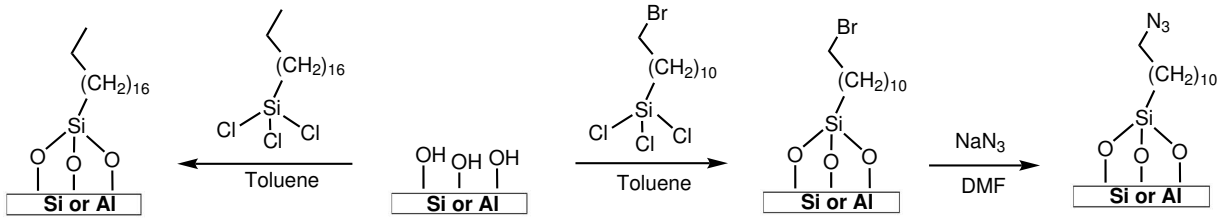

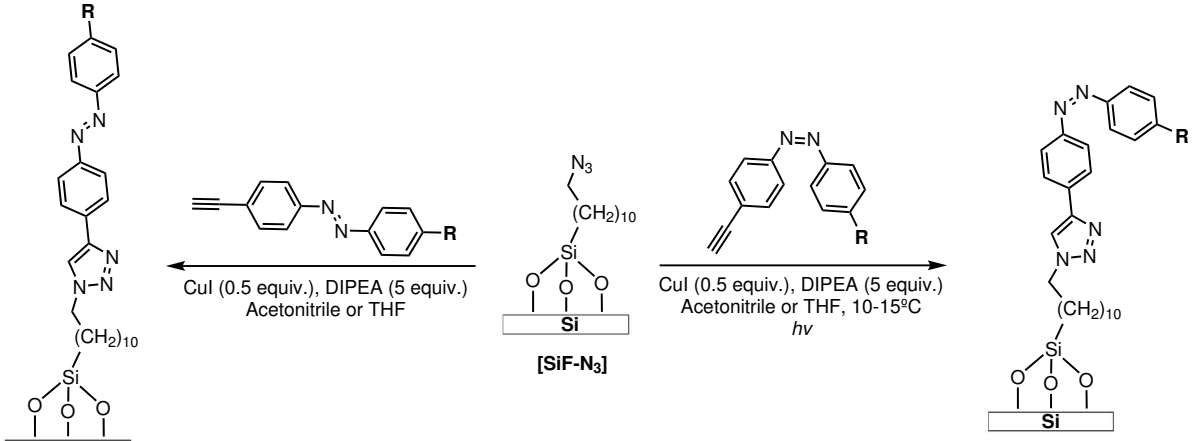

[SiF-41*trans*]
[SiF-11e*trans*]
[SiF-46*trans*]

[SiF-N3]

[SiF-41*cis*]
[SiF-11e*cis*]
[SiF-46*cis*]
[SiF-36*cis*]

	[SiF-41*trans*] [SiF-41*cis*]	[SiF-11e*trans*] [SiF-11e*cis*]	[SiF-46*trans*] [SiF-46cis]	[SiF-36cis]
R	-CF_3	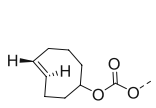	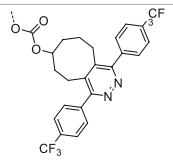	-SH

Die approbierte gedruckte Originalversion dieser Dissertation ist an der TU Wien Bibliothek verfügbar.
The approved original version of this doctoral thesis is available in print at TU Wien Bibliothek.
TU Bibliothek Your knowledge hub WIEN

A.7 Biotin modifications

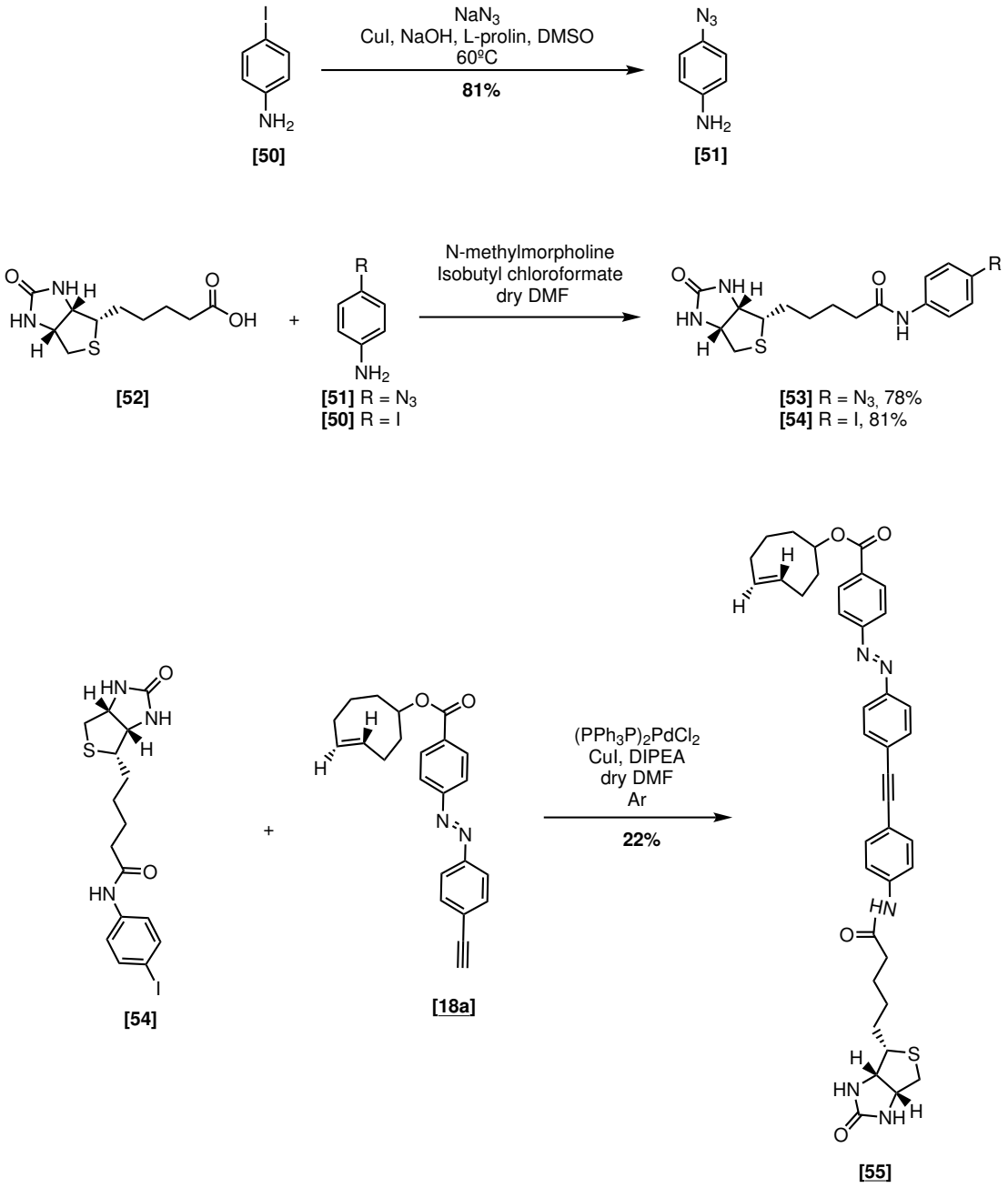

Die approbierte gedruckte Originalversion dieser Dissertation ist an der TU Wien Bibliothek verfügbar.
The approved original version of this doctoral thesis is available in print at TU Wien Bibliothek.

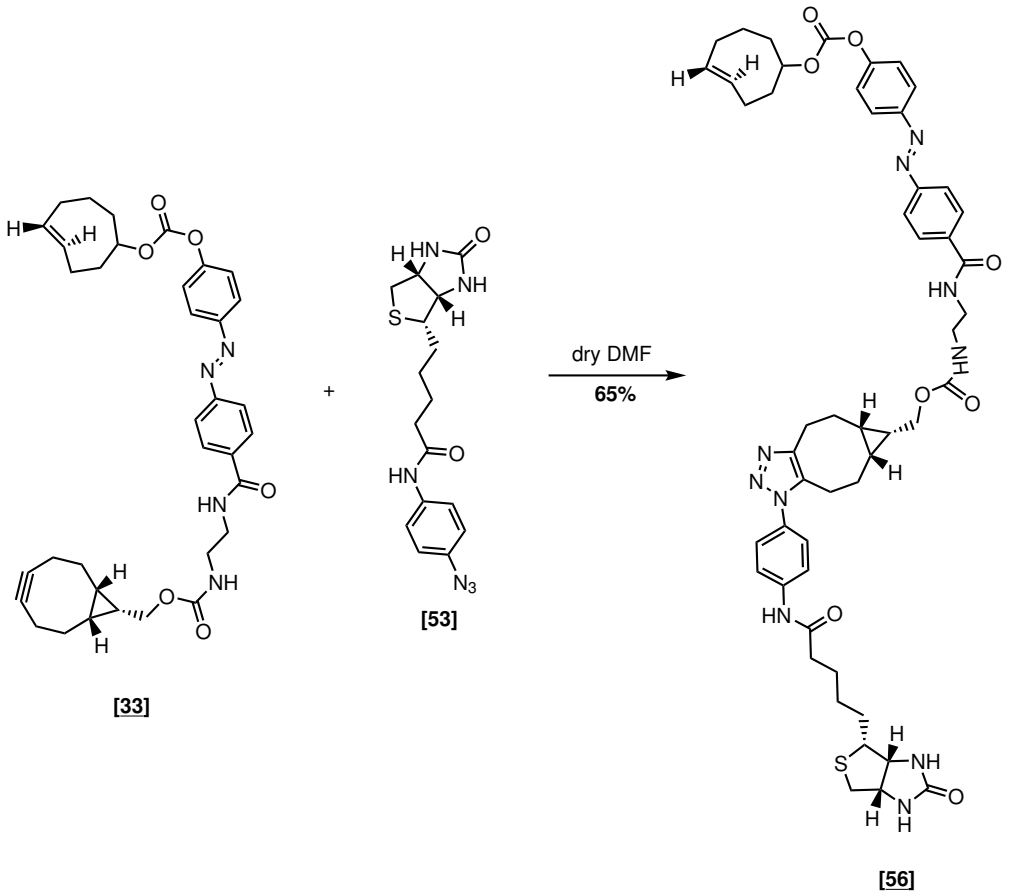

[33] + **[53]** → **[56]**

Die approbierte gedruckte Originalversion dieser Dissertation ist an der TU Wien Bibliothek verfügbar.
The approved original version of this doctoral thesis is available in print at TU Wien Bibliothek.

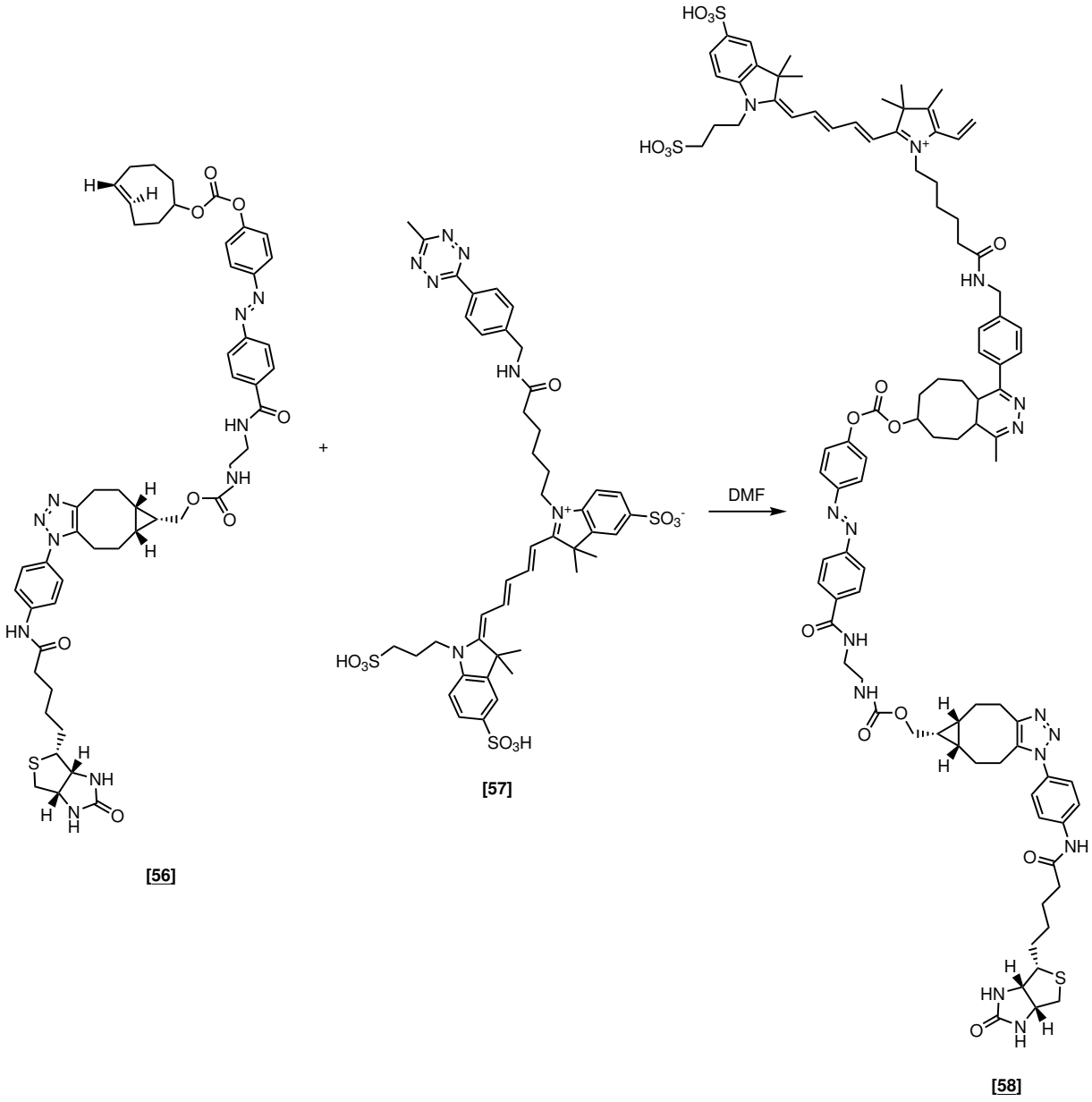

[56] + **[57]** → **[58]**

Die approbierte gedruckte Originalversion dieser Dissertation ist an der TU Wien Bibliothek verfügbar.
The approved original version of this doctoral thesis is available in print at TU Wien Bibliothek.

Die approbierte gedruckte Originalversion dieser Dissertation ist an der TU Wien Bibliothek verfügbar.
The approved original version of this doctoral thesis is available in print at TU Wien Bibliothek.

Chapter B

Introduction

B.1 Photoswitches and photopharmacology

Light has emerged as an important stimulus in the field of biological sciences. Its high spacial and temporal resolution, orthogonality towards most components of living systems, non-toxicity and the ability to regulate its intensity and wavelength has led to the development of tools that rely on light to study biological processes, such as fluorescent proteins (e.g. green fluorescent protein - GFP) and fluorescent probes. Notwithstanding, tolls that rely on fluorescence do not allow to control the activity of the biomolecules of interest, unlike photocages and photoswitches.[1–4] Photocages (e.g. coumarins, *orto*-nitrobenzyl), also known as photocleavable protecting groups, are chemicals that irreversibly undergo the cleavage of a chemical bond after the absorption of one photon, releasing the previously bound molecule and restoring its biological activity.[5] Figure 1 presents an example where an *orto*-nitrobenzyl derivate, α-carboxy-2-nitrobenzyl, was used to cage glutamate, an excitatory neurotransmitter that activates glutamate receptors. After irradiation the glutamate is released and regains its biological activity. Caged glutamate has been used to study glutamate receptors and elucidate the mechanisms behind synapses.[6–8]

Photoswitches are another option that allows to control the activity of biomolecules. Like photocages, they undergo a chemical reaction upon the absorption of a photon, but present two main advantages. In the first place this reaction is reversible, which means that each photoswitch interconverts between 2 different configurations that present different absorption max-

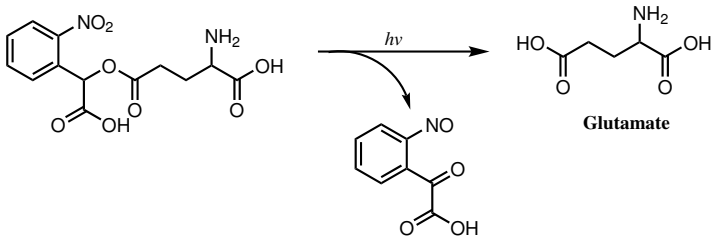

Figure 1: A caged glutamate for the study of glutamate receptors.[8]

imums. These maximum wavelengths determine the wavelength required for controlling the direction of the reaction. In the second place, photoswitches do not generate byproducts upon irradiation, that could be toxic.[1,2,9]

Figure 2 presents several classes of photoswitches found in the literature. In a simplistic manner the photoswitches can be divided according to the reaction they undergo: azobenzenes[10,11], stilbenes[12], hemithioindigos[13–15] and iminothioindoxyls (a recent photoswitch resulting form the combination of azobenzenes and thioindigos)[16] undergo a *trans-cis* isomerization, while diarylethenes[17,18], thiophenefulgides[19], spiropyrans[20,21] and donor-acceptor Stenhouse adducts[22–24] undergo a cyclization-ring opening reaction.

Among all the classes of photoswitches, azobenzenes are probably the most well-studied and applied, due to their high isomerization quantum yields, fast photoisomerization, optical fatigue resistance (repeated photoswitching cycles), synthetic versatility and difference in the dipole moment after isomerization ($\sim$0 D for *trans* and $\sim$3 D for *cis*).[25–27]

Thanks to the importance of azobenzenes, a huge variety of synthetic methods to obtain these chemicals has been developed. Among these the Mills reaction and the azo coupling reaction have been the most applied. In the Mills reaction (Figure 3) a nitrosobenzene derivative in acetic acid is coupled with an aniline, which acts as a nucleophile, and upon H_2O elimination the azobenzene is obtained. The azo coupling reaction (Figure 4) results from the coupling of a diazonium salt and a benzene with an electron-donor group, such as hydroxyl, that directs substitution for the *para* position. In the first place, the nitrosonium cation is formed under strong acidic conditions from nitrite - nitrous acid is formed upon protonation of nitrite and further protonation and H_2O elimination generates the desired cation. The aniline then attacks the nitrosonium forming the diazonium salt. Finally, the diazonium salt undergoes electrophilic

Die approbierte gedruckte Originalversion dieser Dissertation ist an der TU Wien Bibliothek verfügbar.
The approved original version of this doctoral thesis is available in print at TU Wien Bibliothek.
TU Bibliothek Your knowledge hub WIEN

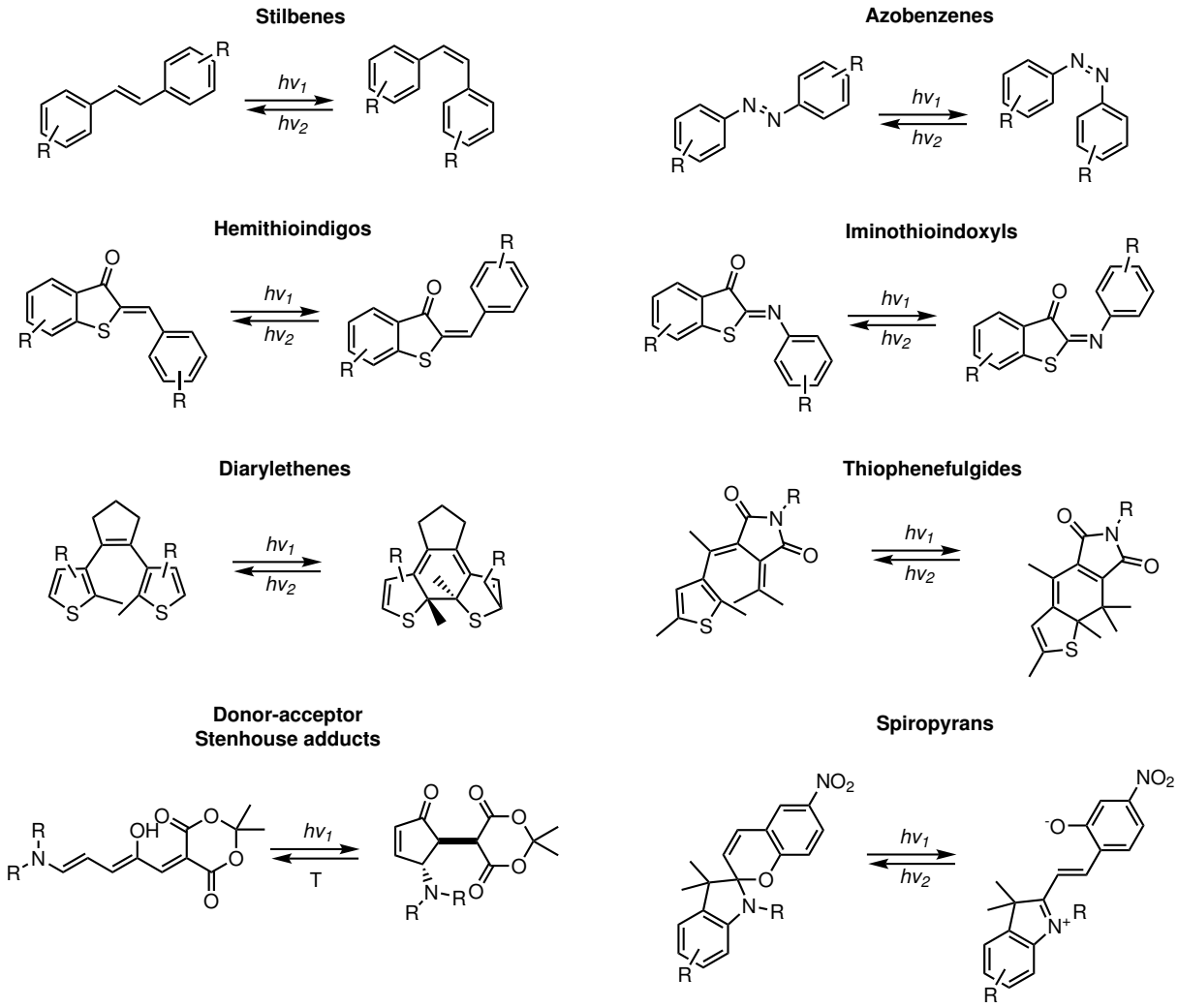

Figure 2: Examples of classes of photoswitches, molecules capable of a reversible chemical reaction upon irradiation.

aromatic substitution.[28]

Azobenzenes can also be obtained by oxidation of anilines or reduction of nitrobenzene derivatives. Nevertheless these methods are not really effective when aiming for heterocoupling.[10,28]

Upon irradiation azobenzenes undergo a *trans-cis* isomerization. More concretely, the switch from *trans* to *cis* is performed with UV light (≈350 nm) and from *cis* and *trans* and with visible light (>460 nm). There are 4 proposed mechanisms that explain the isomerization of the azobenzene: rotation, inversion, concerted inversion and inversion-assisted rotation (Figure 5).

Die approbierte gedruckte Originalversion dieser Dissertation ist an der TU Wien Bibliothek verfügbar.
The approved original version of this doctoral thesis is available in print at TU Wien Bibliothek.

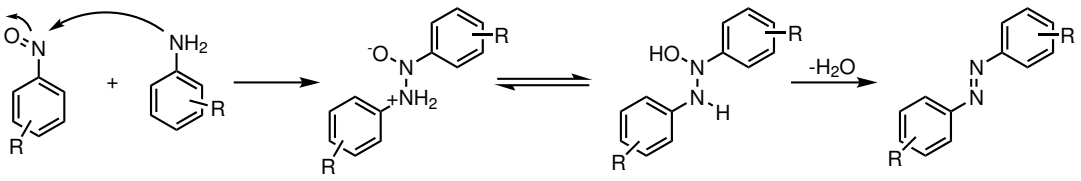

Figure 3: Mills reaction mechanism.

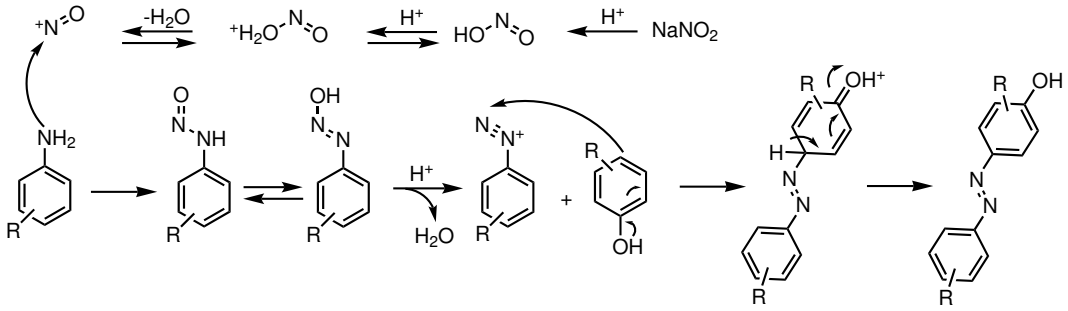

Figure 4: Azo couling mechanism.

The rotation mechanism suggests that the N=N bound is broken to form a single bond that can freely rotate to change the angle. The inversion states that the N=N-C angle increases to 180° and a transition state with an sp hybridized N-azo atom is formed. In the concerned inversion mechanism, both N=N-C angles increase to 180° and the isomerization proceeds through a linear transition state. Finally, the inversion-assisted rotation proceeds via both rotation and assisted mechanisms. Regarding the *cis-trans* photoisomerization, most studies predict that the photoisomerization occurs via rotation while thermal relaxation via inversion.[10,29]

Figure 6 presents the UV-Vis spectra of the unsubstituted azobenzene in the *trans* and *cis* form. The *trans* isomer presents a strong absorption $\pi \rightarrow \pi^*$ band at approximately 320 nm and a $n \rightarrow \pi^*$ weak band, due to a symmetry forbidden transition, near 420 nm. The *cis* presents a slightly stronger $n \rightarrow \pi^*$ also at 420 nm and two $\pi \rightarrow \pi^*$ bands at 280 and 250 nm.[2,11] As a consequence of these absorption bands the photoswitching from *trans* to *cis* is performed using UV light, taking advantage of the $\pi \rightarrow \pi^*$ absorption band, while the reverse with visible light (>460 nm), using the $n \rightarrow \pi^*$ band. Nevertheless, these spectra are overlapping and, consequently, upon irradiation complete conversion to *cis* or switch-back to *trans* is not achieved. Normally an equilibrium, named photostationary state (PSS), is reached at approximately 80% of *cis* or 95% of *trans*.[11] In addition, the use of UV light can present a problem for biological applications not only because of the damage to cells but also due to its low penetration in tis-

Die approbierte gedruckte Originalversion dieser Dissertation ist an der TU Wien Bibliothek verfügbar.
The approved original version of this doctoral thesis is available in print at TU Wien Bibliothek.

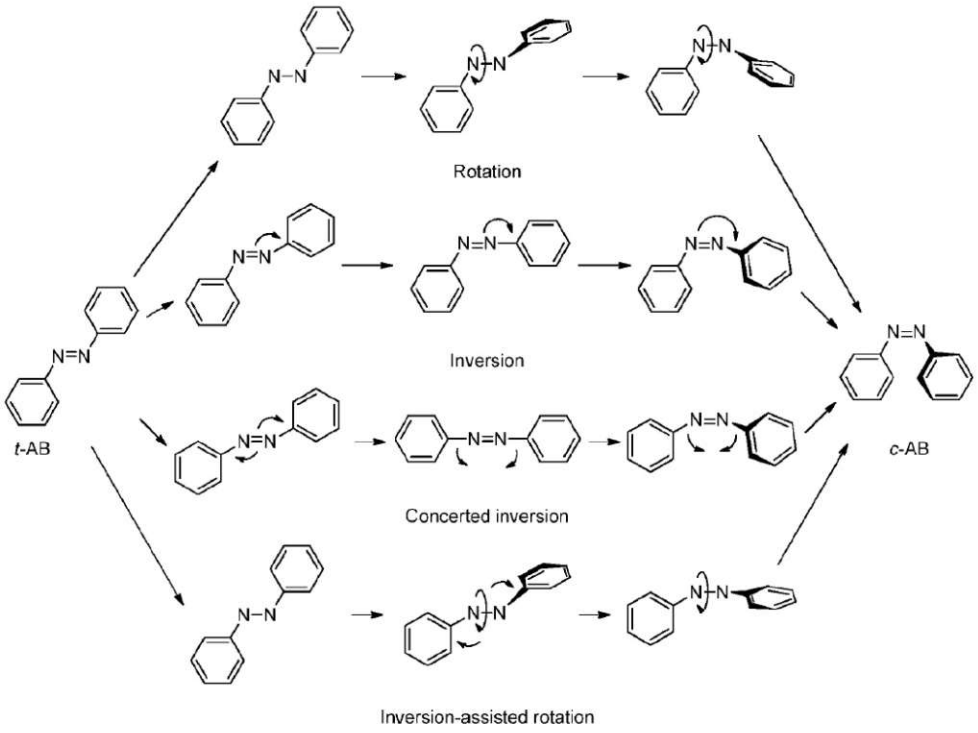

Figure 5: Proposed mechanisms to explain azobenzene isomerization.[29]

sues. Besides the used wavelengths and the completeness of the switching, the thermal stability of each isomer should also be considered.[30] Since the *cis* configuration is 10-12 kcal mol^{-1} thermodynamically less stable than the *trans*, the unmodified azobenzene undergoes thermal relaxation under the dark at room temperature over a couple days, which may be not stable enough in some applications.[11]

To improve the photophysical properties of azobenzenes substituents can be added to the benzene rings or the benzene can be replaced by another heterocycle. Figure 7A shows some examples where the photophysical properties of azobenzenes were tuned by introduction of substituents in the benzene ring. Hammerich et al. reported an azobenzene switchable completely with visible light, 5,6-dihydrodibenzo[c,g][1,2]diazocine, a bridged azobenzene. In this azobenzene, the $n \rightarrow \pi^*$ bands of the *cis* and *trans* isomers are separated by 100 nm which allows to use visible light to switch in both directions and leads to complete isomerization upon switching. Nevertheless, the most thermodynamically stable form of this azobenzene is the *cis*, which can be an inconvenience for biological applications.[31,32] Tetra-*orto* substitution of

Die approbierte gedruckte Originalversion dieser Dissertation ist an der TU Wien Bibliothek verfügbar.
The approved original version of this doctoral thesis is available in print at TU Wien Bibliothek.

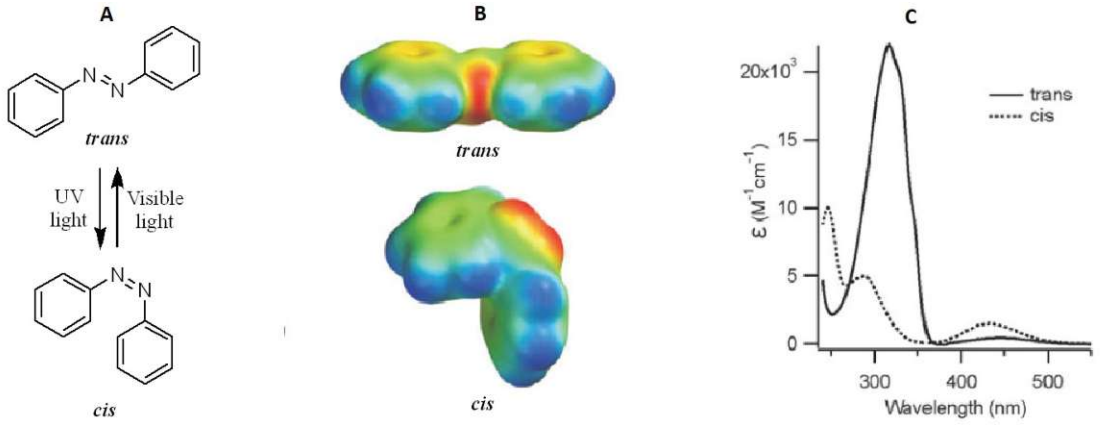

Figure 6: (A) Photoisomerization of unsubstituted azobenzene using UV light for *trans-cis* isomerization and visible light or thermal relaxation for *trans-cis*. **(B)** *Trans* and *cis* azobenzene colored by electrostatic potential (red to blue = negative to positive). **(C)** UV-Vis spectra of the unsubstituted *trans* and *cis* azobenzene in ethanol.[11]

azobenzenes with cloro[33], amines[34], methoxy[35] and fluoro[36] groups has also shown to lead to an increased separation between the $n \rightarrow \pi^*$ bands of the *cis* and *trans* isomers, generating azobenzenes addressable with visible light and with complete isomerization. When the *orto*-substitution is combined with the addition of *para*-electron-withdrawing groups the *trans* and *cis* $n \rightarrow \pi^*$ bands can be even further separated. The tetra-*orto* fluoro azobenzenes present in addition the remarkable feature of half-life times up to 2 years.[36] An azobenzene containing fused dioxan rings has also shown promise as a photoswitch completely addressable by visible light. This dioxan combines the $n \rightarrow \pi^*$ red-shift of a *meta*-methoxy substitution with the increased half-life time of a *orto*-methoxy substitution. Furthermore, the protonation of the amine in *para* position, expected under biological conditions, increases even further the $n \rightarrow \pi^*$ red-shift.[37]

Figure 7B presents examples where the substitution of the benzene ring lead to improved photophysical properties. In the BF_2 adducts, unlike before, the $\pi \rightarrow \pi^*$ is red-shifted to the visible region, allowing a complete switch using visible light. By modifying the R groups the wavelength can be tuned. However, the applicability of this scaffold for biological purposes is limited since in water they are hydrolyzed to hydrazones.[38,39] The azobenzene ring has also been replaced by several 5-membered nitrogen heterocycles such as pyrazoles[30,40], pyrroles[30,40], imidazole[41,42], triazole[30], tetrazole[30] and oxazole[43]. This replacement has

Die approbierte gedruckte Originalversion dieser Dissertation ist an der TU Wien Bibliothek verfügbar.
The approved original version of this doctoral thesis is available in print at TU Wien Bibliothek.
TU Bibliothek Your knowledge hub WIEN

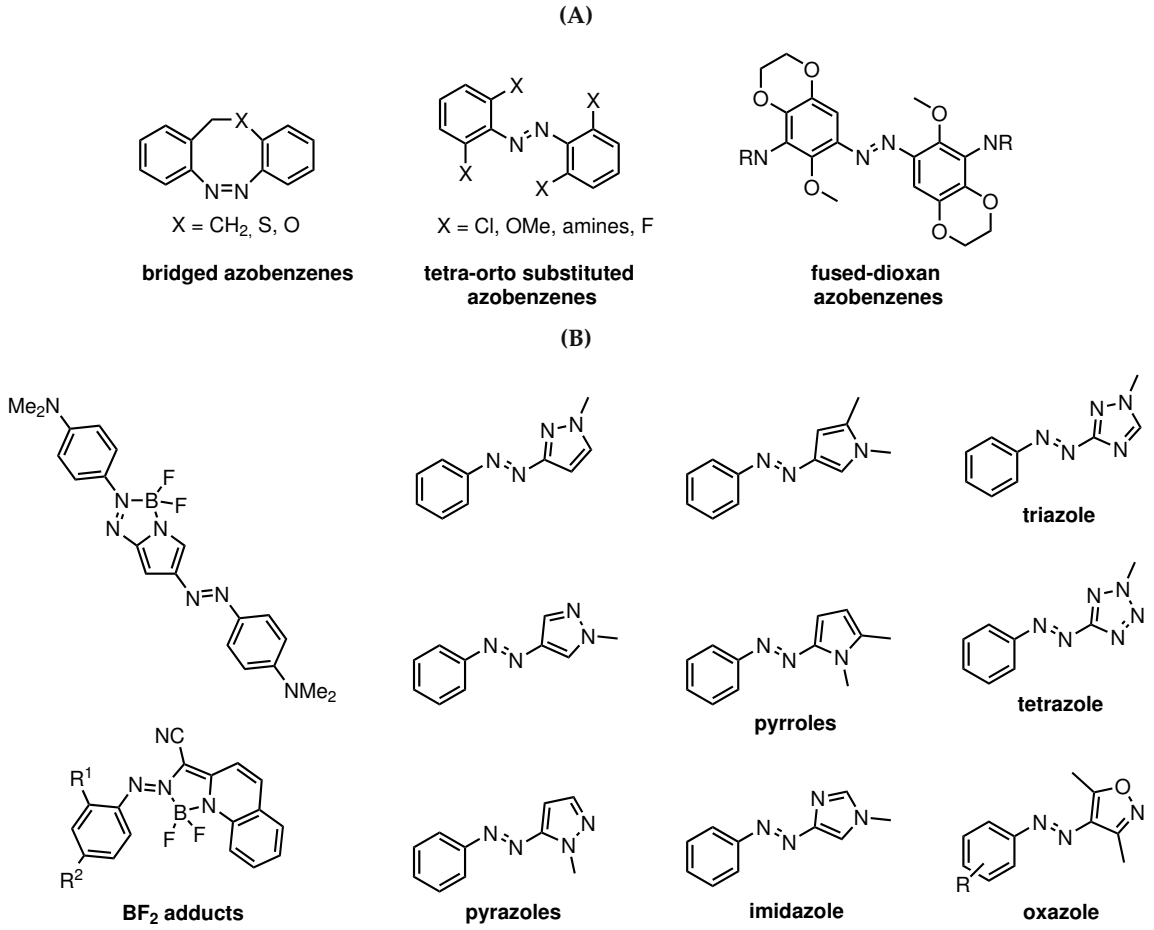

Figure 7: Azobenzenes completely addressable with visible light obtained by **(A)** substituent tuning on the benzene ring and **(B)** benzene ring replacement.

also proven quite successful since a lot of these derivatives have become completely switchable with visible light, with long half-life times and have near-quantitative switched-back to *cis*.[9,30]

Photopharmacology is the field that uses photoswitches to control the activity of biomolecules.[44,45] The photoswitch can modulate the activity of the biomolecule either by a non-covalente or covalent interaction. In the former case, a ligand is modified with a photoswitch forming a photochromic ligand, whose ability to interact with its target potentially depends on the configuration of the photoswitch (Figure 8). Ideally one configuration will have a high affinity towards the target while the other a reduced affinity. In the latter case, the photoswitch is covalently tethered to the target biomolecule, and the change in the configuration of the pho-

Die approbierte gedruckte Originalversion dieser Dissertation ist an der TU Wien Bibliothek verfügbar.
The approved original version of this doctoral thesis is available in print at TU Wien Bibliothek.
TU Bibliothek Your knowledge hub WIEN

toswitch may cause the binding of the ligand to the active center or to change the conformation of the active center itself.[2,4,46]

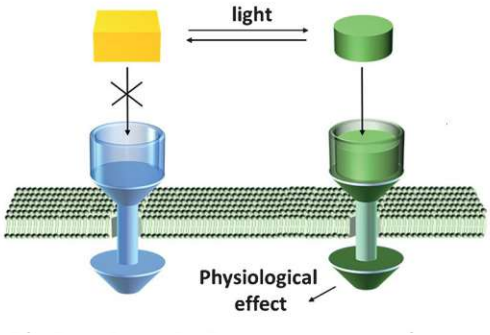

Figure 8: Representation of the mode of action of photochromic ligands: from the 2 configuration only one should interact with the target and lead to a biological response.[46]

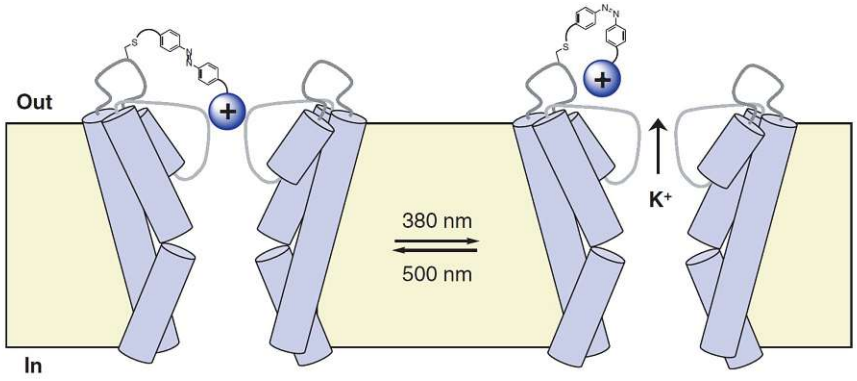

Figure 9: Tethered azobenzene for the control of a K^+ channel and neural firing.[47]

Azobenzenes have been frequently applied in photopharmacology both as tethered ligands and as photochromic ligands. As tethered ligands azobenzenes have been used for example to modify oligonucleotides to control the structure and replication of DNA[48,49], aminoacids to produce photochromic proteins and regulate cell growth or apoptosis[50–52], enzymes[53], and oligosaccharides to switch bacterial cells adhesion to surfaces[54]. Figure 9 presents an example where an azobenzene was tethered to a potassium channel in order to regulate neuron firing. The azobenzene was tethered to the ion channel via a cysteine and a quaternary ammonium group was placed on the azobenzene to block the channel. When the azobenzene is in the *trans* configuration the quaternary ammonium group reaches the pore of the channel and blocks the flow of K^+ and, consequently, neuron firing. Upon irradiation with UV light, the azobenzene

Die approbierte gedruckte Originalversion dieser Dissertation ist an der TU Wien Bibliothek verfügbar.
The approved original version of this doctoral thesis is available in print at TU Wien Bibliothek.
TU Bibliothek Your knowledge hub WIEN

switches to *cis* and the ammonium is removed from the pore and the channel regains its activity.[47]

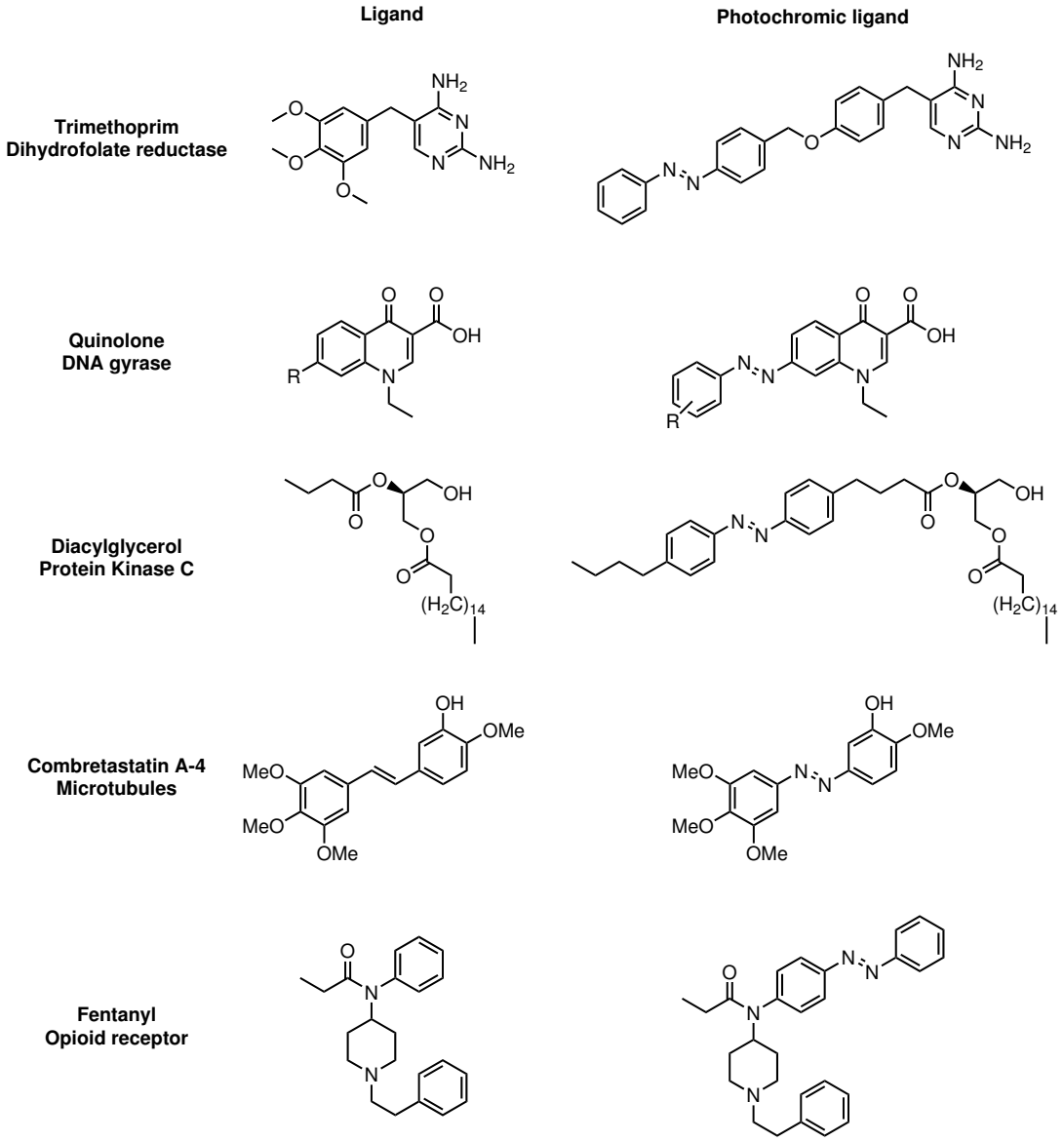

Figure 10: Examples of azobenzene-containing photochromic ligands: trimethoprim[57], quinolone[58], diacylglycerol[59], combretastatin A-4[60] and fentanyl[61]. On the left it is presented the original ligand while on the right the photochromic ligand. Each ligand is labeled with its chemical name (upper line) and its target (bottom line).

Regarding photochromic ligands, they have been used to modulate the activity of ion channels, transporters, pumps, enzymes, antibiotics and cell adhesion, for example.[4,9,55] Figure 10 presents some specific cases where azobenzene-containing photochromic ligands have

Die approbierte gedruckte Originalversion dieser Dissertation ist an der TU Wien Bibliothek verfügbar.
The approved original version of this doctoral thesis is available in print at TU Wien Bibliothek.
TU Bibliothek Your knowledge hub WIEN

been used. To obtain these ligands two approaches can be used: either the azobenzene can be attached to the biomolecule (azo-extension) or it can be incorporated in the biomolecule (azoligation).[44,56] Looking at the examples in Figure 10, the trimethoprim and diacylglycerol photochromic ligands were obtained by azo-extension while the remaining by azoligation.

Die approbierte gedruckte Originalversion dieser Dissertation ist an der TU Wien Bibliothek verfügbar.
The approved original version of this doctoral thesis is available in print at TU Wien Bibliothek.
TU Bibliothek Your knowledge hub WIEN

B.2 Smart light-responsive surfaces

Smart surfaces have attracted attention due to their ability to change their physical and chemical properties in response to specific stimulus such as temperature, pH, light and electrochemical potential. Among these stimuli, light has become increasingly popular due to its non-invasive nature and other advantages previously stated in Section B.1. One approach to obtain these light-responsive surfaces is to coat the surface with a photoswitch. As already indicated, azobenzenes have a privileged position among this class of molecules, therefore they have been frequently used to develop these types of systems.[62]

Possible applications of azobenzene light-responsive surfaces include the development of photocontrollable systems that mimic and control biological processes. This is achieved by immobilizing on a surface a photochromic ligand to control the biological process of interest.[63]

One of the most studied biological processes with these systems is cell adhesion. The controlled adhesion of several mammalian cells such as fibroblasts[64–66], endothelial[67], epithelial[63,68] and osteoblasts[69] has already been achieved by immobilizing on surfaces RGD peptide (arginine–glycine–aspartate) derivatives. This peptide mediates cell-adhesion by interacting with integrins a class of heterodimeric transmembrane cell receptors.[66,69] Figure 11 presents one of the example where RGD peptide has been used to turn on and off cell adhesion. Liu et al. have prepared a self-assembled monolayer (SAM) with a photoswitchable RGD peptide on a gold surface. The idea is that when the azobenzene is on the *trans* configuration the RGD peptide is ”exposed” and can mediate cell adhesion. Photoswitching for *cis* ”hides” the RGD peptide and cell adhesion is no longer possible (Figure 11A). Figure 11B shows that the NIH 3T3 fibroblasts bind to the surface when the azobenzene is in the *trans* configuration (*E* configuration) while Figure 11C shows that the same does not happen on the *cis* configuration (*Z* configuration). If the *cis* surface is irradiated with visible light to switch-back to *trans*, adhesion is once again possible (Figure 11C). Notice, that from Figure 11B to Figure 11C the cells had to be removed from the platform by addition of RGD peptide in solution (the RGD in solution competes with the RGD on the platform for the integrin receptor). This means that UV light is not enough to lead to the detachment of the cells from the surface.[65]

Another interesting aspect of the platform developed by Liu et al. is that the azobenzene-

Die approbierte gedruckte Originalversion dieser Dissertation ist an der TU Wien Bibliothek verfügbar.
The approved original version of this doctoral thesis is available in print at TU Wien Bibliothek.
TU Bibliothek Your knowledge hub WIEN

RGD peptide was immobilized on the gold together with a non-photoswitchable molecule, a PEG chain that works as a lateral spacer (Figure 11A). This spacer intends to prevent surface overcrowding, meaning a too high concentration of azobenzene on the surface that would lead to a non-photoswitchable surface due to lack of space for the *trans-cis* isomerization.[65]

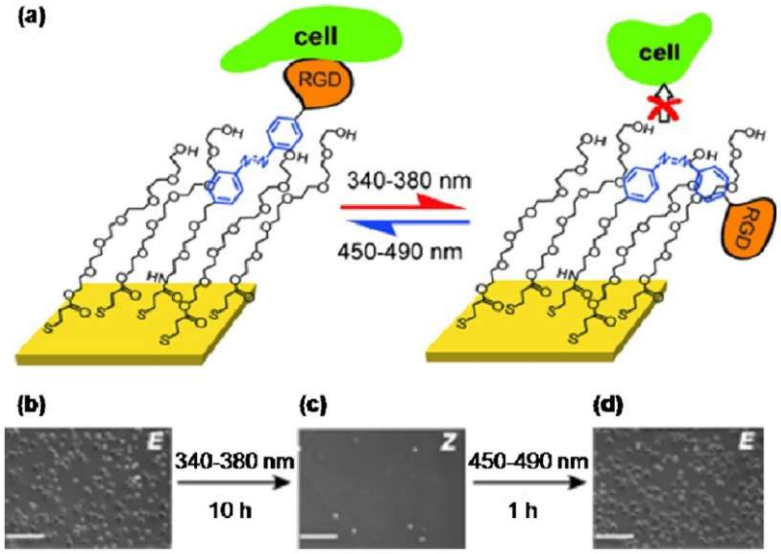

Figure 11: (A) Photoswitchable platform using the RGD peptide for the control of cell adhesion. **(B),(C)** and **(D)** Phase contrast images of the NIH 3T3 fibroblast that show the reversible cell adhesion and detachment using light.[62,65]

Notice that the RGD peptide is not the only motif that can be used to mediate cell adhesion. Zhang et al. have immobilized mannose and galactose on a gold surface to promote cell-adhesion via specific sugars receptors that are overexpressed in cancer cells. The same surface can be used also to specifically recognize lectines (sugar-recognition proteins).[63]

Sugars also have the ability to promote bacterial adhesion. Despras et al. have used α-D-mannoside to not only reversibly photocontrol the adhesion of *E.coli* to a gold surface but also of oligosaccharide engineered human microvascular endothelial cells, mimicking a bacterial infection.[70]

To produce a completely light-controlled reversible system for cell adhesion, host-guest systems with azobenzenes can be built. Cyclodextrin for example can form inclusion complexes with azobenzenes in *trans*, but not in *cis* because it does not fit any longer in its cavity.[71]

Die approbierte gedruckte Originalversion dieser Dissertation ist an der TU Wien Bibliothek verfügbar.
The approved original version of this doctoral thesis is available in print at TU Wien Bibliothek.
TU Bibliothek Your knowledge hub WIEN

This means that after the formation of the inclusion complex cyclodextrin/*trans*-azobenzene the azobenzene can be removed from its cavity simply by irradiation with UV light and switch to *cis*. Gong et al. prepared a self-assembled monolayer of α-cyclodextrin on a quartz surface and the azobenzene-RGDpeptide was added to form the inclusion complex (Figure 12). As expected if this surface was irradiated with UV light the azobenzene would be expelled from the cyclodextrin cavity and this process is reversible. The attachment of HeLa cells (cervical cancer cells) is verified on this surface after the formation of the inclusion complex cyclodextrin/azobenzene-RGD and UV light leds to the expulsion of the azobenzene of the cyclodextrin and cell detachment.[72]

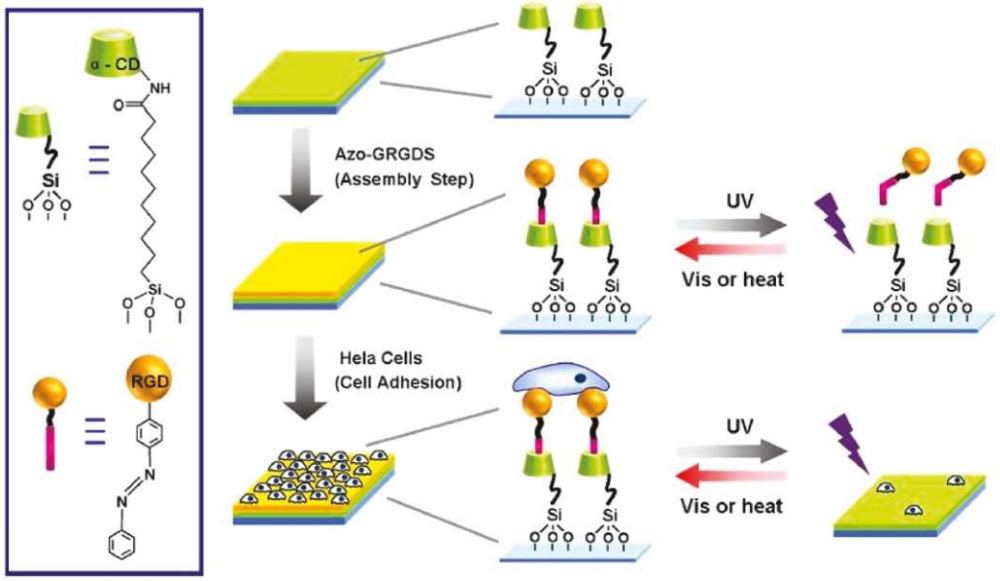

Figure 12: Regulation of cell adhesion with light taking advantage of the host-guest interaction between α-cyclodextrin and azobenzene.[72]

Although the previous system permits to reversibly photocontrol the attachment and detachment of cancer cells, the RGD peptide is not a specific system for cancer cells. Bian et al. have produced a photocontrolable platform specific for the capture and release of breast cancer cells using the cyclodextrin/azobenzene host-guest interaction and, instead of the RGD peptide, a DNA aptamer, a short DNA sequence that forms a unique 3D structure and binds a target molecule with high affinity.[73]

In addition to the capture of mammal cells, these supramolecular systems have already

Die approbierte gedruckte Originalversion dieser Dissertation ist an der TU Wien Bibliothek verfügbar.
The approved original version of this doctoral thesis is available in print at TU Wien Bibliothek.
TU Bibliothek Your knowledge hub WIEN

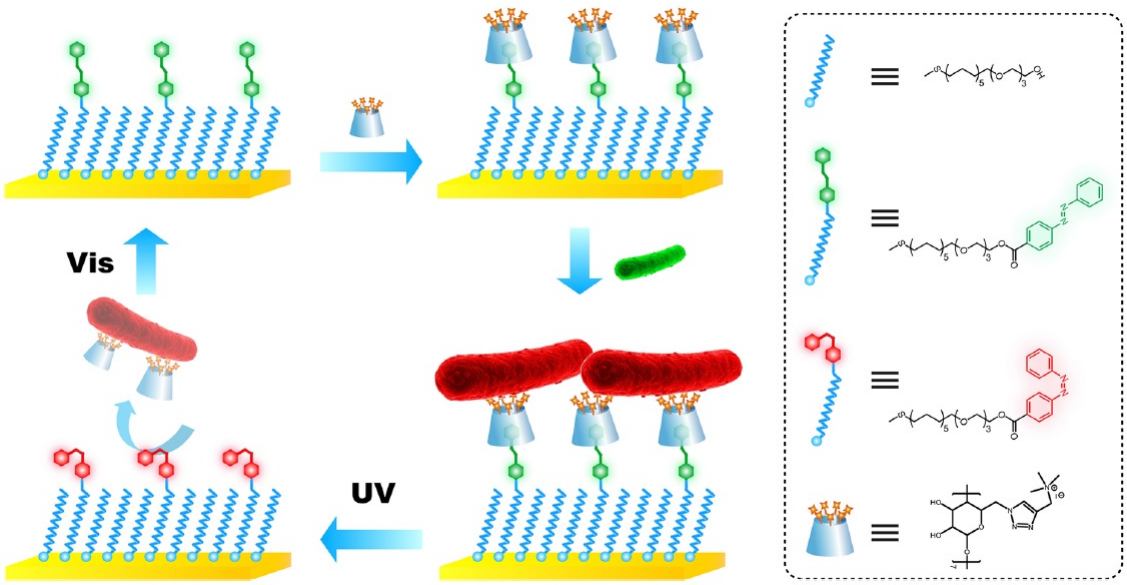

Figure 13: A biocidal photoswitchable surface that can be reused.[71]

been used to capture and release bacteria[74]. The supramolecular platform developed by Wei et al. not only captures and releases bacteria, but also kills the captured bacteria before release, taking advantage of a biocidal β-cyclodextrin (Figure 13).[71] This cyclodextrin contains seven units of a quaternary ammonium salt (potent and commonly used cationic antimicrobial agent), that have been covalently attached to the glucopyranose units of β-cyclodextrin-N_3 *via* CuAAC.[75,76] After preparation of an azobenzene-containing gold surface, the biocidal β-cyclodextrin was incorporated on this surface exploiting the azobenzene-cyclodextrin host-guest interaction. Upon attachment of the bacteria to the biocidal surface, the Ca^{2+} and Mg^{2+} in the bacterial cytoplasmic membrane are replaced by the quaternary ammonium salts, destabilizing its intracellular matrix and leading to cell death. Using UV light, the azobenzene will be isomerized to *cis*, the host-guest interaction will be destabilized and the cyclodextrin will be release together with the dead bacteria, regenerating a surface that can once again be reused.[71,76]

Azobenzene light-responsive surfaces can be used for other biological applications besides the control of cell adhesion. For example, the control of the activity of enzymes is also possible. Person et al. have developed a reversible photocontrolable platform that controls the activity of α-chymotrypsin, a member of the protease family. This platform was decorated with a phenylalanine-based trifluoromethylketone capable of inhibiting the activity of the enzyme

Die approbierte gedruckte Originalversion dieser Dissertation ist an der TU Wien Bibliothek verfügbar.
The approved original version of this doctoral thesis is available in print at TU Wien Bibliothek.
TU Bibliothek Your knowledge hub WIEN

(Figure 14A). When the azobenzene is on the *trans* configuration the enzyme has a reduced affinity to the platform but upon irradiation with UV light it increases almost 2 fold (Figure 14B). If the surface is irradiated with visible light the affinity is once again decreased.[77,78]

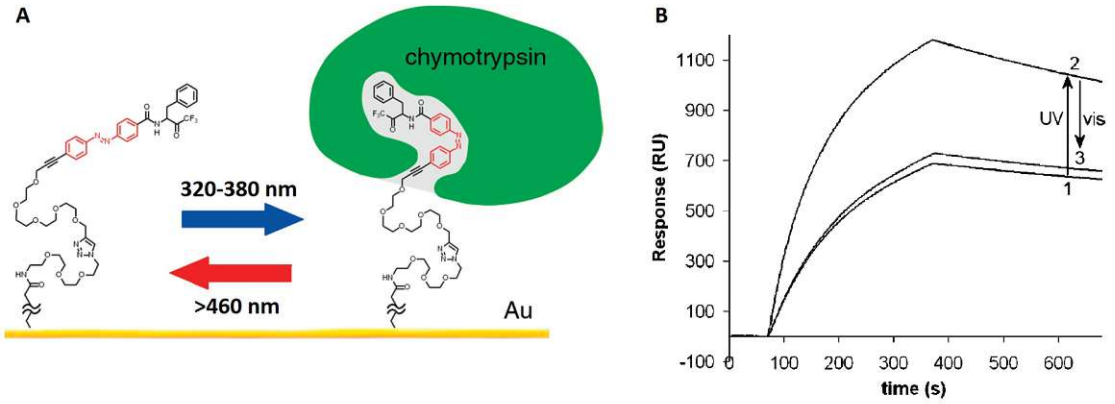

Figure 14: **(A)** Photoreversible inhibition of α-chymotrypsin using an azobenzene coated gold surface.**(B)** Surface plasmon resonance response of the surface before irradiation (1), after irradiation with UV (2) and after irradiation with visible light (3).[77]

The activity of enzymes has also been controlled with systems using cyclodextrin. Wan et al. have reported a platform to control the activity of glucose oxidase, which catalyzes the conversion of glucose to gluconic acid (Figure 15). Normally, glucose oxidase uses flavin adenine dinucleotide (FAD) as a cofactor that works as an electron acceptor. Nevertheless, Wan et al. have taken advantage of ferrocene that can act as an electron acceptor and is capable of forming an inclusion complex with cyclodextrin. In the first place an azobenzene containing self assembled monolayer was prepared and used to attach on the platform polymer grafted β-cyclodextrins. The free cyclodextrins were used for the second host-guest interaction with ferrocene, which can work as an electron acceptor. When the azobenzene is in the *trans* form, the cyclodextrin and ferrocene stay on the platform and catalysis takes place. However, after irradiation with UV light, the cyclodextrin/ferrocene is expelled from the surface and the reaction does not happen any longer.[79]

Die approbierte gedruckte Originalversion dieser Dissertation ist an der TU Wien Bibliothek verfügbar.
The approved original version of this doctoral thesis is available in print at TU Wien Bibliothek.

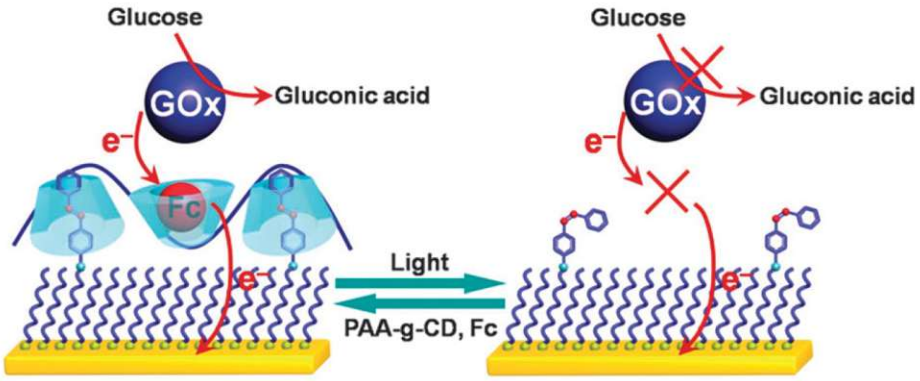

Figure 15: Photoswitchable bioelectrocatalysis of glucose.[79]

Azobenzene smart light-responsive surfaces seem to be actually quite versatile for biological applications. Other examples include photoresponsive surfaces to control DNA hybridization[80] and peptide-RNA interaction[81], to catch and release porphyrin[82], to separate naproxen (nonsteroidal anti-inflammatory drug) enantiomers[83], to reversible immobilize virus particles[84] and to produce surfaces that switch between anticoagulant and hemostatic.[85]

Another interesting property of azobenzenes is the difference in the polarity of both isomers. The *trans* isomer presents a dipole moment of $\sim$0 D while the *cis* isomer of $\sim$3 D.[25] This means that once an azobenzene is immobilized the polarity of the surface changes with light and, as a consequence, the switching of an azobenzene on a surface can be followed by simply placing a drop of water on the surface. Figure 16 presents an example of a glass surface coated with an azobenzene-RGD peptide. After irradiation with UV light the water contact angle (WCA) of the surface decreases from approximately 82° to 74° due to the higher polarity of the *cis* isomer. Over time the angle increases to 81° thanks to the back-switch to *trans* via thermal relaxation.[67]

The difference in the WCA between the *trans* and *cis* isomer is highly dependent on the hydrophobicity/hydrophilicity of the group on top of the azobenzene. If the azobenzene contains on top a hydrophobic group such as a CF_3 this difference is increased since the more apolar *trans* isomer becomes even more apolar. However this difference is still normally less than 10°.[86] Increasing this difference would be convenient for two reasons. In the first place

Die approbierte gedruckte Originalversion dieser Dissertation ist an der TU Wien Bibliothek verfügbar.
The approved original version of this doctoral thesis is available in print at TU Wien Bibliothek.
TU Bibliothek Your knowledge hub WIEN

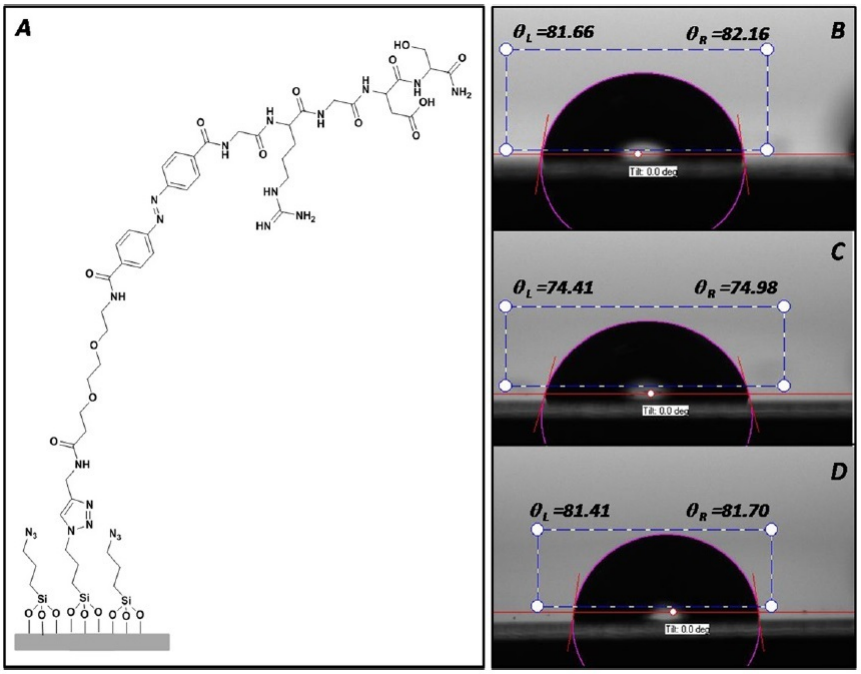

Figure 16: Tracking of azobenzene photoswitching on a surface by water contact angle measurements. **(A)** Glass surface coated with an azobenzene-RGD peptide. **(B)** WCA before irradiation. **(C)** WCA after irradiation with UV light and **(D)** WCA after 3 days on the dark.[67]

the larger the difference the better the read-out of the switching of the azobenzene. Small differences of 1° or 2° would probably lead to doubts if the azobenzene has indeed switched or if that value is simply the error of the measurement. In the second place a bigger difference would make azobenzene light-responsive surfaces potentially applicable in the development of smart self-cleaning material or microfluid devices, for example.[87]

A higher difference in the water contact angle (ΔWCA) can be achieved when the morphology of the surface is changed from flat to rough (non-flat). To understand how roughness influences the WCA, lets look at the models presented in Figure 17 that describe surface wetting. While the wetting on a flat surface is described by the Young model that states that the angle depends on the liquid surface tension (γ_{LS}), solid surface tension (γ_{SV}) and liquid-solid tension (γ_{SL}) (Figure17A), the Cassie-Baxter (Figure17B) and the Wenzel (Figure17C) models are normally used to describe the wetting on a rough surface. In the Cassie-Baxter state air pockets are formed between the surface and the drop, therefore the Cassie-Baxter angle (θ_{CB}) depends on the solid-area fraction (the solid area in contact with the drop) and is always higher

Die approbierte gedruckte Originalversion dieser Dissertation ist an der TU Wien Bibliothek verfügbar.
The approved original version of this doctoral thesis is available in print at TU Wien Bibliothek.
TU Bibliothek Your knowledge hub WIEN

than the angle on a flat surface (θ).[88] The Wenzel model describes a system where the drop penetrates trough the pores and no air pockets are formed. This means that the Wenzel angle (θ_W) depends on the surface roughness and it can be higher or lower than the angle on a flat surface. If the angle on the flat surface is higher than 90° θ_W will be even higher, if lower than 90° θ_W will be even lower and if equal to 90° θ_W will be equal.[89]

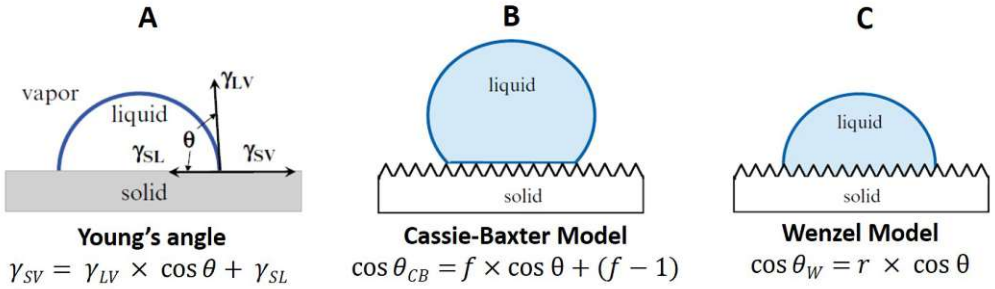

Figure 17: (A) The Young model to describe the wetting on a flat surface. **(B)** The Cassie-Baxter and the **(C)** Wenzel model that describe the wetting on rough surfaces.[89]

Rough surfaces for an increased ΔWCA can be obtained by either coating a substrate with a rough surface layer or by modifying its morphology (roughening by chemical or mechanical methods).

Azobenzene-containing polymers have been used to coat surfaces and create roughness. In 2006, Lim et al. created a multilayer film that switches from superhydrophobic to superhydrophilic, by coating a flat surface with several layers of a polyelectrolyte followed by chemisorption of a photoswitchable azobenzene layer. Figure 18A shows that the ΔWCA between *trans* and *cis* increases with the number of deposited layers of polymer. While in the flat surface the ΔWCA is about 5°, after 9 deposition cycles a ΔWCA of 147° is reached. The increase of the ΔWCA with the number of polymer layers is explained by the increase of the surface roughness and nanoporosity. Figure 18B shows that several irradiation cycles between *trans* and *cis* are possible for these surfaces.[86]

Gao et al.[90] and Chen et al.[91] relied on the assembly of the azobenzene-containing polymers to respectively generate nanofibers and nanogrooves that led to surfaces with an increased ΔWCA. CF_3Azobenzene- containing nanoparticles have also been sprayed on surfaces aiming to create photoswitchable rough surfaces.[92]

Die approbierte gedruckte Originalversion dieser Dissertation ist an der TU Wien Bibliothek verfügbar.
The approved original version of this doctoral thesis is available in print at TU Wien Bibliothek.
TU Bibliothek Your knowledge hub WIEN

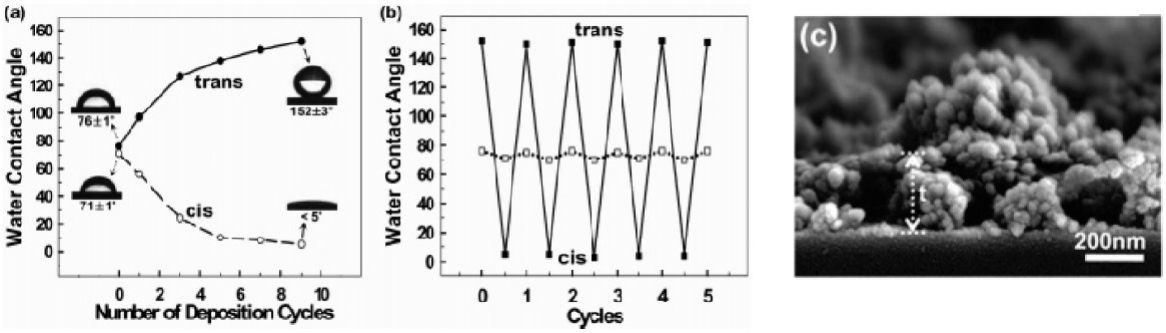

Figure 18: (A) The difference of the WCA between *trans* and *cis* increases with the number of polymer layers. **(B)** Photoreversible switching between *trans* and *cis* for 5 irradiation cycles on the flat surface (non-colored marker) and surface with 9 layers of polymer (black-colored marker). **(C)** Cross-section view of the surface coated with 9 layers of polymer. The thickness of the film is approximately 250 nm.[86]

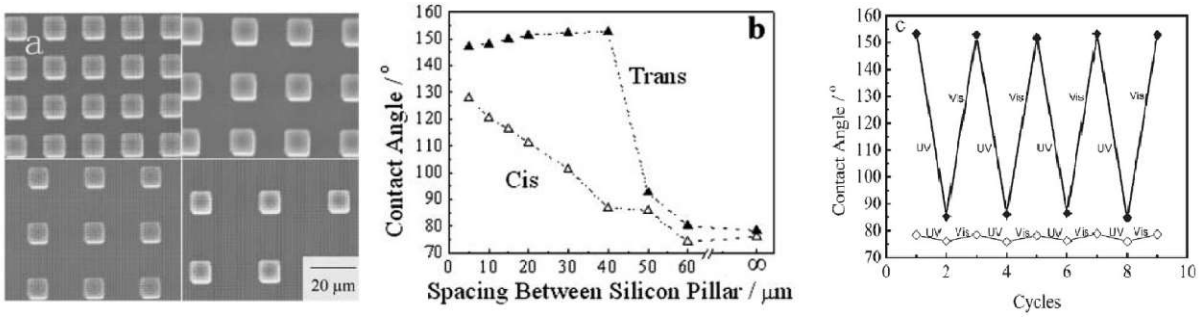

Figure 19: (A) Scanning microscope images of the silicon substrates with pillars spaced by 5, 10, 15 and 20 µm. **(B)** Relation between the spacing of the pillars and the ΔWCA. **(C)** Photoreversible switching between *trans* and *cis* for 10 irradiation cycles on the flat surface (non-colored marker) and surface with 40 µm spacing between the pillars (black-colored marker).[93]

Regarding the direct creation of roughness on the substrate, Bian et al.[68] and Jiang et al.[93] have used photolithography to prepare micro-patterned silicon that was later coated with one layer of a CF_3azobenzene-containing polymer *via* electrostatic assembly, generating surfaces with an increased ΔWCA. Figure 19 shows the results obtained by Bian et al. They reported that the ΔWCA strongly depends on the distance between the pillars in the substrate. From 5 till 40 µm there is a remarkable increase in the ΔWCA from 19° to 66° provoked by a superhydrophobic *trans* state and an increasingly hydrophilic *cis* state. After 40 µm the ΔWCA decreases sharply due to collapse of the *trans* state. As expected the photoswitching on these surfaces was also reversible (Figure 19C).[68]

Die approbierte gedruckte Originalversion dieser Dissertation ist an der TU Wien Bibliothek verfügbar.
The approved original version of this doctoral thesis is available in print at TU Wien Bibliothek.
TU Bibliothek Your knowledge hub WIEN

Figure 20 shows a photoswitchable filter paper surface. Jin et al. have coated this naturally rough substrate with a titania/azobenzene film to generate a surface that switches between superhydrophobic and superhydrophilic.[94]

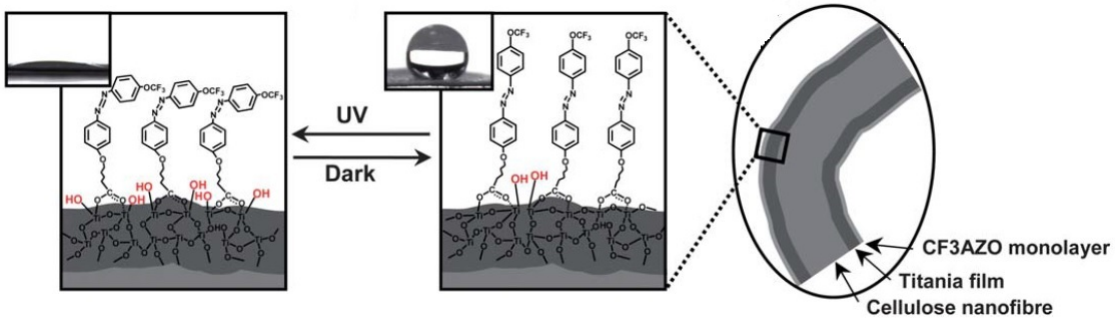

Figure 20: Filter paper coated with a titania/azobenzene monolayer.[94]

Die approbierte gedruckte Originalversion dieser Dissertation ist an der TU Wien Bibliothek verfügbar.
The approved original version of this doctoral thesis is available in print at TU Wien Bibliothek.

B.3 Click chemistry

The term "click chemistry" was firstly introduced in 2001 by K. Barry Sharpless to describe reactions with a high yield and selectivity, wide scope and simple reaction conditions.[95] Some reactions that fit these criteria such as the copper-catalyzed alkyne-azide cycloaddition (CuAAC), strain-promoted alkyne-azide cycloaddition (SPAAC), tetrazine ligation and the thiol-Michael addition are presented in Figure 21. Ever since the term click chemistry was introduced, this practical and convenient approach has been frequently applied in fields such as bioconjugation, material science and drug discovery.[96]

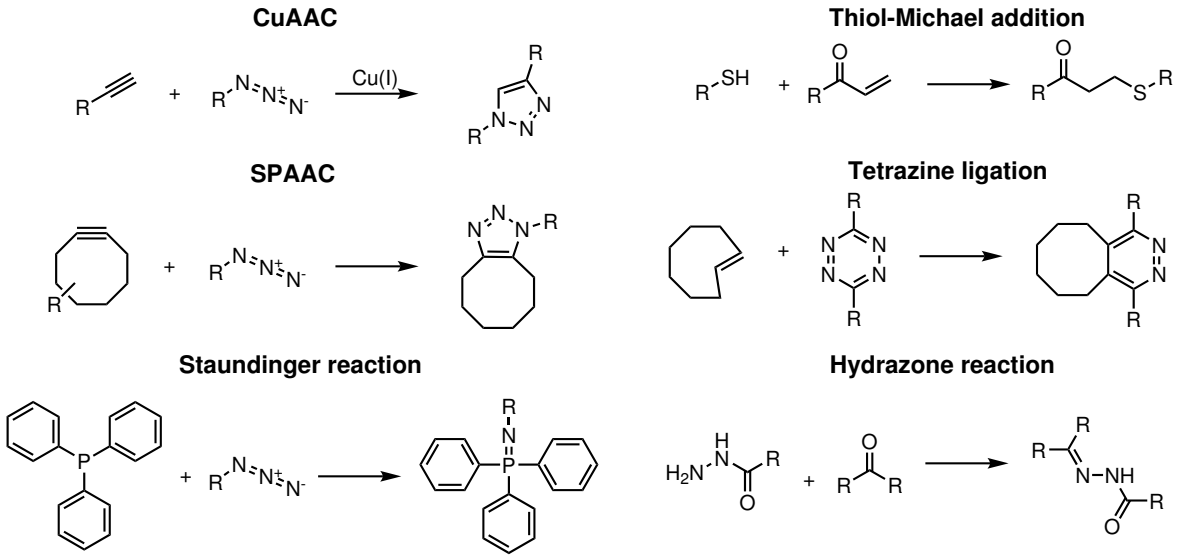

Figure 21: Examples of reactions that fit the definition of a click reaction.

The Huisgen 1,3-dipolar cycloaddition between alkynes and azides, first reported in 1960 by Huisgen,[97] is probably one of the most practical examples of a click reaction. Not only are alkynes and azides easily synthetically accessible starting materials, but also stable and tolerant to several functional groups and reaction conditions.[96] The big breakthrough in these reaction took place when it was discovered that copper(I) dramatically accelerates this reaction and removes the needs of elevated temperatures for the reaction. Furthermore, the use of copper(I) also circumvents the regiospecificity problem of this reaction affording only the 1,4-disubstituted 1,2,3-triazole (without copper the 1,5 can also be formed).[98,99] The mechanism of this copper-catalyzed alkyne-azide cycloaddition reaction is presented in Figure 22. In the

Die approbierte gedruckte Originalversion dieser Dissertation ist an der TU Wien Bibliothek verfügbar.
The approved original version of this doctoral thesis is available in print at TU Wien Bibliothek.

first place there is the formation of the copper(I) acetylide **I**. Density functional theory calculations indicate that a concerned [2+3] cycloaddition (B-direct) is disfavored and that a step-wise annealing process takes place. The annealing sequence starts with the binding of the azide to the copper(I) acetyline, followed by the formation of the copper(III) metallacycle (**III**), ring contraction (**IV**) and protonolysis to afford the desired 1,2,3-triazole.[98,100] Notice that other metals have also been exploited to conduct this reaction such as Ruthenium, Nickel and Palladium, however, none has achieved the same efficiency as the copper catalyzed version.[101] This reaction is also quite versatile and has been applied in polymer chemistry[102,103], drug discovery[104], biochemistry[105,106] and material science[107,108], for example.

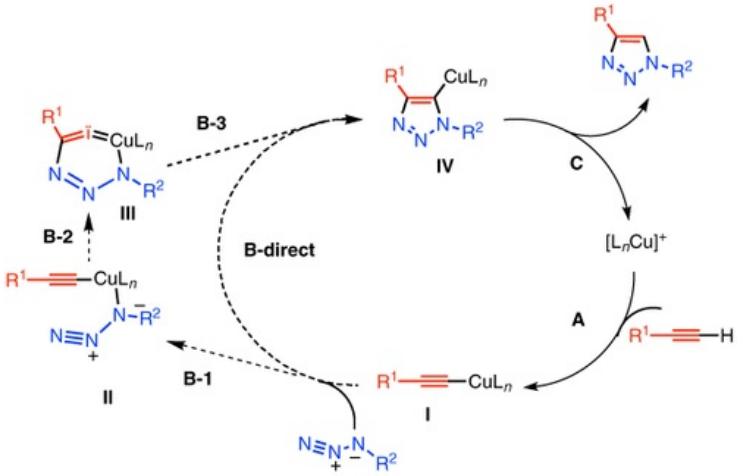

Figure 22: Proposed reaction mechanism of the CuAAC.[98]

Despite the versatility, selectivity, compatibility with water and the speed of the CuAAC its applicability in biological conditions is limited since copper is toxic for both mammalian and bacterial cells, even at low concentrations.[109] Not only is the normal function of these cells compromised, but copper may also induce the degradation of oligonucleotides and polysaccharides.[110,111] This problem raised the need for the development of click reactions that could proceed without the need of a metal catalyst and are compatible with biological systems, now known as bioorthogonal reactions.[112]

The Staudinger ligation, first reported in 1919 by Staudinger and Mayer, was probably the first reaction considered bioorthogonal.[113,114] Figure 23 presents the reaction mechanism of this reaction. The triaryl phosphane **1** and the azide **2** react to form the phosphazide **4**,

Die approbierte gedruckte Originalversion dieser Dissertation ist an der TU Wien Bibliothek verfügbar.
The approved original version of this doctoral thesis is available in print at TU Wien Bibliothek.
TU Bibliothek Your knowledge hub WIEN

which will decompose by loss of nitrogen, forming iminophosphorane **3**. It is supposed that the loss of nitrogen proceeds via the formation of the 4-membered-ring transition state **5**.[115,116] The biocompatibilty of this reaction led to a panoply of applications such as modification of cell surfaces,[117,118] labeling of nucleic acids[119] and protein engineering[120]. Nevertheless, the phosphines are easily oxidized and the reaction kinetics are rather slow.[121] Even though increasing the electron density of the phosphine substituents leads to higher reaction rates the propensity to oxidation also increases.[122]

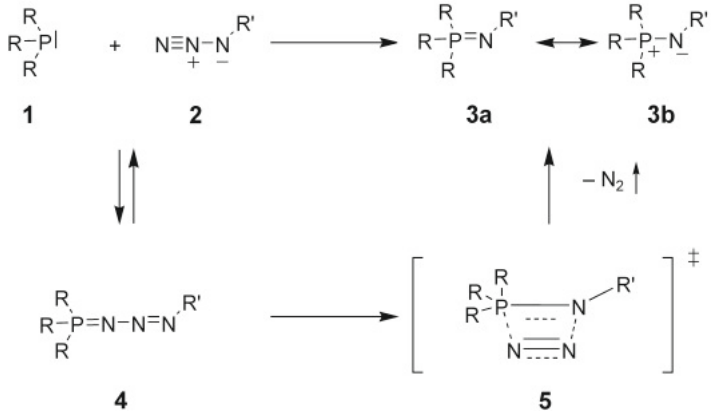

Figure 23: Proposed reaction mechanism of the Staudinger ligation.[115]

Inspired by the findings of Wittig in 1961 that cyclooctyne and phenyl azide react fast at room temperature generating only one product[123], Bertozzi and coworkers developed another click reaction, the strain-promoted alkyne-azide cycloaddition (SPAAC).[124] This reaction takes advantage of the ring strain of the cyclooctyne, that destabilizes its ground state and reduces the activation barrier energy required for the reaction. This allows to obtain a 1,2,3-triazole without the need for a catalyst, via the 1,3-dipolar cycloaddition between the strained alkyne and the azide (Figure 24).[124,125] However, in comparison with the CuAAC this reaction presents a rather slower kinetics (10–100 $M^{-1}s^{-1}$ with 20 µM of Cu(I) vs 1-60 $M^{-1}s^{-1}$).[113,121] The strained-alkyne can also be "clicked" with a nitrone (strain-promoted alkyne nitrone cycloaddition - SPANC) to achieve higher kinetics but these are still not comparable with the CuAAC.[111,121]

The introduction of the tetrazine ligation by Devaraj et al.[126] and Blackman et al.[127] represented a milestone regarding reaction kinetics of click reactions, since it can be up to 10 000-

Die approbierte gedruckte Originalversion dieser Dissertation ist an der TU Wien Bibliothek verfügbar.
The approved original version of this doctoral thesis is available in print at TU Wien Bibliothek.

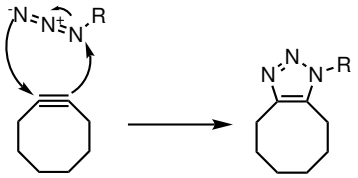

Figure 24: Strain-promoted alkyne-azide cycloaddition, a 1,3-dipolar cycloaddition between a strained alkyne and a azide.

fold faster than the CuAAC.[121] This reaction between 1,2,4,5-tetrazines and olefins is based on the inverse electron demand Diels-Alder (iEDDA) and Figure 25 presents its reaction mechanism. Unlike the normal electron demand Diels-Alder where an electron-rich diene reacts with a electron-poor dienophile, in the iEDDA the opposite takes place. The [4+2] cycloaddition takes place between the electron-rich tetrazine diene and the electron-poor olefin dienophile generating the highly strained bicyclic adduct **2** (rate determining step). This is converted to the 4,5-dihydropyridazine **3** via *retro*-Diels-Alder with release of nitrogen, that latter is isomerized to the 1,4-dihydropyridazine **4**. 1,4-dihydropyridazines can be quite stable, depending on the used olefin, therefore the oxidation step to afford the pyridazine **5** can be rather slow. When it is important that the obtained product is in the oxidized form, oxidation agents such as isoamyl nitrite or hydrogen peroxide can be used to push oxidation.[127,128] Several olefins have been tested as dienophiles for the iEDDA and so far *trans*-cyclooctene (TCO) derivatives have show to be the most reactive, therefore, the tetrazine ligation is normally performed between a tetrazine and a *trans*-cyclooctene.[128]

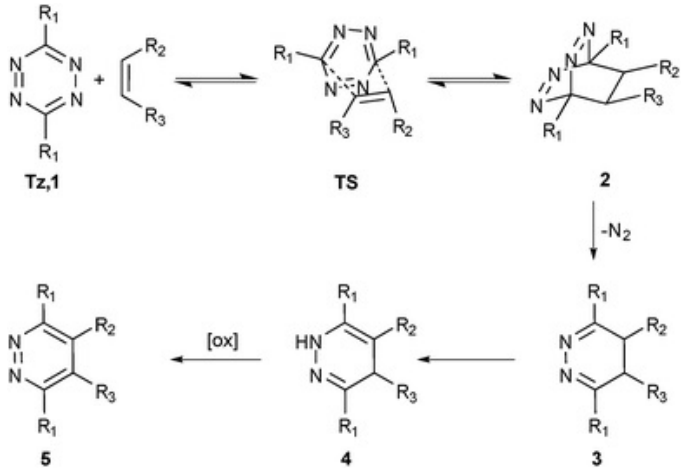

Figure 25: Proposed mechanism for the tetrazine ligation, an iEDDA between tetrazines and olefins.[128]

Die approbierte gedruckte Originalversion dieser Dissertation ist an der TU Wien Bibliothek verfügbar.
The approved original version of this doctoral thesis is available in print at TU Wien Bibliothek.
TU Bibliothek Your knowledge hub WIEN

Ever since the SPAAC and the tetrazine ligation have shown their potential as viable bioorthogonal reactions several *in vivo*, *ex vivo* and *in vitro* applications have been developed[113], for example to image tubulin,[129] drug targets,[130,131] glycans in the brain,[132] tumor vascular endothelial growth factor receptor 2,[133] to analyze microvesicles from the blood of glioblastomas patients[134] and to bind nucleotides in the CRIPSR-Cas9 system.[135]

The previously presented click reactions display remarkable properties. Notwithstanding neither alkynes, azides, TCO or tetrazine can be found in biological molecules, such as proteins or DNA. This means that when the labeling of one of these biomolecules is required, these groups need to be specially introduced.[136] Since thiols are found in cystein-containing protein, the thiol-Michael additions has been exploited to circumvent this obstacle. In the thiol-Michel addition the thiol (Michael donor) reacts normally with a α,β-unsaturated carbonyl (Michael acceptor), under basic catalysis (Figure 26). Since the difference in pKa of thiols and water is large, the thiol-michael addition proceeds in water.[137] Besides the functionalization of proteins,[138,139] the thiol-Michael addition has found a wide range of application in polymer and material chemistry.[136,140,141]

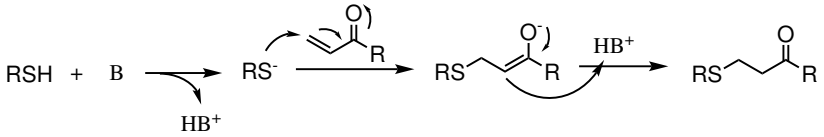

Figure 26: Base-catalyzed mechanism of the thiol-Michael addition .[142]

Die approbierte gedruckte Originalversion dieser Dissertation ist an der TU Wien Bibliothek verfügbar.
The approved original version of this doctoral thesis is available in print at TU Wien Bibliothek.

B.4 Project overview

The field of photopharmacology has been growing at a tremendous rate in the last decades due to its potential in the development of prodrugs,[44] the restoration of vision,[61,143] the study of biological mechanisms by contact-less switchability(e.g. synapses)[8] and the development of photoswitchable surfaces that mimic biological processes.[62]

When aiming to functionalize a biomolecule with a photoswitch for such an application, the traditional approach consists in structure analysis and identification of possible groups for functionalization (without compromising its biological activity). Once this task has been accomplished, the design and synthesis of a suitable photoswitch can start.[45] Here the choice of adequate functional groups to enable an easy and reliable binding to the biomolecule is crucial.[2] Click chemistry has shown a tremendous potential with regards to reaction efficiency, practicality, simplicity and scope, making this group of reactions an ideal choice for the such a task.[96] Additionally, nowadays several important biomolecules already functionalized with click moieties can be found in the catalogs of chemical companies.

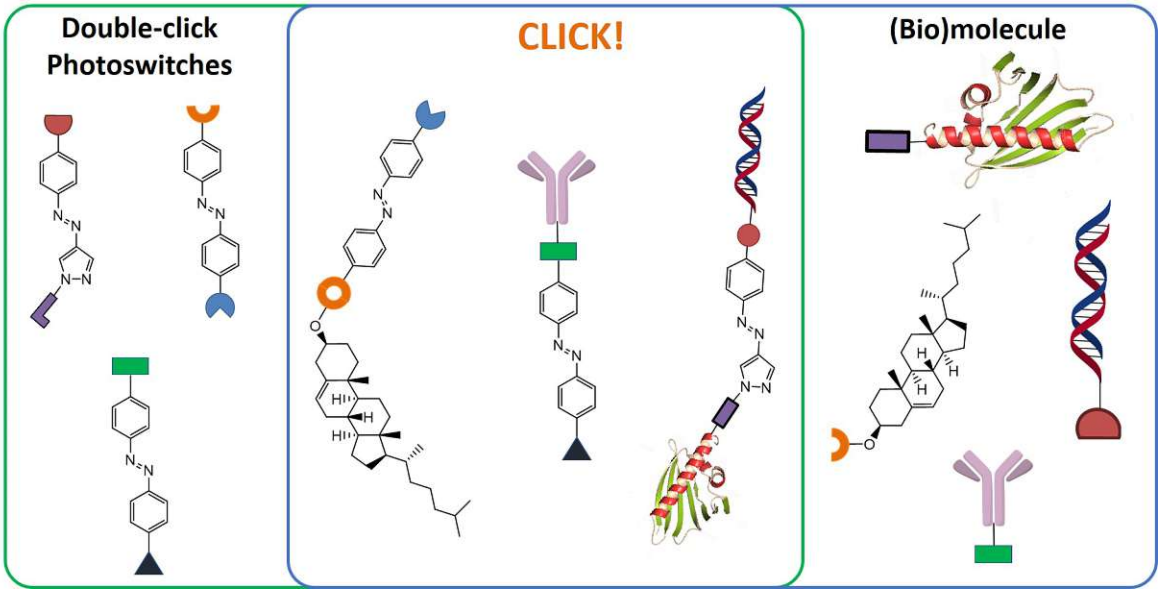

Figure 27: Double-click azobenzenes as an easy approach to selectively functionalize (bio)molecules.

The aim of this project is to enable a more efficient and faster development of photopharmacological applications by providing a library of photoswitches that not only contain func-

Die approbierte gedruckte Originalversion dieser Dissertation ist an der TU Wien Bibliothek verfügbar.
The approved original version of this doctoral thesis is available in print at TU Wien Bibliothek.
TU Bibliothek Your knowledge hub WIEN

tional groups for a convenient/reliable binding to the desired target biomolecule, but also desirable photophysical behavior (photoswitching velocity, absorption wavelength and $t_{1/2}$). For this purpose several types of photoswitches with different click chemistry moieties should be synthesized. To widen the applicability of this approach, each one of these photoswitches should incorporate two different, orthogonal click chemistry moieties to enable the binding of two different entities, when required, e.g. two different biomolecules or even one biomolecule and a surface. This approach is schematized in (Figure 27) and we have named these molecules double-click photoswitches.

Die approbierte gedruckte Originalversion dieser Dissertation ist an der TU Wien Bibliothek verfügbar.
The approved original version of this doctoral thesis is available in print at TU Wien Bibliothek.
TU Bibliothek Your knowledge hub WIEN

B.5 Objective

In this thesis we wish to take the first steps towards the creation of the previously stated library. Thanks to all the advantages of azobenzenes as photoswitches (high isomerization yields, fast photoswitching and optical fatigue resistence), we will focus on the synthesis of double-click azobenzenes. Azobenzenes containing different and orthogonal click moieties such as TCOs, alkynes, strained alkynes and thiols will be synthesized and their photophysical properties will be studied. Additionally, the obtained double-click azobenzenes will be clicked with simple model molecules to test how the photophysical properties of these compounds might chance upon conjugation with a target biomolecule.

In the context of this thesis, these molecules will be applied in the functionalization of surfaces, aiming to obtain a photoswitchble platform for the immobilization of biomolecules. On the way to reach this goal, we aim to also provide solutions for two basic problems related with the preparation of photoswitchable surfaces: surface overcrowding and a small difference in the WCA between the *trans* and *cis* surface. Regarding the former problem, surface overcrowding, we propose to attempt the immobilization of the azobenzene while in the *cis* configuration. To address the later, we propose to test the immobilization of the azobenzenes on rough surfaces with difference morphologies and analyse the difference in WCA upon isomerization.

Finally, we will contribute for the development of a photoswitchable DNA origami platform as a prototype application of the methods worked out within this thesis for the study of T-cell activation - a crucial process in our adaptive immune response. More precisely, our goal is to conjugate one of the synthesized double-click azobenzenes to biotin, a motif required for binding of an azobenzene to the DNA origami platform. After conjugation, the ability of the azobenzene-biotin conjugate to bind to strepavidin will be tested in solution.

Die approbierte gedruckte Originalversion dieser Dissertation ist an der TU Wien Bibliothek verfügbar.
The approved original version of this doctoral thesis is available in print at TU Wien Bibliothek.
TU Bibliothek Your knowledge hub WIEN

Die approbierte gedruckte Originalversion dieser Dissertation ist an der TU Wien Bibliothek verfügbar.
The approved original version of this doctoral thesis is available in print at TU Wien Bibliothek.

Chapter C

Results and discussion

C.1 Synthesis of double-click azobenzenes

In this chapter, we present the synthesis of several azobenzenes substituted in *para* position with different known click chemistry moieties, such as a *trans*-cyclooctene (TCO) for tetrazine ligation, alkyne for CuAAC, thiol for the thiol-Michael addition and a strained cyclic ring-containing alkyne for SPAAC. Furthermore, the photoswithing and the thermal half-life time of these azobenzenes was studied. In later chapters, possible applications of these molecules will be explored.

C.1.1 CuAAC-tetrazine ligation

In our first design we have aimed for an azobenzene containing both an alkyne for the CuAAC and a TCO for tetrazine ligation. In the literature, several TCOs containing a functional groupa for subsequent modification are presented, however, we decided to use TCO **[4]** due to its good balance between a high reaction rate and high stability (Figure 28A).[127,144] To synthesize this compound, the first step is represented by an epoxidation reaction with *meta*-CPBA, followed by reduction of the epoxide with LAH to afford alcohol **[3]**. Finally a photoisomerization is carried out using a flow photoreactor (Figure 28B). In this reactor, starting material **[3]** is exposed to UV light (254 nm) to isomerize from *cis* to *trans*. Afterwards, the reaction mixture passes through a column containing $AgNO_3$ impregnated silica gel. The product will form a

complex with the silver and stay in the column, while the starting material will be continuously pumped through the system untill it is isomerized and stays in the column (Figure 28C). Once the reaction is completed, the silica is washed with aqueous ammonia to release the desired product **[4]**.[144,145] During the reaction two diasteromers are formed, the *minor* axial **[4a]** and *major* equatorial **[4e]**, which were separated by column chromatography

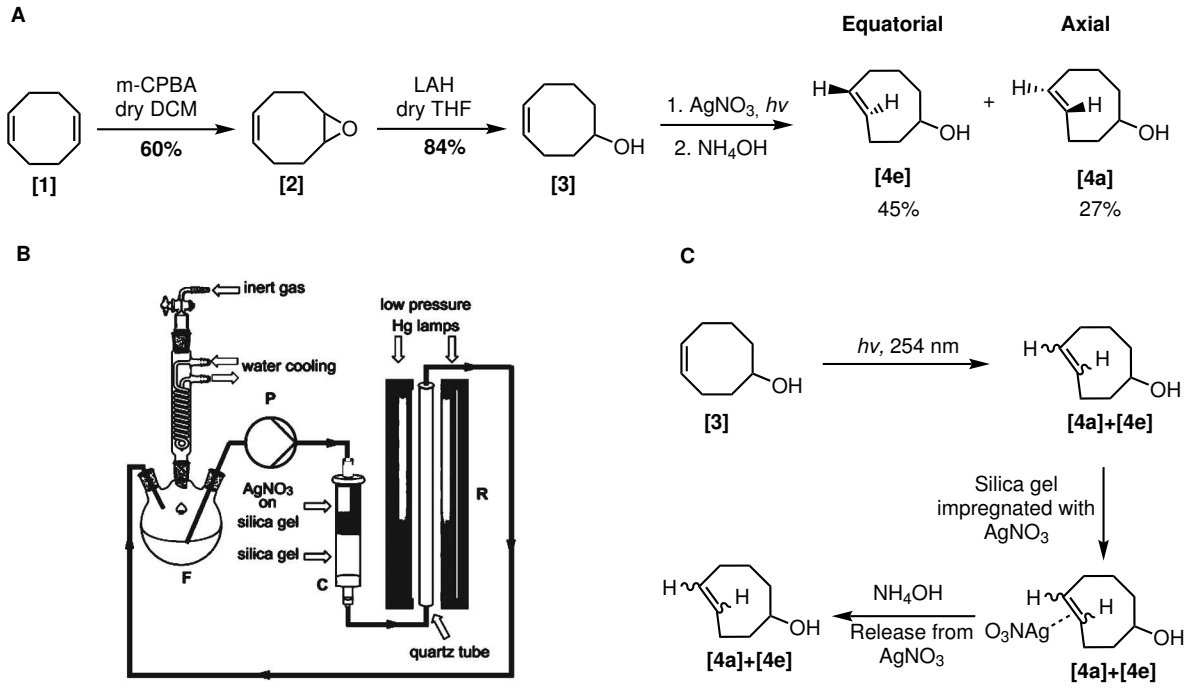

Figure 28: **A**: Synthetic route towards TCO **[4a]** and **[4e]**. **B**: The photochemical apparatus used for the photoisomerization of compound **[3]**. **C**: Clarification of the photoisomerization process.[144,145]

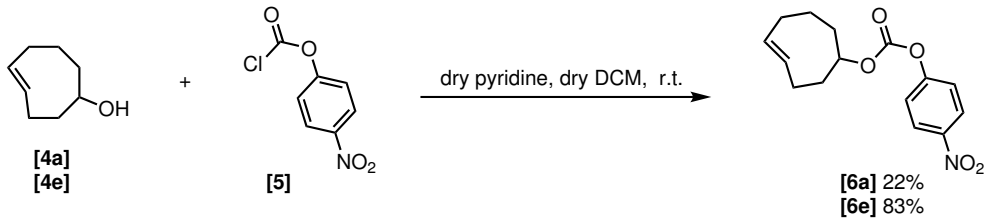

Scheme 1: Activation of TCO **[4a]** and **[4e]** for nucleophilic substitution.

Normally, upon isomerization compounds **[4a]** and **[4e]** are activated in the form of a carbonate to allow further nucleophilic substitution by the molecule of interest.[146,147] We opted to start by following this already known route. In Scheme 1 the activation of the TCO **[4a]** and

Die approbierte gedruckte Originalversion dieser Dissertation ist an der TU Wien Bibliothek verfügbar.
The approved original version of this doctoral thesis is available in print at TU Wien Bibliothek.

[4e] using 4-nitrophenyl-chloroformate is presented.

Compounds **[6a]** and **[6e]** could now be used as reactive intermediates for the generation of azobenzenes containing a phenol attachment moiety. The synthesis of such azobenzene is presented in Scheme 2. The first step consisted of an azo coupling reaction between 4-iodoaniline and phenol affording azobenzene **[8]**, with the iodo function to allow the introduction of alkyne for the CuAAC. This alkyne was introduced in protected form as hydroxymethylakyne *via* Sonogashira coupling and deprotection was subsequently conducted by refluxing in NaOH to afford azobenzene **[10]**.[148] Finally, TCO **[6a]** and **[6e]** were coupled affording double-click azobenzenes with an axial TCO **[11a]** and an equatorial TCO **[11e]**.

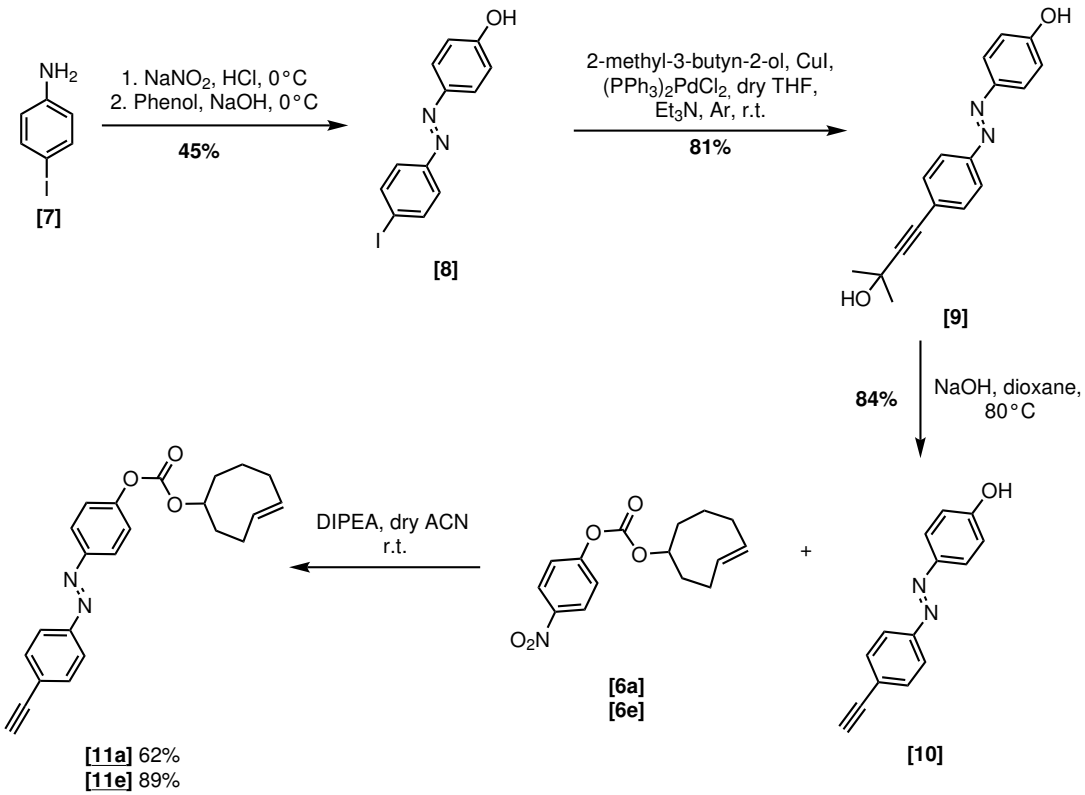

Scheme 2: Synthesis of the double-click azobenzenes **[11a]** and **[11e]**.

Another approach to obtain an azobenzene with a TCO would be *via* a direct esterification between the TCO **[4a]** or **[4e]** and an acid-containing azobenzene. Scheme 3 presents the synthesis of an azobenzene containing an alkyne for the CuAAC and an acid for an esterification with TCO **[4]**. Firstly, methyl 4-nitrosobenzoate **[13]** was prepared by an amine oxida-

Die approbierte gedruckte Originalversion dieser Dissertation ist an der TU Wien Bibliothek verfügbar.
The approved original version of this doctoral thesis is available in print at TU Wien Bibliothek.
TU Bibliothek Your knowledge hub WIEN

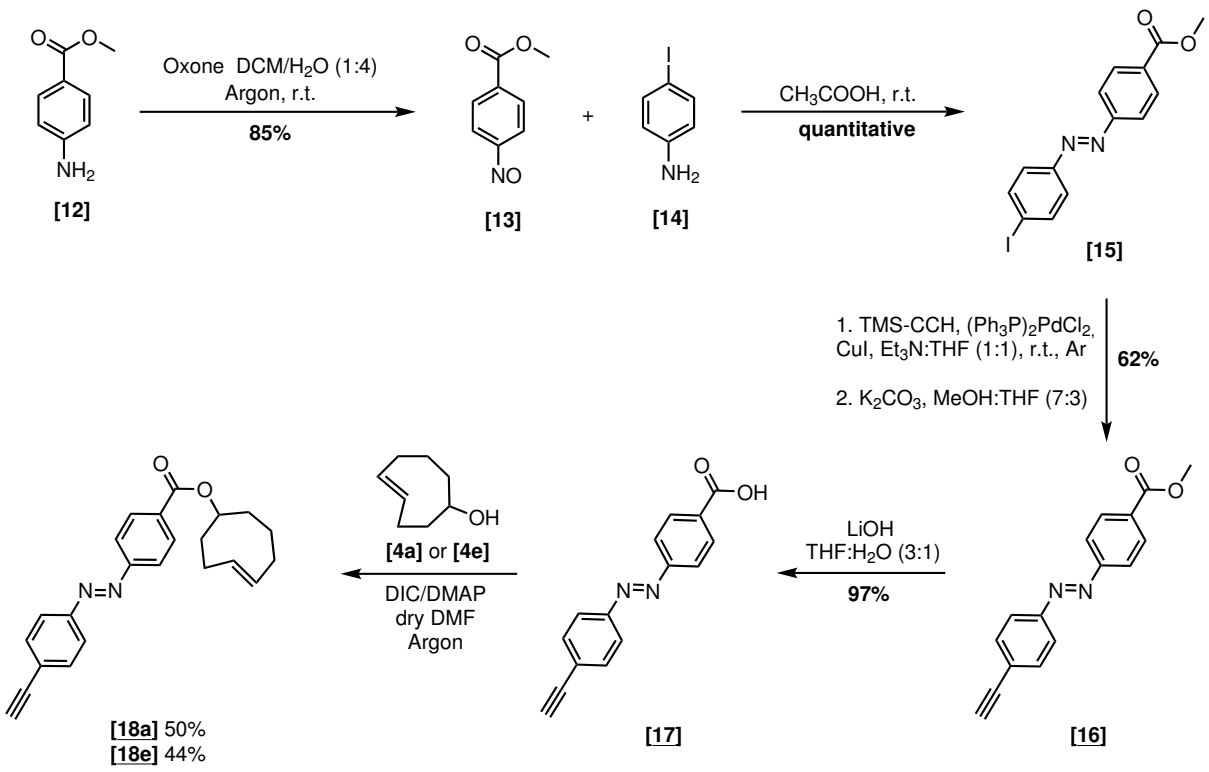

Scheme 3: Synthesis of double-click azobenzenes **[18a]** and **[18e]**.

tion of methyl 4-aminobenzoate **[12]** with Oxone. A Mills reaction between nitroso **[13]** and 4-iodoaniline **[14]** afforded azobenzene **[15]**.[149] The alkyne was introduced in TMS-protected form *via* Sonogashira coupling and immediately deprotected with K_2CO_3, affording compound **[16]**. To obtain the acid containing azobenzene **[17]**, the ester was hydrolyzed with LiOH. Finally, a Steglich esterification using DIC as the acid-activating agent and DMAP as catalyst afforded the desired double-click azobenzenes **[18a]** and **[18e]**.

C.1.2 SPAAC-tetrazine ligation

In biological applications the presence of copper may present a problem. Therefore we also aimed for a double-click azobenzene with two different bioorthogonal clicks: the tetrazine ligation and the SPAAC.

The first step was to choose an appropriate strained-alkyne for the SPAAC. We opted for bicyclo[6.1.0]non-4-yne **[22]** since it presents one of the highest rate constants for SPAAC, a high

Die approbierte gedruckte Originalversion dieser Dissertation ist an der TU Wien Bibliothek verfügbar.
The approved original version of this doctoral thesis is available in print at TU Wien Bibliothek.

stability and the simplest synthetic route among all strained alkynes in the literature.[150] The synthesis is presented in Scheme 4. The first step is a cyclopropanation of 1,5-cyclooctadiene **[1]** with ethyl 2-diazoacetate and rhodium (II) acetate as catalyst, affording the *endo* **[19endo]** and the *exo* product **[19exo]**, which were separated by column chromatography.[151] From here on, the remaining steps of the synthesis were carried out with the *endo* isomer due to its higher reactivity in the SPAAC.[111] A reduction with $LiAlH_4$ of **[19endo]** afforded the alcohol **[20endo]**. The alkyne **[22endo]** was obtained in 2 more steps: bromination of the alkene afforded dibromo coumpound **[21endo]** followed by an elimination with KOtBu. The elimination reaction turned out to be a challenging step. Upon the addition of KOtBu at 0°C, a first intermediate is formed, resulting from the elimination of one bromine (confirmed by ^{1}H NMR). However, for the second elimination, reflux is required and under these conditions, besides product **[22endo]**, the formation of side products was also observed. Additionally, longer reaction times have led to lower yields, indicating that over time **[22endo]** decomposes. After several attempts, the highest reaction yield was 33% after 2 hours under reflux. This challenge seems to be also verified in the literature, where reported yields are not higher than 50%.[152,153] A hypothesis to try to improve this yield in the future might be to perform a two-step elimination, using KOtBu for the first elimination and LDA for the second. This approach avoids the need to reflux and has been previously used in the literature for similar substrates with moderate to high yield.[154–156]

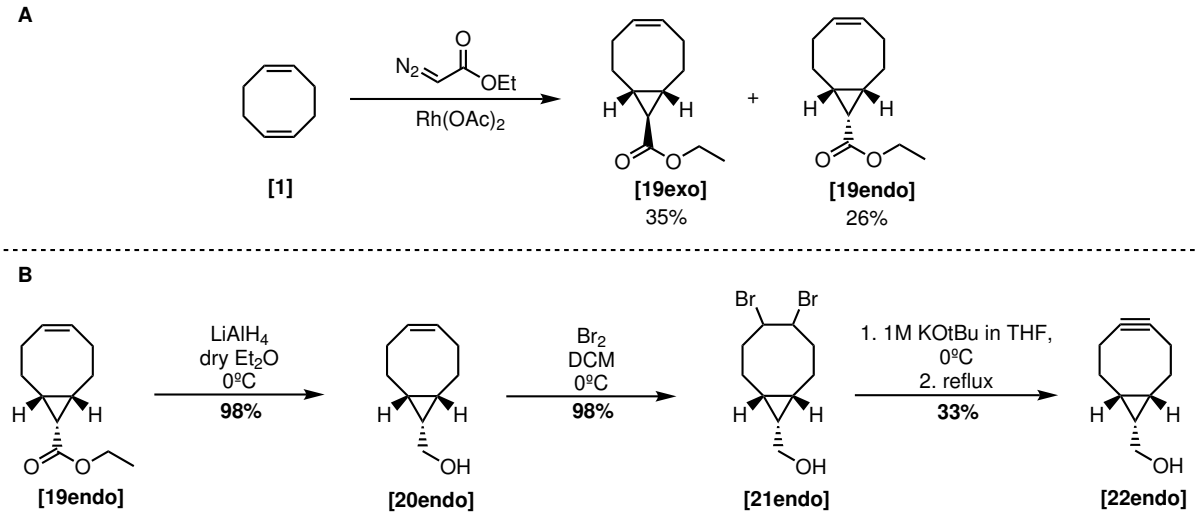

Scheme 4: Synthesis of a strained-alkyne for SPAAC.

Taking advantage of the previously synthesized TCOs (see Section C.1.1), the next step

Die approbierte gedruckte Originalversion dieser Dissertation ist an der TU Wien Bibliothek verfügbar.
The approved original version of this doctoral thesis is available in print at TU Wien Bibliothek.

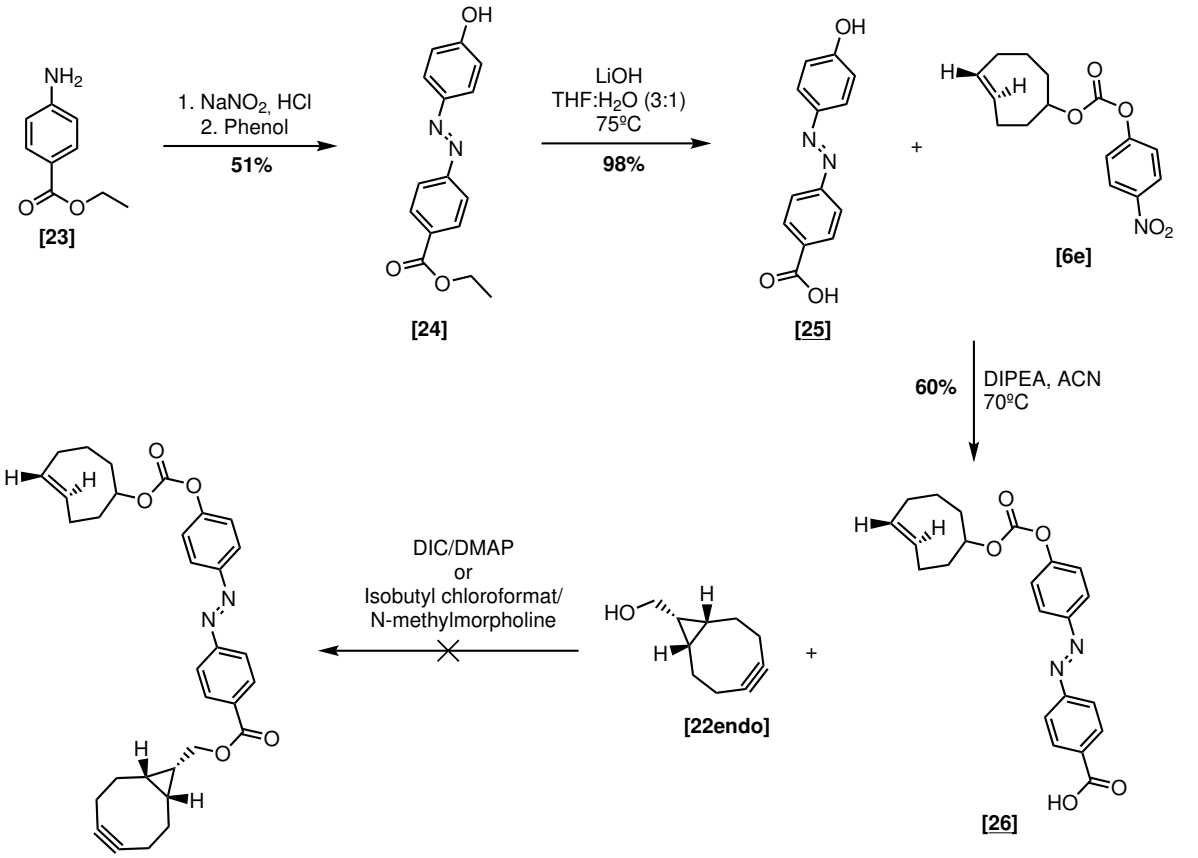

Scheme 5: Synthesis of TCO-containing azobenzene **[26]** and first trial to obtain a double-click SPAAC-tetrazine ligation azobenzene.

would be to assemble an azobenzene containing both **[21endo]** and TCO **[6e]**. Scheme 5 presents a first trial for the synthesis of this azobenzene. Initially, azobenzene **[24]** was synthesized *via* an azo coupling reaction between phenol and ethyl 4-aminobenzoate **[23]**.[157,158] Azobenzene **[25]** was obtained by hydrolysis with LiOH at 75°C and afterwards TCO **[6e]** was conjugated with **[25]**. However, the last step, the esterification was not successful.

In the first place, a Steglich esterification using the activating agent DIC and the catalyst DMAP was attempted with no success. Figure 29 shows a HPLC-MS analysis of the reaction. The activation of the azobenzene **[26]** by the DIC reagent takes place, as confirmed by the peak with a retention time of 2.42 minutes with the a $[M+H^+] = 521.2$. However, a peak with the mass $[M+H^+] = 369.15$ at 1.6 minutes is also found, corresponding to activated acid with a cleaved carbonate. Over time the intensity of this peak increases, indicating that the starting material is not stable under these reaction conditions. Furthermore, neither a peak with $[M+H^+] =$

Die approbierte gedruckte Originalversion dieser Dissertation ist an der TU Wien Bibliothek verfügbar.
The approved original version of this doctoral thesis is available in print at TU Wien Bibliothek.
TU Bibliothek Your knowledge hub WIEN

526.6 (the desired product's mass) or [M+H$^+$] = 375.1 (successful esterification but hydrolyzed carbonate) was found, indicating that the esterification is simply not happening under these conditions.

A second approach relying on a mixed anhydride formation was also tested, where isobutyl chloroformate was used as an activating agent. Even though in these conditions the azobenzene starting material seems to be stable and activation occurs, no product formation was detected. Both the activated acid and the alcohol are not consumed. Unfortunately, harsher conditions such as the formation of an acyl chloride cannot be used in this case since the double bond of the TCO is not compatible and would be protonated, destroying the required moiety for the tetrazine ligation.

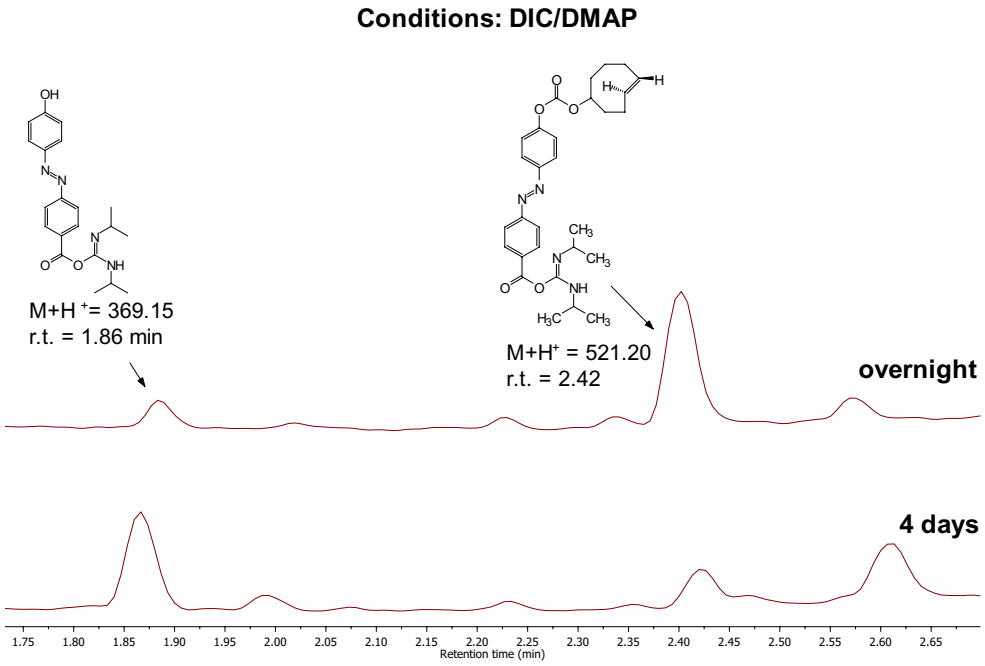

Figure 29: HPLC analysis of the steglich esterification between azobenzene **[26]** and alcohol **[22endo]** using DIC/DMAP.

In the literature it is only possible to find a few examples where bicyclo[6.1.0]non-4-yne **[22]** has been used in a direct esterification with the molecule of interest.[159,160] In these cases, the esterification has taken place with an aliphatic acid, unlike our case where an intrinsically less reactive aromatic acid has been used. Therefore, a similar approach was followed

Die approbierte gedruckte Originalversion dieser Dissertation ist an der TU Wien Bibliothek verfügbar.
The approved original version of this doctoral thesis is available in print at TU Wien Bibliothek.
TU Bibliothek Your knowledge hub WIEN

(Scheme 6). Beta-alanine **[27]** was successfully introduced as an aliphatic spacer in our azobenzene **[26]** *via* the formation of a mixed anhydride with isobutyl chloroformate. We opted for these conditions considering the starting material stability. Once again an esterification with alcohol **[22endo]** *via* mixed anhydride approach was tested, but in vain. HPLC-MS shows that the acid **[28]** is activated, however, as previously, the activated acid and the alcohol **[22endo]** do not react.

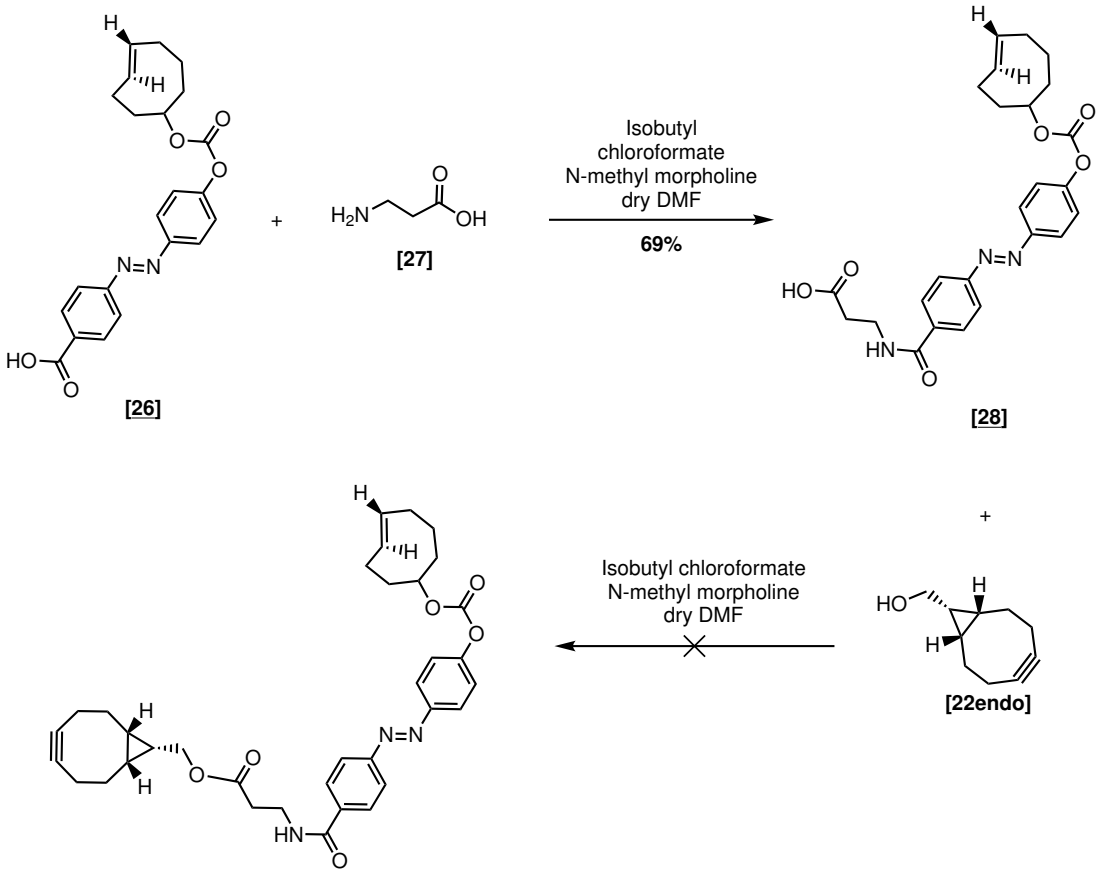

Scheme 6: Second approach to synthesize a double-click SPAAC-tetrazine ligation azobenzene.

Due to the apparent difficulty to further functionalize alcohol **[22endo]**, we opted to use the most common and well established path in the literature. In this path, the alcohol is activated for further nucleophilic substitution as a carbonate *via* condensation with 4-nitrophenyl chloroformate (Scheme 7).[111] Afterwards, ethylenediamine was used as a nucleophile affording compound **[32endo]**, which was used in an amidation with azobenzene **[26]** ultimately leading to the desired double-click azobenzene **[33]**.

Die approbierte gedruckte Originalversion dieser Dissertation ist an der TU Wien Bibliothek verfügbar.
The approved original version of this doctoral thesis is available in print at TU Wien Bibliothek.

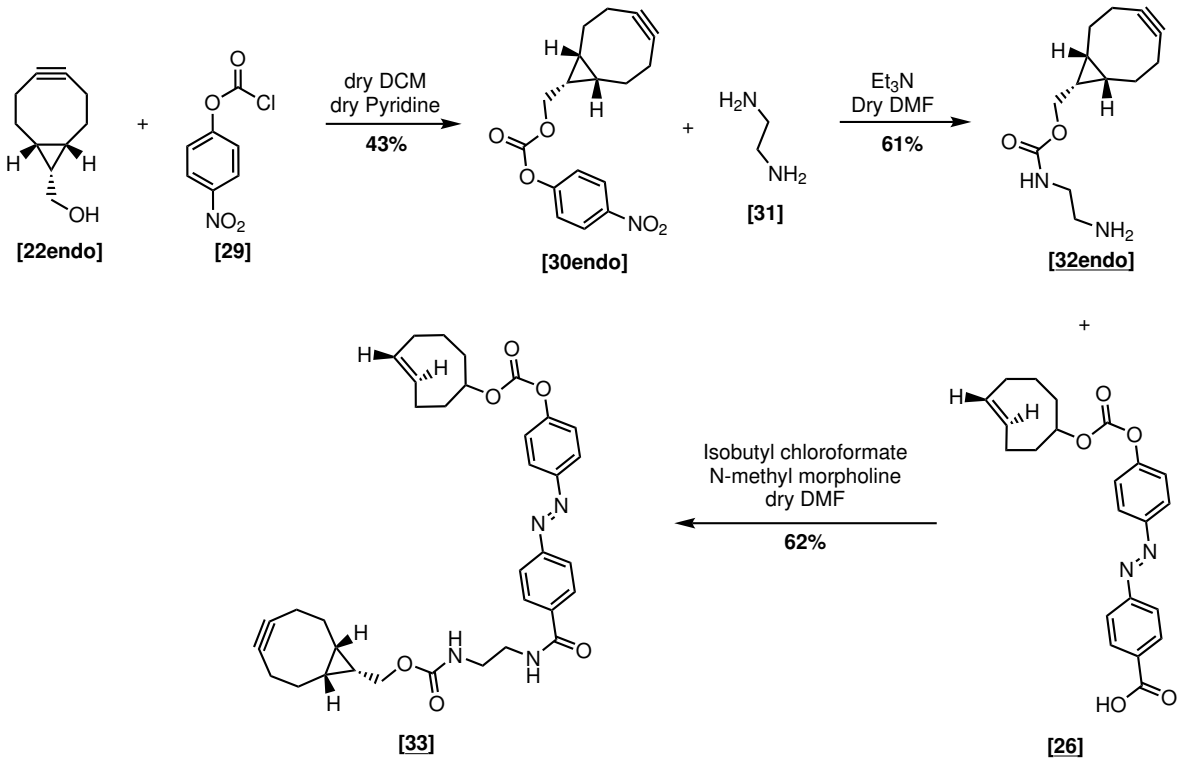

Scheme 7: Successful route towards double-click tetrazine ligation-SPAAC azobenzene.

C.1.3 CuAAC-thiol azobenzene

Another interesting combination of click chemistry is the CuAAC and the thiol/maleimide addition. Since previously we have already synthesized azobenzenes containing an alkyne for the CuAAC, we tried to reuse one of these to reduce the synthetic effort.

Scheme 8 presents the synthesis of this double-click azobenzene. By starting with azobenzene **[10]** it is possible to obtain the thiol in 3 steps.[161] Firstly, a nucleophilic substitution with the azobenzene **[10]** and 1,5-dibromopentane affords azobenzene **[34]**. In the next step, alkylthiosulfate **[35]** is formed by nucleophilic displacement of the bromine. Finally, aqueous HCl hydrolysis alkylthiosulfate **[35]** and the thiol **[36]** is obtained.The yield of this hydrolysis reaction, 54%, is a bit lower than the 75% reported in the literature for a similar derivative.[161] Nevertheless, the reaction was performed in a smaller scale which makes the purification via crystallization more challenging and might explain this difference.

Die approbierte gedruckte Originalversion dieser Dissertation ist an der TU Wien Bibliothek verfügbar.
The approved original version of this doctoral thesis is available in print at TU Wien Bibliothek.

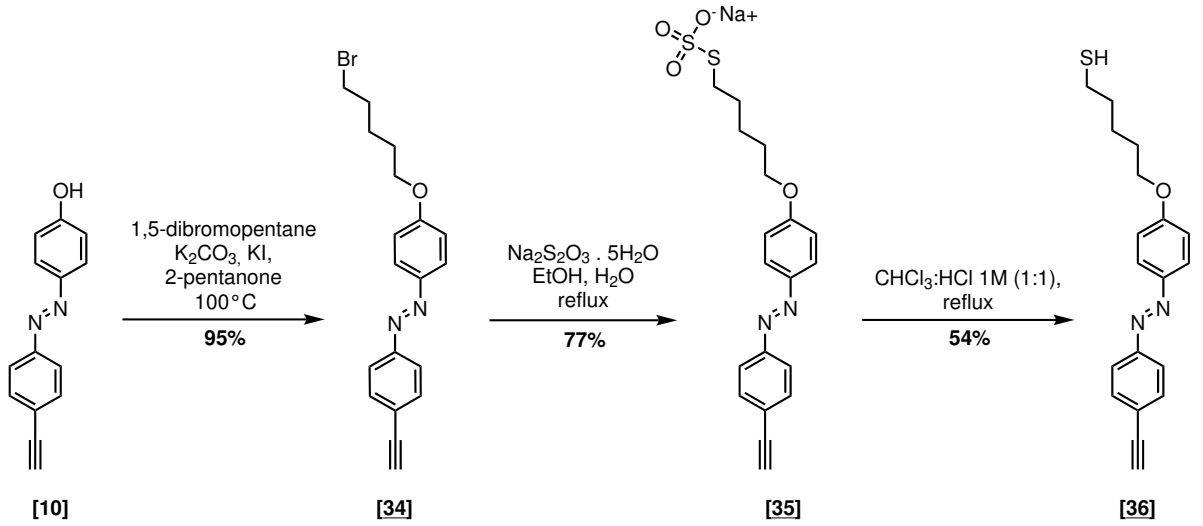

Scheme 8: Synthesis of a double-click CuAAC-thiol azobenzene.

C.1.4 Photoswitching and thermal half-life time of the double-click azobenzenes

Whenever working with azobenzenes, it is important to properly characterize the key parameters of the photoswtiching steps, which include thermal half-life time ($t_{1/2}$, which can vary from seconds to years[30,36,162]) and photoswitching wavelengths. Therefore these photophysicals properties of our double-click azobenzenes were tested (Figure 30).

Following the protocols previously developed in our research group to study the properties of photoswitchable compounds, including azobenzenes and arylazopyrazoles, we have started by testing the *trans-cis* photoswitching of the synthesized azobenzenes.[163] A 0.04 mM solution of each azobenzene in DMSO was prepared and a UV/Vis spectra was recorded, showing the typical azobenzene bands: the $\pi \rightarrow \pi^*$ at a maximum wavelength (λ_{max}) of approximately 350 nm and the much less intense n$\rightarrow \pi^*$ at $\lambda_{max} \approx 450$ nm. Afterwards, this solution was irradiated with a 365 nm LED for 10 seconds and the UV/Vis spectra was once again recorded, showing a decrease in the intensity of the $\pi \rightarrow \pi^*$ band and a small increase of the n$\rightarrow \pi^*$ band. These observations are consistent with the switching from *trans* to *cis*. Since this process should be reversible, the solution was irradiated with a 460 nm LED for 10 seconds leading to the increase of the $\pi \rightarrow \pi^*$ band and a decrease in the n$\rightarrow \pi^*$ band, confirming the back-switch from *cis* to *trans*. Notice that the absorption at the λ_{max} of the $\pi \rightarrow \pi^*$ band after irradiation with 460 nm is slightly lower than before irradiation, indicating that the switch-back

Die approbierte gedruckte Originalversion dieser Dissertation ist an der TU Wien Bibliothek verfügbar.
The approved original version of this doctoral thesis is available in print at TU Wien Bibliothek.
TU Bibliothek Your knowledge hub WIEN

to *trans* is not complete. The increase of the irradiation time does not lead to any increase in the absorption, indicating that the photostationary state was already reached. Nevertheless this is expected due to the overlap of the absorption bands of the *cis* and *trans* isomers, that normally results in a photostationary state where approximately 5% of *cis* isomer is left.[11] In Figure 31 the n $\rightarrow \pi^*$ band of the *cis* and *trans* azobenzene **[11e]** is displayed as an example. Here it is clearly noticeable that both isomers absorb at 460 nm, which means that complete switch back to *cis* is not possible at 460 nm.

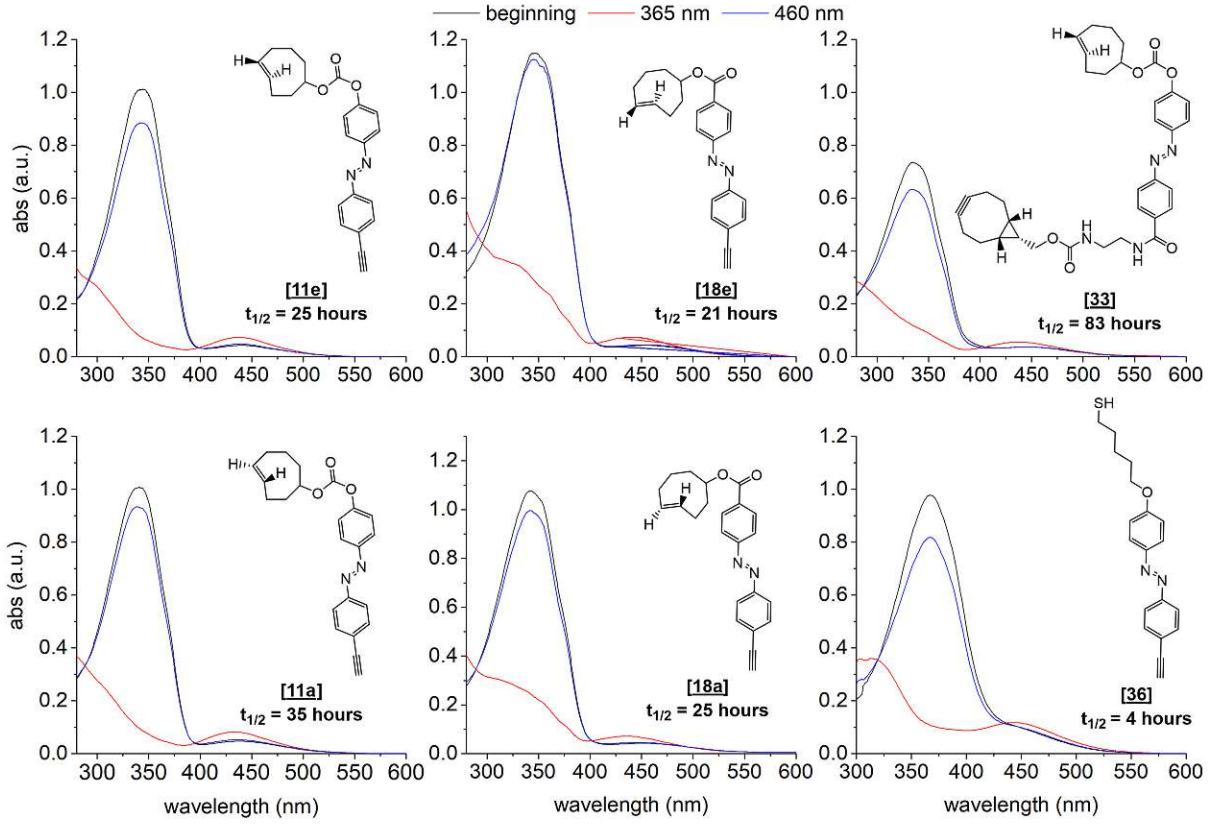

Figure 30: Determination of the photophysical properties of the double-click azobenzenes. The black lines correspond to the UV/Vis spectra before irradiation, the red lines after irradiation with 365 nm and the blue lines after irradiation with 460 nm. Below the structure of each compound the determined thermal $t_{1/2}$ can be found.

For the determination of the thermal relaxation half-life time ($t_{1/2}$) the same azobenzene concentration was used, since the absorption is still within the range where it should be directly proportional to concentration according to the Beer-Lambert law. After switching the compound to *cis*, the increase of the absorption at λ_{max} of the $\pi \rightarrow \pi^*$ of the *trans* isomer was

Die approbierte gedruckte Originalversion dieser Dissertation ist an der TU Wien Bibliothek verfügbar.
The approved original version of this doctoral thesis is available in print at TU Wien Bibliothek.
TU Bibliothek Your knowledge hub WIEN

followed for 18 hours and the data were analyzed according to a first-order kinetics. The determined $t_{1/2}$ can be found as inserts in the graphs of Figure 30 below the structures and range from 4 hours to 83 hours. As expected, azobenzene **[36]** has the lowest thermal $t_{1/2}$ thanks to the electron-donating effect of the oxygen. On the other side, compound **[33]** has the highest thermal $t_{1/2}$ due to the two electron-withdrawing groups in the azobenzene.[36]

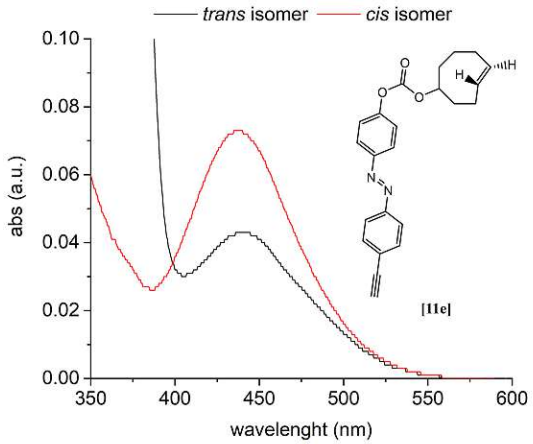

Figure 31: n $\rightarrow \pi^*$ absorption bands of the *cis* and *trans* isomers of azobenzene **[11e]**.

Die approbierte gedruckte Originalversion dieser Dissertation ist an der TU Wien Bibliothek verfügbar.
The approved original version of this doctoral thesis is available in print at TU Wien Bibliothek.

C.2 Preparation of photoswitchable azobenzene functionalized surfaces

As previously stated, one of the goals of this thesis is to prepare a light-responsive azobenzene coated surface for the development of a biological application. As shown in Figure 32, for the preparation of this surface we want to take full advantage of the potential of click chemistry to selectively bind the azobenzene to the surface and to a bioactive compound. For that we can select one of the previously synthesized double-click azobenzene. Since CuAAC has already been successfully used for surface coating[67,164] and the tetrazine ligation is the fastest known click reaction ideal for biomolecule functionalization[127,146,165,166], azobenzene **[11e]** was chosen as a prototype for surface immobilization.

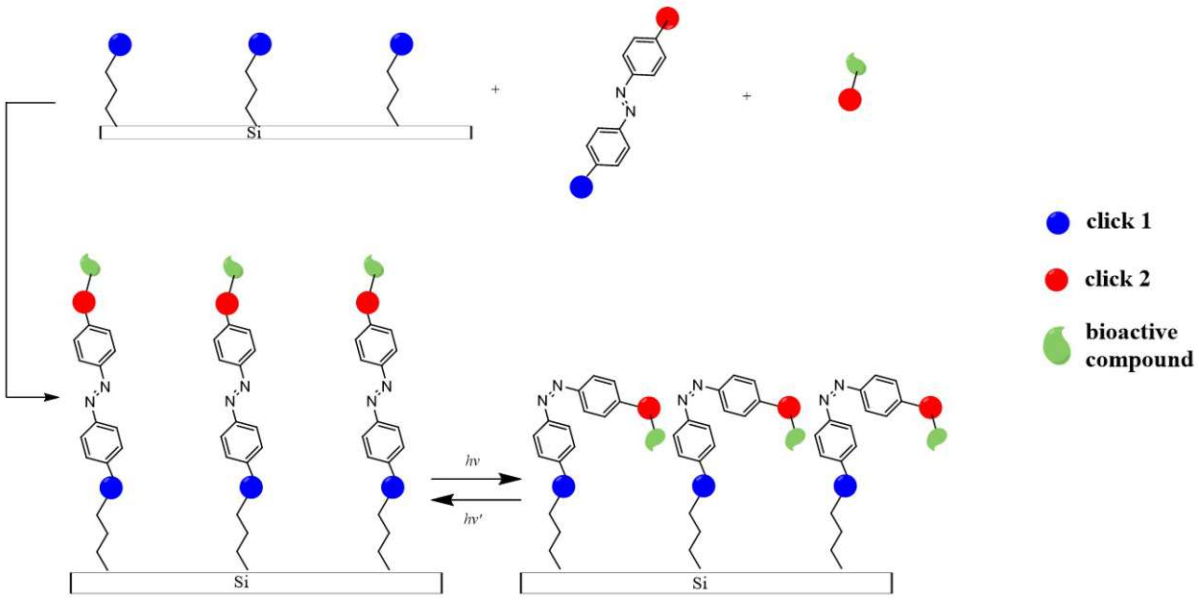

Figure 32: Our approach to obtain a bioactive light-responsive surface using a double-click azobenzene.

This section focuses not only on the preparation of a surface with azobenzene **[11e]** for biological application, but also on approaches to deal with azobenzene surface overcrowding and the small difference between the water contact angle (WCA) of the surface on the *trans* and *cis* states.

Die approbierte gedruckte Originalversion dieser Dissertation ist an der TU Wien Bibliothek verfügbar.
The approved original version of this doctoral thesis is available in print at TU Wien Bibliothek.
TU Bibliothek Your knowledge hub WIEN

C.2.1 Synthesis of a model azobenzene for surface functionalization

Previous to immobilizing the intended azobenzene **[11e]**, we decided to use a simpler model system to understand the basics of azobenzene immobilization since there was no experience in this subject in our research group and also available literature data was arbitrary.

Considering our goal to use the CuAAC to immobilize the azobenzene on an azide functionalized surface, an alkyne containing azobenzene is required. The photoswitching of the surface will be evaluated by WCA, therefore the addition of a hydrophobic group at the "end" of the azobenzene is beneficial because the already more hydrophobic *trans* configuration will become even more hydrophobic, generating a higher response in the WCA. The synthesis of such azobenzene is presented in Scheme 9.

The synthesis starts with the oxidation of 4-(trifluormethyl)aniline **[37]** using oxone, leading to 1-nitroso-4-(trifluoromethyl)benzene **[38]**.[167] Purification of this compound was not successful due to its high instability: proton NMR indicates that the material obtained by recrystallization or sublimation contained higher amounts of the decomposition products (azoxybenzene and azobenzene) than the crude. Hence the crude material was used for the next step, a Mills reaction with 4-iodoaniline **[39]** affording the azobenzene **[40]**. Finally, a Sonogashira coupling was used to introduce a TMS-protected alkyne that was deprotected using K_2CO_3, affording azobenzene **[41]**.[168]

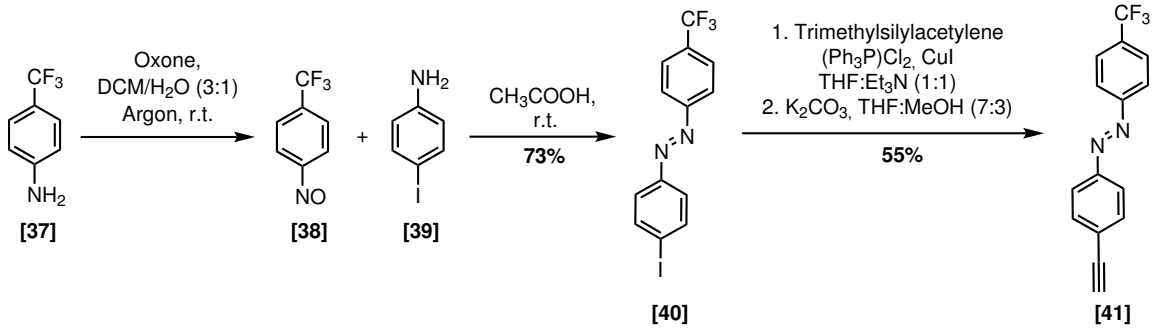

Scheme 9: Synthesis of a model azobenzene for surface functionalization.

Die approbierte gedruckte Originalversion dieser Dissertation ist an der TU Wien Bibliothek verfügbar.
The approved original version of this doctoral thesis is available in print at TU Wien Bibliothek.

C.2.2 Test in solution of the click reactions

It is important to make sure that reaction conditions are working in solution, since reaction analytics on the surface is substantially more complicated. Therefore, we synthesized two model molecules, an aliphatic azide and a tetrazine, to test both the CuAAC and the tetrazine ligation. For the azide, we have chosen 1-azidododecane **[43]** since it is a long alkane chain like the one that will be present on the azide functionalized surface (see Section C.2.3). For its synthesis, shown in Scheme 10A, a simple nucleophilic substitution of 1-bromododecane **[42]** with NaN_3 was carried out.[169]. Regarding the tetrazine, we opted for a trifluormethyl-containing symmetric tetrazine thanks to its easy synthesis and with the expectation that the trifluormethyl generates an increased WCA response upon photoswitching.[86,170] Scheme 10B presents the synthesis of tetrazine **[45]** *via* Pinner synthesis, a two step-procedure: the condensation between 4-(trifluoromethyl)benzonitrile **[44]** and hydrazine generating a dihydrotetrazines that is subsequently oxidized with diacetoxyiodobenzene, forming the tetrazine **[45]**.[171]

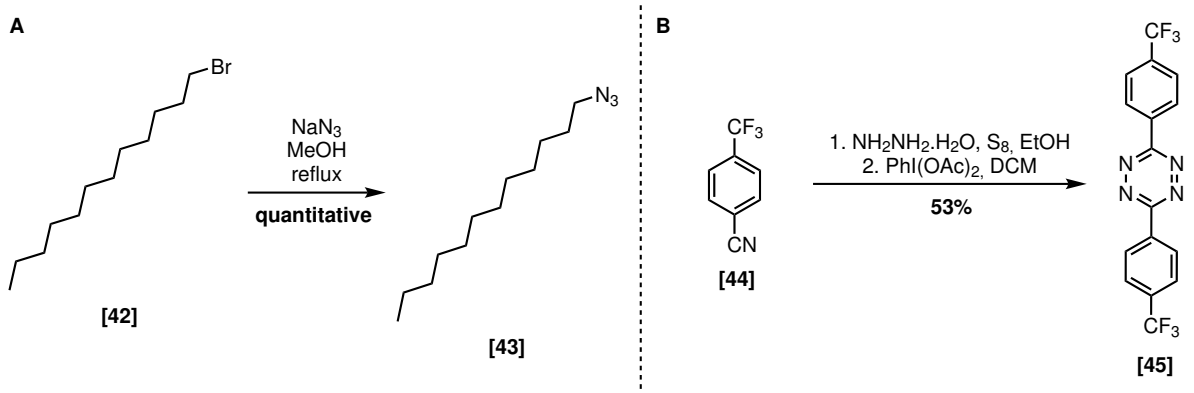

Scheme 10: Synthesis of a model aliphatic azide and a tetrazine for the click reaction testing.

Scheme 11 presents the tetrazine ligation between tetrazine **[45]** and azobenzene **[11e]**. A minute after both compounds being mixed in THF, there is full conversion of the azobenzene starting material. However, two 1,4-dihydropyridazines (regioisomers), which are a non-oxidized forms of the desired pyridazine, are obtained as the main product of this reaction together with small ammounts of the pyridazine (according to MS-HPLC). Since the oxidation was apparently slow and the oxidation state of the product might affect the WCA of the functionalized surface, (diacetoxyiodo)benzene was added to the reaction mixture after complete

Die approbierte gedruckte Originalversion dieser Dissertation ist an der TU Wien Bibliothek verfügbar.
The approved original version of this doctoral thesis is available in print at TU Wien Bibliothek.
TU Bibliothek Your knowledge hub WIEN

conversion of the starting material to push forward oxidation.[128]

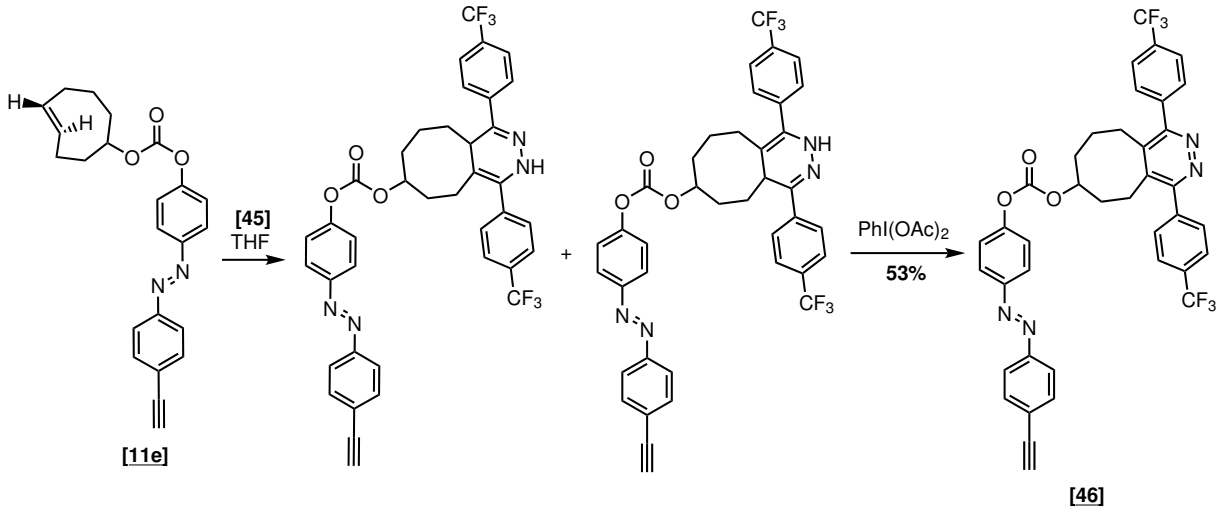

Scheme 11: Test of the tetrazine ligation between azobenzene **[11e]** and tetrazine **[45]**.

11-Azidododecane **[43]** was clicked via CuAAC with azobenzenes **[41]**, **[11e]** and **[46]** (Scheme 12). Firstly, $CuSO_4$/ascorbic acid was the chosen system for this CuAAC since the presence of ascorbic acid prevents the oxidation of the Cu(I), therefore higher yields would be expected.[100] Under these condition, both click products **[47]** and **[49]** were obtained, however, azobenzene **[11e]** decomposed and no click product **[48e]** was recovered. Therefore, another Cu(I) source, Cu(I) iodide was tested for these clicks. These conditions not only afforded click product **[48e]** in 57% yield, but also led to higher yields for the click reactions of **[41]** and **[46]** (73% to quantitative and 42% to 82%, respectively). Therefore, Cu(I) iodide was chosen as the catalyst for subsequent surface immobilization.

Die approbierte gedruckte Originalversion dieser Dissertation ist an der TU Wien Bibliothek verfügbar.
The approved original version of this doctoral thesis is available in print at TU Wien Bibliothek.

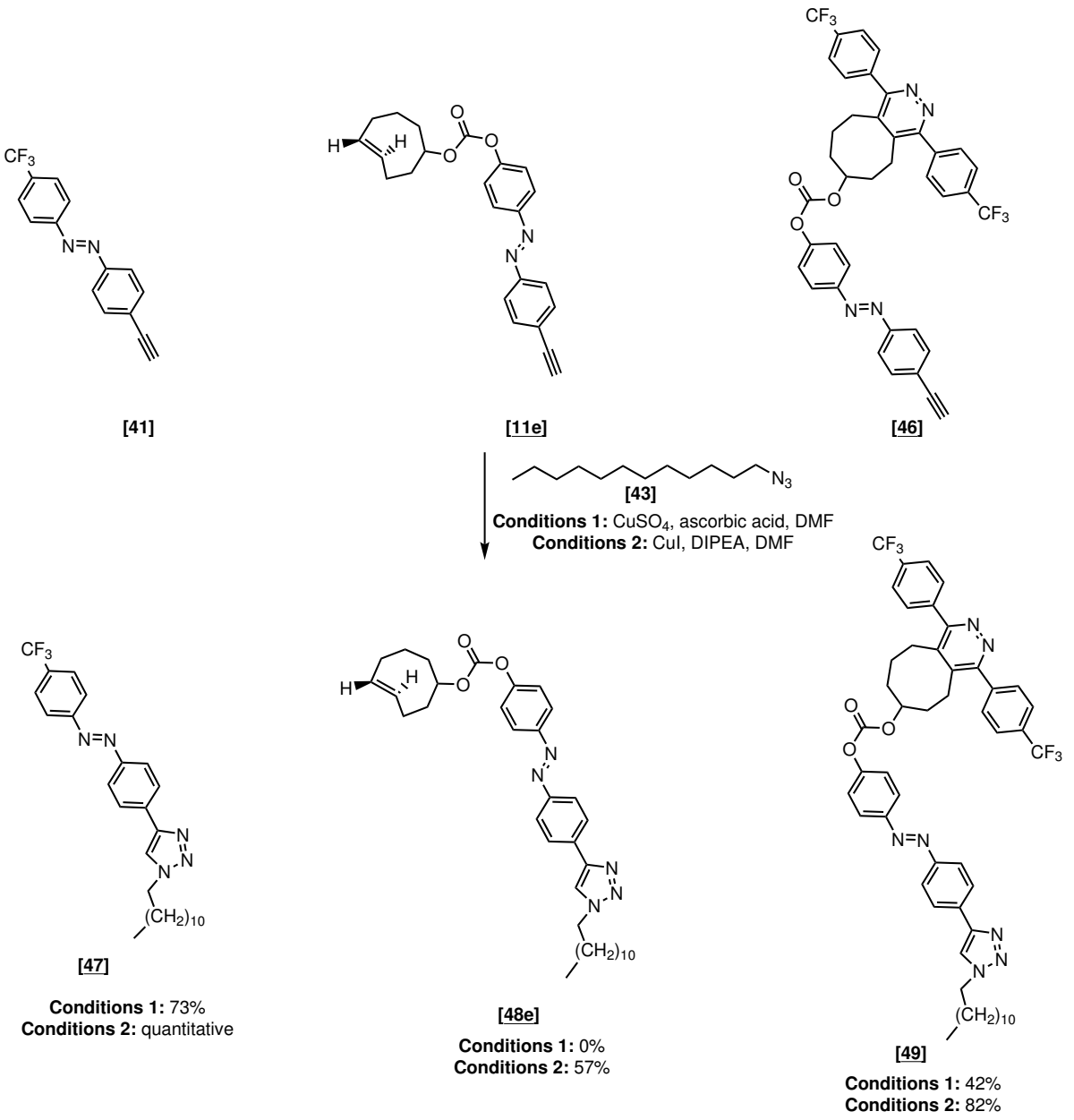

Scheme 12: Test of the CuAAC reactions of azobenzenes **[11e]**,**[41]** and **[46]** with azide **[43]**.

The photophysical properties of model azobenzene **[41]** and clicked products **[46]**, **[47]**, **[48e]** and **[49]** were also determined and compared with their respective azobenzene starting materials (Figure 33). The reversible photoswitching between *trans* and *cis* still occurs after the click reaction as expected. It is also noticeable in the spectra before irradiation (black lines) that the λ_{max} of the $\pi \rightarrow \pi^*$ band of the CuAAC click products has been red-shifted due to

Die approbierte gedruckte Originalversion dieser Dissertation ist an der TU Wien Bibliothek verfügbar.
The approved original version of this doctoral thesis is available in print at TU Wien Bibliothek.

the increased conjugation of the system, when compared with their starting materials (see the missing SM spectra in Section C.1.4).

The thermal half-life times of the click products are within the same range as the starting materials. The determined values are always higher than 20 hours, which means that choosing a configuration of the azobenzene and maintain it on the surface should be possible. This is important because if the thermal half-life times were in the order of seconds, there would not be enough time to analyze the surface on the *cis* configuration. Notice that the CuAAC leads to a small reduction in the $t_{1/2}$ due to the electron-donating effect of the 1,2,3-triazole.[172,173]

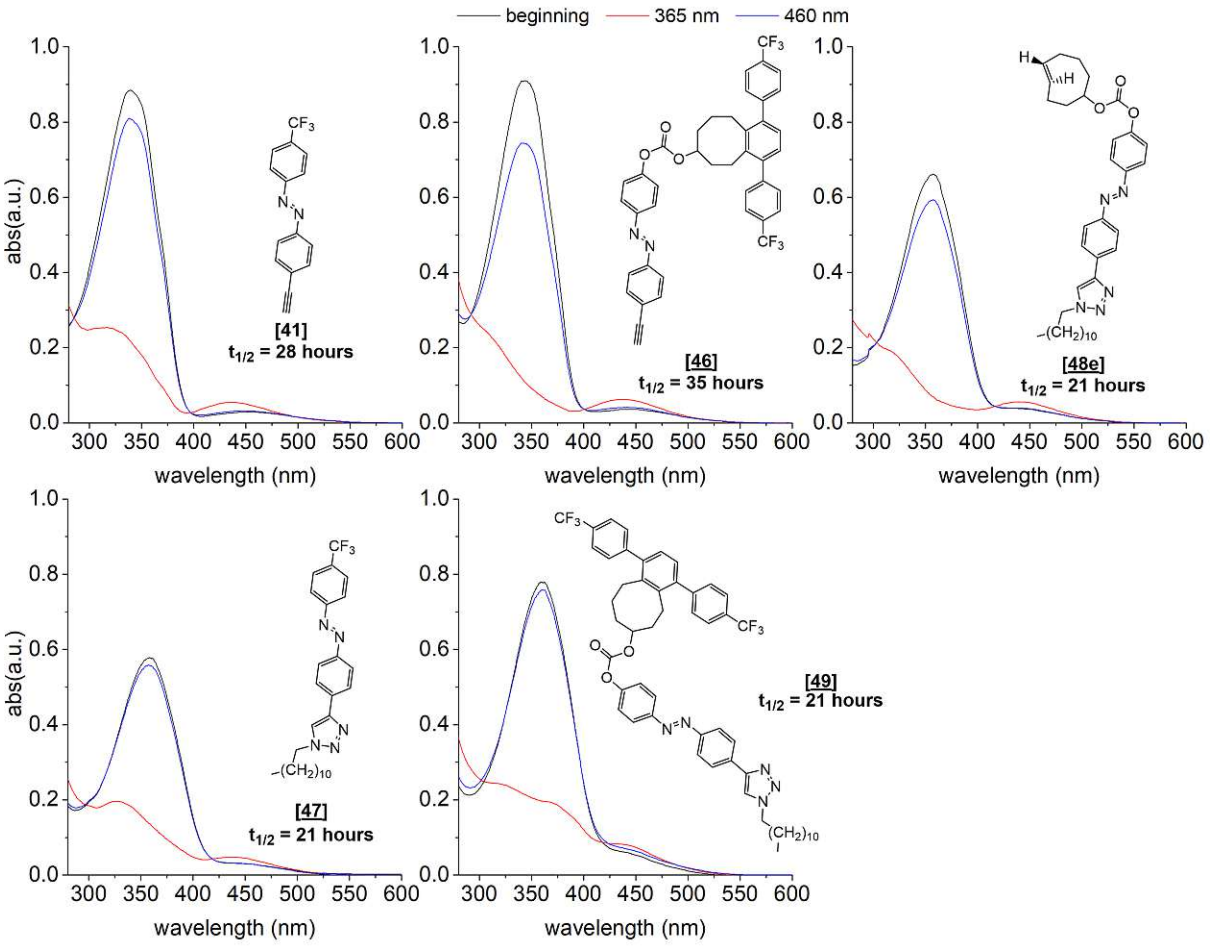

Figure 33: Determination of the photophysical properties of the model azobenzene **[41]** and the click products. The black lines correspond to the UV/Vis spectra before irradiation, the red lines after irradiation with 365 nm and the blue lines after irradiation with 460 nm. Below the structure of each compound the determined thermal $t_{1/2}$ can be found.

Die approbierte gedruckte Originalversion dieser Dissertation ist an der TU Wien Bibliothek verfügbar.
The approved original version of this doctoral thesis is available in print at TU Wien Bibliothek.

C.2.3 Preparation of an azide coated flat silicon surface

For this work, silicon was chosen as the substrate due to its biocompatibility, surface tailorability and high surface-to-volume rations.[174] As previously referred, we envisioned and approach *via* CuAAC to bind the azobenzenes to the surface, therefore an azide-coated silicon surface was prepared (Scheme 13). A reliable approach to prepare organic monolayers on silicon is the adsorption of organo-trichlorosilanes.[175] In this process the trichlorosilane is hydrolyzed by catalytic amounts of water present in the solvent, forming a trisilanol which will react with the hydroxy groups on the oxidized silicon. In our case, the oxidized silicon was coated with 11-bromoundecyltrichlorosilane (BUTS) and ellipsometry confirmed monolayer formation: the measured thickness of the organic layer was 20.9 Å $\pm$ 0.7 (theoretical value 15.6 Å), which is according to the literature.[170]

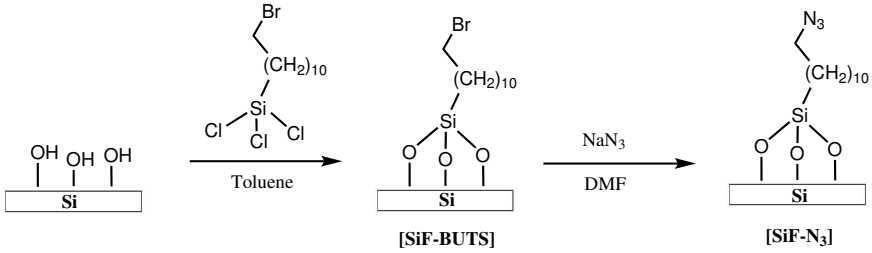

Scheme 13: Preparation of a flat silicon surface coated with azide **[SiF-N_3]**.

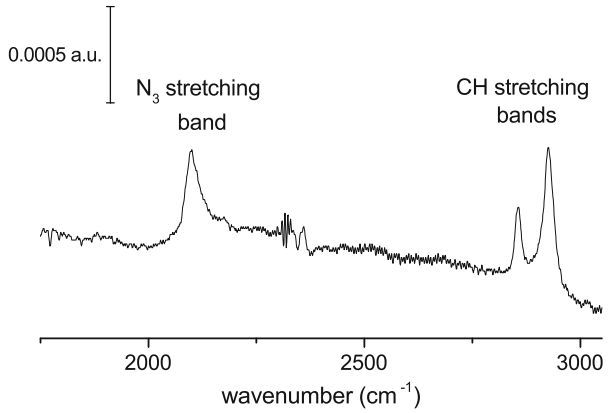

Figure 34: Analysis of the azide coated surface **[SiF-N_3]** by FTIR.

The azide was introduced by nucleophilic substitution with NaN_3 affording the surface **[SIF-N_3]** and FTIR was used to confirm the success of this reaction. The FTIR of **[SIF-N_3]**

Die approbierte gedruckte Originalversion dieser Dissertation ist an der TU Wien Bibliothek verfügbar.
The approved original version of this doctoral thesis is available in print at TU Wien Bibliothek.
TU Bibliothek Your knowledge hub WIEN

present in Figure 34 shows a stretching band at approximately 2130-2080 cm^{-1} corresponding to the azide as well as stretching bands between 2770-3000 cm^{-1} corresponding to the CH. This proves the attainment of the azide-coated surface **[SiF-N_3]**.

C.2.4 *Trans* immobilization on flat silicon

To obtain an azobenzene photoswitchable surface the optimization of the reaction time is crucial, since too much azobenzene on the surface leads to lack of space for the *trans* to *cis* isomerization (surface overcrowding). Therefore, the reaction time needs to be optimized in order to reduce the density of the azobenzene on the surface and to prevent overcrowding.[65,176,177] Figure 35 represents the above mentioned problem.

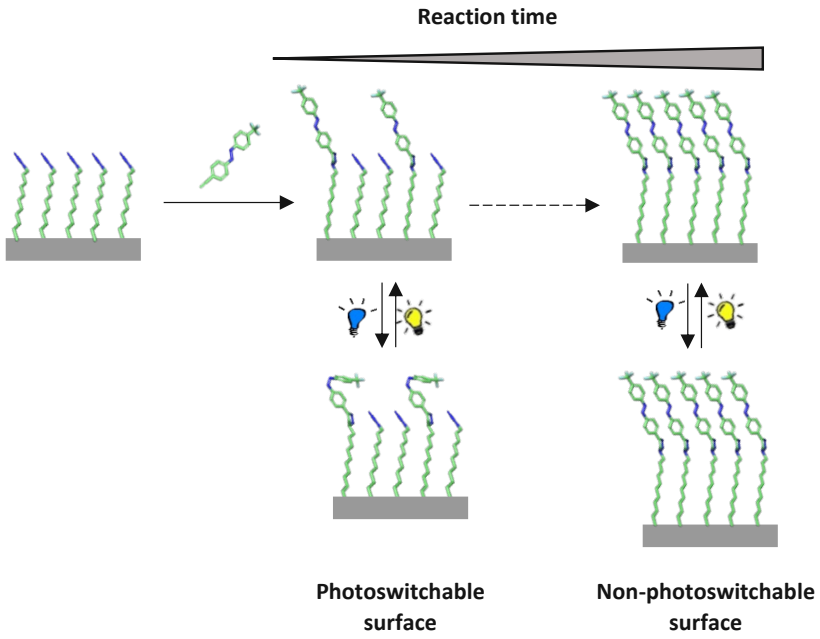

Figure 35: The optimization of the reaction time as a crucial step to prevent overcrowding and obtain photoswitchable surfaces.

Model azobenzene **[41]**, biologically relevant azobenzene **[11e]** and model product of the tetrazine click **[46]** were immobilized on **[SiF-N_3]** using the previously tested reaction conditions with Cu(I) iodide and DIPEA (Figure 36). The surfaces obtained from this process were named **[SiF-x*trans*]**, where **Si** stands for silicon, **F** for flat, **x** for the immobilized azobenzene

Die approbierte gedruckte Originalversion dieser Dissertation ist an der TU Wien Bibliothek verfügbar. The approved original version of this doctoral thesis is available in print at TU Wien Bibliothek.

and ***trans*** for the immobilization method. For clarity reasons, in this thesis the particular mode for immobilization will be referred as *trans* immobilization, since the azobenzene is clicked in the *trans* configuration.

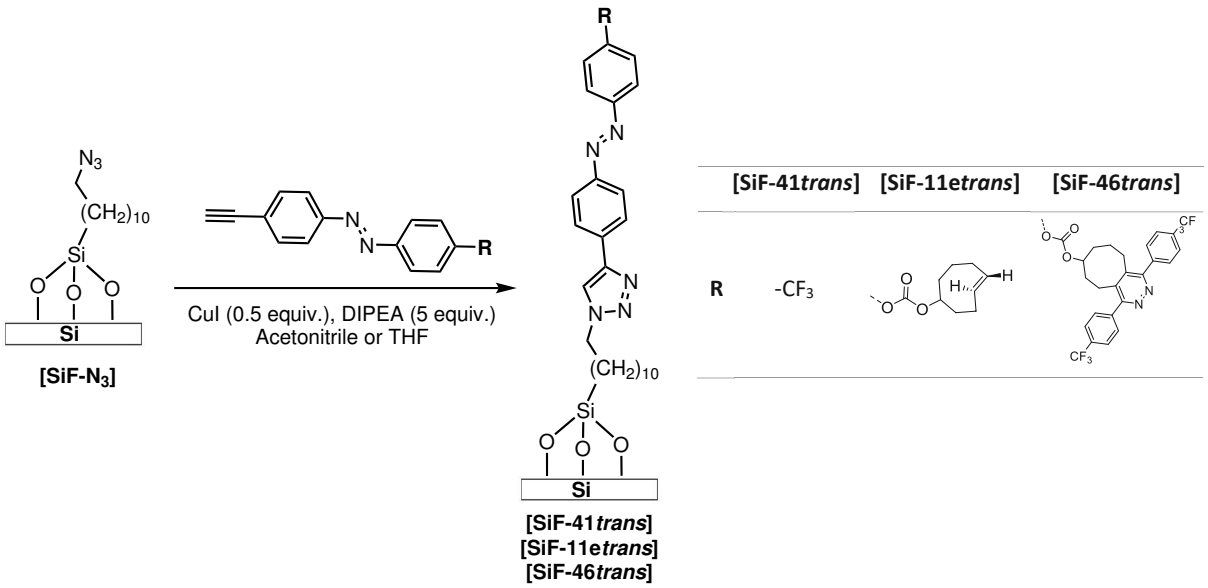

Figure 36: Immobilization of azobenzenes **[41]**, **[11e]** and **[46]** on flat silicon by CuAAC to obtain three distinct photoswitchable surfaces: **[SiF-41*trans*]**, **[SiF-11e*trans*]** and **[SiF-46*trans*]**.

The first immobilized compound was model azobenzene **[41]**. Following a literature precedent[67], we started by running the reaction overnight and the photoswitching of the surface was analyzed by WCA. Upon irradiation with 365 nm, there was no difference in WCA, which indicated that no photoswitching from *trans* to *cis* occurred, presumably due to surface overcrowding. Therefore, we reduced the reaction time to 380, 180, 60, 30, 15 and 7 minutes. The surfaces obtained from reaction times 380, 180 and 60 minutes presented the same behavior as overnight. Only for 30 minutes, 15 minutes and 7 minutes a difference in the WCA is verified upon irradiation with 365 nm, thus these surfaces were irradiated with a halogen lamp to switch-back to *trans* since azobenzene photoswitching should be a reversible process (Figure 37A). A total of 6 cycles alternating between the 365 nm and the halogen lamp were performed, proving the switchability of the obtained surfaces (Figure 37A).

In Figure 37B the previous data were condensed to present the relation between the reaction time and the difference in the WCA (ΔWCA). Here we observe that ΔWCA increases from 30 minutes reaction time to 15 minutes (4° to 7°) which indicates that at 30 minutes reaction

Die approbierte gedruckte Originalversion dieser Dissertation ist an der TU Wien Bibliothek verfügbar.
The approved original version of this doctoral thesis is available in print at TU Wien Bibliothek.
TU Bibliothek Your knowledge hub WIEN

time the concentration of the azobenzene on the surface is probably already too high leading to inefficient photoswitching. When the reaction time is reduced from 15 minutes to 7 minutes, the ΔWCA decreases to 3.5°. We think that this reduction is due to a too low amount of azobenzene on the surface. We conclude that the ideal reaction time for the *trans* immobilization of **[41]** is approximately 15 minutes.

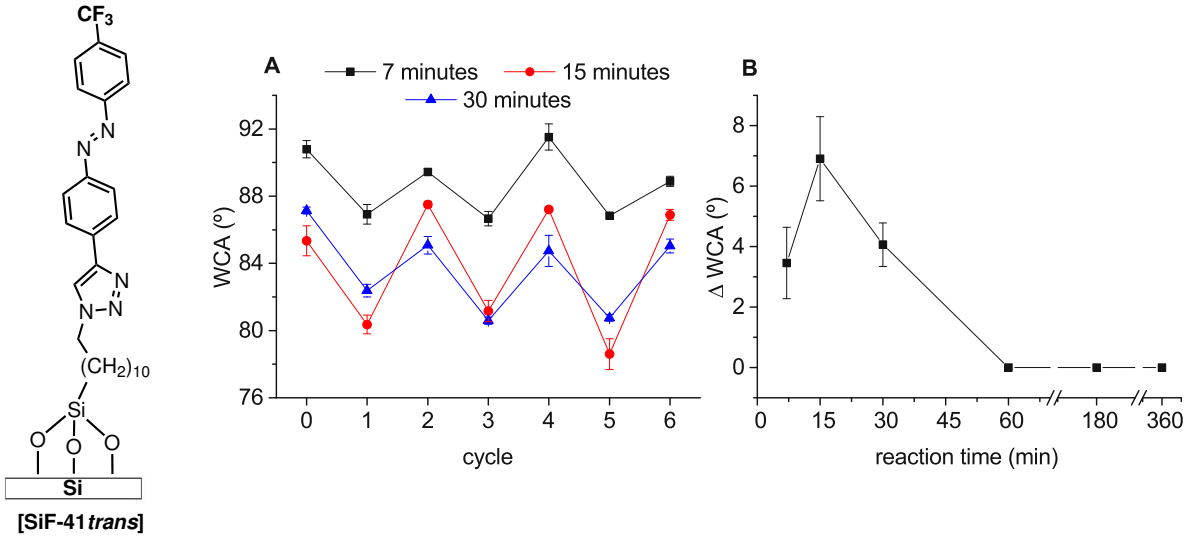

Figure 37: (A) Analysis by WCA of the photoswitching of **[SiF-41*trans*]** after 7 minutes, 15 minutes and 30 minutes reaction time. Cycle 0 corresponds to the WCA before irradiation, odd number cycles to irradiation with 365 nm and even number cycles to irradiation with a halogen lamp (i.e.switch-back). **(B)** Relation between the reaction time and ΔWCA. The presented data are the average of the 6 irradiation cycles.

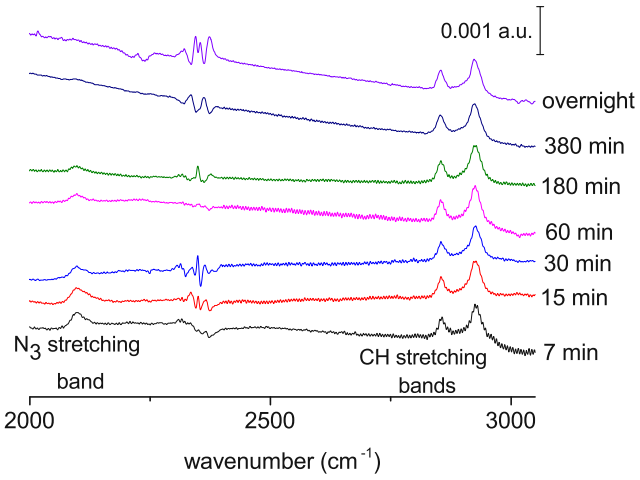

Figure 38: FTIR of the obtained **[SiF-41*trans*]** after 7, 15, 30, 60, 180, 380 minutes and overnight.

Die approbierte gedruckte Originalversion dieser Dissertation ist an der TU Wien Bibliothek verfügbar.
The approved original version of this doctoral thesis is available in print at TU Wien Bibliothek.
TU Bibliothek Your knowledge hub WIEN

The FTIR of all the obtained **[SiF-41*trans*]** was measured to see how much azide had been consumed during the CuAAC (Figure 38). Overnight and after 380 minutes reaction no azide band (2130-2080 cm^{-1}) is observed, meaning that the surface is fully coated with azobenzene and explaining the lack of photoswitchablity. As expected, the shorter the reaction time, the more intense the azide stretching band becomes, indicating a reduction of overcrowding till photoswitchable surfaces are obtained at 7, 15 and 30 minutes.

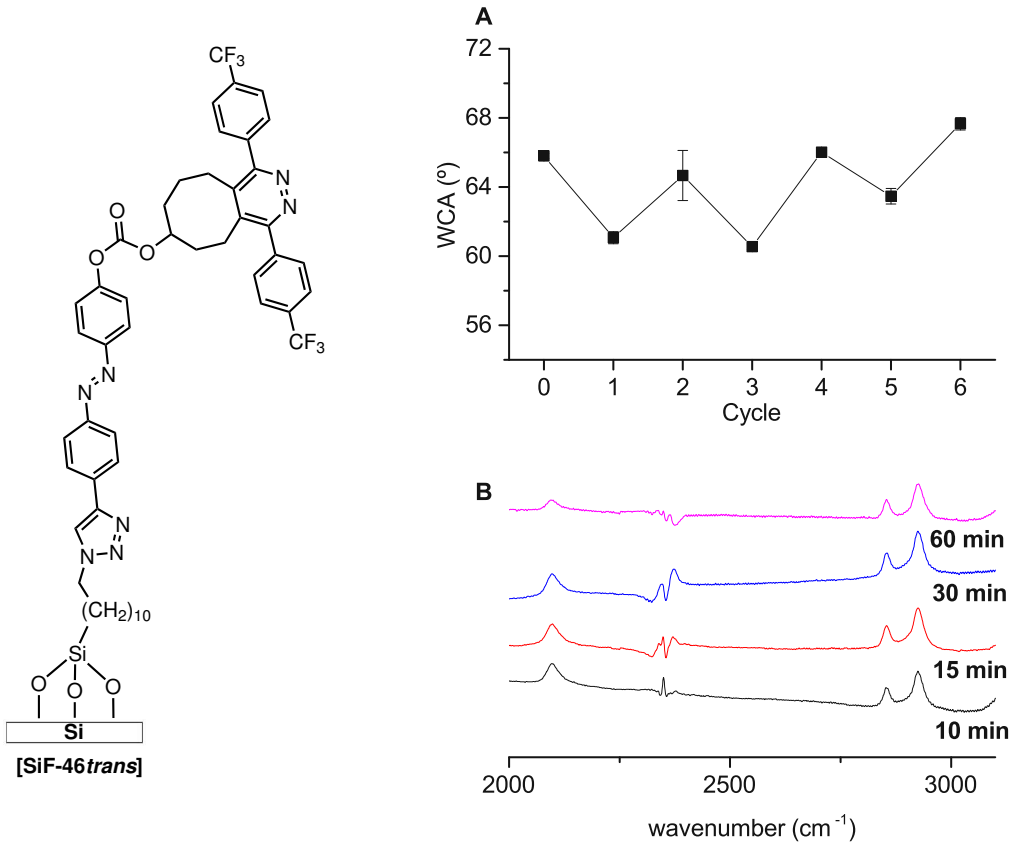

Figure 39: (A) Analysis by WCA of the photoswitching of **[SiF-46*trans*]** after 10 minutes reaction. Cycle 0 corresponds to the WCA before irradiation, odd number cycles to irradiation with 365 nm and even number cycles to irradiation with a halogen lamp. **(B)** FTIR of the obtained **[SiF-46*trans*]**.

Taking into account the knowledge obtained with the *trans* immobilization of azobenzene **[41]**, for the immobilization of **[46]** we started with shorter reaction times: 60, 30, 15 and 10 minutes. From these, only 10 minutes produced a photoswitchable surface. Like before 6 irradiation cycles alternating between a 365 nm LED and a halogen lamp were performed and the average of these cycles is 4.4°. This ΔWCA is smaller than the optimized ΔWCA of **[SiF-**

Die approbierte gedruckte Originalversion dieser Dissertation ist an der TU Wien Bibliothek verfügbar.
The approved original version of this doctoral thesis is available in print at TU Wien Bibliothek.

41*trans*], which we found surprising since the additional CF_3 should contribute to a higher difference. Not only that, but the absolute value of the WCA is on average 64°, much lower than the 84° obtained for **[SiF-41*trans*]**. To try to explain these results, we used chemdraw 3D to obtain a model of the clicked azobenzene **[46]** (Figure 40). In this model we have observed that the rings containing the CF_3 are actually perpendicular to the azobenzene, therefore the hydrophilic carbonyl is probably the main contributor responsible for the obtained WCA. Once again the FTIR of the obtained **[SiF-46*trans*]** were measured (Figure 39B). As expected we have verified that a higher reaction time has led to a higher azide consumption and that there must be azide left on the surface in order to obtain photoswitchable surfaces.

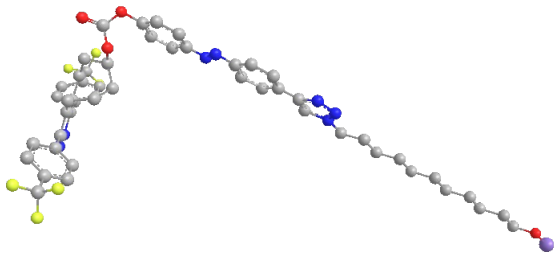

Figure 40: Chemdraw 3D model of the click product of surface **[11-N_3]** and azobenzene **[46]**. The color code is as follows: gray = carbon, blue = nitrogen, red = oxygen, yellow = fluorine, and purple = silicon.

Finally, the compound relevant for the development of a bioapplication, azobenzene **[11e]**, was immobilized. In this case we started with an even smaller reaction time, 30 minutes, which afforded a non-photoswitchable surface, therefore the time was reduced to 10 minutes and 5 minutes. Only 5 minutes afforded a photoswitchable surface (Figure 41A) with an average ΔWCA for the 6 irradiation cycles of 3.9° and an average absolute WCA of 63.1°. These results were expected since in this case there is no hydrophobic group on "top" to increase the apolarity of the *trans* state. The values obtained for **[SiF-46*trans*]** and **[SiF-11e*trans*]** are similar, corroborating that in the case of **[SiF-46*trans*]** the WCA results are probably influenced by the carbonyl group. The FTIR of the obtained **[SiF-11e*trans*]** are shown in Figure 41B and the previous observations regarding reaction and azide consumption as well as the presence of azide on the surface and photoswitchability are still observed.

Die approbierte gedruckte Originalversion dieser Dissertation ist an der TU Wien Bibliothek verfügbar.
The approved original version of this doctoral thesis is available in print at TU Wien Bibliothek.

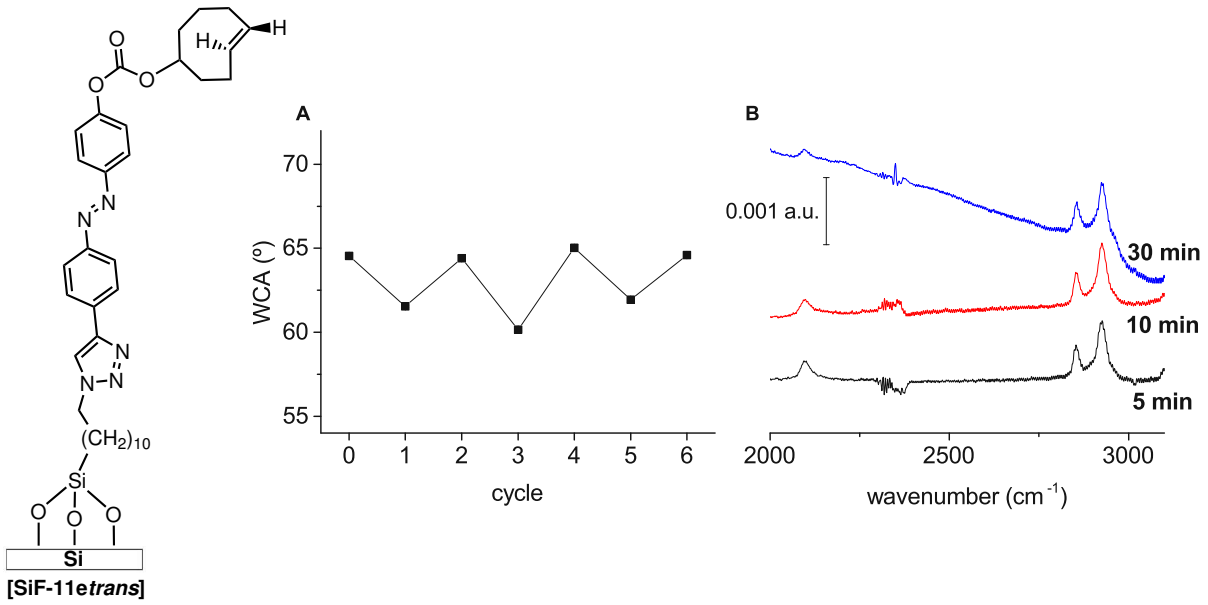

Figure 41: (A) Analysis by WCA of the photoswitching of **[SiF-11e*trans*]** after 5 minutes reaction. Cycle 0 corresponds to the WCA before irradiation, odd number cycles to irradiation with 365 nm and even number cycles to irradiation with a halogen lamp. **(B)** FTIR of the obtained **[SiF-11e*trans*]**.

C.2.5 Preventing surface overcrowding - *cis* immobilization

As previously referred, when the density of the azobenzene on the surface is too high the azobenzene may not have enough space to switch from the *trans* to the *cis* (surface overcrowding), making the surface useless. There are two approaches to circumvent this problem: optimize the reaction time so that the density of azobenzene on the surface is low (as we have done in C.2.4) or to immobilize the azobenzene together with a non-switchable molecule, which acts as a lateral spacer.[65] In both cases a high amount of tedious optimization is required, either reaction time or azobenzene:lateral spacer ratio. We hypothesized that if the azobenzene is immobilized in the most spatially demanding *cis* configuration, upon immobilization the azobenzene moieties should always keep the necessary space required for photoswitching (Figure 42).

To test our hypothesis we have immobilized azobenzenes **[46]**, **[11e]** and **[41]** while in the *cis* configuration (Figure 43). The reaction mixtures were prepared in analogous fashin to the *trans* immobilization and irradiated with a 365 nm LED to switch the azobenzenes to *cis*. The temperature of the reaction also had to be reduced to prevent overheating by the LED and

Die approbierte gedruckte Originalversion dieser Dissertation ist an der TU Wien Bibliothek verfügbar.
The approved original version of this doctoral thesis is available in print at TU Wien Bibliothek.
TU Bibliothek Your knowledge hub WIEN

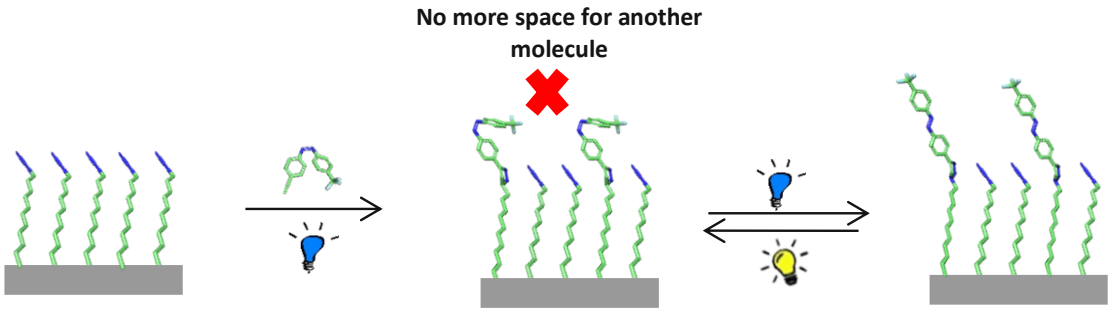

Figure 42: *Cis* immobilization, a practical method to prevent surface overcrowding.

evaporation of the solvent.

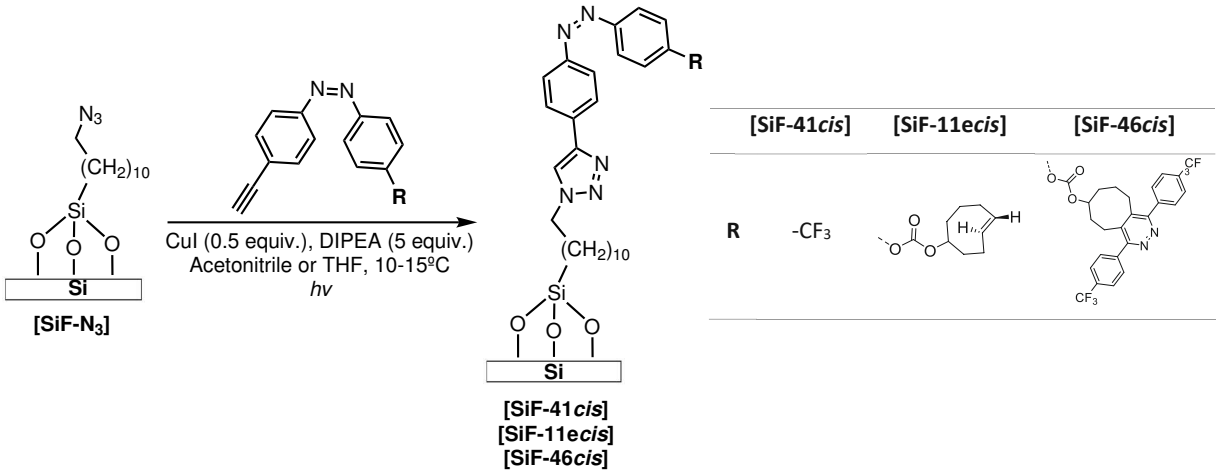

Figure 43: Immobilization of azobenzenes **[41]**, **[11e]** and **[46]** on flat silicon using *cis* immobilization, to afford **[SiF-11e*cis*]**, **[SiF-41*cis*]** and **[SiF-46*cis*]**.

UV/Vis spectroscopy was used to confirm the isomerization of the reaction mixture of the *cis* immobilization (Figure 44). After 30 minutes irradiation there was a decrease in the absorption of the $\pi \rightarrow \pi^*$ band as well as a small increase in the n$\rightarrow \pi^*$ band consistent with switching to the *cis* isomer. Upon confirmation of isomerization by UV/Vis, surface **[SiF-N_3]** was added to the reaction mixtures and kept under irradiation for 180 minutes. This reaction time was chosen because our previous data indicates that with *trans* isomerization the surfaces coated with these compounds get overcrowded way before 180 minutes (**[SiF-41*trans*]** non-photoswitchable after 30 minutes, **[SiF-11e*trans*]** after 5 minutes and **[SiF-46*trans*]** after 10 minutes). At the end of the reaction, a new UV/Vis spectrum was recorded to make sure that during the reaction the azobenzenes had been kept in the *cis* configuration.

Die approbierte gedruckte Originalversion dieser Dissertation ist an der TU Wien Bibliothek verfügbar.
The approved original version of this doctoral thesis is available in print at TU Wien Bibliothek.
TU Bibliothek Your knowledge hub WIEN

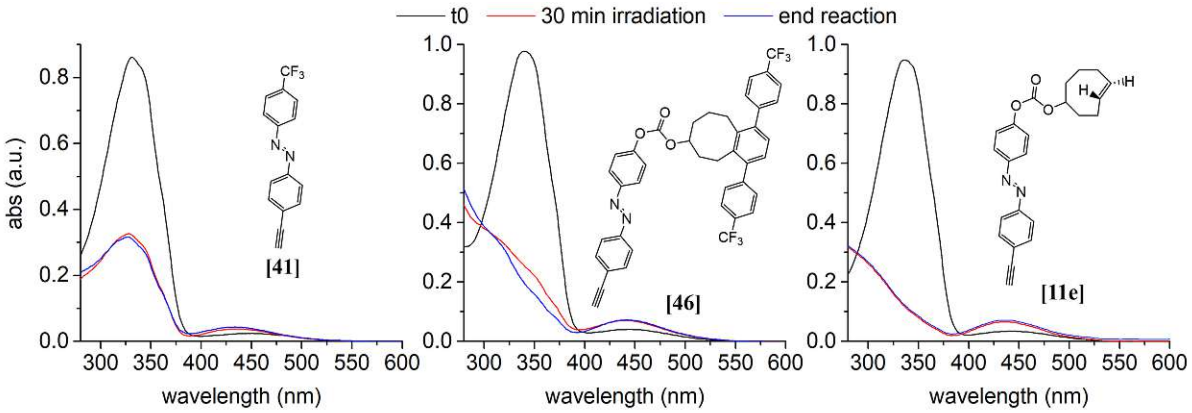

Figure 44: UV spectra of the reaction mixtures for *cis* immobilization for azobenzenes **[41]**, **[46]** and **[11e]**. The black lines represent the spectra before irradiation of the reaction mixture, the red ones after 30 minutes irradiation with the 365 nm LED and the blue ones the reaction mixture at the end of the reaction (180 minutes).

Figure 45 presents the photoswitchability analysis by WCA as well as the FTIR of the obtained surfaces. It seems that even though we used such a long reaction time, all the obtained surfaces are photoswitchable. Since the azobenzenes were immobilized in the *cis* configuration, the first irradiation cycle was performed with a halogen lamp to switch the compound to *trans*. This process led to an increase in the WCA showing that the obtained surfaces are photoswitchable and that indeed the compound was successfully immobilized on the *cis* configuration. Like before a total of 6 irradiation cycles alternating between a halogen lamp and a 365 nm LED were carried. The ΔWCA of these 6 cycles is 9.5° for **[SiF-41*cis*]**, 4.3° for **[SiF-46*cis*]** and 3.5° for **[SiF-11e*cis*]**. These values are the same as previously obtained with the *trans* immobilization, except for **[SiF-41*cis*]**. In this case the *cis* immobilization led to a 2° higher ΔWCA. This shows that with the *cis* immobilization we were able to obtain photoswitchable surfaces with similar or better properties as with the *trans* immobilization, but with no need for optimization.

Die approbierte gedruckte Originalversion dieser Dissertation ist an der TU Wien Bibliothek verfügbar.
The approved original version of this doctoral thesis is available in print at TU Wien Bibliothek.

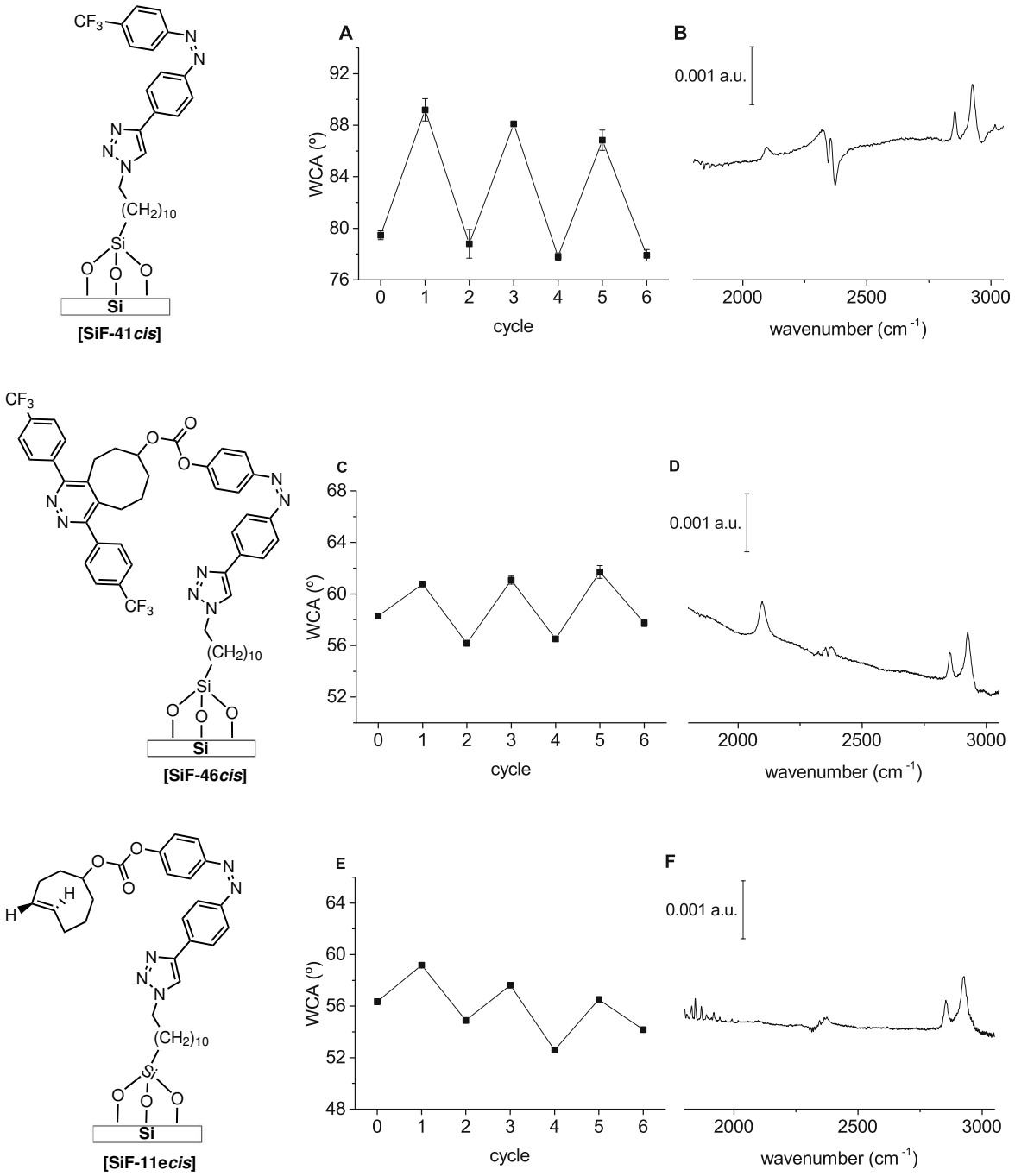

Figure 45: (A,C,E) Analysis by WCA of the photoswitching of **[SiF-41*cis*]**, **[SiF-46*cis*]** and **[SiF-11e*cis*]**, respectively. The cycle 0 corresponds to the WCA before irradiation, odd number cycles to irradiation with a halogen lamp and even number cycles to irradiation with 365 nm. **(B,D,F)** FTIR spectra of **[SiF-41*cis*]**, **[SiF-46*cis*]** and **[SiF-11e*cis*]**, respectively.

Looking at the FTIR of **[SiF-41*cis*]** and **[SiF-46*cis*]** we can see that there is still azide on the

Die approbierte gedruckte Originalversion dieser Dissertation ist an der TU Wien Bibliothek verfügbar.
The approved original version of this doctoral thesis is available in print at TU Wien Bibliothek.

surface after the reaction. However, for **[SiF-11e*cis*]** it seems like there is no azide left which we found puzzling since this should mean that the surface is overcrowded and no photoswitching is possible. Trying to explain this observation, a control experiment was performed to see if there is any azide decomposition during azobenzene immobilization, since organic azide can be decomposed by UV light (normally lower wavelengths than the one used for *cis* immobilization).[178] For that, surface **[SiF-N$_3$]** was treated under the CuAAC conditions with CuI/DIPEA and under irradiation, but no azobenzene was added. After the usual 180 minutes a FTIR of this surface was recorded and compared with the one obtained before irradiation (Figure 46), showing that before and after irradiation nothing happens to the azide. Therefore the FTIR of **[SiF-11e*cis*]** cannot be explained by any azide decomposition.

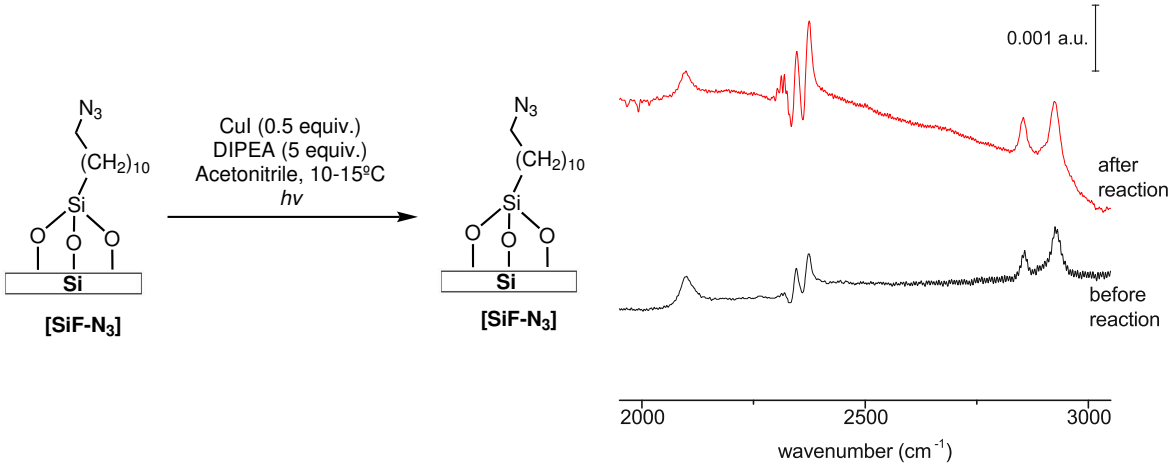

Figure 46: Control experiment to check if the azide is not decomposed in the reaction conditions of the *cis* immobilization.

Since in the *cis* immobilization the temperature of the reaction also had to be reduced, a final control experiment was performed to check if the lower temperature for this step influenced our results. For that azobenzene **[41]** was chosen as a model compound. The reaction mixture was prepared such as in the *cis* immobilization but not placed under irradiation, meaning that if the temperature was responsible for the prevention of the surface overcrowding we should obtain in this case also a photoswitchable surface. As expected a photoswitchable surface was not obtained (no decrease in the WCA after irradiation) and the azide on the surface was almost completely consumed (Figure 47). Therefore we conclude that the temperature has

Die approbierte gedruckte Originalversion dieser Dissertation ist an der TU Wien Bibliothek verfügbar.
The approved original version of this doctoral thesis is available in print at TU Wien Bibliothek.
TU Bibliothek Your knowledge hub WIEN

not significantly affected our results.

Another possible control experiment to be performed in the future would be, after the cis immobilization protocol, to reuse the surfaces and try to completely coat them and confirm that no azide band is present and no photoswitching is observed.

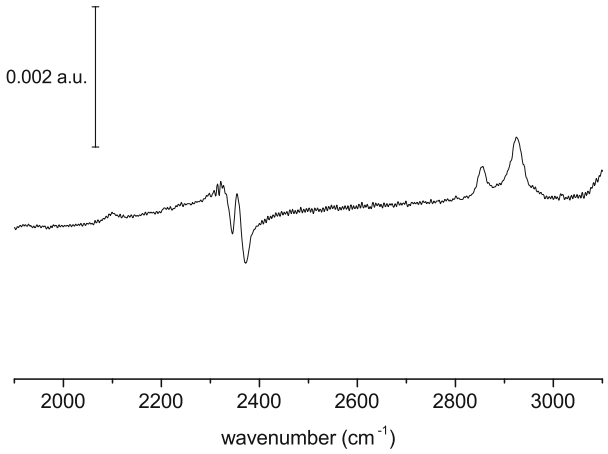

Figure 47: FTIR of the obtained surface after the temperature control experiment.

C.2.6 Aiming for an increased difference in the WCA - immobilization on rough surfaces

Thanks to the difference in the dipole moment of the *trans* and *cis* isomers, WCA has been used as a simple tool to follow the photoswitching of azobenzenes immobilized on surfaces. However, the difference in the WCA upon irradiation on flat surfaces is normally small and highly dependent on the hydrophobicity/hydrophilicity of the group on top of the azobenzene.

As previously stated in Section B.2 several approaches have been used to increase the difference in WCA between the *trans* and *cis* isomers. In all of the previously mentioned approaches the azobenzene has not been directly chemisorbed on a rough substrate with a modified morphology. To the best of our knowledge Bian et al. were the only ones that have tried it, however the ΔWCA of their azobenzene-chemisorbed micropatterned-silicon was only of 4°.[68]

Die approbierte gedruckte Originalversion dieser Dissertation ist an der TU Wien Bibliothek verfügbar.
The approved original version of this doctoral thesis is available in print at TU Wien Bibliothek.
TU Bibliothek Your knowledge hub WIEN

In this section we aimed to achieve an increased ΔWCA by chemisorption of azobenzene **[41]**. Silicon nanowires, porous silicon and rough aluminum were tested as possible substrates to achieve this goal.

C.2.6.1 Silicon nanowires

As previously explained silicon is an ideal substrate (see Section C.2.3). Taking that into account and the known chemistry for the preparation of organic monolayers on silicon (used in C.2.3), we have started by using silicon for the preparation of rough substrates.

Silicon nanowires (SiNW) were our first choice since their properties (e.g. shape, diameter, length and orientation) can be easily tuned with metal-assisted chemical etching, a versatile method that uses a noble metal as a catalyst to generate nanostructures on silicon.[179] Figure 48 schematically explains the metal-assisted chemical etching process used in this thesis to prepare the SiNW. First the silicon is placed in a mixture of $AgNO_3$ and HF to be covered with the catalyst, silver. The silver covered silicon is afterwards transferred to H_2O_2/HF, leading to the electrochemical etching of the silicon, where two main reactions take place. In the first place the silver reduces the H_2O_2 (Reaction 1). The hole generated by this process is transferred to the silicon, oxidizing it, and the HF dissolves the oxidized silicon (Reaction 2), generating the nanowire. Here the corresponding reactions can be found:[180]

$$2\,Ag + H_2O_2 + 2\,H^+ \longrightarrow 2\,Ag^+ + 2\,H_2O \qquad \textbf{Reaction 1}$$

$$Si + 4\,Ag^+ + 6\,F^- \longrightarrow 4\,Ag + {SiF_6}^{2-} \qquad \textbf{Reaction 2}$$

$$Si + 2\,H_2O_2 + 6\,F^- + 4\,H^+ \longrightarrow {SiF_6}^{2-} + 2\,H_2O \qquad \textbf{Net Reaction}$$

To stop the etching process the silicon is transferred to a HNO_3 solution that dissolves the silver and, finally, a strong oxidizing solution, piranha solution (H_2SO_4 96% : H_2O_2 36% = 1:4) is used to clean and oxidize the surface.

Die approbierte gedruckte Originalversion dieser Dissertation ist an der TU Wien Bibliothek verfügbar.
The approved original version of this doctoral thesis is available in print at TU Wien Bibliothek.
TU Bibliothek Your knowledge hub WIEN

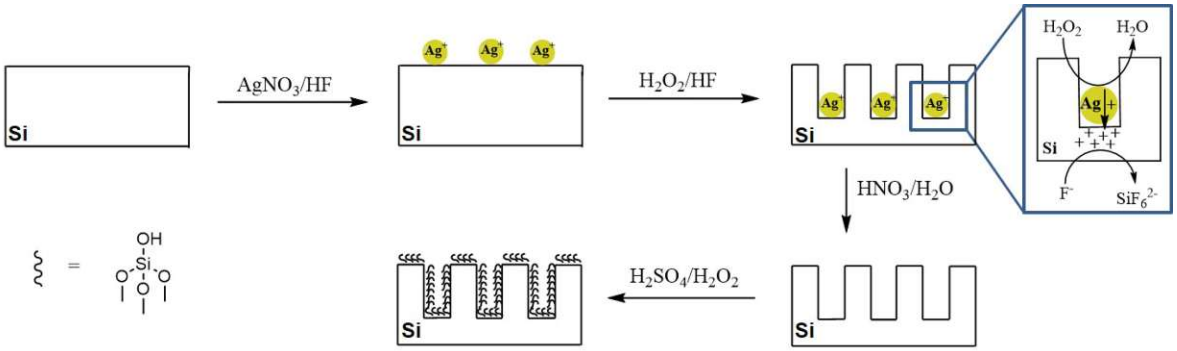

Figure 48: Preparation of silicon nanowires (SiNW) by metal-assisted chemical etching using $AgNO_3$, H_2O_2 and HF.

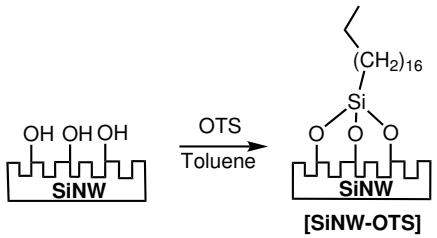

Scheme 14: Coating of SiNW with octadecyltrichlorosilane (OTS).

Since the preparation of SiNW is a complex process, in the first place we wanted to control the quality of the SiNW produced by us. For that nanowires were etched at different H_2O_2 concentrations (0.03 M, 0.06 M, 0.12 M and 0.24 M), coated with octadecyltrichlorosilane (OTS) (Scheme 14) and analyzed by FTIR (Figure 49). If the etching procedure is working smoothly the length of the wires should increase with the concentration of H_2O_2, generating a higher area for coating. As a consequence the area of the CH stretching bands (2770-3000 cm^{-1}) in the FTIR should increase. Figure 49B shows the FTIR of the obtained surfaces and as expected the area of the CH stretching bands increases with the H_2O_2. The area of the CH peaks was also integrated showing that the doubling of the $[H_2O_2]$ generates an area two times bigger, meaning that the area for functionalization also doubles.

The obtained OTS coated SiNW were also analyzed by WCA. According to the literature, SiNW etched in the previously stated conditions and coated with OTS should be superhydrophobic ($\theta > 150°$) and give a drop in the Cassie-Baxter state.[89,170] It is important that we use a system with these properties for azobenzene immobilization since the biggest ΔWCA be-

Die approbierte gedruckte Originalversion dieser Dissertation ist an der TU Wien Bibliothek verfügbar.
The approved original version of this doctoral thesis is available in print at TU Wien Bibliothek.
TU Bibliothek Your knowledge hub WIEN

tween *cis* and *trans* should be obtained if we start with a superhydrophobic Cassie-Baxter state and upon irradiation we attain a superhydrophilic Wenzel state.[92] A way to determine if the drop is in the Cassie-Baxter or Wenzel state is to determine the angle hysteresis, meaning the difference between the advancing and receding contact angles. These angles can be measured by tilting the surface with a drop and the advancing and receding angles correspond to the angles on each side of the drop just before it starts to slide. If the hysteresis is low, it is assumed that the drop is on the Cassie-Baxter state. In the Wenzel state the drop is "stuck" in the pores and sliding becomes much harder.[181]

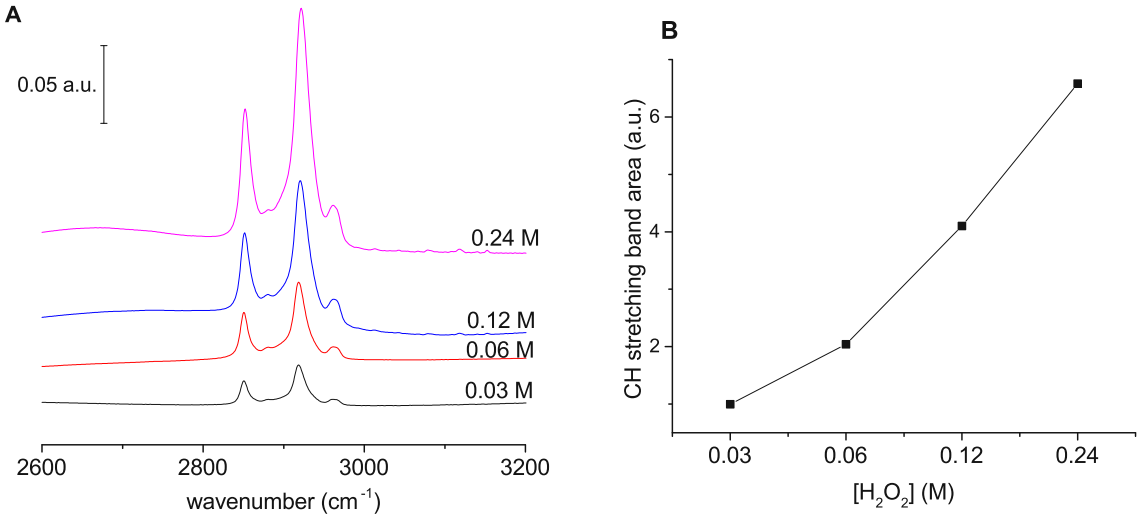

Figure 49: (A) FTIR of the OTS coated SiNW etched with 0.03 M, 0.06 M, 0.12 M and 0.24 M of H_2O_2. **(B)** Relation between the $[H_2O_2]$ and the area of the CH stretching bands (2770-3000 cm^{-1}).

Table 1: Static, advancing and receding angles (water contact angles) as well as angle hysteresis for flat silicon (non-etched, $[H_2O_2]$ = 0 M) and SiNW etched with 0.03 M, 0.06 M, 0.12 M and 0.24 M, all coated with OTS.

$[H_2O_2]$ (M)	Static angle θ (°)	Advancing angle θ_{adv} (°)	Receding angle θ_{rec} (°)	Angle hysteresis (°)
0	110.6	111.4	92.5	18.9
0.03	159.3	159.9	134.9	25
0.06	158.9	162.9	144.2	18.7
0.12	160.7	162.1	142.1	20
0.24	158.9	163.7	141.1	22.6

Die approbierte gedruckte Originalversion dieser Dissertation ist an der TU Wien Bibliothek verfügbar.
The approved original version of this doctoral thesis is available in print at TU Wien Bibliothek.
TU Bibliothek Your knowledge hub WIEN

Table 1 presents the static angles and the angle hysteresis (water contact angles) for the OTS coated SiNW and flat silicon. It is possible to see that all of the obtained SiNW have a higher angle than the flat silicon (110.6°) and are superhydrophobic, with angles varying from 158.9° to 160.7°. The angle hysteresis is also always below 25°, therefore we assume that the drops are in the Cassie-Baxter state. These results match relating findings in the literature.[170]

According to the literature, at [H_2O_2] higher than 0.06 M the wires generated during the etching process start to clump together due to its higher length.[170] Therefore we have chosen to use SiNW etched with 0.06 M to immobilize our azobenzene **[41]**, due to its good balance between increased roughness and stable structure. Before coating this SiNW with the azobenzene, scanning electron microscopy (SEM) was used to confirm its structure. The images of the cross-section and the top-view of the SiNW etched with 0.06 M H_2O_2 are presented in Figure 50. On the cross-section we see homogeneous wires with a length of approximately 2.24 µm and on the top-view small pores. These results are in conformity with the literature.[170]

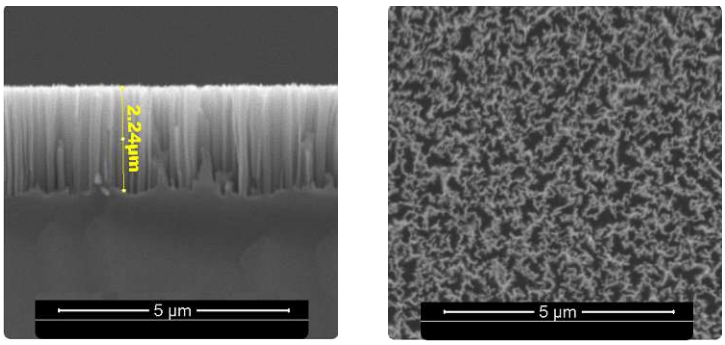

Figure 50: Scanning electron microscopy images of a SiNW etched with 0.06 M H_2O_2. On the left the cross-section and on the right the top-view.

The next step is then to prepare an azide-coated SiNW and immobilize azobenzene **[41]** *via* CuAAC. To obtain the azide-coated SiNW **[SiNW-N_3]** we have employed the same protocol used to attain the azide coated-flat silicon surface (see Section C.2.3). To confirm the formation of the azide coated SiN [SiNW-N_3] a FTIR was measured, showing the expected azide stretching band at 2130-2080 cm^{-1} (Figure 51). Unfortunately, the monolayer formation cannot be checked by ellipsometry for the SiNW since ellipsometry cannot be used with rough surfaces.

Afterwards, the *trans* immobilization of azobenzene **[41]** on the **[SiNW-N_3]** was performed using the optimized conditions previously found for the flat surface - CuI/DIPEA and 15

Die approbierte gedruckte Originalversion dieser Dissertation ist an der TU Wien Bibliothek verfügbar.
The approved original version of this doctoral thesis is available in print at TU Wien Bibliothek.
TU Bibliothek Your knowledge hub WIEN

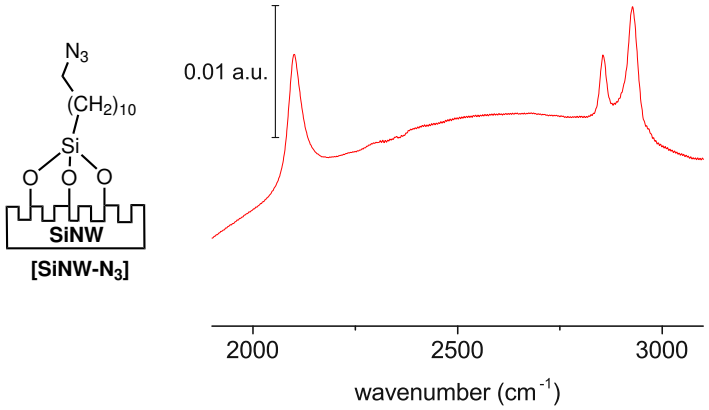

Figure 51: FTIR of an azide-coated SiNW **[SiNW-N_3]**.

minutes reaction. Figure 52A presents the analysis of the surface photoswitching by WCA. As expected, the WCA of this surface is much higher than on the flat surface (85° to 136°) since we would expect to obtain a rough surface in the Cassie-Baxter state, where the WCA is always higher on a rough surface. However, there is no decrease in the WCA after irradiation with 365 nm. Since the surface area is higher for the SiNW than for the flat surface, we increased the CuAAC reaction time for 30, 60 and 180 minutes, in case the coverage of the SiNW with the azobenzene was not high enough. The WCA of the surfaces increases with the reaction time due to the higher amount of hydrophobic azobenzene on top of the SiNW. Unfortunately, this has not led to a decrease of the WCA after irradiation with 365 nm. The FTIR (Figure 52B) shows that for all the cases there is still azide left on the surfaces after reaction, even after 180 minutes, unlike on the flat surface, therefore surface overcrowding does not explain these results.

One possible explanation for this behavior might be that the pore size of the SiNW is too small. Jiang et al. showed that when coating a micro-patterned silicon with an CF_3azobenzene-containing polymer, the ΔWCA between *trans* and *cis* is dependent on the distance between the pillars on the structure. They prepared structures with pillars distanced by 5, 10, 20, 40, 50 and 60 µm and the ΔWCA increased from 19° (5 µm) to 66° (40 µm). To distances higher than 40° the ΔWCA reduces again drastically.[93] Even their smallest size, 5 µm, is much bigger than the pore in our nanowires. Maybe this relation is also true for chemisorption of the azobenzene

Die approbierte gedruckte Originalversion dieser Dissertation ist an der TU Wien Bibliothek verfügbar.
The approved original version of this doctoral thesis is available in print at TU Wien Bibliothek.
TU Bibliothek Your knowledge hub WIEN

and the pore size must be bigger in order to obtain an observable ΔWCA.[93]

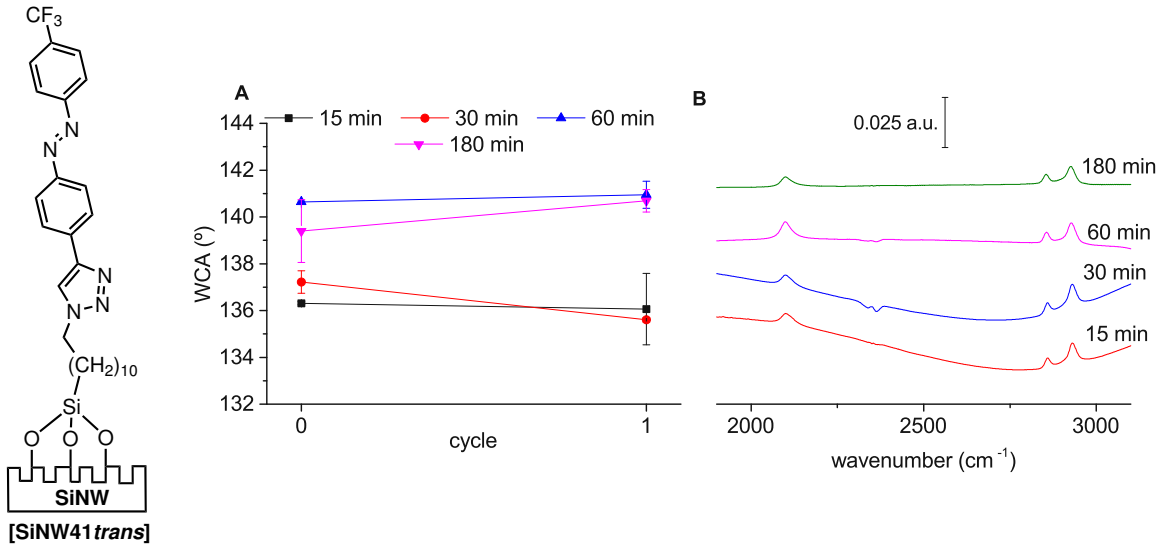

Figure 52: (A) Analysis by WCA of the photoswitching of the **[SiNW41*trans*]** obtained at different reaction times: 15, 30, 60 min and 180 min. Cycle 0 represents the WCA before irradiation and cycle 1 after irradiation with 365 nm. **(B)** FTIR of **[SiNW41*trans*]** after 15, 30, 60 and 180 minutes.

C.2.6.2 Porous silicon

Porous silicon (PSi) is another type of rough silicon, which has a porous surface as the name indicates .[182] We have decided to use a commercially available PSi with a pore size between 10-15 nm to check if this substrate would be viable to obtain an azobenzene-coated surfaces with an increased ΔWCA. For that the SiP was coated with OTS (**[SiP-OTS]**) and the static WCA was measured hoping to obtain a superhydrophobic surface. However, the WCA was of only 116.7° (Table 2) which is in the same range as the WCA for a flat silicon surface coated with OTS. Before functionalization of the SiP, it was sonicated in toluene and then oxidized. In case the toluene is still in the pores, the oxidation will not be efficient, therefore, we introduced an extra drying step before oxidation. After sonication the SiP was placed in acetone for 2 hours and afterwards overnight in high-vacuum at 50°C. Afterwards it was oxidized and coated with OTS (**[SiP-OTS]**+drying). Once again we were not able to obtain a superhydrophobic surface. In fact, the obtained WCA is even lower than before (101.3°). This decrease may be due to the removal of some residual water that could be on the SiP or to some structural change provoked by the heating and vacuum.

Die approbierte gedruckte Originalversion dieser Dissertation ist an der TU Wien Bibliothek verfügbar.
The approved original version of this doctoral thesis is available in print at TU Wien Bibliothek.
TU Bibliothek Your knowledge hub WIEN

Table 2: Static water contact angles for **[SiP-OTS]**.

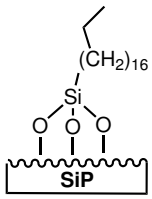

Substrate	Static angle θ (°)
[SiP-OTS]	116.7
[SiP-OTS] + drying	101.3

We conclude that probably the porosity of this SiP substrate is not high enough to generate a superhydrophobic surface. Metal-assisted chemical-etching could also be used to produce SiP with higher porosity to try to attain a superhydrophobic SiP.[179]

C.2.6.3 Aluminum

Aluminum was another practical choice of a substrate to prepare rough surfaces. While the etching process of silicon is somehow complex and requires the use of non-friendly chemicals such as HF, aluminum rough surfaces can be simply obtained by boiling the flat aluminum in water.[183–187] When it is placed in boiling water, a part of the aluminum is dissolved and aluminum oxy hydroxide colloidal particles (bohemite) are formed and deposit on the aluminum, forming a porous structure. The thickness of this layer can be controlled by changing the boiling times.[183,184]

In addition, several superhydrophobic surfaces have been produced in the literature by coating rough aluminum[183,185,187,188] and there are reports of aluminum coated with trichlorosilanes, indicating that the already established chemistry (Section C.2.3) could also be applicable also for this material silicon.[186,189]

For this work, three aluminum substrates were tested: one 99.998% aluminum from ABCR, one aluminum alloy with 97.7% Al/Mg 2%/Mn 0.3% from Sigma-Aldrich and one 99.5% aluminum from Conrad. For practicality reasons these substrates will be named **AlA**, **AlS** and **AlC**, respectively. The name refers to the material (Al) and the first letter of the company where the material was acquired.

In the first place, we aimed to confirm the formation of Bohemite structures on these aluminum substrates. For that, each one was placed in boiling water for 10 and 20 minutes and

Die approbierte gedruckte Originalversion dieser Dissertation ist an der TU Wien Bibliothek verfügbar.
The approved original version of this doctoral thesis is available in print at TU Wien Bibliothek.
TU Bibliothek Your knowledge hub WIEN

SEM images were obtained for these and the untreated samples. The SEM images are presented in Figure 53. Looking at the untreated samples (left column) it is possible to see that **AlA** contains imperfections. Actually these imperfections can be seen by the naked eye.

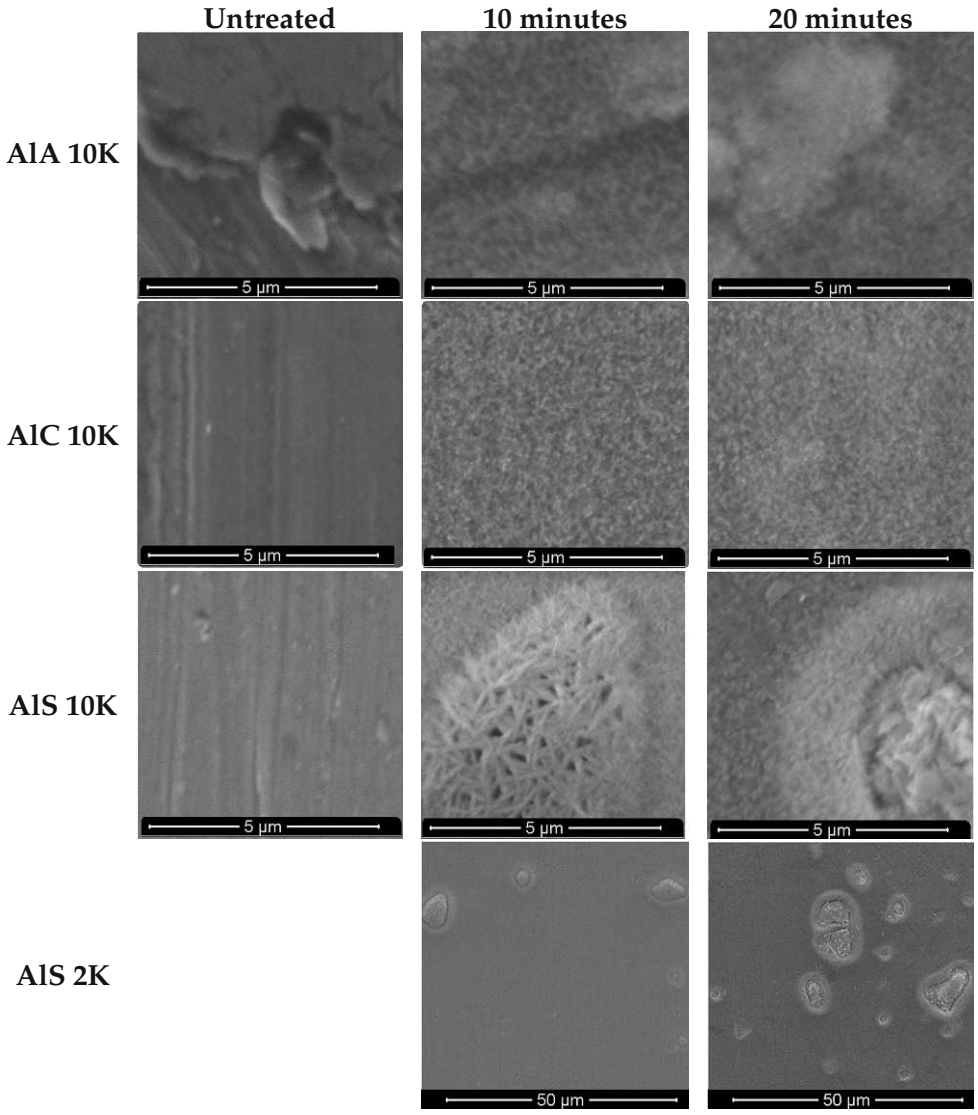

Figure 53: SEM images of the three different aluminum substrates: **AlA** (first row), **AlC** (second row) and **AlS** (third and fourth row) at 2K or 10K magnification. The samples are untreated (first column), boiled 10 minutes (second column) or boiled 20 minutes (third column).

AlS and **AlC** have a much more homogeneous structure. In all the substrates there is a clear morphology change after boiling (middle and right column). In **AlA** it is possible to see the pores formed on the substrate imperfections, while **AlC** has a very homogeneous structure.

Die approbierte gedruckte Originalversion dieser Dissertation ist an der TU Wien Bibliothek verfügbar.
The approved original version of this doctoral thesis is available in print at TU Wien Bibliothek.
TU Bibliothek Your knowledge hub WIEN

Surprisingly on **AlS** a heterogeneous surface is obtained after boiling. After 10 minutes, besides the usual pores, there is the formation of localized wire structures that seem to collapse after 20 minutes. At a lower magnification (2k) it is possible to see that the number of localized structures also increases with the boiling time. Unlike **AlA** and **AlC**, **AlS** is an aluminum alloy with 2% Mg and 0.3% Mn. Nevertheless, other aluminum alloys (also including Mg) have been before treated with hot water to form pores and such wire-like structures have not been observed.[186,190] Saadi et al. found out that actually several other metals besides aluminum can be subjected to hot water treatment to generate nanostructures such as cubes, pyramids, plates, wires, spheres and leaf-like. In this list Mg and Mn are included, forming respectively a leaf-like structure and spheres. Actually, magnesium forms nanostructures even faster than aluminum when in hot water. Since the morphology of the structure depends on the crystal structure of the formed oxide upon boiling, maybe in our **AlS** there is the formation of other particles besides bohemite due to the Mg and Mn generating this wire-like structures.[190] Since 10 minutes seems to be enough to generate bohemite structures, henceforward a rough aluminum surface will refer to aluminum boiled for 10 minutes.

The next step was to coat the flat and rough aluminum surfaces with OTS, like the SiNW (see Figure 49A), and check if rough superhydrophobic surfaces are obtained. Table 3 presents the obtained static water contact angle for the obtained surfaces. **[AlA-OTS]** presents as expected a big difference in the static contact angle for flat and rough. While the flat surface presents a static angle of 95°, the rough surface is almost superhydrophobic with 143.8°. We also have tried to measure the angle hysteresis, however unsuccessfully. The imperfections present on these surface seem to affect the sliding of the drop since the movement of the drop depended on its position on the surface: sometimes it would not move, sometimes it would move and get stuck again, probably in one of these imperfections. Regarding **AlS**, we have obtained a flat surface with a static angle of 22.9° and a rough surface with 115.3°. Since the value for the flat surface is so low we conclude that probably these surfaces have not been completely coated with OTS. Finally for **AlC** we obtained quite inconsistent results. The angle variation between surfaces was quite big, both for the flat and rough, as displayed by the error.

Unfortunately, ellipsometry could not be used to confirm the formation of a monolayer on top of the flat aluminum since the polarized light is scattered by the aluminum, preventing a

Die approbierte gedruckte Originalversion dieser Dissertation ist an der TU Wien Bibliothek verfügbar.
The approved original version of this doctoral thesis is available in print at TU Wien Bibliothek.
TU Bibliothek Your knowledge hub WIEN

Table 3: Static water contact angles for **AlA**, **AlS** and **AlC**, flat and rough, coated with OTS.

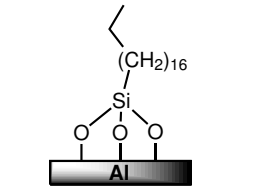

[AlAF-OTS] [AlAR-OTS]
[AlCF-OTS] [AlCR-OTS]
[AlSF-OTS] [AlSR-OTS]

	Static angle (°)	
	Flat	**Rough**
[AlA-OTS]	95.0±4.2	143.8±3.4
[AlS-OTS]	22.9±4.2	115.3±4.9
[AlC-OTS]	83.5±12.2	128.8±13.9

proper measurement. Therefore, to better understand the previous results we could only rely on IRRAS (Infra-red reflection absorption spectroscopy). The IR of the obtained surfaces are presented in Figure 54. In the IRs of **[AlA-OTS]** the CH stretching bands are more intense for the rough surface than for the flat. This reflects the higher coated area in the rough surface and is consistent with the static angles. On the other hand, for **[AlS-OTS]** no CH stretching bands are observable for the flat surface, explaining the low contact angle for this surface. Finally, the IRs of the **[AlC-OTS]** express the inconsistent results for the static contact angle. In Figure 54 two examples of a rough and flat surfaces are presented. We have observed that the intensity of the CH stretching bands was quite different comparing the same type of substrate (rough or flat) and there are flat surfaces that present CH stretching bands with the same intensity as rough.

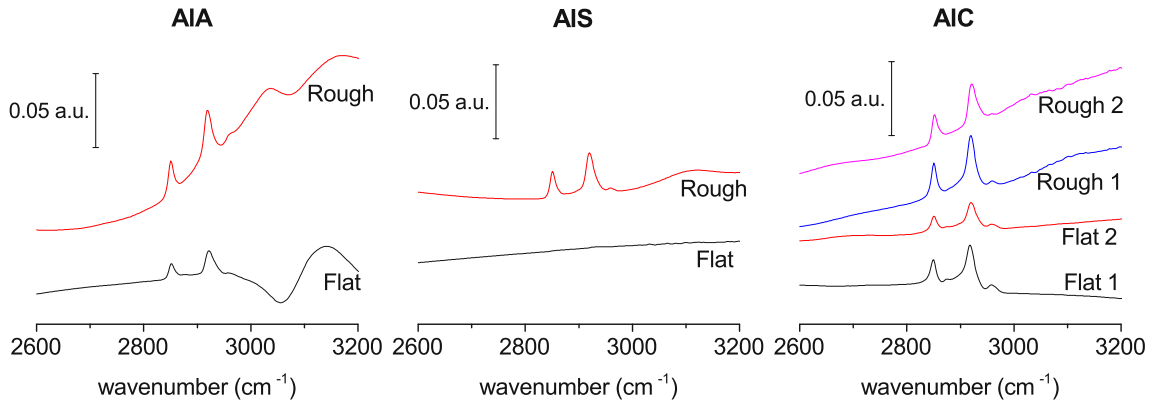

Figure 54: IRRAS of the obtained flat and rough OTS coated Aluminum: **AlA** flat and rough (left), **AlS** flat and rough (middle) and **AlC** flat and rough (right).

Taking into account the previous data, we decided to use **AlA** for azobenzene **[41]** immobilization. To obtain an azide-coated **AlA** surface we have used the same process as for the

Die approbierte gedruckte Originalversion dieser Dissertation ist an der TU Wien Bibliothek verfügbar.
The approved original version of this doctoral thesis is available in print at TU Wien Bibliothek.
TU Bibliothek Your knowledge hub WIEN

silicon (see Scheme 13). First the surface is coated with BUTS and afterwards NaN_3 is used to insert the azide. Table 4 presents the static water contact angle for the obtained BUTS coated **[AlA-BUTS]** and azide coated **[AlA-N_3]** aluminum. After coating with BUTS the flat surface presents a angle of 31.5°±1.4 and the rough surface is superhydrophilic. Upon azide coating the angle increases for 54.6°±1 and 43.8°±3.9, respectively. This increase shows that the nucleophilic substitution is probably taking place as expected.

Table 4: Static water contact angles for **[AlA-BUTS]** and **[AlA-N_3]**. The * sign means that a specific angle could not be measured because the water drop would immediately completely wet the surface and become invisible.

	Static angle (°)	
	Flat	**Rough**
[AlA-BUTS]	31.5±1.4	*
[AlA-N_3]	54.6±1	43.8±3.9

IR of the obtained **[AlA-N_3]** surfaces were also measured to verify the presence of both the CH and azide stretching bands. The spectra are presented in Figure 55. In the flat **[AlA-N_3]** no stretching bands are observable while on the rough one weak bands are present. This shows that there is a problem in the coating of the surfaces. Probably, the monolayer formation is not taking place efficiently.

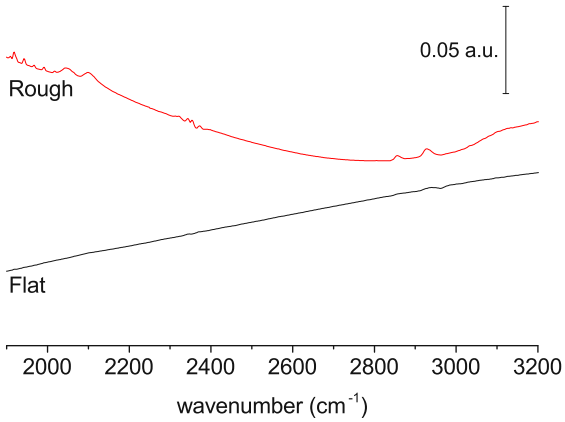

Figure 55: IRRAS of the obtained flat and rough N_3 coated Aluminum **[AlA-N_3]**.

Notwithstanding, the static WCA show that there must be some compound on the surface, therefore, we have proceeded to attempt the immobilization of azobenzene **[41]** as described

Die approbierte gedruckte Originalversion dieser Dissertation ist an der TU Wien Bibliothek verfügbar.
The approved original version of this doctoral thesis is available in print at TU Wien Bibliothek.
TU Bibliothek Your knowledge hub WIEN

in Section C.2.4 (CuI/DIPEA, 15 minutes). Figure 56 shows the analysis of the photoswitchability of the obtained flat surface **[AlAF41*trans*]**. It seems that a photoswitchable surface is nevertheless obtained with a ΔWCA of 7.5°.

Unfortunately, the immobilization of azobenzene **[41]** on rough **[AlAR-N_3]** was not successful. Upon using the same reaction conditions as to obtain **[AlAF41*trans*]** the WCA is only of 65°, quite distant from the hydrophobic surface we would be expecting. In addition, upon irradiation with 365 nm no decrease in the WCA is observed. Even when coating the surface completely (overnight reaction) the WCA only increases to 83.1° and once again no decrease in the WCA is observed upon irradiation. It seems that without a complete monolayer it is not possible to get close to the superhydrophobic range and observe a ΔWCA.

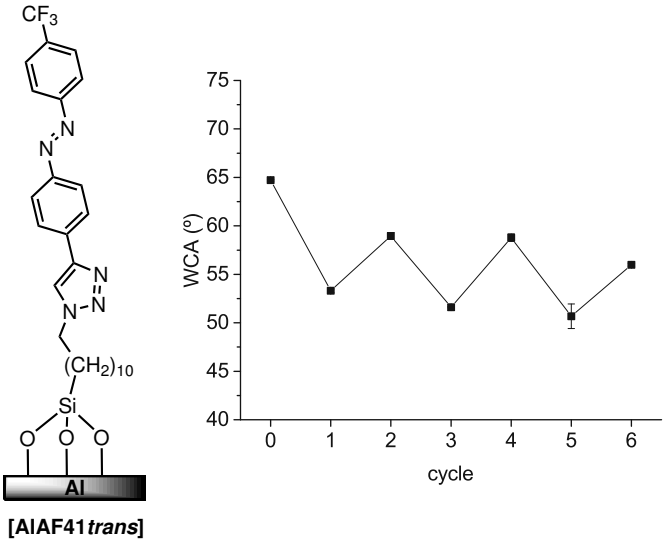

Figure 56: Immobilization of azobenzene **[41]** on flat **[AlAF-N_3]** by CuAAC and analysis by WCA of the photoswitchability of the obtained surface **[AlAF41*trans*]**. Cycle 0 corresponds to the WCA before irradiation, odd number cycles to irradiation with 365 nm and even number cycles to irradiation with a halogen lamp.

Acids and phosphonic acids are commonly used in the literature to coat aluminum substrates, therefore being a good alternative to try to solve the previously presented coating problems.[184,185,187,191] Another improvement could also be done in the preparation of the rough aluminum in boiling water. In the literature it is stated that treatment of aluminum in water at 75°C is sufficient to generate a porous structure.[190] Maybe reducing the temperature could help with the reproducibility issues of **AlC**.

Die approbierte gedruckte Originalversion dieser Dissertation ist an der TU Wien Bibliothek verfügbar.
The approved original version of this doctoral thesis is available in print at TU Wien Bibliothek.
TU Bibliothek Your knowledge hub WIEN

C.3 Towards a photoswitchable DNA origami platform for T-cell activation

T-cells are a component of our adaptive immune system, meaning that they take part in a specific immune response against an antigen (foreign substance to our body). Nevertheless, T-cells are not capable of directly recognizing an antigen. They rely on antigen-presenting cells (APC), such as dendritic cells and macrophages, to first process the antigen and then display it on their surface.[192] Figure 57 presents a representation of this process. The processed antigen is presented on the APC's cell surface by the major histocompatibility complex (MHC), a membrane protein. The MHC with the antigen is afterwards recognized by a receptor on the membrane of the T-cell, named T-cell receptor (TCR), initiating the immune response.

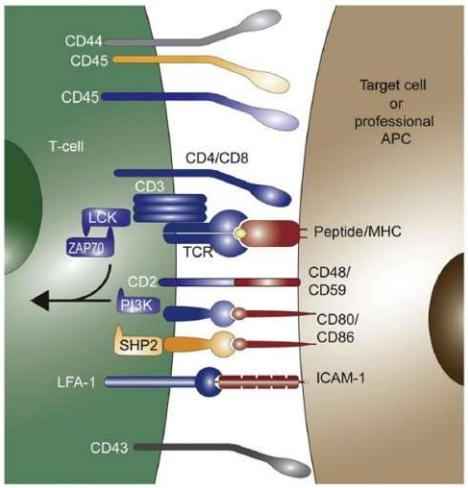

Figure 57: T-cell receptor interaction with an antigen-presenting cell via interaction with the MHC.[193]

For a long time scientists have been interested in the study of such an important biological process.[194,195] One method to study this process consists in using DNA origami. DNA origami is a technique that allows a relatively easy preparation of 2D and 3D nanostructures of DNA. Taking advantage of the highly specific Watson-Crick base pairing, a single-stranded DNA scaffold is folded into a specific shape by using smaller single-stranded DNAs called staples (Figure 58A).[196–198] Ever since 2006, when Rothumend has for the first time used the DNA origami technique to assemble simple 2D DNA nanostructures such as rectangles and five-point stars and a more complex DNA smiley face, several other 2D and 3D shapes have been

Die approbierte gedruckte Originalversion dieser Dissertation ist an der TU Wien Bibliothek verfügbar.
The approved original version of this doctoral thesis is available in print at TU Wien Bibliothek.
TU Bibliothek Your knowledge hub WIEN

assembled.[199] Among these, pyramids, cubs, nanoflasks and even flowers and rabbits (Figure 58B-K). In addition to the creation of structurally interesting and beautiful nanostructures, DNA origami allows to precisely spatially arrange any molecule on the nanoscale by modifying its staples. Therefore, these systems have been applied to study molecule interactions (e.g. DNA-enzyme activity, protein-protein, aptamer-protein interaction, enzymatic cascades) used as a biosensors and for drug delivery.[196–198]

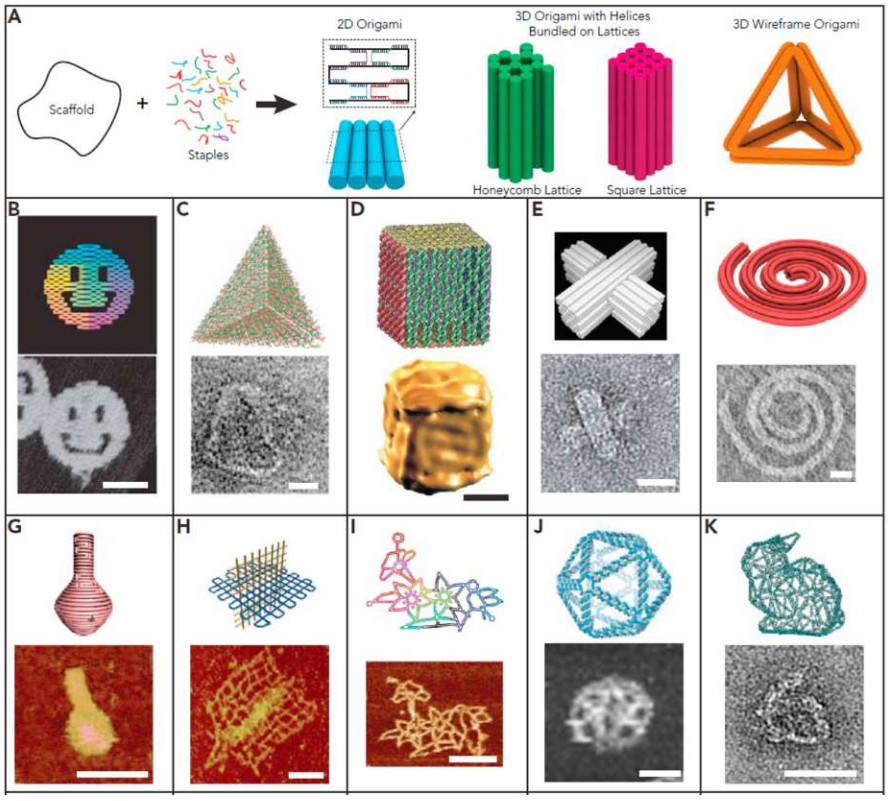

Figure 58: (A) Assembly process of DNA origami nanostructures. **(B-K)** Images of structures designed using the DNA origami technique.[198]

To study T-cell activation Motsch et al. have decorated a DNA origami platform with TCR ligands (either a single-chain antibody fragment or a peptide-loaded MHC II), forming a surface that mimics an APC (Figure 59A).[200] To attach the ligands on the DNA origami, they have taken advantage of the well-known Streptavidin(SA)-biotin technology. SA is a 56 KDa homotetrameric protein from the bacterium *Streptomyces avidinii*, which is known for its high thermostability, resistance against extreme pH and proteolytic enzymes, high tolerance for extensive mutations and a highly specific and stable binding ($K_d \approx 10^{-14}$ M) to biotin. These features

Die approbierte gedruckte Originalversion dieser Dissertation ist an der TU Wien Bibliothek verfügbar.
The approved original version of this doctoral thesis is available in print at TU Wien Bibliothek.
TU Bibliothek Your knowledge hub WIEN

have led to development of several application using SA-biotin technology as a foundation, such as the rational design of novel host–guest systems for organometallic chemistry applications, labeling, separation (affinity chromatography e.g.) and targeting of structures.[201–203]

(A) DNA origami platform for the study of T-cell activation

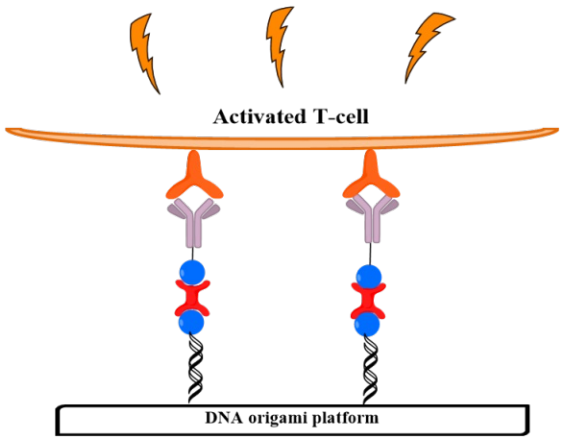

(B) Photoswitchable DNA origami platform for the study of T-cell activation

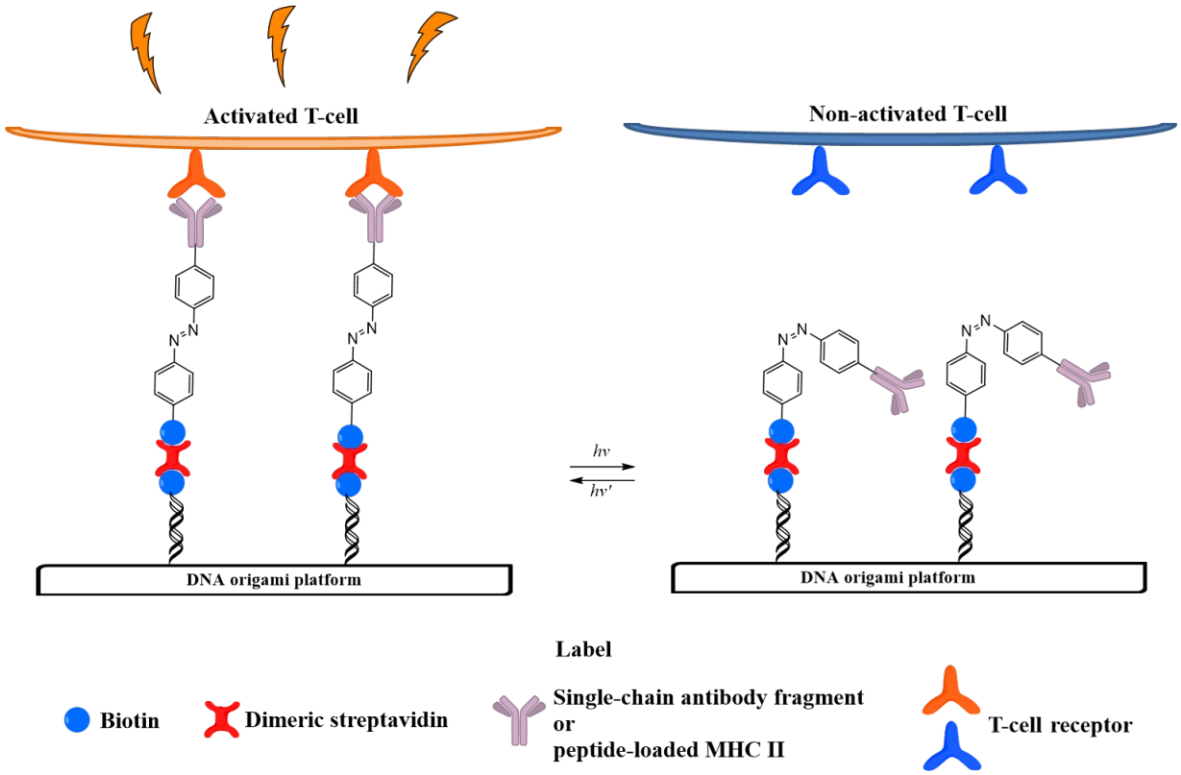

Figure 59: The DNA origami platform used by Motsch et al. (**A**)[200] vs our design of a photoswitchable DNA origami platform (**B**).

Die approbierte gedruckte Originalversion dieser Dissertation ist an der TU Wien Bibliothek verfügbar.
The approved original version of this doctoral thesis is available in print at TU Wien Bibliothek.

In the specific case of Motsch et al., the single-stranded DNA was folded with some staples containing biotin to obtain a DNA origami with biotin that was used to attach a dimeric SA to the platform. The second binding site of the SA allowed to bind a biotin functionalized TCR ligand to the platform.[200]

Our goal was to modify the previously referred DNA origami platform to be able to temporally control the activation of the T-cells by using an azobenzene. Figure 59B presents our approach to obtain such a system. In our design an azobenzene contains both a biotin to enable the attachment to the DNA origami and a single-chain antibody fragment or a peptide loaded MHC II to activate the T-cell. The idea is that when the azobenzene is in the *trans* configuration the T-Cell is activated while in the *cis* it is inactivated. This means that we hope to be able to reversibly activate and deactivate the immune response.

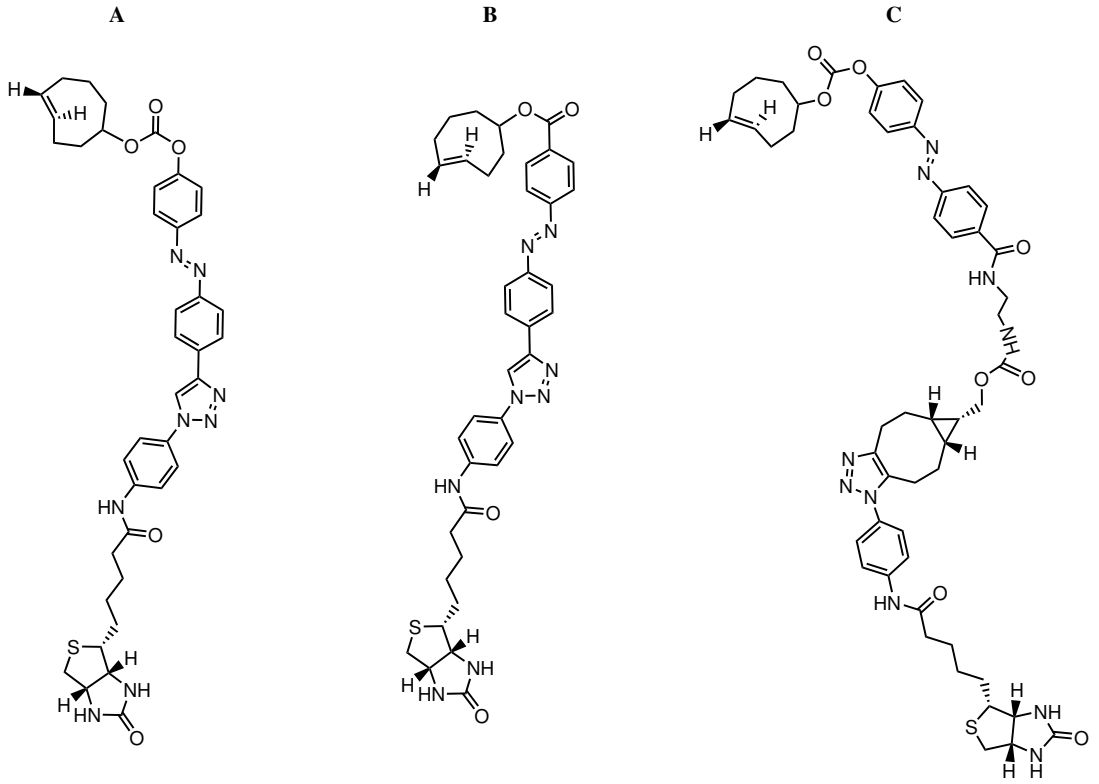

Figure 60: Target structures resulting from the coupling of azobenzenes **[11]** (**A**), **[18]** (**B**) and **[33]** (**C**) with biotin.

To synthesize the azobenzene we have planned to take advantage of our double-click azobenzene approach. To bind the azobenzene and the T-cell ligand we have envisioned to

Die approbierte gedruckte Originalversion dieser Dissertation ist an der TU Wien Bibliothek verfügbar.
The approved original version of this doctoral thesis is available in print at TU Wien Bibliothek.
TU Bibliothek Your knowledge hub WIEN

use the tetrazine ligation click since it is the fastest know click reaction and bioorthogonal. Taking into account this requirement and the double-click azobenzene previously synthesized, azobenzenes **[11]**, **[18]** and **[33]** were considered viable targets to obtain the desired azobenzene with biotin and TCR ligand. Figure 60 presents the target conjugation products resulting from the coupling of the azobenzenes **[11]**, **[18]** and **[33]** with biotin.

C.3.1 Functionalization of double-click azobenzenes with biotin

Taking into account the double-click azobenzenes that we will use in this Section (**[11]**, **[18]** and **[33]**), a biotin functionalized with an azide is necessary since an alkyne and a strain-promoted alkyne are left on these azobenzenes for binding to the biotin (TCO will bind to the TCR ligand).

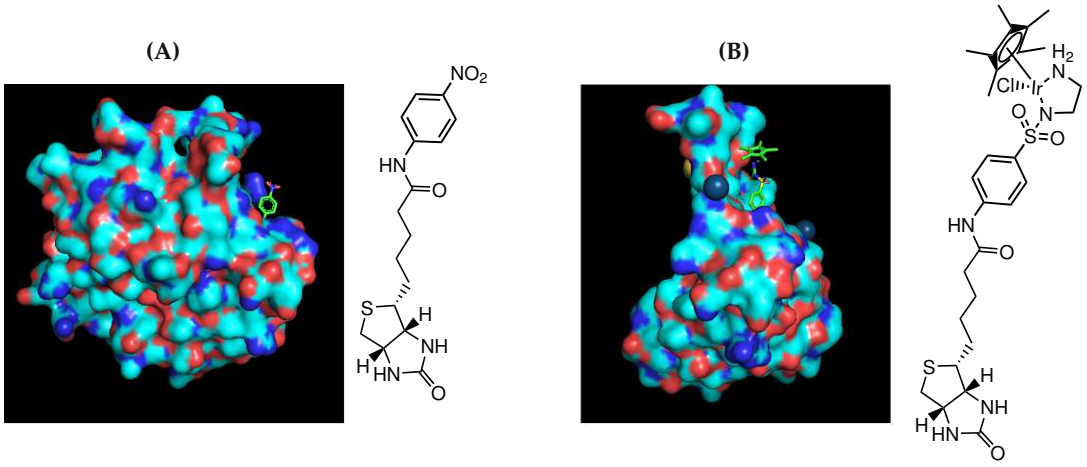

Figure 61: Pymol image of the crystal strucure of SA mutant L123R (M1) complexed with biotynyl *para*-nitroanilide (PDBcode 1RXH) **(A)**[204] and of SA mutant S112A-N118O-K121A-S122M complexed with [Cp*Ir(biot-p-L)Cl] (PDBcode 6ESS) **(B)**[205].

In the design of the biotin modified azobenzene there are another two requirements that must be fulfilled: the modified biotin-azobenzene must still be able to bind to SA and, if it binds, the azobenzene needs to be outside of SA's binding site in order to keep the necessary space to switch to the *cis* configuration. According to the literature, one modification that would respect these requirements would be to insert a benzene ring. Figure 61 presents two examples were biotin was modified with a benzene ring.[204,205] In the images it is possible to see that this modification does not prevent the binding of biotin and the benzene ring is already outside the binding site. Therefore, we opted to modify our biotin with a benzene and

Die approbierte gedruckte Originalversion dieser Dissertation ist an der TU Wien Bibliothek verfügbar.
The approved original version of this doctoral thesis is available in print at TU Wien Bibliothek.

afterwards click the azobenzene.

Scheme 15 presents the synthesis of the modified biotin. In the first place, 4-azidoaniline **[51]** was obtained from 4-iodoaniline **[50]** *via* a Ullmann-type copper-catalyzed reaction (copper-catalyzed nucleophilic aromatic substitution).[206,207] Afterwards biotin **[52]** was activated using isobutyl chloroformate to form a mixed-anhydride that undergoes an amidation with 4-azidoaniline **[51]**, forming amide **[53]**.[208] Amide **[54]** was also synthesized using the same method from biotin **[52]** and 4-iodoaniline **[50]** since it could be used for a Sonogashira coupling with azobenzenes **[11]** and **[18]**.

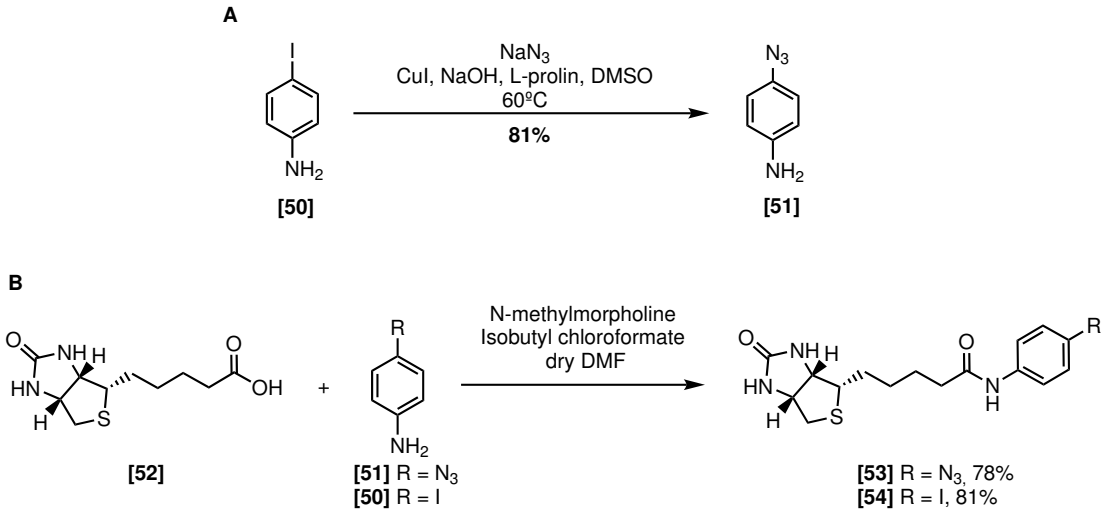

Scheme 15: Synthesis of 4-azidoaniline **[51] (A)** and modified biotin **[53]** and **[54] (B)**.

In first the first place the CuAAC between biotin **[53]** and azobenzenes **[11e]** and **[18e]** was performed (Scheme 16). In the case of coupling between **[11e]** and **[53]** the CuAAC happens, nevertheless the carbonate is cleaved during the reaction. For the coupling of **[18e]** with biotin **[53]**, small amounts of the product are formed but we were not able to isolate it.

Afterwards we have tried a Sonogashira coupling between the azobenenes **[11e]** or **[18a]** and biotin **[54]** (Scheme 17). Even though the coupling between azobenzene **[11e]** and biotin **[54]** has not delivered satisfactory results, the reaction between **[18a]** and **[54]** was successful affording compound **[55]** in 22% yield.

Control experiments were performed to test the stability of azobenzenes **[11e]** and **[18e]** under these reaction conditions. In the case of the CuAAC, three diferent mixtures were

Die approbierte gedruckte Originalversion dieser Dissertation ist an der TU Wien Bibliothek verfügbar.
The approved original version of this doctoral thesis is available in print at TU Wien Bibliothek.
TU Bibliothek Your knowledge hub WIEN

prepared: azobenzene/DIPEA, azobenzene/CuI and azobenzene/DIPEA/CuI. After stirring overnight, decomposition of the starting material was observed in all cases, except in the azobenzene/DIPEA mixture (according to TLC), indicating that the azobenzenes are unstable under the presence of CuI. Regarding the Sonogashira coupling, a similar control experiment was performed, where 4 mixtures were prepared: azobenzene/DIPEA, azobenzene/CuI, azobenzene/$(Ph_3P)_2PdCl_2$ and azobenzene/DIPEA/CuI/$(Ph_3P)_2PdCl_2$. Here it was verified that whenever CuI, $(Ph_3P)_2PdCl_2$ or both are present, the azobenzenes are not stable. These observation explain the previously obtained results. We hypothesize that the instability of the SMs may be due to the complexation of the metal catalysts to the strained double bond of the TCO.

Finally, the SPAAC between biotin **[53]** and azobenzene **[33]** was conducted, affording product **[56]** in 65% yield (Scheme 18).

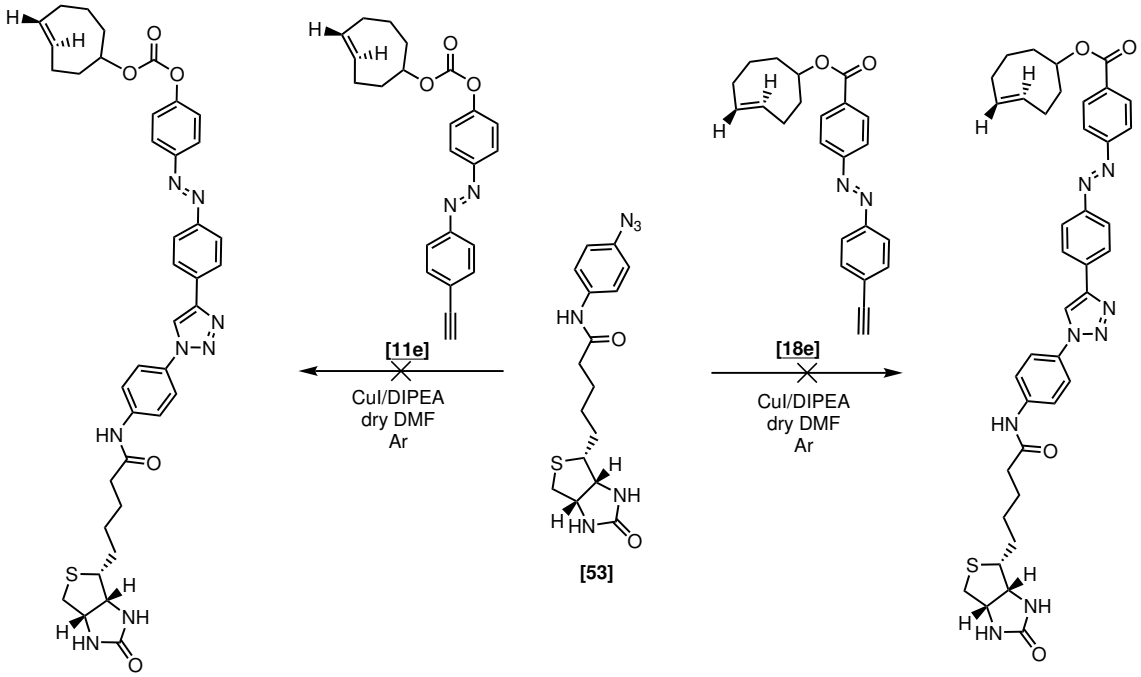

Scheme 16: Unsuccessful CuAAC between modified biotin **[53]** and azobenzenes **[11e]** and **[18e]**.

Die approbierte gedruckte Originalversion dieser Dissertation ist an der TU Wien Bibliothek verfügbar.
The approved original version of this doctoral thesis is available in print at TU Wien Bibliothek.

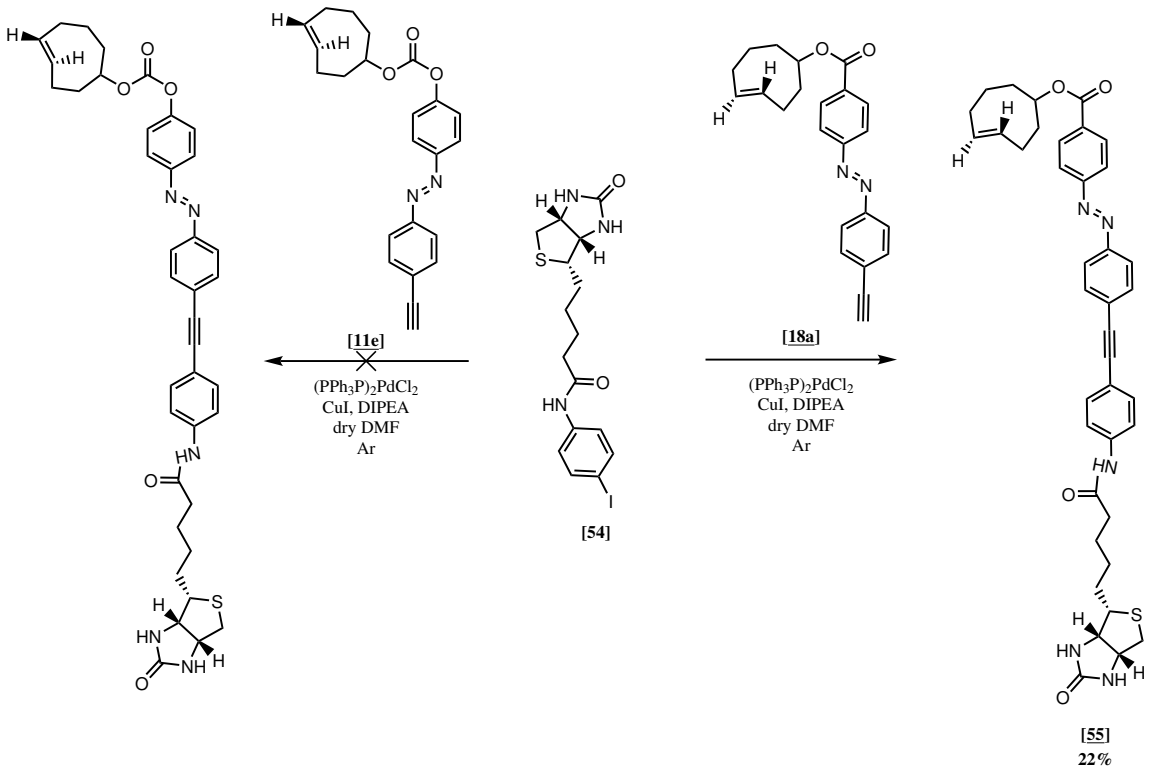

Scheme 17: Sonogashira coupling between **[54]** and azobenzenes **[11e]** and **[18a]**. Sonogashira coupling product **[55]** was successfully obtained.

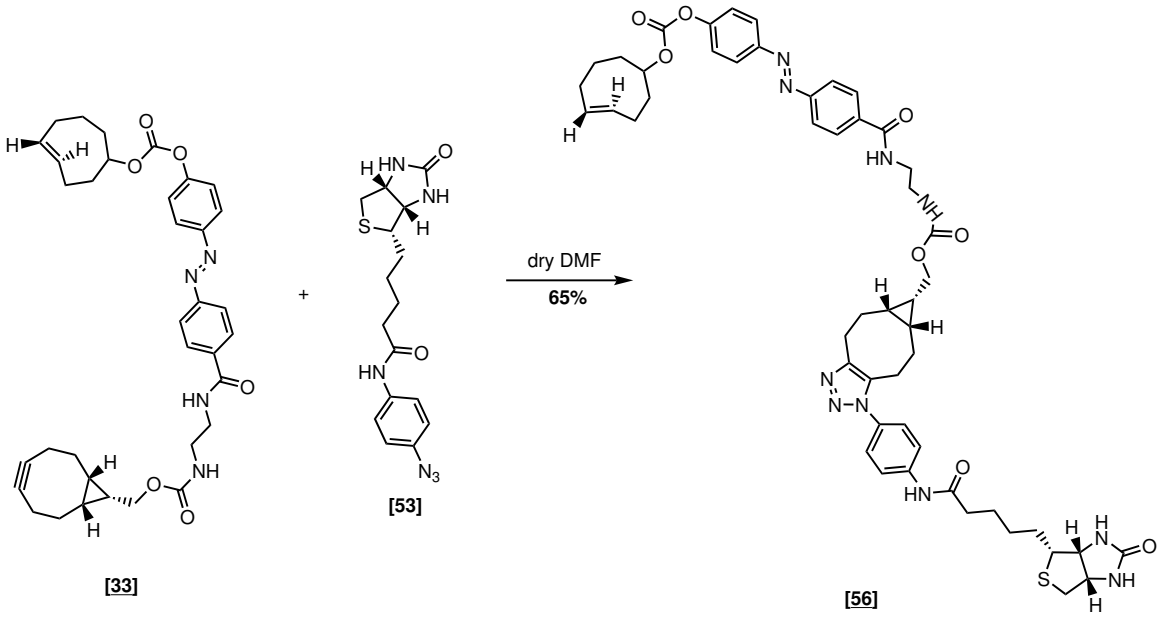

Scheme 18: SPAAC between azobenzene **[33]** and biotin **[53]**.

Die approbierte gedruckte Originalversion dieser Dissertation ist an der TU Wien Bibliothek verfügbar.
The approved original version of this doctoral thesis is available in print at TU Wien Bibliothek.

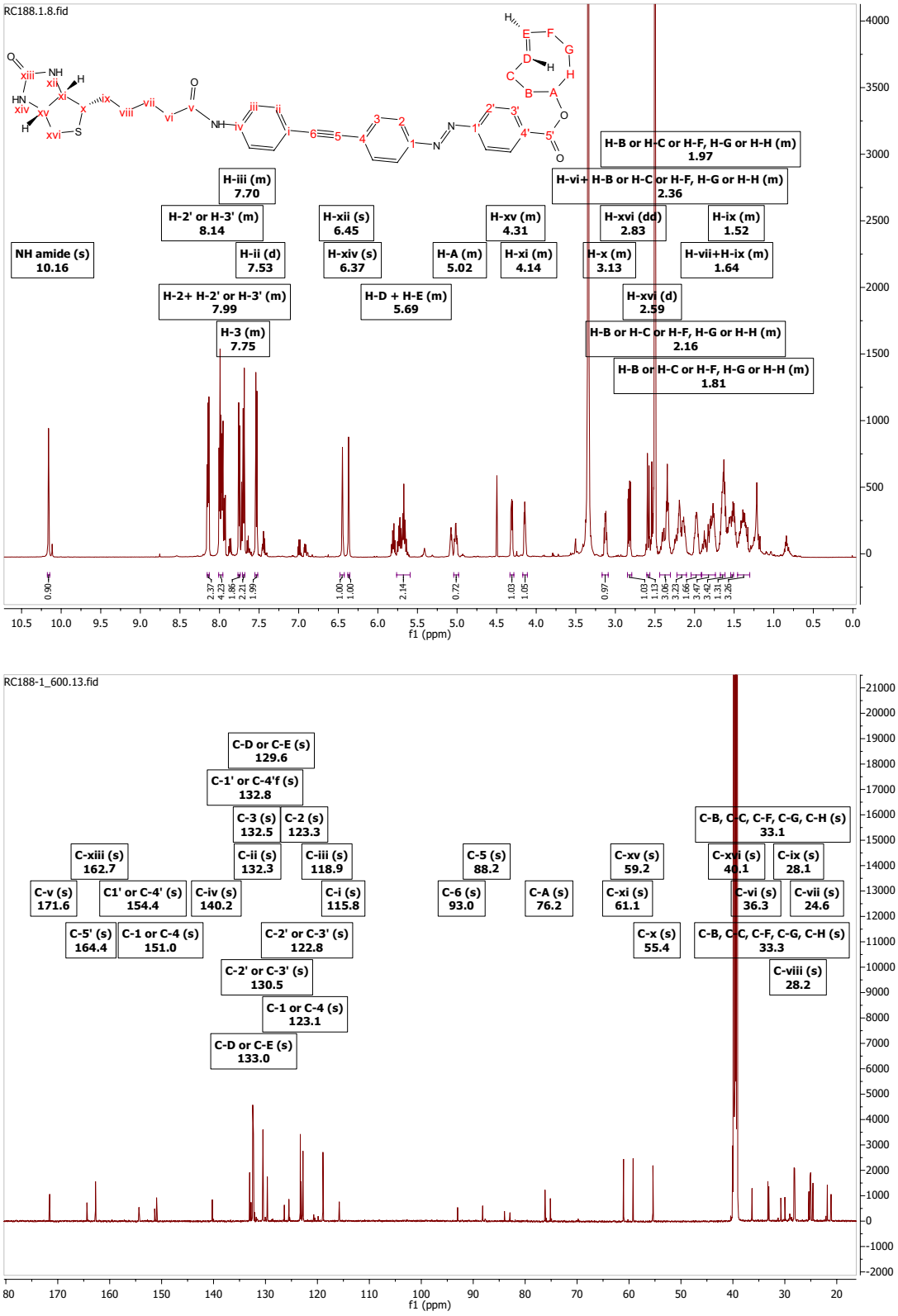

Figure 62: ^{1}H and ^{13}C NMR of azobenzene **[55]**.

Die approbierte gedruckte Originalversion dieser Dissertation ist an der TU Wien Bibliothek verfügbar.
The approved original version of this doctoral thesis is available in print at TU Wien Bibliothek.
TU Bibliothek Your knowledge hub WIEN

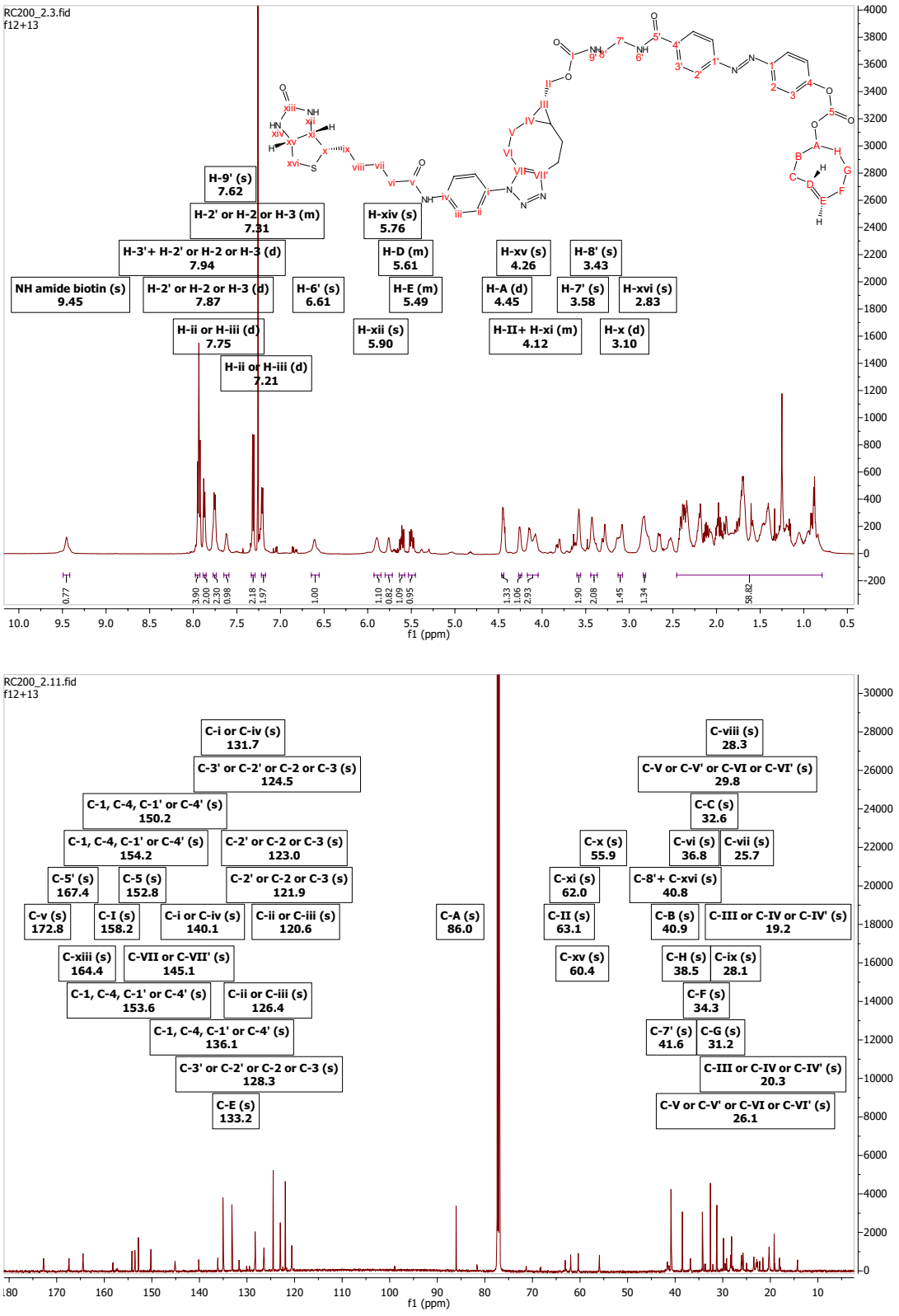

Figure 63: ^{1}H and ^{13}C NMR of azobenzene **[56]**.

Die approbierte gedruckte Originalversion dieser Dissertation ist an der TU Wien Bibliothek verfügbar.
The approved original version of this doctoral thesis is available in print at TU Wien Bibliothek.
TU Bibliothek Your knowledge hub WIEN

Figure 62 and 63 present the ^{1}H and ^{13}C NMR of conjugation products **[55]** and **[56]**, respectively. Here it is possible to observe the complexity of these molecules, specially **[56]**. Once analyzing the NMRs of both compounds, besides aromatics, a couple of aliphatic signals stand out at higher chemical shifts. From the TCO moiety, **D**/**E** (^{1}H $\approx$ 5.5 ppm, ^{13}C $\approx$ 130-135 ppm) and **A** (**[55]**: ^{1}H 5.02 ppm, ^{13}C 76 ppm; **[56]**: ^{1}H 4.45 ppm, ^{13}C 86 ppm). Notice that there is a big different in the chemical shift of the signal **A** for both compounds (0.5 ppm in the ^{1}H and 10 ppm in the ^{13}C). This can be explained by two factors: the different diastereomers (**[55]** is axial and **[56]** is equatorial) and the difference in the chemical group (carbonate vs ester). Regarding the biotin moiety, the signals from the heterocyclic part **xii** (**[55]** ^{1}H 6.45 ppm; **[56]** ^{1}H 5.9 ppm), **xiv** (**[55]** ^{1}H 6.37 ppm; **[56]** ^{1}H 5.76 ppm), **xv** (^{1}H 4.3 ppm, ^{13}C 60 ppm) and **xi** (^{1}H 4.1 ppm, ^{13}C: 62 ppm), as well as the amide proton (**[55]**: ^{1}H 10.16 ppm; **[56]**: 1H^{1}H 9.45 ppm) are noteworthy. Notice that the NMRs have been measured in different deuterated solvents (**[55]**: DMSO-d_6; **[56]**: $CDCl_3$) which explains the different shifts of the NH signals in both compounds.

For each compound, a couple of specific signals are also worth to mention. From conjugation product **[55]**, in the ^{13}C the signals from the alkyne, **C-5** (88.2 ppm) and **C-6** (93 ppm). Regarding product **[56]**, **II** (^{1}H 4.12 ppm, ^{13}C 63.1 ppm) , **8'** (^{1}H 3.43 ppm, ^{13}C 40.8 ppm) and **7'** (^{1}H 3.58 ppm, ^{13}C 41.6 ppm).

After the click reactions we have ended up with 2 possible click products to bind to the platform, azobenzene-biotin **[55]** and **[56]**. It is important to check if the photophysical properties of these products were unaffected by the binding to biotin. Figure 64 presents the photoswitching tests for these compounds. Looking at the UV/Vis spectra of azobenzene-biotin **[55]** in the beginning (before irradiation), it is possible to notice that the typical $\pi \rightarrow \pi^*$ and n$\rightarrow \pi^*$ bands do not appear, but instead a broad band. Probably the $\pi \rightarrow \pi^*$ and n$\rightarrow \pi^*$ bands have overlapped because of the increased conjugation of this system. As consequence, it would be expected that the photoswitching of this compound would be quite inefficient, which was indeed observed. Upon irradiation with 365 nm only a small decrease in the intensity of the broad band is observed. Even when the irradiation time is increased the results do not differ. After irradiation with 460 nm a recovery of the absorption is observed. On the other hand, azobenzene-biotin **[56]** presents the classic behavior of an azobenzene. In addition, the $t_{1/2}$ was

Die approbierte gedruckte Originalversion dieser Dissertation ist an der TU Wien Bibliothek verfügbar.
The approved original version of this doctoral thesis is available in print at TU Wien Bibliothek.
TU Bibliothek Your knowledge hub WIEN

also determined to be 86.3 hours, similar to its azobenzene starting material **[33]**. Taking into account these results, azobenzene-biotin **[56]** was decided as candidate for subsequent studies.

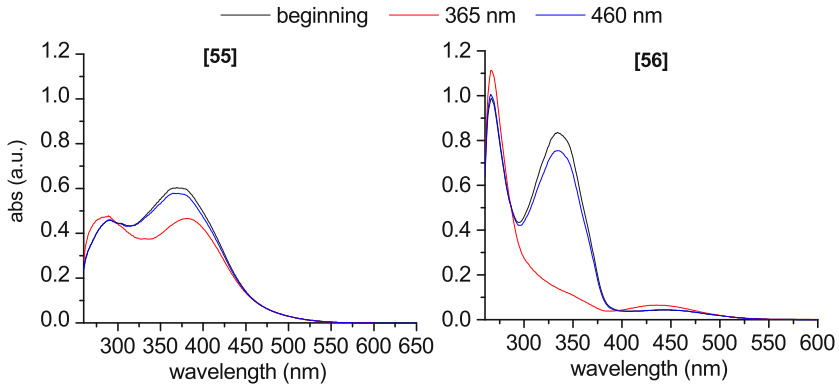

Figure 64: Photoswitching of compounds **[55]** (left) and **[56]** (right). The black line represents the UV-Vis spectra before irradiation, the red light after irradiation with 365 nm and the blue line the back switch with 460 nm.

C.3.2 Testing the binding to the DNA origami platform

As previously stated, to attain our goal the modified biotin must bind to SA. To check the binding two different experiments were carried out. The first assay is a colorimetric procedure that uses 4-hydroxyazobenzene-2'-carboxylic acid (HABA). This compound binds to the biotin and forms a complex with a maximum absorption at 500 nm. Since the affinity of biotin for SA is higher, if biotin is added to the mixture it displaces HABA and the absorption at 500 nm decreases.[209,210] Figure 65 presents the results from this assay. In Figure 65A a control experiment using SA's natural substrate, biotin **[52]**, was performed. As expected upon the addition of biotin **[52]** (100 µL of 10 mM) there is a sharp decrease in the absorption at 500 nm, indicating that biotin has bound to the SA and displaced HABA. Figure 65B shows the same assay but for the compound of interest **[56]**, using also a 10 mM solution in DMSO. In this case, upon the addition of 100 µL precipitation occurred, therefore compound **[56]** was added in portions of 2 µL. Upon the addition of 2 µL a decrease in the absorption at 500 nm is observed and this decrease is even more accentuated after 4 µL. At 6 µL precipitation occurs so no more measurements could be performed. These results indicate that the azobenzene-modified biotin **[56]** retained the ability to bind to the SA, corroborating the initial design and validity of the approach.

Die approbierte gedruckte Originalversion dieser Dissertation ist an der TU Wien Bibliothek verfügbar.
The approved original version of this doctoral thesis is available in print at TU Wien Bibliothek.
TU Bibliothek Your knowledge hub WIEN

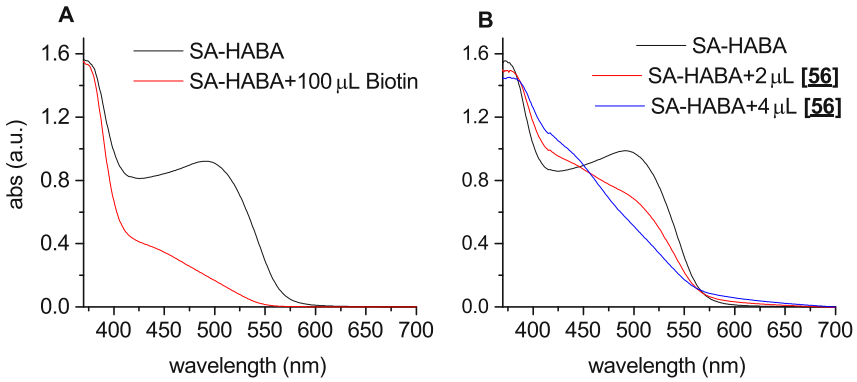

Figure 65: HABA assay to test the binding to SA. **(A)** Positive control using 10 µM biotin in DMSO. **(B)** Test of the binding of **[56]** to SA also using a 10 µM solution in DMSO.

Afterwards, we aimed to test the direct binding of our azobenzene directly to the SA in the DNA origami platform. For that, azobenzene **[56]** was conjugated with cyanine fluorophore **[57]** (Scheme 19). The idea is that if compound **[58]** binds to the platform localized fluorescence will be observed where SA and azobenzene-fluorophore **[58]** have bound. Since this reaction had to be carried in a scale below 1 mg, purification would be a challenge. Therefore the reaction between **[56]** and **[57]** was carried using excess of **[57]**, since **[56]** can also bind to SA. The reaction was followed by HPLC and the fluorescence and absorption chromatograms of compounds **[57]**, **[56]** and the reaction mixture **[58]** can be found in Figure 66. In the absorption chromatograms it is visible that azobenzene **[56]** has been completely consumed, since in the reaction mixture **[58]** the peak at 2.39 minutes, which corresponds to the azobenzene, is not visible. Two new peak are also observed both in the absorption (1.20 and 1.70 minutes) and fluorescence (1.30 and 1.78 minutes) chromatograms, which probably correspond to the desired product **[58]**, oxidized and non-oxidized form.

Die approbierte gedruckte Originalversion dieser Dissertation ist an der TU Wien Bibliothek verfügbar.
The approved original version of this doctoral thesis is available in print at TU Wien Bibliothek.

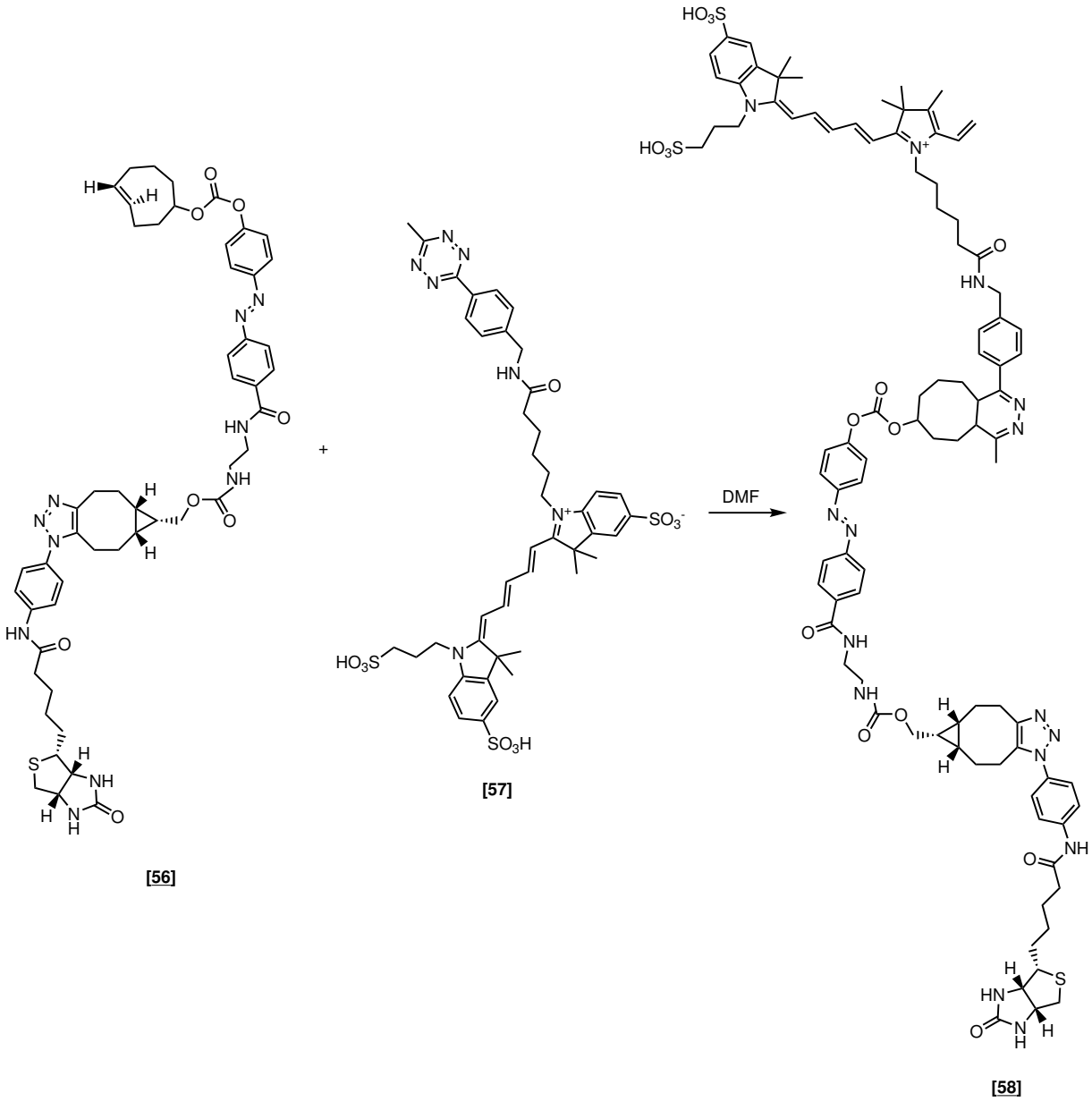

Scheme 19: Conjugation between azobenzene **[56]** and fluorophore Cy5 **[57]**, affording the conjugate **[58]**.

Die approbierte gedruckte Originalversion dieser Dissertation ist an der TU Wien Bibliothek verfügbar.
The approved original version of this doctoral thesis is available in print at TU Wien Bibliothek.

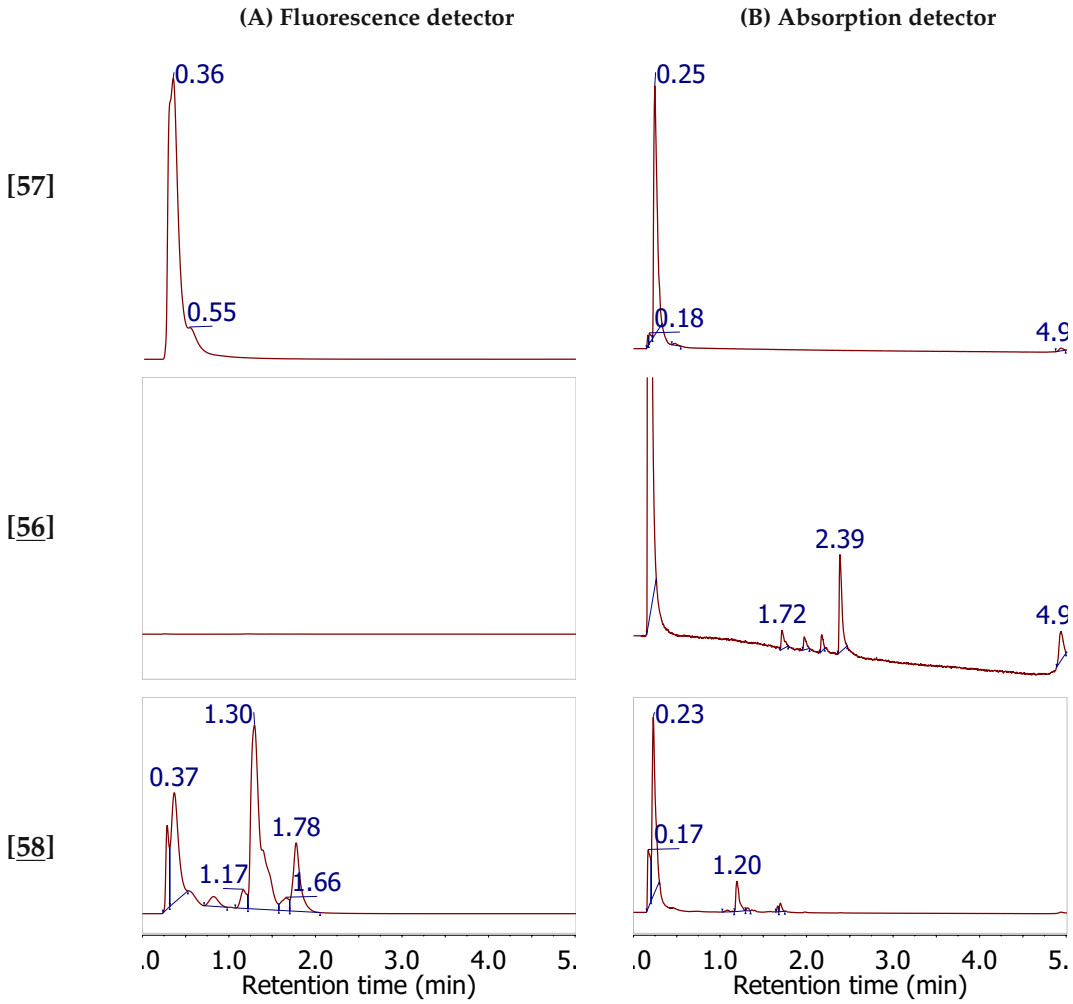

Figure 66: HPLC analysis of the conjugation reaction to afford **[58]**. The first column presents the fluorescence chromatograms **(A)** and the second column the absorption chromatograms **(B)** for compounds **[57]** (fluorophore, first row), **[56]** (biotin-azobenzene, second row) and **[58]** (the biotin-azobenzene-fluorophore conjugate, third row).

C.3.3 Determining the force generated by the photoswitching of a single azobenzene

In the previous sections we outlined a strategy towards activating and deactivating T-cells, by using an azobenzene to break the interaction between the TCR and the T-cell ligand. Physically this means that the force generated by the photoswitching of the azobenzene must be higher than the force of the interaction between the TCR and T-cell ligand. Nevertheless, the force generated by the photoswitching of an azobenzene on a single molecule level is till the moment

Die approbierte gedruckte Originalversion dieser Dissertation ist an der TU Wien Bibliothek verfügbar.
The approved original version of this doctoral thesis is available in print at TU Wien Bibliothek.
TU Bibliothek Your knowledge hub WIEN

not known.

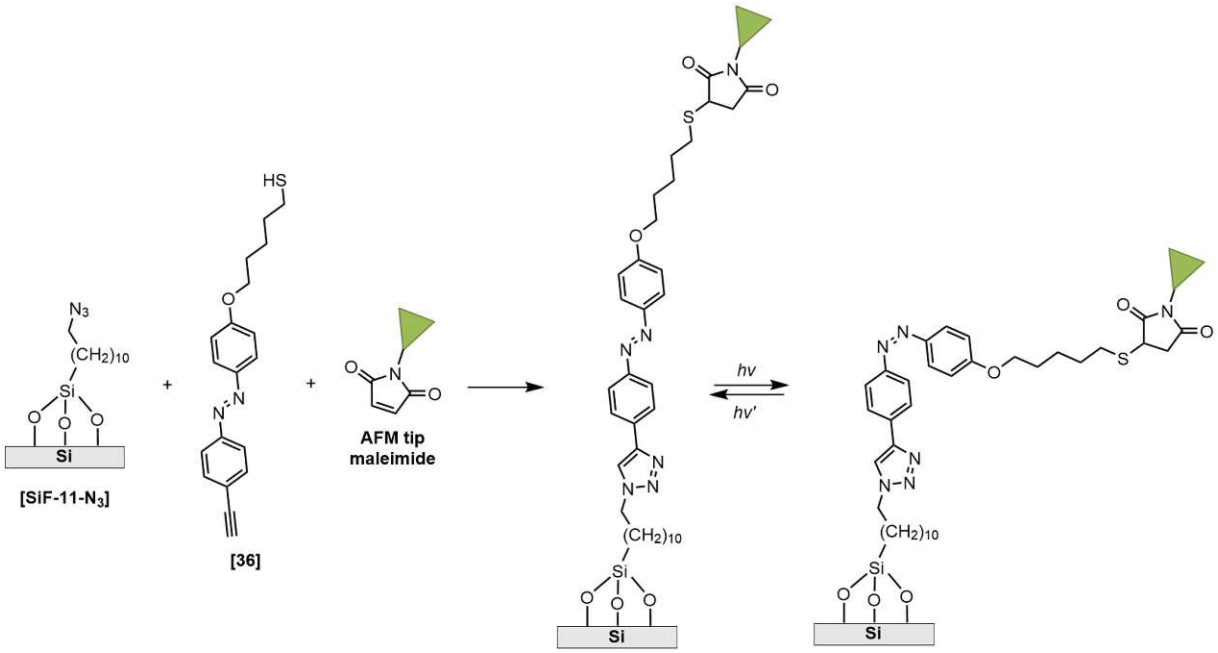

Figure 67: Our approach to obtain an azobenzene-functionalized AFM tip bound to a silicon surface, that can be used to measure the force generated by the photoswitching of the azobenzene.

Holland et al. have used atom force microscopy (AFM) to determine the force exerted by an azobenzene polymer with 46 monomers. The polymer was covalently attached both to the tip of the AFM cantilever and to a glass surface. Afterwards, the photoswitching from *trans* to *cis* was tested against an external force and till 400 pN photoswitching was verified.[211,212]

In our case, we have aimed to determine the force generated by the photoswitching of a single azobenzene molecule. Like in Holland et al., to be able to measure the force exerted by an azobenzene we will have to bind it to an AFM tip and a surface. To attain our goal we intend to once again take advantage of click chemistry and use one of our double-click azobenzenes. The first step was to find an AFM tip functionalization and surface modification that is compatible with our designs. Gruber has developed a protocol to obtain a maleimide functionalized AFM tip that are compatible with our azobenzene **[36]**, that contains a thiol.[213] This azobenzene also has a alkyne, which means that we could also reuse the azide-coated silicon surface previously obtained (see Section C.2.3). Figure 67 shows our approach using azobenzene **[36]**, a maleimide-functionalized AFM tip and our azide-coated silicon surface.

Die approbierte gedruckte Originalversion dieser Dissertation ist an der TU Wien Bibliothek verfügbar.
The approved original version of this doctoral thesis is available in print at TU Wien Bibliothek.
TU Bibliothek Your knowledge hub WIEN

After the assembly of these components the deflection of the cantilever should allow to measure the force exerted by the switching of the azobenzene.

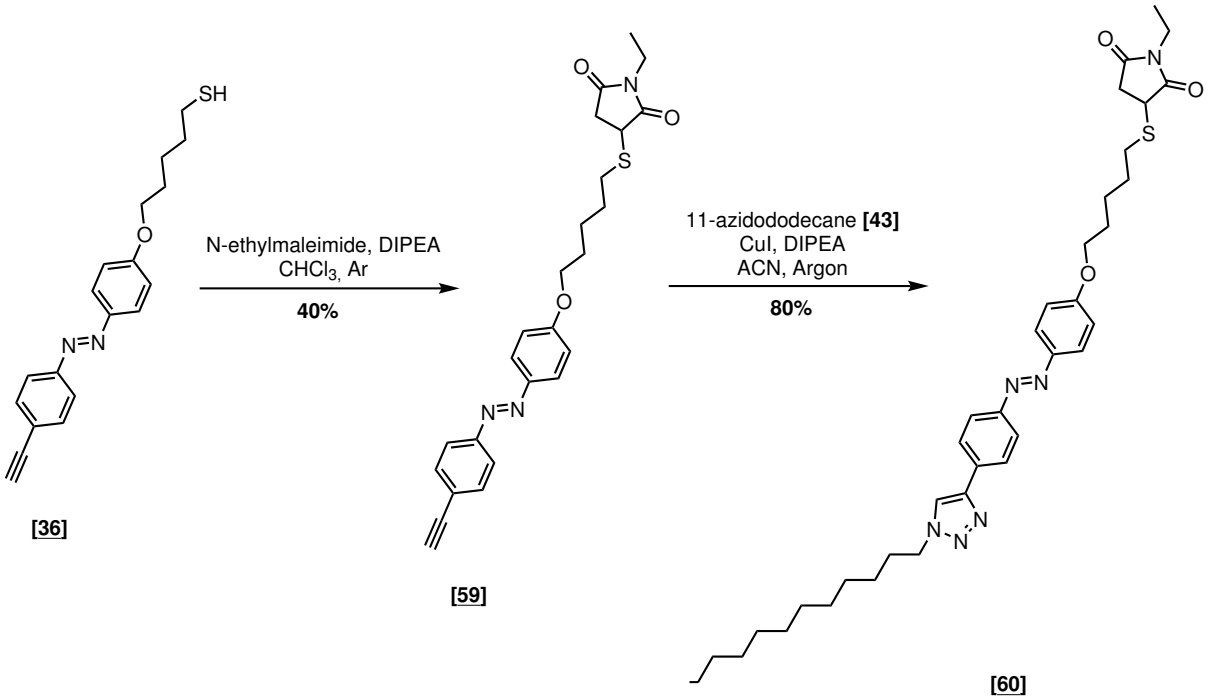

Scheme 20: Test of the click reactions for the surface and AFM tip functionalization in solution.

Before attaching the azobenzene to the surface **[SiF-N_3]** and the AFM tip, we have tested the click reactions in solution. Scheme 20 shows the test reactions. In the first place, azobenzene **[36]** was clicked with N-ethylmaleimide, a commercially available maleimide, affording product **[59]** in 40% yield. Afterwards, the CuAAC catalyzed reaction with 11-azidododecane **[43]** was performed affording azobenzene **[60]** in 80% yield.

The photophysical properties of the click products of azobenzene **[36]** were also tested (Figure 68). Upon the click reactions both azobenzene **[59]** and **[60]** keep their ability to photoswitch as expected. The $t_{1/2}$ of the click products **[59]** and **[60]** are respectively 9 and 8 hours, which is slightly higher in comparison with their SM **[36]** ($t_{1/2}$ = 4 hours). Once again it is verified that the introduction of the electron-donating 1,2,3-triazole leads to a small reduction of the $t_{1/2}$ (9 to 8 hours) as well as to a red shift of the maximum absorption wavelength due to the increased conjugation of the system (367 nm for **[59]** and 372 nm for **[60]**).

Die approbierte gedruckte Originalversion dieser Dissertation ist an der TU Wien Bibliothek verfügbar.
The approved original version of this doctoral thesis is available in print at TU Wien Bibliothek.
TU Bibliothek Your knowledge hub WIEN

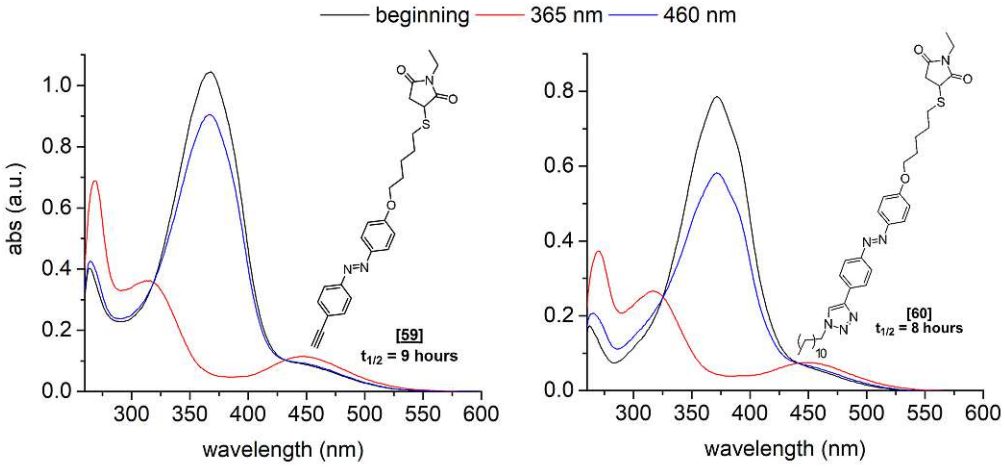

Figure 68: Determination of the photophysical properties of the click products of azobenzene **[36]**. The black lines correspond to the UV/Vis spectra before irradiation, the red lines after irradiation with 365 nm and the blue lines after irradiation with 460 nm. Below the structure of each compound the determined thermal $t_{1/2}$ can be found.

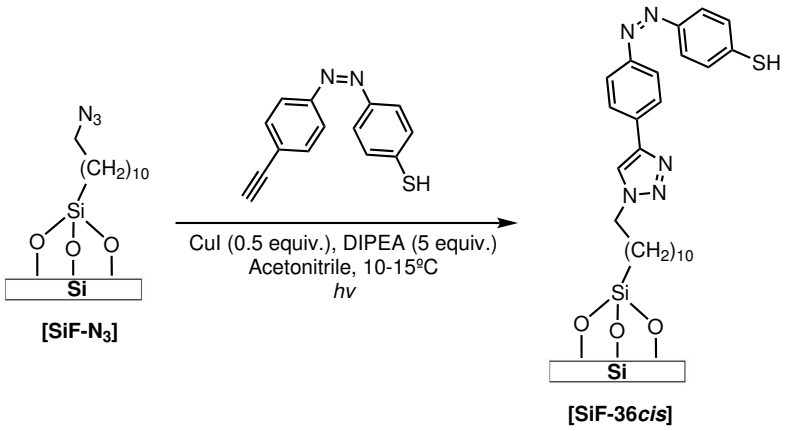

Scheme 21: Immobilization of azobenzene **[36]** on **[SiF-N_3]** via *cis* immobilization affording **[SiF-36*cis*]**.

After testing the clicks and verifying the photophysical properties of azobenzenes **[59]** and **[60]**, the next step is to immobilize azobenzene **[36]** on surface **[SiF-N_3]**. For the azobenzene immobilization we have decided to use the *cis* immobilization method in order to save the optimization time (Scheme 21).

Figure 69A presents the photoswitchability of **[SiF-36*cis*]**. The irradiation cycles were performed like discussed in Section C.2.5 and we have obtained a surface with a ΔWCA of 4.7°. A FTIR of this surface was also measured and as expected we still see unreacted azide on the sur-

Die approbierte gedruckte Originalversion dieser Dissertation ist an der TU Wien Bibliothek verfügbar.
The approved original version of this doctoral thesis is available in print at TU Wien Bibliothek.

face (Figure 69B). One concern that should be addressed is how much thiol has oxidized during the immobilization process. Since thiols are prone to dimerization, the addition of a reducing agent such as (tris(2-carboxyethyl)phosphine) could prove advantageous for this specific immobilization.

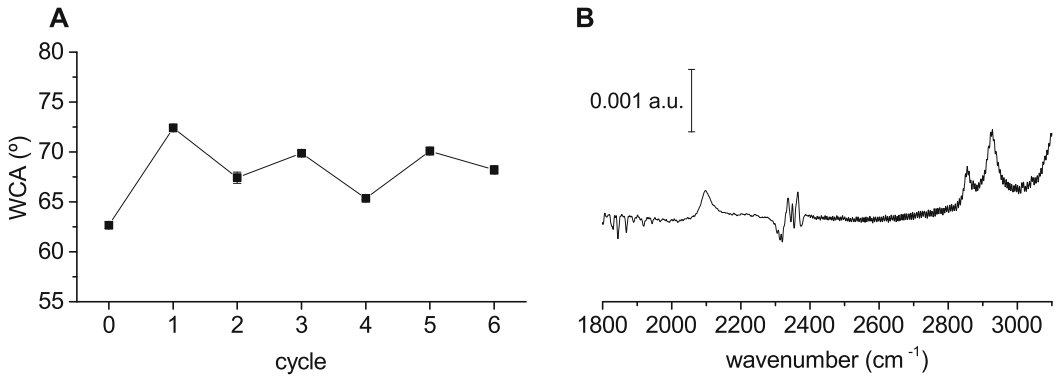

Figure 69: (A) Analysis of the photoswitchability of **[SiF-36*cis*]**. The cycle 0 corresponds to the WCA before irradiation, odd number cycles to irradiation with a halogen lamp and even number cycles to irradiation with 365 nm. **(B)** FTIR spectra of **[SiF-36*cis*]**.

Since the AFM measurements are based on optical beam deflection, the irradiation required for our experiments generates artifacts in the measurements. Once this question has been addressed, the AFM tip will be connected to our surface **[SiF-36*cis*]** and the force generated by the switching will be determined by our partners in the Institute of Lightweight Design and Structural Biomechanics at TU Wien.

Die approbierte gedruckte Originalversion dieser Dissertation ist an der TU Wien Bibliothek verfügbar.
The approved original version of this doctoral thesis is available in print at TU Wien Bibliothek.

Die approbierte gedruckte Originalversion dieser Dissertation ist an der TU Wien Bibliothek verfügbar.
The approved original version of this doctoral thesis is available in print at TU Wien Bibliothek.
TU Bibliothek Your knowledge hub WIEN

Chapter D

Summary and outlook

In this thesis 6 double-click azobenzenes were synthesized containing moieties for CuAAC, SPAAC and maleimide-thiol Michael addition (**[11a]**, **[11e]**, **[18a]**, **[18e]**, **[33]** and **[36]**). The photophysical properties of these azobenzenes were determined showing that photoswitching from *trans* to *cis* is possible by irradiation with 365 nm and back-switching to *trans* is possible by irradiation with 460 nm. The thermal relaxation half-life times of these compounds were always in the range of hours, indicating that these compounds do not switch-back to *cis* too fast and can be comfortably manipulated in biological applications.

The obtained azobenzenes were applied in the development of azobenzene photoswitchable surfaces for biological applications. In the first place, we focused on the preparation of a silicon surface that could be used to immobilize in the future compounds of biological interest. Before immobilizing the double-click azobenzene of interest **[11e]**, azobenzene **[41]** was clicked on azide coated silicon surface **[SiF-N_3]** to better understand the process of azobenzene immobilization (**[SiF41*trans*]**). The results have shown that reaction time optimization is a determining factor in this process since a too long reaction time leads to an overcrowded not-photoswitchable surface and a too low reaction to a low concentration of azobenzene on the surface (according to the ΔWCA between the *trans* and *cis* surface). Afterwards, azobenzene **[11e]** was immobilized and photoswitchable surface **[SiF11e*trans*]** was obtained. This surface can serve in the future as a platform to immobilize biomolecules via mild and selective chemistry for the development of bioapplications. A model click product of azobenzene **[11e]**, azobenzene **[46]**, was also immobilized on the silicon showing the feasibility of this approach.

Click chemistry moieties can be used to increase the scope of application of the double-click azobenzenes. In addition, double-click azobenenes derivatives that take advantage of the better photophysical properties of bridged azobenenes and arylazopyrazoles, arylazopyrroles or arylazoimidazoles, for example, can be synthesized. This way a library can be developed where an azobenzene could be chosen according not only the required click chemistry but also the desired photophysical properties.

Trying to circumvent the problem of surface overcrowding, we have decided to immobilize the azobenzenes while on the *cis* configuration by continuous UV irradiation of the azobenzene solution during the adsorption process. We have hypothesized that if the azobenzene was immobilized in the most spatially demanding configuration, it should always keep the required space for switching while preventing surface overcrowding. Using this method we have immobilized azobenzenes **[41]**, **[11e]** and **[46]**. Not only have we obtained photoswitchable surfaces (**[SiF41*cis*]**, **[SiF11e*cis*]** and **[SiF46*cis*]**) but also a ΔWCA that was the same or higher than with the first method with no need for optimization.

Aiming for an increased difference in the WCA between the *trans* and *cis* surface we have immobilized the azobenzene **[41]** (while on the *trans* configuration) on rough surfaces. In the first place, we have utilized silicon nanowires as a substrate. Even though the data indicate that the preparation and functionalization of the SiNW was successful, we have not observed any difference in the WCA upon irradiation with UV light. A hypothesis that could explain this observation is that the size (diameter and length) of the wires is still too small. An increase in ΔWCA upon switching from a flat to a rough surface can only be expected, if the *trans* and the *cis* configuration adopt two different wetting states: Cassie Baxter wetting for *trans* and Wenzel wetting for *cis*. This requires systematic variations of the surface morphology (pore size, pore density, etc) which was beyond the scope of this work. Therefore, it would be worth it to try immobilization on a surface with pores with bigger diameters. Porous silicon was also tested as a substrate. Nevertheless, upon immobilization with OTS a superhydrophobic surface was not obtained, meaning that the porosity of this silicon is not high enough for our purpose. Finally, 3 different rough aluminum substrates were prepared and after coating with OTS one of the substrates (**[AlA]**) afforded a superhydrophobic surface. Hence, **[AlA]** was used for the immobilization of the azobenzene **[41]** both on flat and rough **[AlA]**. This immobilization

Die approbierte gedruckte Originalversion dieser Dissertation ist an der TU Wien Bibliothek verfügbar.
The approved original version of this doctoral thesis is available in print at TU Wien Bibliothek.
TU Bibliothek Your knowledge hub WIEN

afforded a photoswitchable flat surface **[AlA41*trans*]**, however not a photoswitchable rough surface. Actually, the obtained rough surface is not even hydrophobic indicating that there is probably a problem in the coating of the surface. This is supported by the IR of the surface that shows really weak CH stretching bands. A way to circumvent this problem would be to use a more common chemistry to coat the aluminum: acids or phosphonic acids instead of the used trichlorosilanes.

The double-click azobenzenes have also been modified for the development of a photoswitchable DNA origami platform for the study of T-cell activation. The first step was to modify our double-click azobenzenes with biotin so that the photoswitchable compound can bind to the SA in the DNA platform. Azobenzenes **[33]** and **[18a]** have both been successfully coupled to biotin, notwithstanding, only the coupling product of **[33]**, azobenzene **[56]**, has retained the ability to efficiently photoswitch. The binding of **[56]** to SA was tested via the HABA assay which indicated that this modified biotin can still bind to SA. In the future, the direct binding on the DNA platform should also be tested with fluorescence microscopy. For that **[56]** was already conjugated with a fluorophore ans switchability of the system was confirmed, hence, the relevant preparation steps for subsequent biological investigations could be successfully demonstrated. If these tests confirm the binding to the platform, azobenzene **[56]** should be conjugated with a single-chain antibody fragment capable of activating T-cells. Afterwards, the activation of the T-cells will be tested upon irradiation.

Die approbierte gedruckte Originalversion dieser Dissertation ist an der TU Wien Bibliothek verfügbar.
The approved original version of this doctoral thesis is available in print at TU Wien Bibliothek.
TU Bibliothek Your knowledge hub WIEN

Die approbierte gedruckte Originalversion dieser Dissertation ist an der TU Wien Bibliothek verfügbar.
The approved original version of this doctoral thesis is available in print at TU Wien Bibliothek.

Chapter E

Experimental part

E.1 Materials and methods - chemical synthesis

Unless otherwise noted, chemicals were purchased from commercial suppliers and used without further purification. The purity of the reported compounds is >95% according to NMR.

E.1.1 NMR spectroscopy

NMR spectra were recorded on a Bruker Avance Ultrashield 400 (^{1}H: 400 MHz, ^{13}C: 101 MHz) and Bruker Avance IIIHD 600 spectrometer equipped with a Prodigy BBO cryo probe (^{1}H: 600 MHz, ^{13}C: 151 MHz). Chemical shifts are given in parts per million (ppm) and were calibrated with internal standards of deuterium labeled solvents $CDCl_3$ (^{1}H 7.26 ppm, ^{13}C 77.16 ppm), MeOD (^{1}H 3.31 ppm, ^{13}C 49.00 ppm) and DMSO-d_6 (^{1}H 2.50 ppm, ^{13}C 39.52 ppm). NMR assignments of unknown compounds were confirmed by ^{1}H - ^{1}H COSY, ^{1}H - ^{13}C HSQC and ^{1}H - ^{13}C HMBC and by comparison to predicted spectra. Proton multiplicities are denoted by the following abbreviations: s (singlet), br s (broad singlet), d (doublet), dd (doublet of a doublet), t (triplet), dt (doublet of a triplet), q (quartet), pent (quintet), hep (septet), m (multiplet). Coupling constants (*J*) are presented in Hz (Hertz). Carbon multiplicities (suppressed CH coupling) are denoted by the following abbreviations: s (singlet), d (doublet), t (triplet) and q (quartet). In case of fluoro structures the coupling constant is denoted generally as " x/y, $^{z}J_{CF}$ = ...Hz " whereby x represents the multiplicity of the CH coupling, y the multiplicity of the

CF coupling and z the order of spin-spin coupling.

E.1.2 Chromatographic methods

TLC was performed using silica gel 60 aluminum plates containing fluorescent indicator from Merck and detected either with UV light at 254 nm or by staining in ninhydrin solution (300 mg ninhydrin, 3 mL acetic acid, 100 mL butanol), potassium permanganate (1 g $KMnO_4$, 6.6 g K_2CO_3, 100 mg NaOH, 100 mL H_2O in 1M NaOH) or *para*-anisaldehyde (4 mL *para*-anisaldehyde, 5 mL H_2SO_4, 150 mL EtOH) with heating.

HPLC chromatography was carried out with an Autopurification system of Waters using an ACQUITY QDa Detector in combination with a 2998 Photodiode Array Detector. Analytical separation was conducted using XSELECT CSH Fluoro-Phenyl 5 µm 4.6 x 150 mm and XSELECT CSH C18 5 µm 4.6 x 150 mm columns. Preparative separation was performed using XSELECT CSH Prep Fluoro-Phenyl 5 µm 30 x 150 mm and XSELECT CSH Prep C18 5 µm OBD 30 x 150 mm columns. As solvents HPLC grade methanol and HPLC grade H_2O were used with or without 0.1% formic acid.

Column chromatography was carried out with a Büchi Sepacore^{TM} MPLC system (2 x Büchi Pump Module C-605, Büchi Pump Manager C-615, Büchi UV Photometer C-635, Büchi Fraction Collector C-660) or standard manual glass columns using silica gel 60 M (particle size 40-63 µm, 230-400 mesh ASTM, Macherey Nagel, Düren). Unless stated otherwise all compounds were purified with a ratio of 1/100 (weight(compound)/ weight (silica)).

GC/MS spectra were measured using a Thermo Trace 1300 / ISQ LT (single quadrupole MS (EI)) using a standard capillary column BGB 5 (30 m x 0.25 mm ID).

Some reactions were analyzed *via* HPLC-MS on a reverse phase Nexera X2 UHPLC system (Shimadzu, Kyoto, Japan) comprised of LC-30AD pumps, a SIL-30AC autosampler, CTO-20AC column oven, DGU-20$A_{5/3}$ degasser module. Detection was accomplished by concerted efforts of SPD-M20A photo diode array, a RF-20Axs fluorescence detector, an ELS-2041 evaporative light scattering detector (JASCO) and finally via a LCMS-2020 mass spectrometer. Separations were performed using either a XSelect CHS Fluoro-Phenyl 2.5 µm 3.0 x 15 mm column or ACQUITY UPLC Protein BEH C4 column 300 $\AA$ 1.7 µm 2.1 mm x 50 mm. Mobile phases are

Die approbierte gedruckte Originalversion dieser Dissertation ist an der TU Wien Bibliothek verfügbar.
The approved original version of this doctoral thesis is available in print at TU Wien Bibliothek.
TU Bibliothek Your knowledge hub WIEN

UPLC grade grade water and acetonitrile containing 0.1% formic acid or 2.5 mM ammonium formiate (pH = 8.5).

E.1.3 Melting points

Melting points were determined using a Leica Galen III Kofler or a Büchi Melting Point B-545.

E.1.4 HR-MS

An Agilent 6230 LC TOFMS mass spectrometer equipped with an Agilent Dual AJS ESI-Source was used for HR-MS analysis. The mass spectrometer was connected to a liquid chromatography system of the 1100/1200 series from Agilent Technologies, Palo Alto, CA, USA. The system consisted of a 1200SL binary gradient pump, a degasser, column thermostat, and an HTC PAL autosampler (CTC Analytics AG, Zwingen, Switzerland). A silica-based Phenomenex C-18 Security Guard Cartridge was used as stationary phase.

Data evaluation was performed using Agilent MassHunter Qualitative Analysis B.07.00. Identification was based on peaks obtained from extracted ion chromatograms (extraction width $\pm$ 20 ppm).

E.2 Chemical synthesis

E.2.1 CuAAC-tetrazine ligation azobenzene

E.2.1.1 (*Z*)-9-Oxabicyclo[6.1.0]non-4-ene [2]

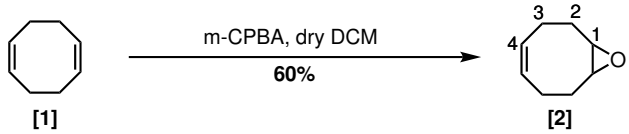

(*Z*)-9-Oxabicyclo[6.1.0]non-4-ene **[2]** was synthesized according to a literature procedure.[145] 1,5-Cyclooctadiene **[1]** (15.0 g, 121.0 mmol, 1 equiv.) was cooled to 0°C and then *meta*-chloroperbenzoic acid (27.12 g, 157.2 mmol, 1.3 equiv.), suspended in 200 mL of dry DCM, was slowly added.

Die approbierte gedruckte Originalversion dieser Dissertation ist an der TU Wien Bibliothek verfügbar.
The approved original version of this doctoral thesis is available in print at TU Wien Bibliothek.
TU Bibliothek Your knowledge hub WIEN

After 4 hours the solid was removed by filtration and washed with chloroform. The filtrate was washed with aqueous saturated Na_2SO_3 solution, aqueous saturated $NaHCO_3$ solution and water. The organic and water phases were separated, the organic phase was dried over Na_2SO_4 and the solvent was evaporated. The crude material was purified by distillation. The analytical data are in accordance with the literature.[145]

Yield: 60% (9.0 g, 72.4 mmol)

Appearance: colorless oil

TLC analysis: R_f = 0.74 (PE:EtOAc = 4:1)

Sum formula: $C_8H_{12}O$

^{1}H NMR (400 MHz, $CDCl_3$): δ = 1.97 – 2.08 (m, 4H, H-2 + H-3), 2.06 – 2.22 (m, 2H, H-2), 2.36 – 2.52 (m, 2H, H-3), 2.93 – 3.20 (m, 2H, H-1), 5.40 – 5.69 (m, 2H, H-4) ppm.

^{13}C NMR (101 MHz, $CDCl_3$): δ = 24.1 (t, 2C, C-3), 28.6 (t, 2C, C-2), 57.2 (d, 2C, C-1), 129.3 (d, 2C, C-4) ppm.

E.2.1.2 (*Z*)-Cyclooct-4-en-1-ol [3]

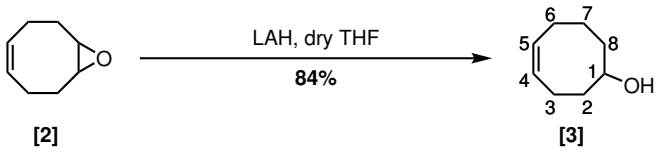

[2] **[3]**

(*Z*)-Cyclooct-4-en-1-ol **[3]** was synthesized according to a literature procedure.[145] Lithium aluminum hydride (2.96 g, 78 mmol, 1.3 equiv.) was cooled to 0°C, placed under argon and suspended in 12 mL of dry THF. Afterwards, (*Z*)-9-oxabicyclo[6.1.0]non-4-ene **[2]** (7.46 g, 60.0 mmol, 1 equiv.) was added dropwise. After 3 hours stirring at room temperature, the reaction mixture was cooled to 0°C, diluted in diethyl ether, quenched by the dropwise addition of aqueous saturated Na_2SO_4 solution and filtered. The organic and water phases were separated, the organic phase was dried over Na_2SO_4 and the solvent was evaporated. The analytical data are in accordance with the literature.[145]

Yield: 84% (6.3 g, 51 mmol)

Die approbierte gedruckte Originalversion dieser Dissertation ist an der TU Wien Bibliothek verfügbar.
The approved original version of this doctoral thesis is available in print at TU Wien Bibliothek.
TU Bibliothek Your knowledge hub WIEN

Appearance: colorless oil

TLC analysis: R_f = 0.36 (n-hexane:EtOAc = 4:1)

Sum formula: $C_8H_{14}O$

^{1}H NMR (400 MHz, $CDCl_3$): δ = 1.48 – 1.56 (m, 2H, H-2 + H-7), 1.59 – 1.75 (m, 2H, H-7 + H-8), 1.79 – 1.99 (m, 2H, H-2 + H-8), 2.04 – 2.22 (m, 3H, H-3 + H-6), 2.22 – 2.39 (m, 1H, H-3), 3.75 – 3.86 (m, 1H, H-1), 5.55 – 5.63 (m, 1H, H-5), 5.65 – 5.74 (m, 1H, H-4) ppm.

^{13}C NMR (101 MHz, $CDCl_3$): δ = 22.9 (t, C-3), 25.0 (t, C-7), 25.8 (t, C-6), 36.4 (t, C-8), 37.9 (t, C-2), 72.9 (d, C-1), 129.7 (d, C-5), 130.3 (d, C-4) ppm.

E.2.1.3 Equatorial *(E)*-cyclooct-4-en-1-ol [4e] and axial *(E)*-cyclooct-4-en-1-ol [4a]

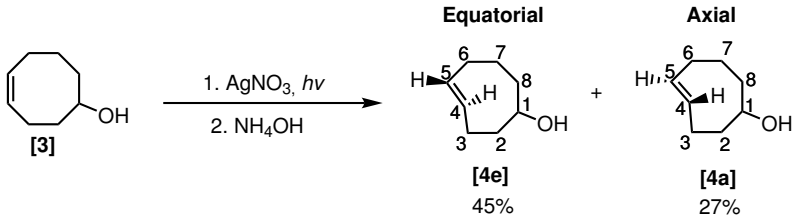

The isomerization of compound (*Z*)-cyclooct-4-en-1-ol **[3]** followed a protocol described in the literature.[144] A column was filled with 35 g of $AgNO_3/SiO_2$ (10%) and flushed with n-hexane:EtOAc (1:1). The reservoir was filled with n-hexane:EtOAc (4:1) and flushed with argon. Then the solvent was pumped through the system using a HPLC pump at a flow rate of 100 cm^3/min. After the system was filled with solvent, compound (*Z*)-cyclooct-4-en-1-ol **[3]** (2.21 g, 17.6 mmol, 1 equiv.) and methyl benzoate (4.78 g, 35 mmol, 2 equiv.) were slowly added to the system. After 15 minutes, the 254 nm lamps were turned on, beginning the isomerization process. The depletion of the starting material was monitored with GC-MS. After 18 hours the impregnated silica gel was placed under stirring in NH_4OH:DCM (2:1), then the silica was filtrated and thoroughly washed with NH_4OH:DCM (2:1). The organic and water phase were separated and the organic phase was washed with distilled water, dried over $MgSO_4$ and the solvent was evaporated. The crude material was purified by column chromatography (silica gel/crude = 100:1) with n-hexane:EtOAc (4:1), affording the major equatorial **[4e]** and minor axial **[4a]** products. The analytical data are in accordance with the literature.[144]

Die approbierte gedruckte Originalversion dieser Dissertation ist an der TU Wien Bibliothek verfügbar.
The approved original version of this doctoral thesis is available in print at TU Wien Bibliothek.
TU Bibliothek Your knowledge hub WIEN

Yield: 45% equatiorial **[4e]** (1.0 g, 8.0 mmol) and 27% axial **[4a]** (0.6 g, 4.7 mmol)

Appearance ([4e] and [4a]): colorless oils

TLC analysis: R_f**[4e]** = 0.21 (n-hexane:EtOAc = 4:1) and R_f**[4a]** = 0.45 (n-hexane:EtOAc = 4:1)

Sum formula: $C_8H_{14}O$

^{1}H NMR [4e] (400 MHz, $CDCl_3$): δ = 1.47 – 1.76 (m, 3H, H-7 + H-8), 1.75 – 2.08 (m, 4H, H-2 + H-6 + H-7), 2.21 – 2.39 (m, 3H, H-3 + H-6), 3.40 – 3.55 (m, 1H, H-1), 5.31 – 5.44 (m, 1H, H-5), 5.51 – 5.65 (m, 1H, H-4) ppm.

^{13}C NMR [4e] (101 MHz, $CDCl_3$): δ = 31.4 (t, C-7), 32.8 (t, C-3), 34.5 (t, C-6), 41.2 (t, C-8), 44.7 (t, C-2), 77.9 (d, C-1), 132.9 (d, C-5), 135.2 (d, C-4) ppm.

^{1}H NMR [4a] (400 MHz, $CDCl_3$): δ = 1.19 – 1.24 (m, 1H, H-8), 1.57 – 1.69 (m, 1H, H-2), 1.71 – 1.92 (m, 3H, H-6 + H-7), 1.99 – 2.15 (m, 2H, H-3 + H-8), 2.16 – 2.28 (m, 2H, H-2 + H-6), 2.28 – 2.44 (m, 1H, H-3), 3.92 – 4.07 (m, 1H, H-1), 5.48 – 5.62 (m, 2H, H-4 + H-5) ppm.

^{13}C NMR [4a] (101 MHz, $CDCl_3$): δ = 27.8 (t, C-7), 29.4 (t, C-3), 34.2 (t, C-6 or C-8), 34.2 (t, C-6 or C-8), 43.1 (t, C-2), 67.5 (d, C-1), 133.2 (d, C-4), 134.4 (d, C-5) ppm.

E.2.1.4 Equatorial *(E)*-cyclooct-4-en-1-yl (4-nitrophenyl) carbonate [6e]

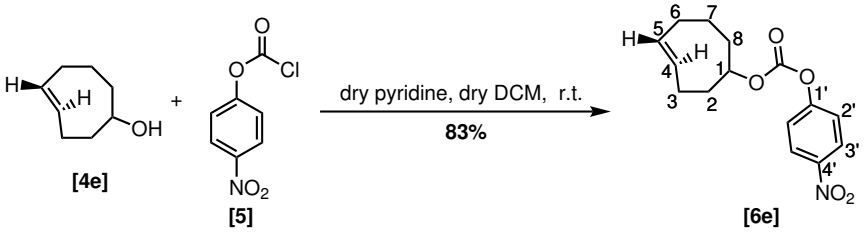

Equatorial *(E)*-cyclooct-4-en-1-yl (4-nitrophenyl) carbonate **[6e]** was synthesized according to a literature protocol.[151] Equatorial *(E)*-cyclooct-4-en-1-ol **[4e]** (1.01 g, 8.0 mmol, 1 equiv.) was dissolved in 80 mL of dry dichloromethane and then dry pyridine (1.62 mL, 20 mmol, 2.5 equiv.) was added. The 4-nitrophenyl chloroformate **[5]** (1.58 g, 8.8 mmol, 1.1 equiv.) was dissolved in 20 mL of dry DCM and added dropwise to the reaction mixture. After 2 hours the reaction was quenched with aqueous saturated NH_4Cl solution and the organic and aqueous phase were

Die approbierte gedruckte Originalversion dieser Dissertation ist an der TU Wien Bibliothek verfügbar.
The approved original version of this doctoral thesis is available in print at TU Wien Bibliothek.
TU Bibliothek Your knowledge hub WIEN

separated. The aqueous phase was extracted twice with dichloromethane. The organic phases were combined and dried over Na_2SO_4. After evaporation of the solvent, the crude material was purified by column chromatography (silica gel/crude = 100:1) with a PE:EtOAc (95:5).The analytical data are in accordance with the literature.[214]

Yield: 84% (1.9 g, 6.7 mmol)

Appearance: beige solid

Melting point: 76.2 - 76.4°C (Lit.[214]: 74-75°C)

TLC analysis: R_f = 0.46 (n-hexane:EtOAc = 4:1)

Sum formula: $C_{15}H_{17}NO_5$

^{1}H NMR (400 MHz, $CDCl_3$): δ = 1.61 – 1.77 (m, 2H, H-7 + H-8), 1.78 – 2.00 (m, 3H, H-6 + H-7 + H-8), 2.01 – 2.17 (m, 2H, H-2), 2.28 – 2.41 (m, 3H, H-3 + H-6), 4.36 – 4.45 (m, 1H, H-1), 5.39 – 5.49 (m, 1H, H-5), 5.51 – 5.61 (m, 1H, H-4), 7.32 (d, *J* = 9.2 Hz, 2H, H-2′ or H-3′), 8.19 (d, *J* = 9.2 Hz, 2H, H-2′ or H-3′) ppm.

^{13}C NMR (101 MHz, $CDCl_3$): δ = 30.9 (t, C-7), 32.2 (t, C-3), 33.9 (t, C-6), 38.1 (t, C-8), 40.4 (t, C-2), 86.1 (d, C-1), 121.6 (d, 2C, C-2′ or C-3′), 125.0 (d, 2C, C-2′ or C-3′), 132.8 (d, C-5), 134.6 (d, C-4), 145.0 (s, C-1′ or C-4′), 151.7 (s, carbonyl), 155.5 (s, C-1′ or C-4′) ppm.

E.2.1.5 Axial *(E)*-cyclooct-4-en-1-yl (4-nitrophenyl) carbonate [6a]

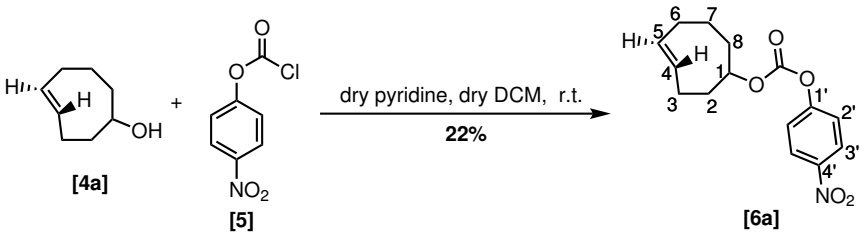

Axial *(E)*-cyclooct-4-en-1-yl (4-nitrophenyl) carbonate **[6a]** was synthesized according to a literature protocol.[147] Axial *(E)*-cyclooct-4-en-1-ol **[4a]** (0.5 g, 4.0 mmol, 1 equiv.) was dissolved in 45 mL of dry DCM and then dry pyridine (0.81 mL, 10 mmol, 2.5 equiv.) was added. The 4-nitrophenyl chloroformate **[5]** (0.88 g, 4.4 mmol, 1.1 equiv.) was dissolved in 10 mL of dry DCM and added dropwise. After 22 hours the reaction was quenched with aqueous saturated

Die approbierte gedruckte Originalversion dieser Dissertation ist an der TU Wien Bibliothek verfügbar.
The approved original version of this doctoral thesis is available in print at TU Wien Bibliothek.
TU Bibliothek Your knowledge hub WIEN

NH_4Cl solution and the organic and aqueous phases were separated. The aqueous phase was extracted twice with DCM. The organic phases were placed combined and dried with anhydrous Na_2SO_4. After evaporation of the solvent, the crude material was purified by column chromatography (silica gel/crude = 100:1) using n-hexane:EtOAc (5:1). The analytical data are in accordance with the literature.[215]

Yield: 22% (0.26 g, 0.8 mmol)

Appearance: beige solid

Melting point: 50.1 - 51.4°C (Lit: not reported)

TLC analysis: R_f = 0.48 (n-hexane:EtOAc = 5:1)

Sum formula: $C_{15}H_{17}NO_5$

^{1}H NMR [4e] (400 MHz, $CDCl_3$): δ = 1.26 – 1.36 (m, 1H, H-8), 1.50 – 1.65 (m, 1H, H-7), 1.67 – 1.78 (m, 1H, H-2), 1.80 – 1.92 (m, 2H, H-6+H-7), 2.09 – 2.19 (m, 1H, H-3), 2.23 – 2.30 (m, 1H, H-6), 2.30 – 2.46 (m, 3H, H-2 + H-3 + H-8), 4.92 – 5.00 (m, 1H, H-1), 5.49 – 5.65 (m, 2H, H-4 + H-5), 7.37 (d, *J* = 9.2 Hz, 2H, H-2' or H-3'), 8.23 (d, *J* = 9.2 Hz, 2H, H-2' or H-3') ppm.

^{13}C NMR (101 MHz, $CDCl_3$): δ = 27.9 (t, C-7), 29.7 (t, C-3), 32.0 (t, C-8), 34.1 (t, C-6), 40.5 (t, C-2), 75.9 (d, C-1), 121.8 (d, 2C, C-2' or C-3'), 125.2 (d, 2C, C-2' or C-3'), 131.4 (d, C-4), 135.3 (d, C-5), 145.2 (s, C-1' or C-4'), 151.8 (s, carbonyl), 155.7 (s, C-1' or C-4') ppm.

E.2.1.6 4-((4-Iodophenyl)diazenyl)phenol [8]

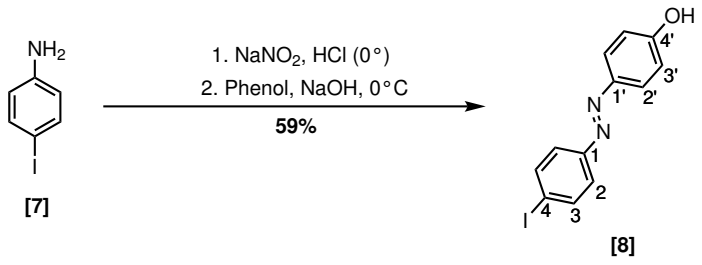

4-Iodoaniline **[7]** (5.19 g, 23.7 mmol, 1 equiv.) was dissolved in 400 mL of 2 M HCl and cooled to 0°C. Then $NaNO_2$ (1.96 g, 28.4 mmol, 1.2 equiv.) was dissolved in 30 mL of H_2O and added dropwise forming a light orange solution with a precipitate. After 5 minutes, this solution

Die approbierte gedruckte Originalversion dieser Dissertation ist an der TU Wien Bibliothek verfügbar.
The approved original version of this doctoral thesis is available in print at TU Wien Bibliothek.
TU Bibliothek Your knowledge hub WIEN

was slowly added to a phenol (2.45 g, 26.1 mmol, 1.1 equiv.) solution in 200 mL of 2 M NaOH, also cooled to 0°C. After 2 hours at r.t., the reaction mixture was acidified with 2 M HCl and extracted with EtOAc. The organic phase was separated and dried over $MgSO_4$. After evaporation of the solvent, the crude material was purified by column chromatography (silica gel/crude = 100:1) with PE:EtOAc (5:1). The analytical data are in accordance with the literature.[216]

Yield: 59% (4.56 g, 14 mmol)

Appearance: orange solid

Melting point: 161.7 - 162.7 °C (Lit.[216]: 163-165 °C)

TLC analysis: R_f = 0.4 (PE:EtOAc = 6:1)

Sum formula: $C_{12}H_9IN_2O$

^{1}H NMR (400 MHz, $CDCl_3$): δ = 5.22 (s, 1H, OH), 6.94 (d, J = 8.9 Hz, 2H, H-2′ or H-3′), 7.61 (d, J = 8.6 Hz, 2H, H-2 or H-3), 7.84 (d, J = 8.7 Hz, 2H, H-2 or H-3), 7.88 (d, J = 8.9 Hz, 2H, H-2′ or H-3′) ppm.

^{13}C NMR (101 MHz, $CDCl_3$): δ = 97.3 (s, C-4), 116.3 (d, 2C, C-2′ or C-3′), 124.7 (d, 2C, C-2 or C-3), 125.6 (d, 2C, C-2′ or C-3′), 138.7 (d, 2C, C-2 or C-3), 147.5 (s, C-4′), 152.5 (s, C-1), 158.9 (s, C-1′) ppm.

E.2.1.7 4-((4-(3-Hydroxy-3-methylbut-1-yn-1-yl)phenyl)diazenyl)phenol [9]

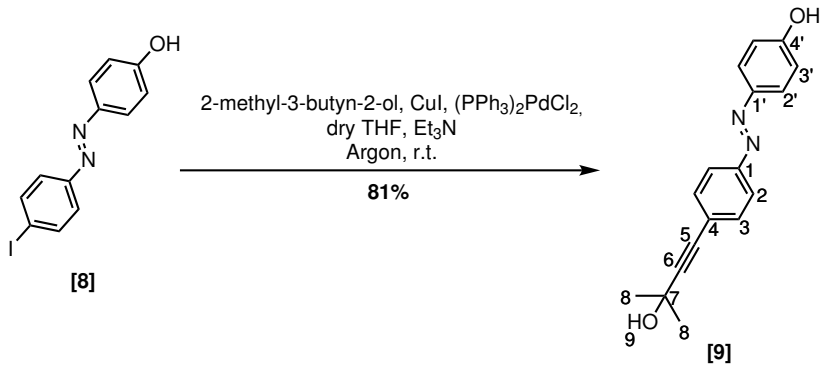

Die approbierte gedruckte Originalversion dieser Dissertation ist an der TU Wien Bibliothek verfügbar.
The approved original version of this doctoral thesis is available in print at TU Wien Bibliothek.
TU Bibliothek Your knowledge hub WIEN

This reaction followed a protocol from the literature.[148] 4-((4-Iodophenyl)diazenyl)phenol **[8]** (2.7 g, 8.3 mmol, 1 equiv.), bis(triphenylphosphine) palladium (II) dichloride (0.233 g, 0.33 mmol, 0.04 equiv.) and copper (I) iodide (31.62 mg, 1.7 mmol, 0.02 equiv.) were dissolved in 230 mL of dry THF and 230 mL of Et_3N and flushed with argon. Then 2-methyl-3-butyn-2-ol (2.09 g, 24.9 mmol, 3 equiv.) was added dropwise and the reaction was kept at room temperature overnight. The solid was removed by filtration, washed with THF and the filtrate was evaporated. The crude material was purified by column chromatography (silica gel//crude = 100:1) using PE:EtOAc (2:1). The analytical data are in accordance with the literature.[148]

Yield: 59% (1.87 g, 6.7 mmol)

Appearance: orange solid

Melting point: 194.1 - 195.8 °C (Lit.: not reported)

TLC analysis: R_f = 0.54 (PE:EtOAc = 1:1)

Sum formula: $C_{17}H_{16}N_2O_2$

^{1}H NMR (400 MHz, DMSO-d_6): δ = 1.49 (s, 6H, CH_3), 5.53 (br s, 1H, H-9), 6.95 (d, J = 8.9 Hz, 2H, H-3'), 7.55 (d, J = 8.7 Hz, 2H, H-3), 7.77 – 7.83 (m, 4H, H-3 and H-6), 10.36 (s, 1H, Ar OH) ppm.

^{13}C NMR (400 MHz, DMSO-d_6): δ = 31.5 (q,CH_3), 63.7 (s, C-7), 80.18 (s, C-5), 98.4 (s, C-6), 116.0 (d, 2C,C-3'), 122.4 (d, 2C, C-2), 124.5 (d, 2C, C-4), 125.0 (2, 2C, C-2'), 132.3 (d, 2C, C-3), 145.3 (s, C-1'), 151.2 (s, C-1), 161.3 (s, C-4') ppm.

E.2.1.8 4-((4-Ethynylphenyl)diazenyl)phenol [10]

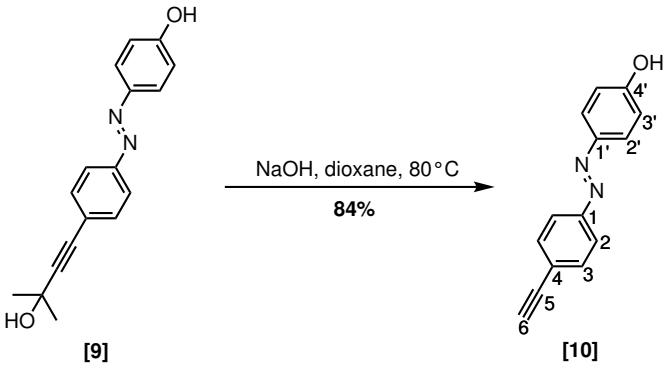

[9] **[10]**

Die approbierte gedruckte Originalversion dieser Dissertation ist an der TU Wien Bibliothek verfügbar.
The approved original version of this doctoral thesis is available in print at TU Wien Bibliothek.
TU Bibliothek Your knowledge hub WIEN

This reaction followed a protocol from the literature.[148] 4-((4-(3-Hydroxy-3-methylbut-1-yn-1-yl)phenyl)diazenyl)phenol **[9]** (1.9 g, 6.7 mmol, 1 equiv.) was dissolved in 350 mL of dry dioxane, then NaOH (2.4 g, 60 mmol, 4.8 equiv.) was added and the mixture was heated to 80°C. After 4 hours TLC shows full consumption of the starting material. The reaction mixture was cooled to room temperature, the dioxane was evaporated and the crude material was dissolved in EtOAc and washed with water. After separation of the organic and water phases, the organic phase was dried over $MgSO_4$, filtered and the solvent was evaporated. The crude material was purified by column chromatography (silica gel/crude = 100:1) with PE:EtOAc (6:1). The analytical data are in accordance with the literature.[148]

Yield: 84% (1.25 g, 5.6 mmol)

Appearance: orange solid

Melting point: 159.4 - 160.5 °C (Lit[148]: not reported)

TLC analysis: R_f = 0.8 (PE:EtOAc = 1:1)

Sum formula: $C_{14}H_{10}N_2O$

^{1}H NMR (400 MHz, DMSO-d_6): δ = 4.40 (s, 1H, C-6), 6.96 (d, J = 8.9 Hz, 2H, H-3'), 7.65 (d, J = 8.6 Hz, 2H, H-3), 7.77 – 7.85 (m, 4H, H-2+H-2'), 10.39 (s, 1H, OH) ppm.

^{13}C NMR (400 MHz, DMSO-d_6): δ = 82.7 (s, C-6), 82.9 (s, C-5), 115.8 (d, 2C, C-3'), 122.1 (d, 2C, C-2), 123.3 (s, C-4), 124.9 (d, 2C, C-2'), 132.6 (d, 2C, C-3), 145.0 (s, C-4'), 151.5 (s, C-1), 161.2 (s, C-1') ppm.

Die approbierte gedruckte Originalversion dieser Dissertation ist an der TU Wien Bibliothek verfügbar.
The approved original version of this doctoral thesis is available in print at TU Wien Bibliothek.

E.2.1.9 Equatorial (*E*)-cyclooct-4-en-1-yl (4-(4-ethynylphenyl)diazenyl)phenyl) carbonate [11e]

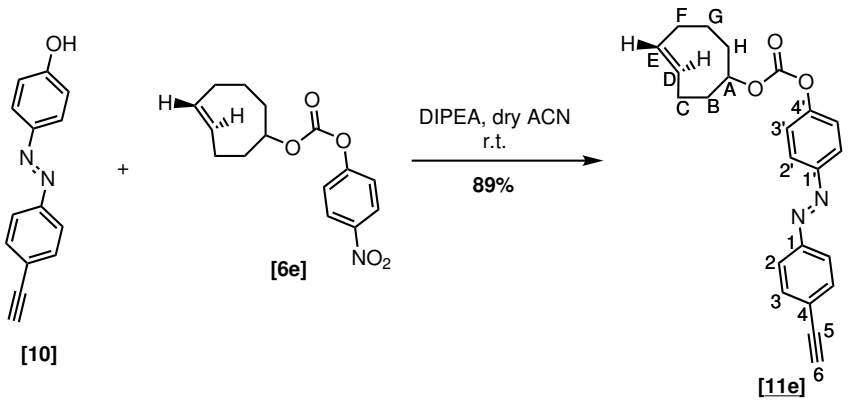

4-((4-Ethynylphenyl)diazenyl)phenol **[10]** (49.4 mg, 0.17 mmol, 1 equiv.) and equatorial *(E)*-cyclooct-4-en-1-yl (4-nitrophenyl) carbonate **[6e]** (75.4 mg, 0.34 mmol, 2 equiv.) were dissolved in 2.5 mL of dry ACN and then DIPEA (0.6 mL, 3.4 mmol, 20 equiv.) was added. The reaction mixture was stirred overnight at room temperature. After evaporation of the solvent, the crude material was purified by column chromatography (silica gel/crude = 100:1) using n-hexane:EtOAc (7:1).

Yield: 89% (56.1 mg, 0.18 mmol)

Appearance: orange solid

Melting point: 131.1-132.8 °C

TLC analysis: R_f = 0.51 (n-hexane:EtOAc = 10:1)

Sum formula: $C_{23}H_{22}N_2O_3$

HR-MS: $[M+H]^+$ calculated = 375.1703 Da; $[M+H]^+$ found = 375.1705; difference = 0.6 mDa

^{1}H NMR (400 MHz, $CDCl_3$): δ = 1.64 – 1.86 (m, 2H, H-G+H-H), 1.87 – 2.07 (m, 3H, H-F + H-G + H-H), 2.06 – 2.26 (m, 2H, H-B), 2.32 – 2.48 (m, 3H, H-C + H-F), 3.24 (s, 1H, H-6), 4.40 – 4.52 (m, 1H, H-A), 5.44 – 5.58 (m, 1H, H-E), 5.56 – 5.68 (m, 1H, H-D), 7.34 (d, J = 8.8 Hz, 2H, H-2′ or H-3′), 7.63 (d, J = 8.5 Hz, 2H, H-3), 7.87 (d, J = 8.5 Hz, 2H, H-2), 7.95 (d, J = 8.8 Hz, 2H, H-2′ or H-3′) ppm.

^{13}C NMR (101 MHz, $CDCl_3$): δ = 31.2 (t, C-G), 32.6 (t, C-C), 34.3 (t, C-F), 38.5 (t, C-H), 40.9

Die approbierte gedruckte Originalversion dieser Dissertation ist an der TU Wien Bibliothek verfügbar.
The approved original version of this doctoral thesis is available in print at TU Wien Bibliothek.
TU Bibliothek Your knowledge hub WIEN

(t, C-B), 79.7 (d, C-6), 83.4 (s, C-5), 85.9 (d, C-A), 121.9 (d, 2C, C-2′ or C-3′), 123.0 (d, 2C, C-2), 124.4 (d, 2C, C-2′ or C-3′), 124.9 (s, C-4), 133.1 (d, 2C, C-3), 133.2 (d, C-E), 135.0 (d, C-D), 150.3 (s, C-1′ or C-4′), 152.2 (s, C-1), 152.8 (s, carbonyl), 153.4 (s, C-1′ or C-4′) ppm.

E.2.1.10 Axial (*E*)-cyclooct-4-en-1-yl (4-(4-ethynylphenyl)diazenyl)phenyl) carbonate [11a]

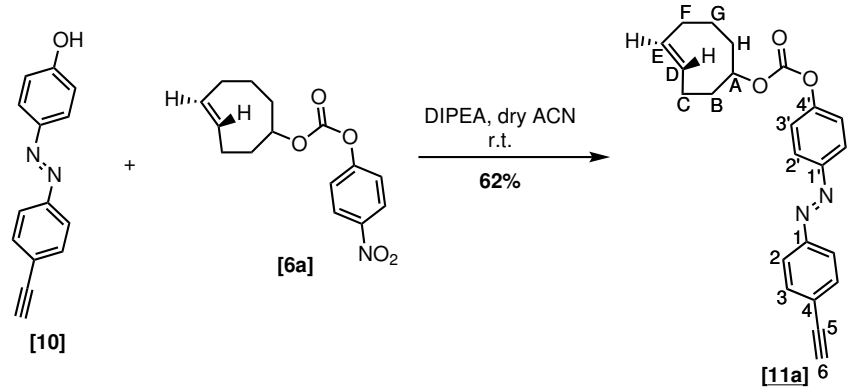

4-((4-Ethynylphenyl)diazenyl)phenol **[10]** (49.6 mg, 0.17 mmol, 1 equiv.) and axial *(E)*-cyclooct-4-en-1-yl (4-nitrophenyl) carbonate **[6a]** (75.7 mg, 0.34 mmol, 2 equiv.) were dissolved in 2.5 mL of dry ACN and then DIPEA (0.6 mL, 3.4 mmol, 20 equiv.) was added. The reaction mixture was stirred overnight at room temperature. After evaporation of the solvent, the crude material was purified by column chromatography (silica gel/crude = 100:1) using n-hexane:EtOAc (10:1).

Yield: 62% (43.5 mg, 0.12 mmol)

Appearance: orange solid

Melting point: 134.5-135.8 °C

TLC analysis: R_f = 0.66 (n-hexane:EtOAc = 6:1)

Sum formula: $C_{23}H_{22}N_2O_3$

HR-MS: $[M+H]^+$ calculated = 375.1703 Da; $[M+H]^+$ found = 375.1718 Da; difference = 1.5 mDa.

^{1}H NMR (400 MHz, $CDCl_3$): δ = 1.25 – 1.37 (m, 1H, H-H), 1.59 – 1.81 (m, 2H, H-B + H-G), 1.83 – 1.96 (m, 2H, H-F + H-G), 2.12 – 2.23 (m, 1H, H-C), 2.27 – 2.36 (m, 1H, H-F), 2.34 – 2.52 (m,

Die approbierte gedruckte Originalversion dieser Dissertation ist an der TU Wien Bibliothek verfügbar.
The approved original version of this doctoral thesis is available in print at TU Wien Bibliothek.
TU Bibliothek Your knowledge hub WIEN

3H, H-B + H-C + H-H), 3.24 (s, 1H, H-6), 4.96 – 5.05 (m, 1H, H-A), 5.49 – 5.73 (m, 2H, H-D+H-E), 7.36 (d, J = 9.0 Hz, 2H, H-2′ or H-3′), 7.64 (d, J = 8.5 Hz, 2H, H-3), 7.88 (d, J = 8.5 Hz, 2H, H-2), 7.98 (d, J = 9.0 Hz, 2H, H-2′ or H-3′) ppm.

^{13}C NMR (101 MHz, $CDCl_3$): δ = 28.1 (t, C-G), 29.9 (t, C-C), 32.3 (t, C-H), 34.3 (t, C-F), 40.8 (t, C-B), 75.5 (d, C-A), 79.7 (d, C-6), 83.4 (s, C-5), 122.0 (d, 2C, C-2′ or C-3′), 123.0 (d, 2C, C-2), 124.4 (d, 2C, C-2′ or C-3′), 124.9 (s, C-4), 131.6 (d, C-D or C-E), 133.1 (d, 2C, C-3), 135.6 (d, C-D or C-E), 150.3 (s, C-1′ or C-4′), 152.2 (s, C-1), 152.8 (s, carbonyl), 153.5 (s, C-1′ or C-4′) ppm.

E.2.1.11 Methyl 4-nitrosobenzoate [13]

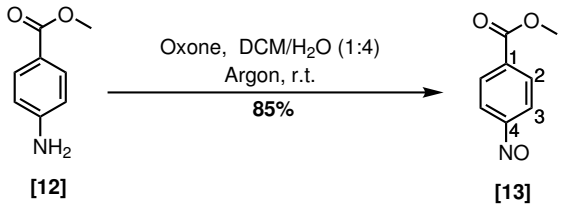

This compound was synthesized according to a literature protocol.[149] Methyl benzoate **[12]** (6.83 g, 45.2 mmol, 1 equiv.) was dissolved in 120 mL of dry DCM and placed under argon. Oxone (41.67 g, 137 mmol, 3 equiv.) was dissolved in 250 mL of water and slowly added to the reaction mixture. After 4 hours stirring at room temperature, the organic and water phases were separated and the water phase was extracted with DCM. The organic phases were combined and washed with HCl 0.5 M, water and dried over Na_2SO_4. After evaporation of the solvent, the crude material was recrystallized using DCM. The analytical data are in accordance with the literature.[149]

Yield: 85% (3.69 g, 22.3 mmol)

Appearance: yellow solid

Melting point: 141.8-142.5°C (Lit.: 122-125 °C[149], 145-150 °C[217])

TLC analysis: R_f = 0.5 (PE:EtOAc = 12:1)

Sum formula: $C_8H_7NO_3$

^{1}H NMR (400 MHz, $CDCl_3$): δ = 3.91 (s, 3H, OCH_3), 7.86 (d, J = 8.5 Hz, 2H, H-3), 8.22 (d, J

Die approbierte gedruckte Originalversion dieser Dissertation ist an der TU Wien Bibliothek verfügbar.
The approved original version of this doctoral thesis is available in print at TU Wien Bibliothek.
TU Bibliothek Your knowledge hub WIEN

= 8.6 Hz, 2H, H-2) ppm.

^{13}C NMR (101 MHz, $CDCl_3$): δ = 52.8 (q, OCH_3), 120.4 (d, 2C, C-3), 131.1 (d, 2C, C-2), 135.2 (s, C-1), 164.4 (s, C-4), 165.8 (s, carbonyl) ppm.

E.2.1.12 Methyl 4-((4-iodophenyl)diazenyl)benzoate [15]

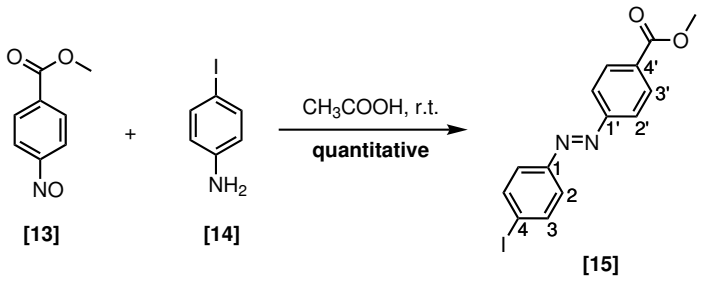

This compound was synthesized according to a literature protocol.[149] Methyl 4-nitrosobenzoate **[13]** (5.65 g, 34.2 mmol, 2 equiv.) was suspended in 200 mL of glacial acetic acid and 4-iodoaniline **[14]** (5.26 g, 17.1 mmol, 1 equiv.) was added, dissolved in 50 mL of glacial acetic acid. After stirring overnight, the precipitate was collected by filtration, washed with glacial acetic acid, water and EtOAc. The analytical data are in accordance with the literature.[149]

Yield: quantitative (7.68 g, 0.02 mmol)

Appearance: orange solid

Melting point: 216.6-216.7 °C (Lit.:[149] 206-208 °C)

TLC analysis: R_f = 0.57 (PE:EtOAc = 8:1)

Sum formula: $C_{14}H_{11}N_2O_2$

^{1}H NMR (400 MHz, $CDCl_3$): δ = 3.96 (s, 3H, OCH_3), 7.68 (d, J = 8.7 Hz, 2H, H-2), 7.89 (d, J = 8.7 Hz, 2H, H-3), 7.95 (d, J = 8.8 Hz, 2H, H-2'), 8.19 (d, J = 8.7 Hz, 2H, H-3') ppm.

^{13}C NMR (101 MHz, $CDCl_3$): δ = 52.5 (q, OCH_3), 98.8 (s, C-1 or C-4), 122.9 (d, 2C, C-2'), 124.8 (d, 2C, C-2), 130.8 (d, 2C, C-3'), 132.3 (s, C-4'), 138.7 (d, 2C, C-3), 152.0 (s, C-1 or C-4), 155.0 (s, C-1'), 166.6 (s, carbonyl) ppm.

Die approbierte gedruckte Originalversion dieser Dissertation ist an der TU Wien Bibliothek verfügbar.
The approved original version of this doctoral thesis is available in print at TU Wien Bibliothek.
TU Bibliothek Your knowledge hub WIEN

E.2.1.13 Methyl 4-((4-ethynylphenyl)diazenyl)benzoate [16]

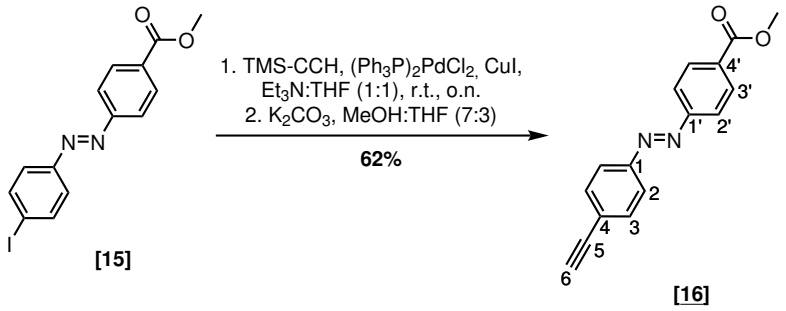

Methyl 4-((4-iodophenyl)diazenyl)benzoate **[15]** (1.76 g, 4.8 mmol, 1 equiv.), CuI (27.4 mg, 0.14 mmol, 0.03 equiv.) and $(Ph_3P)_2PdCl_2$ (101 g, 0.14 mmol , 0.03 equiv.) were dissolved in 300 mL of dry THF:Et_3N (1:1) and placed under argon. Then trimethylsilylacetylene (0.95 g, 9.6 mmol, 2 equiv.) was added dropwise to the reaction mixture and the reaction was stirred overnight. The reaction mixture was evaporated to almost dryness, diluted in DCM and filtered through a pad of silica. After evaporation of the filtrate, the obtained solid was dissolved in 500 mL of dry methanol:dry THF (3:7), K_2CO_3 (1.99 g, 14.4 mmol, 3 equiv.) was added and the mixture was stirred for 2 hours. The reaction mixture was diluted with EtOAc and the organic phase was washed with brine, dried over Na_2SO_4 and the solvent was evaporated. The crude material was purified by column chromatography (silica gel/crude = 100:1) with n-hexane:EtOAc (4:1).

Yield: 62% (0.782 g, 3 mmol)

Appearance: orange solid

Melting point: 182.1-182.5 °C

TLC analysis: R_f = 0.54 (PE: EtOAc = 8:1)

Sum formula: $C_{16}H_{12}N_2O_2$

HR-MS: $[M+H]^+$ calculated = 265.0972 Da; $[M+H]^+$ found = 265.0981 Da; difference = 0.9 mDa

^{1}H NMR (400 MHz, $CDCl_3$): δ = 3.26 (s, 1H, H-6), 3.96 (s, 3H, OCH_3), 7.65 (d, J = 8.6 Hz, 2H, H-3), 7.91 (d, J = 8.6 Hz, 2H, H-2), 7.95 (d, J = 8.6 Hz, 2H, H-2'), 8.19 (d, J = 8.6 Hz, 2H, H-3')

Die approbierte gedruckte Originalversion dieser Dissertation ist an der TU Wien Bibliothek verfügbar.
The approved original version of this doctoral thesis is available in print at TU Wien Bibliothek.
TU Bibliothek Your knowledge hub WIEN

ppm.

^{13}C NMR (101 MHz, $CDCl_3$): δ = 52.5 (q, OCH_3), 80.1 (d, C-6), 83.3 (s, C-5), 122.9 (d, 2C, C-2′), 123.3 (d, 2C, C-2), 125.6 (s, C-4), 130.8 (d, 2C, C-3′), 132.2 (s, C-4′), 133.2 (d, 2C, C-3), 152.2 (s, C-1), 155.1 (s, C-1′), 166.6 (s,carbonyl) ppm.

E.2.1.14 4-((4-Ethynylphenyl)diazenyl)benzoic acid [17]

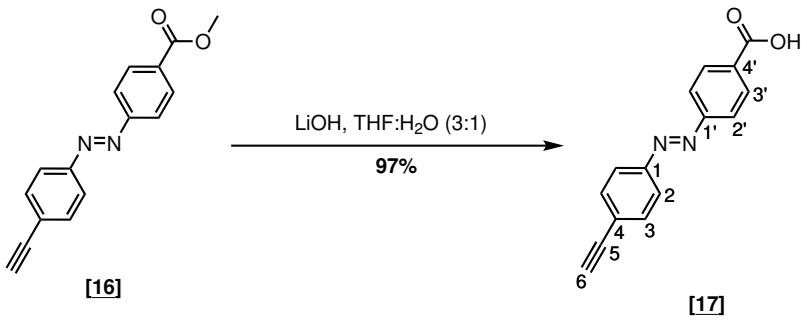

[16] [17]

Methyl 4-((4-ethynylphenyl)diazenyl)benzoate **[16]** (0.115 g, 0.43 mmol, 1 equiv.) was dissolved in 13.5 mL of THF and LiOH (0.259 g, 10.8 mmol, 25 equiv.) was added, dissolved in 4.5 mL of water. After stirring overnight, the reaction mixture was acidified using 2 M HCl, EtOAc was added and the organic and water phases were separated. The water phase was extracted with EtOAc, all of the organic phases were combined, dried over $MgSO_4$ and the solvent was evaporated.

Yield: 97% (0.105 g, 0.40 mmol)

Appearance: orange solid

Melting point: 242.4-245.1 °C

TLC analysis: R_f = 0.54 (DCM:MeOH = 20:1)

Sum formula: $C_{15}H_{10}N_2O_2$

HR-MS: $[M+H]^+$ calculated = 251.0815 Da; $[M+H]^+$ found = not found.

^{1}H NMR (400 MHz, DMSO-d_6): δ = 4.49 (s, 1H, H-6), 7.72 (d, J = 8.5 Hz, 2H, H-3), 7.93 (d, J = 8.5 Hz, 2H, H-2), 7.98 (d, J = 8.5 Hz, 2H, H-2′), 8.15 (d, J = 8.5 Hz, 2H, H-3′), 13.18 (br s, 1H, COOH) ppm.

Die approbierte gedruckte Originalversion dieser Dissertation ist an der TU Wien Bibliothek verfügbar.
The approved original version of this doctoral thesis is available in print at TU Wien Bibliothek.
TU Bibliothek Your knowledge hub WIEN

^{13}C NMR (101 MHz, DMSO-d_6): δ = 82.92 (d, C-6), 83.91 (s, C-5), 122.70 (d, 2C, C-2′), 123.09 (d, 2C, C-2), 125.27 (s, C-4), 130.65 (d, 2C, C-3′), 133.02 (d, 2C, C-3), 133.13 (s, C-4′), 151.36 (s, C-1), 154.17 (s, C-1′), 166.63 (s, carbonyl) ppm.

E.2.1.15 Equatorial (E)-cyclooct-4-en-1-yl 4-(4-ethynylphenyl)diazenyl)benzoate [18e]

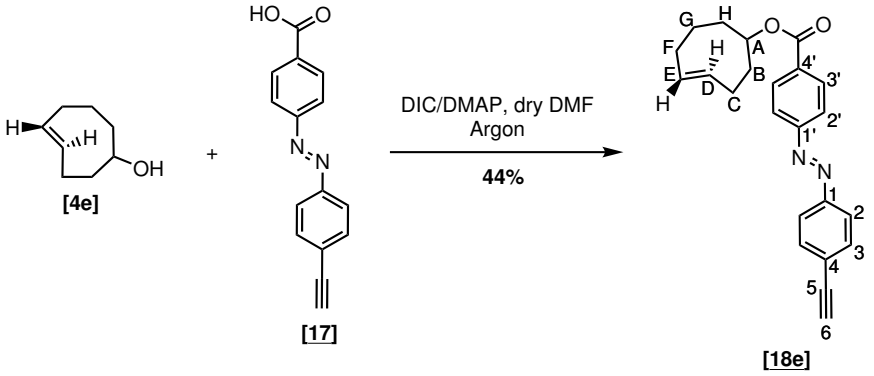

4-((4-Ethynylphenyl)diazenyl)benzoic acid **[17]** (0.406 g, 1.6 mmol, 2 equiv.), equatorial *(E)*-cyclooct-4-en-1-ol **[4e]** (0.102 g, 0.81 mmol, 1 equiv.) and DMAP (0.149 g, 1.2 mmol, 1.5 equiv.) were dissolved in 2 mL of dry DMF, placed under argon and cooled to 0°C. After 20 minutes, DIC (0.42 mL, 2.6 mmol, 3.2 equiv.) was added to the reaction mixture, which was then allowed to warm to room temperature. After 4 hours, the solvent was evaporated and the crude material was purified by column chromatography (silica gel/crude = 100:1) using n-hexane:EtOAc (12:1).

Yield: 44% (0.129 g, 0.36 mmol)

Appearance: orange solid

Melting point: 116.5-117.6 °C

TLC analysis: R_f = 0.52 (n-hexane:EtOAc = 12:1)

Sum formula: $C_{23}H_{22}N_2O_2$

HR-MS: $[M+H]^+$ calculated = 359.1754 Da; $[M+H]^+$ found = 359.1759 Da; difference = 0.5 mDa

^{1}H NMR (400 MHz, $CDCl_3$): δ = 1.67 – 1.77 (m, 1H, H-H), 1.81 – 1.93 (m, 2H, H-G + H-H),

Die approbierte gedruckte Originalversion dieser Dissertation ist an der TU Wien Bibliothek verfügbar.
The approved original version of this doctoral thesis is available in print at TU Wien Bibliothek.
TU Bibliothek Your knowledge hub WIEN

1.96 – 2.05 (m, 2H, H-F + H-G), 2.12 – 2.22 (m, 2H, H-B), 2.39 – 2.47 (m, 3H, H-C + H-F), 3.25 (s, 1H, H-6), 4.66 – 4.79 (m, 1H, H-A), 5.55 – 5.70 (m, 2H, H-D+ H-E), 7.65 (d, J = 8.7 Hz, 2H, H-3), 7.89 – 7.95 (m, 4H, H-2 + H-2'), 8.15 (d, J = 8.9 Hz, 2H, H-3') ppm.

^{13}C NMR (101 MHz, $CDCl_3$): δ = 31.1 (t, C-G), 32.6 (t, C-C), 34.3 (t, C-F), 38.7 (t, C-H), 41.0 (t, C-B), 79.9 (d, C-6), 81.3 (t, C-A), 83.2 (s, C-5), 122.7 (d, 2C, C-2'), 123.1 (d, 2C, C-2), 125.4 (s, C-4), 130.5 (d, 2C, C-3'), 132.9 (s, C-4'), 133.1 (d, 2C, C-3), 133.2 (d, C-E), 135.0 (d, C-D), 152.1 (s, C-1), 154.9 (s, C-1'), 165.3 (s, carbonyl) ppm.

E.2.1.16 Axial (E)-cyclooct-4-en-1-yl 4-(4-ethynylphenyl)diazenyl)benzoate [18a]

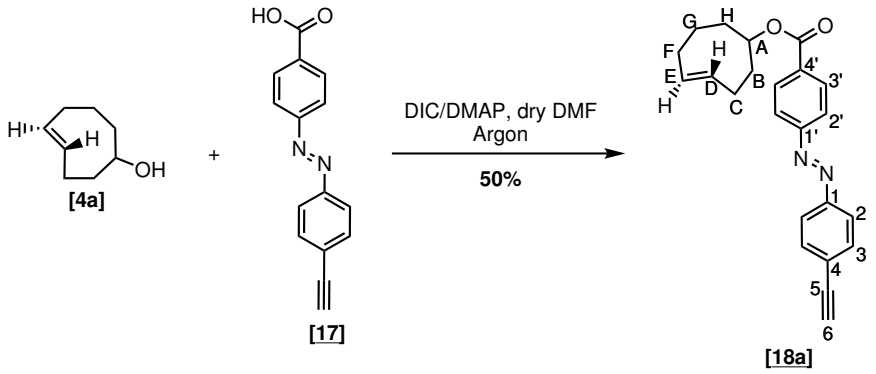

4-((4-Ethynylphenyl)diazenyl)benzoic acid **[17]** (0.222 g, 0.89 mmol, 2 equiv.), axial *(E)*-cyclooct-4-en-1-ol **[4a]** (0.056 g, 0.44 mmol, 1 equiv.) and DMAP (0.081 g, 0.66 mmol, 1.5 equiv.) were dissolved in 2 mL of dry DMF, placed under argon and cooled to 0°C. After 20 minutes, DIC (0.22 mL, 1.4 mmol, 3.2 equiv.) was added to the reaction mixture, which was allowed to warm up to room temperature. After 4 hours, the solvent was evaporated and the crude material was purified by column chromatography (silica gel/crude = 100:1) using n-hexane:EtOAc (12:1).

Yield: 50% (0.080 g, 0.22 mmol)

Appearance: orange solid

Melting point: 108.2 - 109.9 °C

TLC analysis: R_f = 0.64 (PE:EtOAc = 15:1)

Sum formula: $C_{23}H_{22}N_2O_2$

Die approbierte gedruckte Originalversion dieser Dissertation ist an der TU Wien Bibliothek verfügbar.
The approved original version of this doctoral thesis is available in print at TU Wien Bibliothek.
TU Bibliothek Your knowledge hub WIEN

HR-MS:$[M+H]^+$ calculated = 359.1754 Da; $[M+H]^+$ found = 359.1768 Da; difference = 1.4 mDa

^{1}H NMR (600 MHz, $CDCl_3$): δ = 1.34 – 1.41 (m, 1H, H-H), 1.48 – 1.57 (m, 1H, H-G), 1.79 – 1.87 (m, 2H, H-B+ H-G), 1.89 – 1.96 (m, 1H, H-F), 2.22 – 2.25 (m, 1H, H-C), 2.28 – 2.33 (m, 1H, H-F), 2.41 – 2.48 (m, 2H, H-H + H-B), 2.49 – 2.55 (m, 1H, H-C), 3.26 (s, 1H, H-6), 5.27 – 5.31 (m, 1H, H-A), 5.63 – 5.69 (m, 1H, H-D), 5.74 – 5.81 (m, 1H, H-E), 7.66 (d, J = 8.6 Hz, 2H, H-3), 7.93 (d, J = 8.5 Hz, 2H, H-2), 7.99 (d, J = 8.6 Hz, 2H, H-2'), 8.25 (d, J = 8.7 Hz, 2H, H-3') ppm.

^{13}C NMR (151 MHz, $CDCl_3$): δ = 28.5 (t, C-G), 30.4 (t, C-C), 32.6 (t, C-H), 34.5 (t, C-F), 41.1 (t, C-B), 71.3 (d, C-A), 80.1 (s, C-4), 83.3 (s, C-5), 123.0 (d, 2C, C-2'), 123.3 (d, 2C, C-2), 125.6 (s, C-4), 130.7 (d, 2C, C-3'), 132.0 (d, C-D), 132.6 (s, C-4'), 133.2 (d, 2C, C-3), 135.4 (d, C-E), 152.2 (s, C-1), 155.2 (s, C-1'), 165.1 (s, carbonyl) ppm.

E.2.2 SPAAC-tetrazine ligation azobenzene

E.2.2.1 Ethyl (1R,8S,9s,Z)-bicyclo[6.1.0]non-4-ene-9-carboxylate [19endo] and ethyl (1R,8S,9r,Z)-bicyclo[6.1.0]non-4-ene-9-carboxylate [19exo]

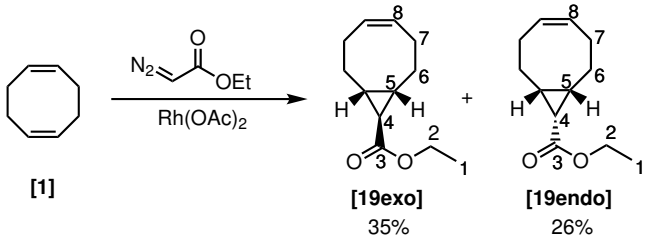

These compounds were prepared according to the literature.[151] A round-bottomed flask was filled with rhodium(II) acetate (1.08 g, 22.6 mmol, 0.043 equiv.) and 1,5-cyclooctadiene **[1]** (45.5 g, 420.7 mmol, 8 equiv.), and placed under argon atmosphere. Ethyl 2-diazoacetate (6.90 g, 52.6 mmol, 1 equiv.) was added with a syringe pump to the reaction mixture over 60 hours. The reaction mixture was filtered through a glass filter with silica and eluted with PE:EtOAc (100:1). The fractions that only contained 1,5-cyclooctadiene were separated and the remaining ones were pooled, the solvent was evaporated and the crude material was purified by column chromatography (silica gel/crude = 100:1) using PE:EtOAc (100:1) affording the compounds

Die approbierte gedruckte Originalversion dieser Dissertation ist an der TU Wien Bibliothek verfügbar.
The approved original version of this doctoral thesis is available in print at TU Wien Bibliothek.

[19endo] and **[19exo]**. The analytical data are in accordance with the literature.[151]

Yield: 26% **[19endo]** (2.7 g, 13.7 mmol) and 35% **[19exo]** (3.5 g, 18.1 mmol) (Lit.: 44%/54%,[151] 58%/24%[111] **endo/exo**)

Appearance ([19endo] and [19exo]): colorless oils

TLC analysis: R_f**[19endo]** = 0.35 (n-heptane:EtOAc = 20:1) and R_f**[19exo]** = 0.24 (n-heptane:EtOAc = 20:1)

Sum formula: $C_{12}H_{20}O_2$

^{1}H NMR [19endo] (600 MHz, $CDCl_3$): δ = 1.26 (t, J = 7.1 Hz, 3H, H-1), 1.35 – 1.43 (m, 2H, H-5), 1.70 (t, J = 8.8 Hz, 1H, H-4), 1.79 – 1.86 (m, 1H, H-6), 2.01 – 2.10 (m, 1H, H-7), 2.13 – 2.26 (m, 1H, H-6), 2.46 – 2.54 (m, 2H, H-7), 4.11 (q, J = 7.1 Hz, 2H, H-2), 5.57 – 5.64 (m, 2H, H-8) ppm.

^{13}C NMR [19endo] (151 MHz, $CDCl_3$): δ = 14.6 (q, C-1), 21. (d,4 C-4), 22.8 (t, 2C, C-6), 24.3 (d, 2C, C-5), 27.2 (t, 2C, C-7), 59.9 (t, C-2), 129.6 (d, 2C, C-8), 172.5 (s, C-3) ppm.

^{1}H NMR [19exo] (600 MHz, $CDCl_3$): δ = 1.17 (t, J = 4.6 Hz, 1H, H-4), 1.24 (t, J = 7.1 Hz, 3H, H-1), 1.42 – 1.50 (m, 1H, H-6), 1.52 – 1.58 (m, 2H, H-5), 2.02 – 2.13 (m, 2H, H-7), 2.15 – 2.23 (m, 2H, H-6), 2.24 – 2.34 (m, 2H, H-7), 4.08 (q, J = 7.1 Hz, 2H, H-2), 5.60 – 5.66 (m, 2H, H-8) ppm.

^{13}C NMR [19exo] (151 MHz, $CDCl_3$): δ = 14.4 (q, C-1), 26.8 (t, 2C, C-7), 27.8 (d, 2C, C-5), 28.0 (d, C-4), 28.4 (t, 2C, C-6), 60.4 (t, C-2), 130.0 (d, 2C, C-8), 174.5 (s, C-3) ppm.

E.2.2.2 (1R,8S,9s,Z)-Bicyclo[6.1.0]non-4-en-9-yl)methanol [20endo]

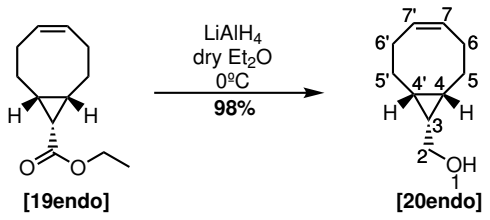

This compound was prepared according to the literature.[111] Lithium aluminum hydride (0.196 mg, 23.1 mmol, 1.8 equiv.) was suspended in 10 mL of dry Et_2O and cooled to 0°C. Ethyl (1R,8S,9s,Z)-bicyclo[6.1.0]non-4-ene-9-carboxylate **[19endo]** (2.5 g, 12.8 mmol, 1 equiv.) was dissolved in 55 mL of dry Et_2O and added dropwise to the reaction mixture with an addition funnel. Upon

Die approbierte gedruckte Originalversion dieser Dissertation ist an der TU Wien Bibliothek verfügbar.
The approved original version of this doctoral thesis is available in print at TU Wien Bibliothek.
TU Bibliothek Your knowledge hub WIEN

complete addition, the reaction mixture was allowed to warm to room temperature. After 1 hour the reaction mixture was diluted with Et_2O, cooled to 0°C and quenched by the slow addition of aqueous saturated Na_2SO_4 solution. The obtained suspension was filtered and the filtrate collected. The organic and water phases were separated, the water phase was extracted with Et_2O, the organic phases were combined, dried over Na_2SO_4 and the solvent was evaporated. The analytical data are in accordance with the literature.[111]

Yield: 98% (1.9 g, 11.4 mmol)

Appearance: beige oil

TLC analysis: R_f = 0.1 (n-heptane:EtOAc = 10:1)

Sum formula: $C_{10}H_{16}O$

^{1}H NMR (600 MHz, $CDCl_3$): δ = 0.94 – 1.02 (m, 2H, H-4), 1.10 (p, J = 8.2 Hz, 1H, H-3), 1.52 – 1.59 (m, 2H, H-5 or H-5'), 1.93 – 2.00 (m, 2H, H-5 or H-5'), 2.05 – 2.11 (m, 2H, H-6 or H-6'), 2.31 – 2.38 (m, 2H, H-6 or H-6'), 3.69 (d, J = 7.6 Hz, 2H, H-2), 5.57 – 5.64 (m, 2H, H-7+H-7') ppm.

^{13}C NMR (151 MHz, $CDCl_3$): δ = 19.1 (d, C-4), 20.8 (d, C-3), 24.0 (t, C-5), 27.8 (t, C-6), 60.3 (t, C-2), 129.8 (d, C-7) ppm.

E.2.2.3 (1R,8S,9s)-4,5-Dibromobicyclo[6.1.0]nonan-9-yl)methanol [21endo]

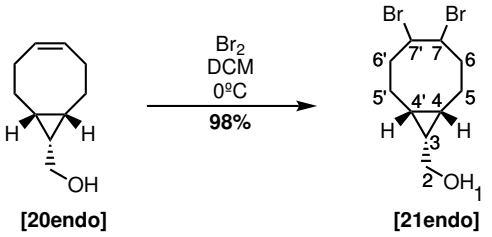

[20endo] **[21endo]**

This compound was prepared according to the literature.[153] (1R,8S,9s,Z)-Bicyclo[6.1.0]non-4-en-9-yl)methanol **[20endo]** (1.92 g, 12.6 mmol, 1 equiv.) was dissolved in 40 mL of DCM and cooled to 0°C. Bromine (0.71 mL, 13.85 mmol, 1.1 equiv.) was diluted in 6 mL of DCM and added dropwise to the reaction mixture with an addition funnel, turning the reaction mixture yellow. The reaction mixture was quenched with aqueous saturated $Na_2S_2O_3$ solution, the organic phase was separated from the water phase, dried over Na_2SO_4 and the solvent was

Die approbierte gedruckte Originalversion dieser Dissertation ist an der TU Wien Bibliothek verfügbar.
The approved original version of this doctoral thesis is available in print at TU Wien Bibliothek.
TU Bibliothek Your knowledge hub WIEN

evaporated. The desired product was obtained pure and used without further purification (purity >95% according to NMR). The analytical data are in accordance with the literature.[153]

Yield: 98% (3.8 g, 12.3 mmol)

Appearance: colorless solid

Melting point: 102.2 - 103.5 °C (Lit.:[153] 104 - 106 °C)

TLC analysis: R_f = 0.22 (PE:EtOAc = 3:1)

Sum formula: $C_{10}H_{16}Br_2O_2$

^{1}H NMR (600 MHz, $CDCl_3$): δ = 1.06 – 1.13 (m, 1H, H-4 or H-4′), 1.14 – 1.19 (m, 1H, H-4 or H-4′), 1.20 – 1.24 (m, 1H, H-3), 1.53 – 1.69 (m, 2H, H-5 or H-5′), 1.86 – 1.98 (m, 2H, H-5 or H-5′), 2.13 – 2.19 (m, 1H, H-6 or H-6′), 2.24 – 2.31 (m, 1H, H-6 or H-6′), 2.62 – 2.77 (m, 2H, H-6 or H-6′), 3.73 – 3.79 (m, 2H, H-2), 4.79 – 4.82 (m, 1H, H-7 or H-7′), 4.83 – 4.86 (m, 1H, H-7 or H-7′) ppm.

^{13}C NMR (151 MHz, $CDCl_3$): δ = 17.3 (d, C-4 or C-4′), 19.1 (t, C-5 or C-5′), 20.1 (t, C-5 or C-5′), 20.2 (d, C-4 or C-4′), 22.0 (d, C-3), 35.1 (t, C-6 or C-6′), 35.1 (t, C-6 or C-6′) 53.4 (s, C-7 or C-7′), 56.3 (s, C-7 or C-7′), 59.8 (t, C-2) ppm.

E.2.2.4 (1R,8S,9s)-Bicyclo[6.1.0]non-4-yn-9-yl)methanol [22endo]

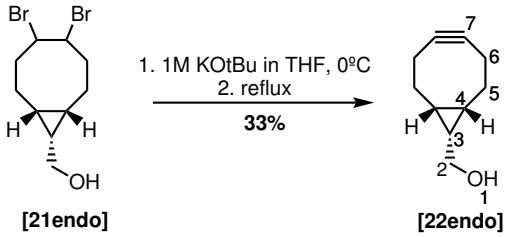

This compound was prepared according to the literature.[111] (1R,8S,9s)-4,5-Dibromobicyclo [6.1.0]nonan-9-yl)methanol **[21endo]** (3.86 g, 12.36 mmol, 1 equiv.) was dissolved in 140 mL of dry THF and cooled to 0°C. 1 M KOtBu in THF (40.8 mL, 40.83 mmol, 3.3 equiv.) was added dropwise and the reaction mixture was heated to 70°C. After 2 hours the reaction mixture was quenched with aqueous saturated NH_4Cl solution, the organic phase was separated, dried over $NaSO_4$ and the solvent was evaporated. The crude material was purified by column chro-

Die approbierte gedruckte Originalversion dieser Dissertation ist an der TU Wien Bibliothek verfügbar.
The approved original version of this doctoral thesis is available in print at TU Wien Bibliothek.
TU Bibliothek Your knowledge hub WIEN

matography (silica gel/crude =100:1) using a PE:EtOAc gradient (3:1 till 1:1). The analytical data are in accordance with the literature.[153]

Yield: 33% (0.612 g, 0.4 mmol)

Appearance: beige oil

TLC analysis: R_f = 0.24 (PE:EtOAc = 1:1)

Sum formula: $C_{10}H_{14}O$

^{1}H NMR (600 MHz, $CDCl_3$): δ = 0.89 – 0.95 (m, 2H, H-4), 1.32 (m, 1H, H-3), 1.55 – 1.62 (m, 2H, H-5), 2.16 – 2.33 (m, 6H, H-6 + H-5), 3.71 (d, J = 7.9 Hz, 2H, H-2) ppm.

^{13}C NMR (151 MHz, $CDCl_3$): δ = 20.1 (d, 2C, C-4), 21.5 (d, C-3), 21.6 (t, 2C, C-6), 29.1 (t, 2C, C-5), 60.0 (t, C-2), 99.0 (s, 2C, C-7) ppm.

E.2.2.5 Ethyl 4-((4-hydroxyphenyl)diazenyl)benzoate [24]

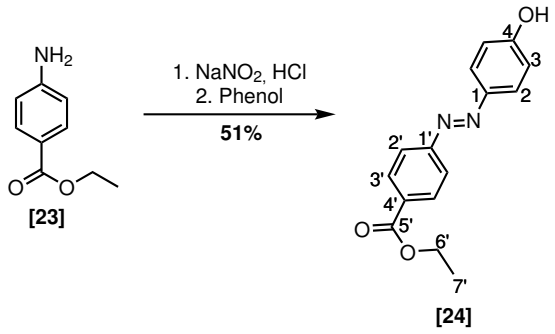

This compound was prepared according to the literature.[158] Ethyl-4-aminobenzoate **[23]** (1.44 g, 8.74 mmol, 1 equiv.) was dissolved in 20 mL of 2 M HCl and cooled to 0°C. The $NaNO_2$ (0.747 g, 10.82 mmol, 1.2 equiv.) was dissolved in 5 mL of water and slowly added to the reaction mixture. After 30 minutes, phenol (1.0 g, 10.63 mmol, 1.2 equiv.) was added to the reaction mixture . After 1h30 aqueous saturated $NaHCO_3$ solution was added until reaching pH 7. The precipitate collected by filtration, washed with water and recrystallized from ethanol. The analytical data are in accordance with the literature.[157]

Yield: 51% (1.15 g, 4.3 mmol)

Appearance: orange solid

Die approbierte gedruckte Originalversion dieser Dissertation ist an der TU Wien Bibliothek verfügbar.
The approved original version of this doctoral thesis is available in print at TU Wien Bibliothek.

Melting point: 161.8 - 162.3 °C (Lit.: 162 °C[158], 164 °C[157])

TLC analysis: R_f = 0.24 (PE:EtOAc = 5:1)

Sum formula: $C_{15}H_{14}N_2O_3$

^{1}H NMR (600 MHz, $CDCl_3$): δ = 1.43 (t, J = 7.1 Hz, 3H, H-7'), 4.42 (q, J = 7.1 Hz, 2H, H-6'), 5.52 (s, 1H, OH), 6.97 (d, J = 8.8 Hz, 2H, H-3), 7.89 – 7.94 (m, 4H, H-2' + H-2), 8.18 (d, J = 8.8 Hz, 2H, H-3') ppm.

^{13}C NMR (151 MHz, $CDCl_3$): δ = 14.48 (q, C-7'), 61.44 (t, C-6'), 116.08 (d, 2C, C-3), 122.50 (d, 2C, C-2'), 125.60 (d, 2C, C-2), 130.72 (d, 2C, C-3'), 131.70 (s, C-4'), 147.30 (s, C-1), 155.39 (s, C-1'), 159.12 (s, C-4), 166.46 (s, C-5') ppm.

E.2.2.6 4-((4-Hydroxyphenyl)diazenyl)benzoic acid [25]

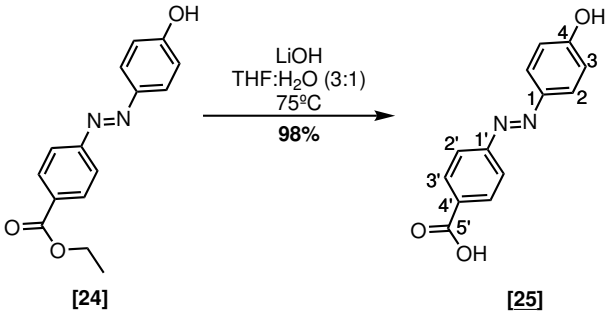

[24] [25]

Ethyl 4-((4-hydroxyphenyl)diazenyl)benzoate **[24]** (0.94 g, 3.7 mmol, 1 equiv.) was dissolved in 250 mL of THF and stirred, LiOH (2.1 g, 92.5 mmol, 25 equiv.) was dissolved in 75 mL of H_2O and added to the reaction mixture. After stirring overnight at 75°C, the reaction mixture was acidified with 2 M HCl till pH approximately 1 and diluted in DCM. The water and organic phases were separated, the water phase was extracted with DCM, the organic phases were combined, dried over $NaSO_4$, filtered and the solvent was evaporated.

Yield: 98% (0.817 g, 3.4 mmol)

Appearance: orange solid

Melting point: $>$ 220°C

TLC analysis: R_f = 0.2 (PE:EtOAc = 1:1)

Die approbierte gedruckte Originalversion dieser Dissertation ist an der TU Wien Bibliothek verfügbar.
The approved original version of this doctoral thesis is available in print at TU Wien Bibliothek.
TU Bibliothek Your knowledge hub WIEN

Sum formula: $C_{13}H_{10}N_2O_3$

HR-MS: $[M+H]^+$ calculated = 243.0764 Da; $[M+H]^+$ found = 243.0767; difference = 0.3 mDa

^{1}H NMR (600 MHz, DMSO-d_6): δ = 6.96 (d, J = 8.8 Hz, 2H, H-3), 7.85 (d, J = 8.8 Hz, 2H, H-2), 7.88 (d, J = 8.6 Hz, 2H, H-2'), 8.11 (d, J = 8.5 Hz, 2H, H-3'), 10.46 (s, 1H, OH), 13.10 (s, 1H, COOH) ppm.

^{13}C NMR (151 MHz, DMSO-d_6): δ = 116.1 (d, 2C, C-2), 122.1 (d, 2C, C-2'), 125.4 (d, 2C, C-3), 130.6 (d, 2C, C-3'), 131.9 (s, C-1), 145.3 (s, C-1'), 154.6 (s, C-4), 161.7 (s, C-4'), 166.8 (s, C-5') ppm.

E.2.2.7 4-(4((((*E*)-Cyclooct-4-en-1-yl)oxy)carbonyl)oxy)phenyl)diazenyl)benzoic acid [26]

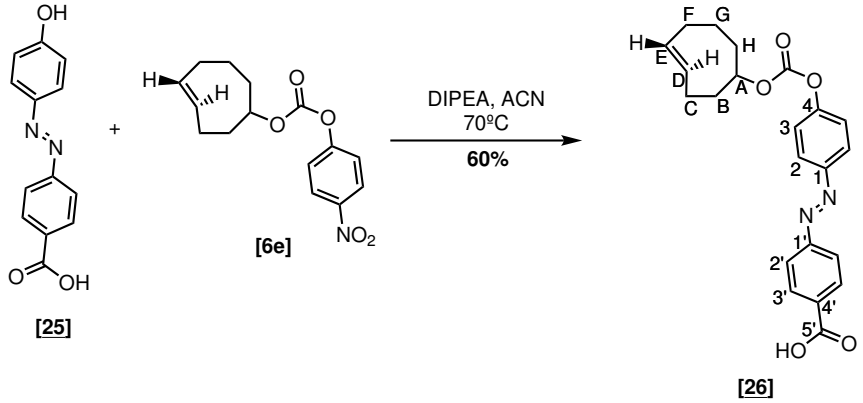

4-((4-Hydroxyphenyl)diazenyl)benzoic acid **[25]** (0.67 mg, 2.75 mmol, 2 equiv.) was dissolved in 2.8 mL of DMF and DIPEA (4.77 mL, 27.4 mmol, 30 equiv.) was added. Compound **[6e]** (0.4 g, 1.37 mmol, 1 equiv.) was dissolved in 2 mL of DMF and added to the reaction mixture. The flask was flushed with argon and stirred overnight at 70°C. The DMF was evaporated and the crude material was purified by column chromatography (silica gel/ crude = 100:1) using DCM:MeOH (100:1 till 100:5).

Yield: 60% (0.325 g, 0.8 mmol)

Appearance: orange solid

Melting point: 208.4-210.2 °C

Die approbierte gedruckte Originalversion dieser Dissertation ist an der TU Wien Bibliothek verfügbar.
The approved original version of this doctoral thesis is available in print at TU Wien Bibliothek.

TLC analysis: R_f = 0.41 (DCM:MeOH = 20:1)

Sum formula: $C_{22}H_{22}N_2O_5$

HR-MS: $[M+H]^+$ calculated = 395.1601 Da; $[M+H]^+$ found = 395.1608 Da ; difference = 0.7 mDa

^{1}H NMR (600 MHz, DMSO-d_6): δ = 1.64 – 1.74 (m, 2H, H-H + H-G), 1.79 – 1.85 (m, 1H, H-H), 1.89 – 1.96 (m, 2H, H-G + H-F), 2.04 – 2.13 (m, 2H, H-B), 2.28 – 2.35 (m, 3H, H-C + H-F), 4.34 – 4.42 (m, 1H, H-A), 5.45 – 5.52 (m, 1H, H-E), 5.58 – 5.70 (m, 1H, H-D), 7.48 (d, J = 8.8 Hz, 2H, H-3), 7.95 – 8.01 (m, 4H, H-2 + H-2′), 8.15 (d, J = 8.6 Hz, 2H, H-3′), 13.26 (s, 1H, COOH) ppm.

^{13}C NMR (151 MHz, DMSO-d_6): δ = 30.7 (t, C-G), 32.0 (t, C-C), 33.6 (t, C-F), 37.6 (t, C-H), 40.1 (t, C-B), 85.3 (d, C-A), 122.6 (d, 2C, C-3), 122.6 (d, 2C, C-2′), 124.2 (d, 2C, C-2), 130.6 (d, 2C, C-3′), 132.6 (d, C-E), 133.2 (s, C-4′), 135.0 (d, C-D), 149.6 (s, C-1), 152.0 (s, C-5), 153.3 (s, C-4), 154.1 (s, C-1′), 166.7 (s, C-5′) ppm.

E.2.2.8 3-(4-((*E*)-(4-(((((*E*)-Cyclooct-4-en-1-yl)oxy)carbonyl)oxy)phenyl)diazenyl) benzamido)propanoic acid [28]

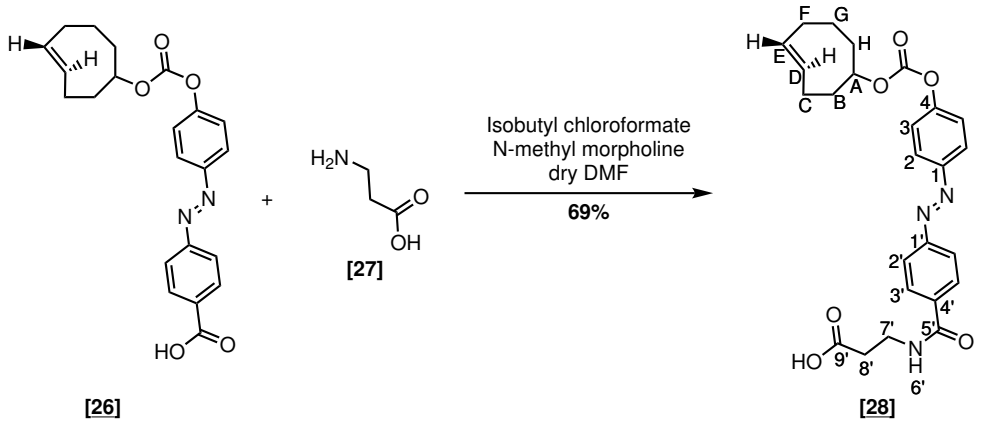

4-(4((((*E*)-Cyclooct-4-en-1-yl)oxy)carbonyl)oxy)phenyl)diazenyl)benzoic acid **[26]** (97.2 mg, 0.25 mmol, 1 equiv.) was dissolved in 5 mL of dry DMF and cooled to 0°C, and the N-methyl-morpholine (35.5 µL, 0.32 mmol, 1.3 equiv.) and the isobutyl chloroformate (52 µL, 0.39 mmol, 1.6 equiv.) were added. After 10 minutes of stirring at 0°C, β-alanine (0.110 g, 1.2 mmol,

Die approbierte gedruckte Originalversion dieser Dissertation ist an der TU Wien Bibliothek verfügbar.
The approved original version of this doctoral thesis is available in print at TU Wien Bibliothek.
TU Bibliothek Your knowledge hub WIEN

5 equiv.) was added to the reaction mixture, which stirred overnight at room temperature. The solvent was evaporated and the crude material was purified by preparative HPLC (C18 column, MeOH/H_2O, 9 minutes method: 2 minutes gradient elution - 5% MeOH till 98% MeOH - followed by 7 minutes isocratic with 98% MeOH). After evaporation of the fractions, the solid was liophilized.

Yield: 69% (78.8 mg, 0.17 mmol)

Appearance: orange solid

Melting point: 147.2-148.6 °C

TLC analysis: R_f = 0.34 (DCM:MeOH = 20:1)

Sum formula: $C_{25}H_{27}N_3O_6$

HR-MS: $[M+H]^+$ calculated = 466.1973 Da; $[M+H]^+$ found = 466.1980 Da; difference = 0.7 mDa

^{1}H NMR (400 MHz, $CDCl_3$): δ = 1.64 – 1.85 (m, 2H, H-G + H-H), 1.86 – 2.05 (m, 3H, H-F + H-G + H-H), 2.09 – 2.26 (m, 2H, H-B), 2.33 – 2.47 (m, 3H, H-C+ H-F), 2.76 (t, J = 5.4 Hz, 2H, H-8'), 3.77 (q, J = 5.7 Hz, 2H, H-7'), 4.41 – 4.51 (m, 1H, H-A), 5.45 – 5.56 (m, 1H, H-E), 5.56 – 5.68 (m, 1H, H-D), 6.96 (s, 1H, H-6'), 7.33 (d, J = 8.9 Hz, 2H, H-2'), 7.86 – 8.03 (m, 6H, H-3'+ H-2 + H-3) ppm.

^{13}C NMR (101 MHz, $CDCl_3$): δ = 31.1 (t, C-G), 32.5 (t, C-C), 33.7 (t, C-8'), 34.2 (t, C-F), 35.4 (t, C-7'), 38.4 (t, C-H), 40.8 (t, C-B), 85.9 (d, C-A), 121.8 (d, 2C, C-2'), 123.0 (d, 2C, C-3), 124.4 (d, 2C, C-2), 128.0 (d, 2C, C-3'), 133.1 (d, C-E), 134.9 (d, C-D), 135.9 (s, C-1, C-4'), 150.1 (s, C-1), 152.7 (s, C-5), 153.5 (s, C-4), 154.2 (s, C-1'), 167.0 (s, C-5'), 176.8 (s, C-9') ppm.

E.2.2.9 ((1R,8S,9s)-Bicyclo[6.1.0]non-4-yn-9-yl)methyl (4-nitrophenyl) carbonated [30endo]

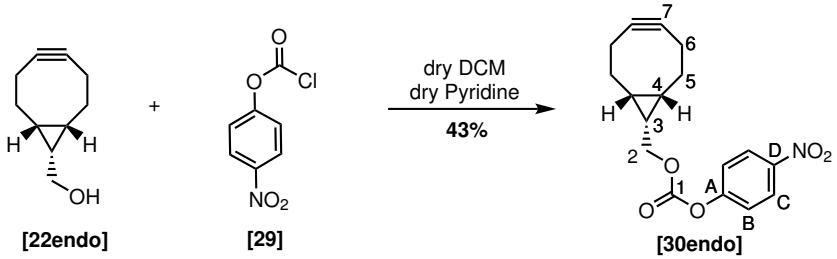

Die approbierte gedruckte Originalversion dieser Dissertation ist an der TU Wien Bibliothek verfügbar.
The approved original version of this doctoral thesis is available in print at TU Wien Bibliothek.

This compound was prepared according to the literature.[111] (1R,8S,9s)-Bicyclo[6.1.0]non-4-yn-9-yl)methanol **[22endo]** (0.116 g, 0.77 mmol, 1 equiv.) was dissolved in 15 mL of dry DCM, and dry pyridine (0.156 mL, 1.9 mmol, 2.5 equiv.) and 4-nitrophenyl chloroformate **[29]** (0.194 g, 0.96 mmol, 1.25 equiv.) were added. After 10 minutes the reaction mixture was quenched with aqueous saturated NH_4Cl solution, the organic phase and the water phases were separated, the water phase was extracted with DCM, the organic phases were combined and dried over $NaSO_4$, filtered and the solvent was evaporated. The crude material was purified by column chromatography (silica gel/crude = 100:1) using PE:EtOAc (3:1). The analytical data are in accordance with the literature.[111]

Yield: 43% (0.104 g, 0.33 mmol)

Appearance: colorless oil

TLC analysis: R_f = 0.6 (PE:EtOAc = 6:1)

Sum formula: $C_{25}H_{27}N_3O_6$

^{1}H NMR (400 MHz, $CDCl_3$): δ = 0.99 – 1.12 (m, 2H, H-4), 1.45 – 1.54 (m, 1H, H-3), 1.55 – 1.66 (m, 2H, H-5), 2.19 – 2.39 (m, 6H, H-5+ H-6), 4.40 (d, J = 8.3 Hz, 2H, H-2), 7.38 (d, J = 9.2 Hz, 2H, H-B), 8.27 (d, J = 9.2 Hz, 2H, H-C) ppm.

^{13}C NMR (101 MHz, $CDCl_3$): δ = 17.4 (d, C-3), 20.6 (d, 2C, C-4), 21.5 (t, 2C, C-6), 29.8 (t, 2C, C-5), 68.1 (t, C-2), 98.8 (s, 2C, C-7), 121.9 (d, 2C, C-B), 125.4 (d, 2C, C-C), 145.5 (s, C-D), 152.7 (s, C-1), 155.7 (s, C-A) ppm.

E.2.2.10 ((1R,8S,9s)-Bicyclo[6.1.0]non-4-yn-9-yl)methyl (2-aminoethyl)carbamate [32endo]

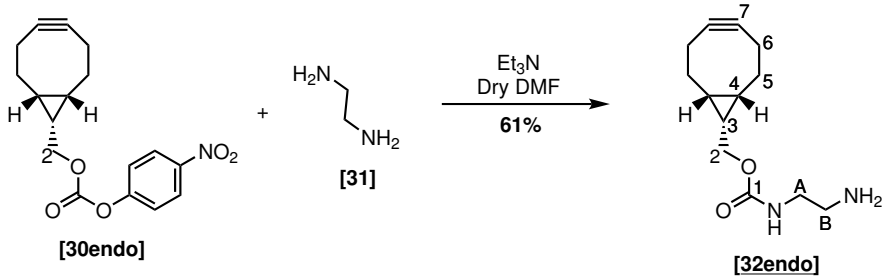

Die approbierte gedruckte Originalversion dieser Dissertation ist an der TU Wien Bibliothek verfügbar.
The approved original version of this doctoral thesis is available in print at TU Wien Bibliothek.
TU Bibliothek Your knowledge hub WIEN

This compound was synthesized by adapting a literature protocol.[111] (1R,8S,9s)-Bicyclo[6.1.0] non-4-yn-9-yl)methyl (4-nitrophenyl) carbonated **[30endo]** (0.117 g, 0.37 mmol, 1 equiv.) was dissolved in 0.6 mL of dry DMF and the triethylamine (0.148 mL, 2.2 mmol, 6 equiv.) and ethylenediamine **[31]** (0.154 mL, 1.1 mmol, 3 equiv.) were added. After 20 minutes, the reaction mixture was diluted in DCM, and washed with 1 M NaOH. The organic and water phases were separated, the water phase was extracted with DCM, the organic phases were dried over $NaSO_4$, filtered and the solvent was evaporated. The crude material was purified by column chromatography (silica gel/crude = 100:1) using DCM:MeOH (20:1 till 5:1, with 1% Et_3N).

Yield: 61% (53.3 mg, 0.23 mmol)

Appearance: yellow oil

TLC analysis: R_f = 0.15 (DCM:MeOH = 20:1 + 1% Et_3N)

Sum formula: $C_{13}H_{20}N_2O_2$

HR-MS: $[M+H]^+$ calculated = 237.1598 Da; $[M+H]^+$ found = 237.1601 Da; difference = 0.03 mDa

^{1}H NMR (400 MHz, CD_3OD: δ = 0.89 – 0.99 (m, 2H, H-4), 1.35 – 1.41 (m, 1H, H-3), 1.56 – 1.66 (m, 2H, H-5), 2.15 – 2.28 (m, 6H, H-5+ H-6), 2.82 (t, J = 6.2 Hz, 2H, H-B), 3.24 (t, J = 6.2 Hz, 2H, H-A), 4.16 (d, J = 8.1 Hz, 2H, H-2) ppm.

^{13}C NMR (101 MHz, CD_3OD): δ = 18.9 (d, C-3), 21.4 (d, 2C, C-4), 21.9 (t, 2C, C-6), 30.2 (t, 2C, C-5), 41.9 (t, C-B), 42.6 (t, C-A), 63.9 (t, C-2), 99.5 (s, 2C, C-7), 159.6 (s, C-1) ppm.

Die approbierte gedruckte Originalversion dieser Dissertation ist an der TU Wien Bibliothek verfügbar.
The approved original version of this doctoral thesis is available in print at TU Wien Bibliothek.

E.2.2.11 ((1R,8S,9s)-Bicyclo[6.1.0]non-4-yn-9-yl)methyl (2-(4-((4-(((((*E*)-cyclooct-4-en-1-yl)oxy) carbonyl)oxy)phenyl)diazenyl)benzamido)ethyl) carbamate [33]

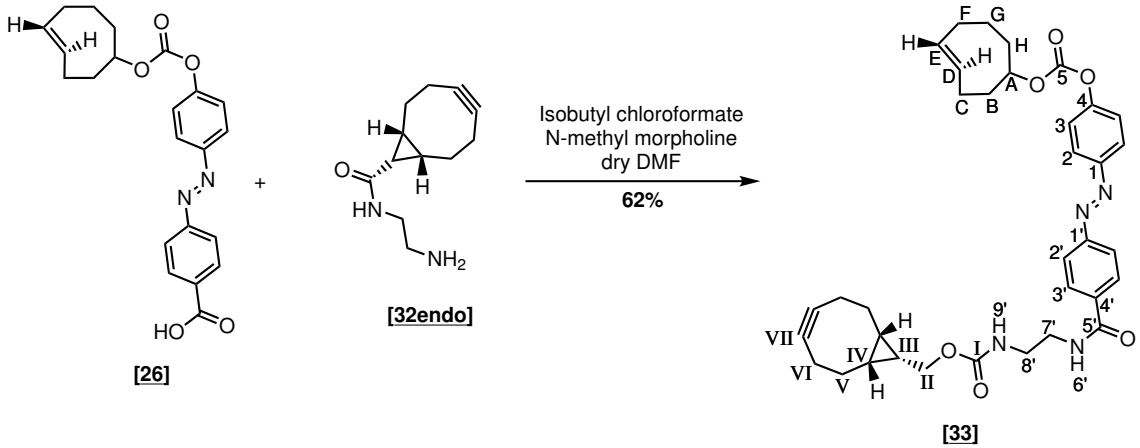

[26] + [32endo] → [33]

4-(4((((*E*)-Cyclooct-4-en-1-yl)oxy)carbonyl)oxy)phenyl)diazenyl)benzoic acid **[26]** (36.1 mg, 0.09 mmol, 1 equiv.) was dissolved in 0.6 mL of dry DMF, cooled to 0°C and the N-methylmorpholine (13 µL, 1.2 mmol, 1.3 equiv.) and isobutyl chloroformate (19 µL, 1.5 mmol, 1.6 equiv.) were added to the reaction mixture. After 10 minutes ((1R,8S,9s)-bicyclo[6.1.0] non-4-yn-9-yl)methyl (2-aminoethyl)carbamate **[32endo]** was added to the reaction mixture, dissolved in 0.2 mL of DMF. After 3 hours the solvent was evaporated and the crude material was purified by column chromatography (silica gel/crude = 100:1) using DCM:MeOH (100:1 + 1% Et_3N).

Yield: 62% (35.1 mg, 0.57 mmol)

Appearance: orange solid

Melting point: 124.5-126.2°C

TLC analysis: R_f = 0.12 (PE:EtOAc (1:1) + 1% Et_3N)

Sum formula: $C_{35}H_{42}N_4O_5$

HR-MS: $[M+H]^+$ calculated = 613.3021 Da; $[M+H]^+$ found = 613.3027 Da; difference = 0.06 mDa

^{1}H NMR (400 MHz, $CDCl_3$): δ = 0.88 – 0.92 (m, 2H, H-IV), 1.35 – 1.37 (m, 1H, H-III), 1.51 – 1.61 (m, 2H, C-V), 1.67 – 1.82 (m, 2H, H-G + H-H), 1.87 – 2.03 (m, 3H, H-F + H-G + H-H), 2.06 – 2.32 (m, 8H, H-V + H-VI + H-B), 2.38 – 2.45 (m, 3H, H-C + H-F), 3.47 – 3.53 (m, 3H, H-8'), 3.58

Die approbierte gedruckte Originalversion dieser Dissertation ist an der TU Wien Bibliothek verfügbar.
The approved original version of this doctoral thesis is available in print at TU Wien Bibliothek.
TU Bibliothek Your knowledge hub WIEN

– 3.67 (m, 2H, H-7′), 4.17 (d, J = 8.1 Hz, 2H, H-II), 4.41 – 4.50 (m, 1H, H-A), 5.46 – 5.56 (m, 1H, H-E), 5.57 – 5.69 (m, 1H, H-D), 7.34 (d, J = 8.9 Hz, 2H, H-2′), 7.91 – 8.02 (m, 6H, H-3′ + H-2 + H-3) ppm.

^{13}C NMR (101 MHz, $CDCl_3$): δ = 17.8 (d, C-III), 20.3 (d, 2C, C-IV), 21.5 (t, 2C, C-VI), 29.2 (t, 2C, C-V), 31.2 (t, C-G), 32.6 (t, C-C), 34.3 (t, C-F), 38.5 (t, C-H), 40.7 (t, C-8′), 40.9 (t, C-B), 42.1 (t, C-7′), 63.5 (t, C-II), 86.0 (d, C-A), 98.9 (s, 2C, C-VII), 121.9 (d, 2C,C-2′), 123.1 (d, 2C, C-3), 124.5 (d, 2C, C-2), 128.2 (d, 2C, C-2, C-3′), 133.2 (d, C-E), 135.1 (d, C-D), 136.1 (s, C-1, C-4′), 150.3 (s, C-1), 152.8 (s, C-5), 153.6 (s, C-4), 154.3 (s, C-1′), 158.5 (s, C-I), 167.2 (s, C-5′) ppm.

E.2.3 CuAAC-thiol azobenzene

E.2.3.1 1-(4-((5-Bromopentyl)oxy)phenyl)-2-(4-ethynylphenyl)diazene [34]

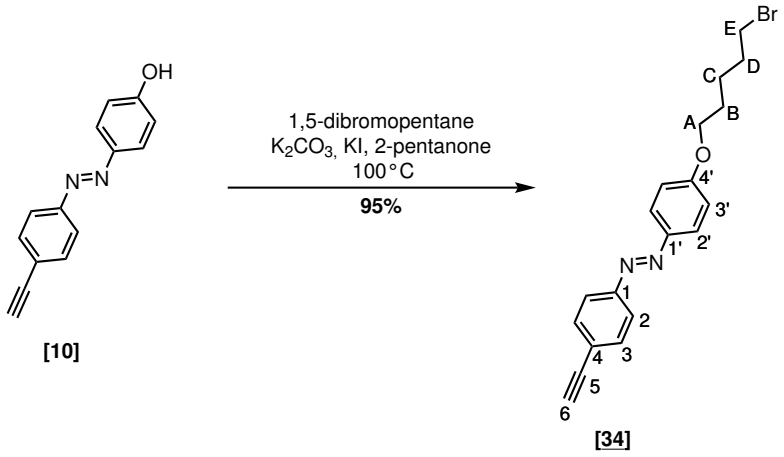

A literature protocol was adapted to synthesize 1-(4-((5-Bromopentyl)oxy)phenyl)-2-(4-ethynyl phenyl)diazene **[34]**.[161] 4-((4-ethynylphenyl) diazenyl)phenol **[10]** (0.294 g, 1.3 mmol, 1 equiv.), KI (6.6 mg, 0.4 mmol, 0.03 equiv.) and K_2CO_3 (0.128 g, 0.9 mmol, 0.7 equiv.) were placed in 2 mL of 2-pentanone. 1,5-Dibromopentane (0.9 mL, 6.6 mmol, 5 equiv.) was added to the reaction mixture which was placed overnight at 100°C. The solid was removed by filtration and, after evaporation of the filtrate, the crude material was purified by column chromatography (silica gel/crude = 100:1) with PE:EtOAc (12:1).

Yield: 95% (0.464 g, 1.125 mmol)

Die approbierte gedruckte Originalversion dieser Dissertation ist an der TU Wien Bibliothek verfügbar.
The approved original version of this doctoral thesis is available in print at TU Wien Bibliothek.
TU Bibliothek Your knowledge hub WIEN

Appearance: orange solid

Melting point: 101.1-102.3 °C

TLC analysis: R_f = 0.67 (PE:EtOAc = 4:1)

Sum formula: $C_{19}H_{19}BrN_2O$

HR-MS: $[M+H]^+$ calculated = 371.0754 Da; $[M+H]^+$ found = 371.0769 Da; difference = 1.5 mDa

^{1}H NMR (400 MHz, $CDCl_3$): δ = 1.62 – 1.70 (m, 2H, H-C), 1.85 (pent., J = 7.6 Hz, 2H, H-B), 1.95 (pent., J = 7.6 Hz, 2H, H-D), 3.22 (s, 1H, H-6), 3.45 (t, J = 6.7 Hz, 2H, H-E), 4.04 (t, J = 6.3 Hz, 2H, H-A), 6.99 (d, J = 9.0 Hz, 2H, H-2'), 7.62 (d, J = 8.5 Hz, 2H, H-3), 7.84 (d, J = 8.5 Hz, 2H, H-2), 7.91 (d, J = 9.0 Hz, 2H, H-3') ppm.

^{13}C NMR (101 MHz, $CDCl_3$): δ = 24.9 (t, C-C), 28.5 (t, H-B), 32.6 (t, C-D), 33.6 (t, C-E), 68.1 (t, C-A), 79.3 (d, C-6), 83.6 (s, C-5), 114.9 (d, 2C, C-2'), 122.7 (d, 2C, C-2), 124.0 (s, C-4), 125.1 (d, 2C, C-3'), 133.1 (d, 2C, C-3), 147.0 (s, C-1'), 152.5 (s, C-1), 161.9 (s, C-4') ppm.

E.2.3.2 Sodium S-(5-(4-((4-ethynylphenyl)diazenyl)phenoxy)pentyl)sulfurothioate [35]

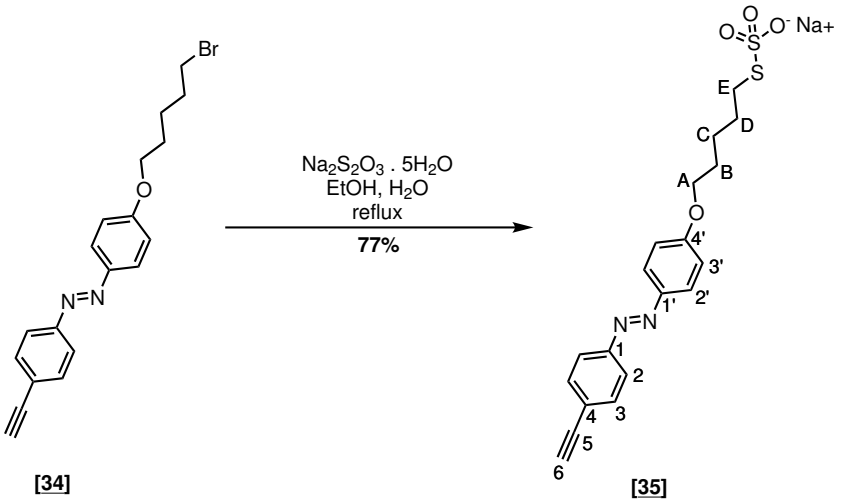

A literature protocol was adapted to synthesize sodium S-(5-(4-((4-ethynylphenyl)diazenyl) phenoxy)pentyl) sulfurothioate **[35]**.[161] 1-(4-((5-Bromopentyl)oxy)phenyl)-2-(4-ethynylphenyl) diazene **[34]** (0.452 mmol, 1.2 mmol, 1 equiv.) was suspended in 16 mL of EtOH, $Na_2S_2O_3$

Die approbierte gedruckte Originalversion dieser Dissertation ist an der TU Wien Bibliothek verfügbar.
The approved original version of this doctoral thesis is available in print at TU Wien Bibliothek.

(0.333 g, 1.3 mmol, 1.1 equiv.) was dissolved in 2 mL of water and added to compound **[34]**. After 4 hours at reflux, the reaction mixture was cooled to room temperature and the solid was collected by filtration and washed with cold Et_2O.

Yield: 77% (0.340 g, 0.98 mmol)

Appearance: orange solid

Melting point: 183.1-183.2°C

Sum formula: $C_{19}H_{19}N_2NaO4_4S_2$

HR-MS: $[M+H]^+$ calculated = 427.0757 Da; $[M+H]^+$ found = 427.0767 Da; difference = 1 mDa

^{1}H NMR (400 MHz, MeOD-d_4): δ = 1.53 (pent., J = 8.5 Hz, 2H, H-C), 1.71 – 1.81 (m, 4H, H-B + H-D), 3.01 (t, J = 7.3 Hz, 2H, H-E), 3.56 (s, 1H, H-6), 3.98 (t, J = 6.4 Hz, 2H, H-A), 6.96 (d, J = 9.0 Hz, 2H, H-2'), 7.50 (d, J = 8.6 Hz, 2H, H-3), 7.72 (d, J = 8.7 Hz, 2H, H-2), 7.79 (d, J = 9.0 Hz, 2H, H-3') ppm.

^{13}C NMR (101 MHz, MeOD-d_4): δ = 24.9 (t, C-C), 28.4 (t, C-B), 29.0 (t, C-D), 34.4 (t, C-E), 68.0 (t, C-A), 79.4 (d, C-6), 82.7 (s, C-5), 114.6 (d, 2C, C-2'), 122.2 (d, 2C, C-2), 124.3 (s, C-4), 124.6 (d, 2C, C-3'), 132.5 (d, 2C, C-3), 146.7 (s, C-1'), 152.3 (s, C-1), 162.3 (s, C-4') ppm.

E.2.3.3 5-(4-((4-Ethynylphenyl)diazenyl)phenoxy)pentane-1-thiol [36]

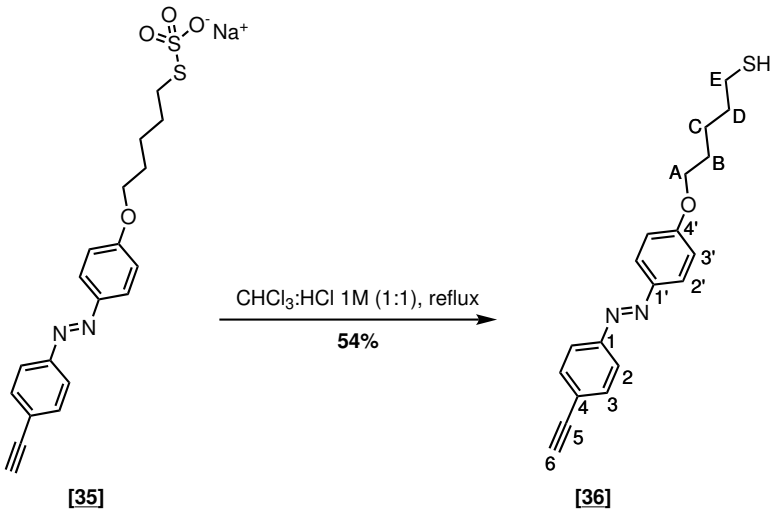

Die approbierte gedruckte Originalversion dieser Dissertation ist an der TU Wien Bibliothek verfügbar.
The approved original version of this doctoral thesis is available in print at TU Wien Bibliothek.
TU Bibliothek Your knowledge hub WIEN

A literature protocol was adapted to synthesize 5-(4-((4-ethynylphenyl)diazenyl)phenoxy)pentane-1-thiol **[36]**.[161] of $CHCl_3$:HCl 1 M (1:1, 12 mL) was degassed with argon and then used to dissolve sodium S-(5-(4-((4-ethynylphenyl)diazenyl) phenoxy)pentyl)sulfurothioate **[35]** (0.314 g, 0.74 mmol, 1 equiv.). The reaction was refluxed overnight. After cooling to room temperature, the organic and water phases were separated, the water phase was extracted with chloroform and all organic phases were collected and dried over Na_2SO_4. After evaporation of the solvent, the crude material was recrystallized with n-hexane:acetone (1:1).

Yield: 54% (0.129 mg, 0.39 mmol)

Appearance: orange solid

Melting point: 194.9-196.3°C

TLC analysis: R_f = 0.68 (n-hexane:EtOAc = 4:1)

Sum formula: $C_{19}H_{20}N_2NaOS$

HR-MS: $[M+H]^+$ calculated = 325.1369 Da; $[M+H]^+$ found = 325.1380 Da; difference = 1.1 mDa

^{1}H NMR (600 MHz, $CDCl_3$): δ = 1.56 – 1.63 (m, 2H, H-C), 1.69 – 1.75 (m, 2H, H-D), 1.83 – 1.87 (m, 2H, H-B), 2.58 (q, J = 7.5 Hz, 2H, H-E), 3.21 (s, 1H, H-6), 4.05 (t, J = 6.4 Hz, 2H, H-A), 7.00 (d, J = 9.0 Hz, 2H, H-3'), 7.61 (d, J = 9.2 Hz, 2H, H-3), 7.83 (d, J = 8.5 Hz, 2H, H-2), 7.91 (d, J = 9.0 Hz, 3H, H-2') ppm.

^{13}C NMR (151 MHz, $CDCl_3$): δ = 24.7 (t, C-E), 25.0 (t, C-C), 28.8 (t, C-B), 33.8 (t, C-D), 68.2 (t, C-A), 79.2 (d, C-6), 83.6 (s, C-5), 114.9 (d, 2C, C-3'), 122.7 (d, 2C, C-2), 124.0 (s, C-4), 125.1 (d, 2C, C-2'), 133.1 (d, 2C, C-3), 147.0 (s, C-1'), 152.5 (s, C-1), 162.0 (s, C-4') ppm.

Die approbierte gedruckte Originalversion dieser Dissertation ist an der TU Wien Bibliothek verfügbar.
The approved original version of this doctoral thesis is available in print at TU Wien Bibliothek.

E.2.4 Compounds for surface immobilization

E.2.4.1 1-Nitroso-4-(trifluoromethyl)benzene [38]

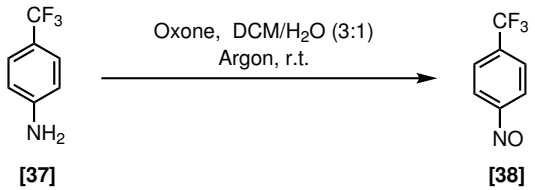

[37] [38]

1-Nitroso-4-(trifluoromethyl)benzene **[38]** was prepared according to the literature.[167] 4-(Trifluoromethyl)aniline **[37]** (5.3 g, 32.7 mmol, 1 equiv.) was dissolved in 30 mL of DCM and placed under argon. Oxone (20.1 g, 66 mmol, 2 equiv.) was dissolved in 100 mL of water and slowly added to the reaction mixture. After 8 hours, the organic and water phases were separated, the organic phase was washed with HCl 0.05 M, water, dried over $MgSO_4$ and the solvent was carefully evaporated due to the products volatility. Upon concentration of the solvent, the crude material was used without any further purification. The analytical data are in accordance with the literature.[167]

Appearance: green liquid

TLC analysis: R_f = 0.85 (DCMCM:PE = 1:1)

Sum formula: $C_7H_4F_3NO$

^{1}H NMR (400 MHz, $CDCl_3$): δ = 7.92 (d, J = 8.2 Hz, 2H), 8.01 (d, J = 8.2 Hz, 2H) ppm.

E.2.4.2 1-(4-Iodophenyl)-2-(4-(trifluoromethyl)phenyl)diazene [40]

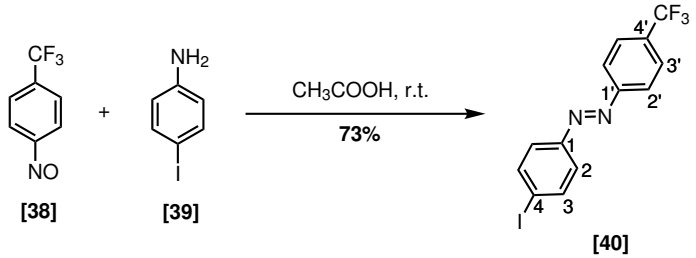

[38] [39] [40]

Die approbierte gedruckte Originalversion dieser Dissertation ist an der TU Wien Bibliothek verfügbar.
The approved original version of this doctoral thesis is available in print at TU Wien Bibliothek.
TU Bibliothek Your knowledge hub WIEN

1-(4-Iodophenyl)-2-(4-(trifluoromethyl)phenyl)diazene **[40]** was prepared according to the literature.[168] Methyl 4-nitrosobenzoate **[38]** (0.56 g, 2.6 mmol, 1 equiv.) was dissolved in 5 mL of acetic acid. Then 4-iodoaniline **[39]** (2.26**g**, 13 mmol, 5 equiv.) was dissolved in 2 mL of glacial acetic acid and added to the reaction mixture. The reaction was stirred at room temperature overnight. The solid was filtered, washed with glacial acetic acid, water and dried under vacuum. The analytical data are in accordance with the literature.[168,218]

Yield: 73% (0.711 g, 1.9 mmol)

Appearance: orange solid

Melting point: 147.1-147.5°C (Lit.:[218] 150-151 °C)

TLC analysis: R_f = 0.5 (PE)

Sum formula: $C_{13}H_8F_3IN_2$

^{1}H NMR (400 MHz, $CDCl_3$): δ = 7.67 (d, J = 8.6 Hz, 2H, H-2 or H-3), 7.77 (d, J = 8.4 Hz, 3H, H-3'), 7.88 (d, J = 8.6 Hz, 2H, H-2 or H-3), 7.98 (d, J = 8.0 Hz, 2H, H-2') ppm.

^{13}C NMR (101 MHz, $CDCl_3$): δ = 99.3 (s, C-4), 123.6 (d, 2C, C-2'), 124.3 (s/q, $^1J_{CF}$ = 275.8 Hz, CF_3), 125.1 (d, 2C, C-2 or C-3), 126.8 (d/q, $^3J_{CF}$ = 3.8 Hz, 2C, C-3'), 132.9 (s/q, $^2J_{CF}$ = 32.6 Hz, C-4'), 138.9 (d, 2C, C-2 or C-3), 152.1 (s, C-1), 154.6 (s, C-1') ppm.

E.2.4.3 1-(4-Ethynylphenyl)-2-(4-(trifluoromethyl)phenyl)diazene [41]

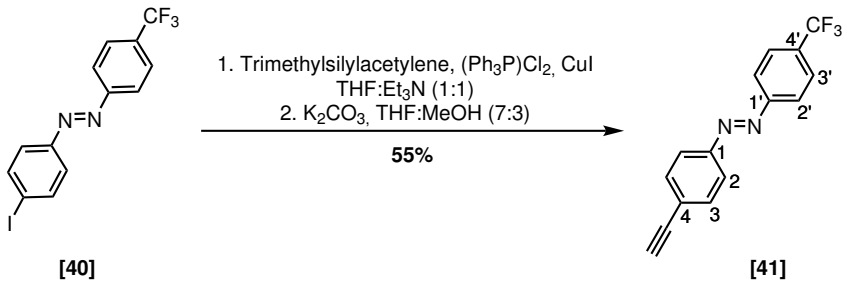

[40] **[41]**

1-(4-Ethynylphenyl)-2-(4-(trifluoromethyl)phenyl)diazene **[41]** was prepared according to the literature.[168] A flask containing 1-(4-iodophenyl)-2-(4-(trifluoromethyl)phenyl)diazene **[40]** (0.30 g, 0.8 mmol, 1 equiv.), $(Ph_3P)_2PdCl_2$ (17 mg, 0.02 mmol, 0.03 equiv.), CuI (4.6 mg, 0.02 mmol, 0.03 equiv.) and 15 mL THF:Et_3N (1:1) was placed under argon atmosphere and trimethylsily-

Die approbierte gedruckte Originalversion dieser Dissertation ist an der TU Wien Bibliothek verfügbar.
The approved original version of this doctoral thesis is available in print at TU Wien Bibliothek.
TU Bibliothek Your knowledge hub WIEN

lacetylene (0.16 g, 1.6 mmol, 2 equiv.) was added dropwise. After stirring overnight at room temperature, the reaction mixture was concentrated under vacuum, filtered through a plug of silica and the solvent was evaporated. The obtained brown solid was dissolved in 7.5 mL of THF:MeOH (7:3) and K_2CO_3 (0.34 g, 2.4 mmol, 3 equiv.) was added. After 3 hours, the mixture was diluted in diethyl ether, washed with aqueous saturated NH_4Cl solution, water, dried over $MgSO_4$ and the solvent was evaporated. The crude material was purified by column chromatography (silica gel/crude = 100:1) with n-hexane:DCM (6:1).The analytical data are in accordance with the literature.[168]

Yield: 55% (0.122 g, 0.45 mmol)

Appearance: orange solid

Melting point: 116.9-118.1°C (Lit.: not reported)

TLC analysis: R_f = 0.46 (n-hexane:DCM = 10:1)

Sum formula: $C_{15}H_9F_3N_2$

HR-MS: $[M+H]^+$ calculated = 275.0791 Da; $[M+H]^+$ found = 275.0794 Da; difference = 0.1 mDa

^{1}H NMR (600 MHz, $CDCl_3$): δ = 3.26 (s, 1H, H-6), 7.66 (d, J = 8.6 Hz, 2H, H-3), 7.79 (d, J = 8.3 Hz, 2H, H-3'), 7.92 (d, J = 8.7 Hz, 2H, H-2), 8.00 (d, J = 8.0 Hz, 2H, H-2') ppm.

^{13}C NMR (151 MHz, $CDCl_3$): δ = 80.0 (d, C-6), 83.1 (s, C5), 123.1 (d, 4C, C-2+C-2'), 123.9 (s/q, $^1J_{CF}$ = 272.4 Hz, CF_3), 125.6 (s, C-4), 126.3 (d/q, $^3J_{CF}$ = 3.8 Hz, 2C, C-3'), 132.5 (s/q, $^2J_{CF}$ = 32.5 Hz, C-4'), 133.1 (d, 2C, C-3), 151.9 (s, C-1), 154.3 (s, C-1') ppm.

E.2.4.4 1-Azidododecane [43]

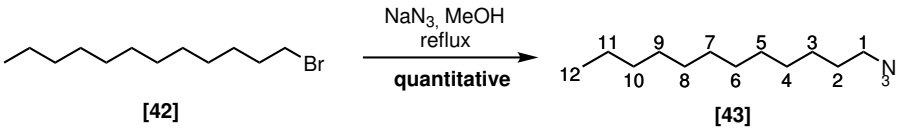

[42] [43]

1-Azidododecane **[43]** was synthesized according to the literature.[169] Sodium azide (28.7 mg, 0.44 mmol, 1.1 equiv.) was placed in 0.5 mL of MeOH, 1-bromododecane **[42]** (0.096 mL,

Die approbierte gedruckte Originalversion dieser Dissertation ist an der TU Wien Bibliothek verfügbar.
The approved original version of this doctoral thesis is available in print at TU Wien Bibliothek.
TU Bibliothek Your knowledge hub WIEN

0.4 mmol, 1 equiv.) was added and the reaction was kept under reflux overnight. After cooling the solvent was evaporated and the crude material was redissolved in chloroform and filtered. After evaporation of the solvent, the pure product was obtained (purity >95% according to NMR). The analytical data are in accordance with the literature.[169]

Yield: quantitative (85 mg, 0.4 mmol)

Appearance: colorless oil

Sum formula: $C_{12}H_{25}N_3$

^{1}H NMR (400 MHz, $CDCl_3$): δ = 0.88 (t, J = 6.7 Hz, 3H, H-12), 1.24 – 1.33 (m, 18H, H-3 - H11), 1.60 (p, J = 7.0 Hz, 2H, H-2), 3.25 (t, J = 7.0 Hz, 2H, H-1) ppm.

^{13}C NMR (101 MHz, $CDCl_3$): δ = 14.3 (q, C1-2), 22.8 (t, C3-C11), 26.9 (t, C-3 - C-11), 29.0 (t, C-2), 29.3 (t,C-3 - C-11), 29.5 (t, C-3 - C-11), 29.6 (t, C-3 - C-11), 29.7 (t, C-3 - C-11), 29.8 (t, C-3 - C-11), 29.8 (t, C-3 - C-11), 32.1 (t, C-3 - C-11), 51.7 (t, C-1) ppm.

E.2.4.5 3,6-Bis(4-(trifluoromethyl)phenyl)-1,2,4,5-tetrazine [45]

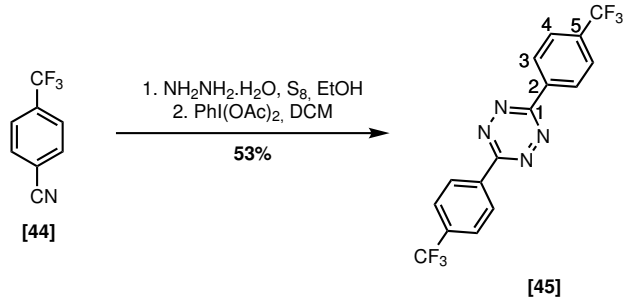

3,6-Bis(4-(trifluoromethyl)phenyl)-1,2,4,5-tetrazine **[45]** was synthesized according to a literature protocol.[171] 4-(Trifluoromethyl)benzonitrile **[44]** (2.4 g, 14.1 mmol, 1 equiv.) and sulfur (0.27 g, 8.5 mmol, 0.6 equiv.) were dissolved in 1.1 mL of absolute EtOH, flushed with argon, placed under stirring and cooled to 0°C. Hydrazine monohydrate (2.74 mL, 56.5 mmol, 4 equiv.) was added dropwise, the reaction mixture was stirred at room temperature during 1 hour and 30 minutes and then placed under reflux during 6 hours. After cooling to room temperature, the reaction mixture was diluted in water and extracted with DCM. The organic phase was washed with brine and dried over $MgSO_4$. After removal of the solvent,

Die approbierte gedruckte Originalversion dieser Dissertation ist an der TU Wien Bibliothek verfügbar.
The approved original version of this doctoral thesis is available in print at TU Wien Bibliothek.
TU Bibliothek Your knowledge hub WIEN

the material was dissolved in 300 mL of DCM and (diacetoxyiodo)benzene (1.95 g, 21.2 mmol, 1.5 equiv.) was added. After 22 hours stirring at room temperature, the reaction mixture was adsorbed in celite gel and purified by column chromatography (silica gel/crude = 100:1) using n-hexane:DCM (0% to 100% DCM).The analytical data are in accordance with the literature.[171]

Yield: 53% (1.38 g, 3.7 mmol)

Appearance: bright pink solid

Melting point: 283.1-283.2 °C (Lit.[171] 273-276 °C)

TLC analysis: R_f = 0.6 (n-hexane:EtOAc = 10:1)

Sum formula: $C_{16}H_8F_6N_4$

^{1}H NMR (600 MHz, $CDCl_3$): δ = 7.91 (d, J= 8.2 Hz, 4H, H-4), 8.82 (d, J = 8.2 Hz, 4H, H-5) ppm.

^{13}C NMR (151 MHz, $CDCl_3$): δ = 122.9 (s/q, $^1J_{C,F}$ = 272.7 Hz, 2C, CF_3) 126.5 (d/q, $^3J_{C,F}$= 3.7 Hz, 4C, C-4), 128.62 (d, 4C, C-3), 134.6 (s/q, $^2J_{C,F}$ = 33.2 Hz, 2C, C-5), 134.89 (s, 2C, C-2), 163.6 (s, C-1) ppm.

E.2.4.6 1,4-Bis(4-(trifluoromethyl)phenyl)-5,6,7,8,9,10-hexahydrocycloocta[d] pyridazin-7-yl (4-((4-ethynylphenyl)diazenyl)phenyl) carbonate [46]

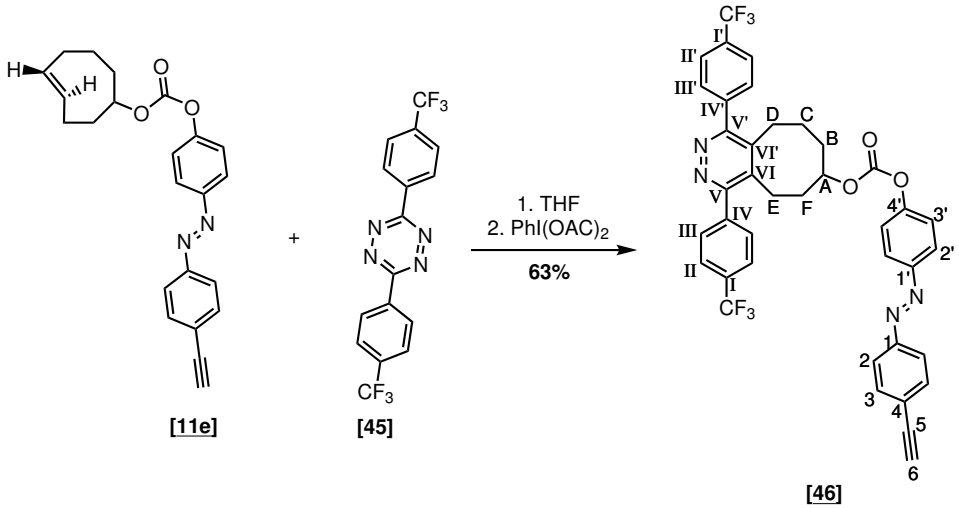

[11e] [45] [46]

Die approbierte gedruckte Originalversion dieser Dissertation ist an der TU Wien Bibliothek verfügbar.
The approved original version of this doctoral thesis is available in print at TU Wien Bibliothek.

3,6-Bis(4-(trifluoromethyl)phenyl)-1,2,4,5-tetrazine **[45]** (0.165 g, 0.45 mmol, 1 equiv.) was dissolved in 10 mL of THF and placed under stirring. Equatorial (*E*)-cyclooct-4-en-1-yl (4-(4-ethynylphenyl)diazenyl)phenyl) carbonate **[11e]** (0.250 g, 0.67 mmol, 1.5 equiv.) was dissolved in 5 mL of THF and added dropwise to the reaction vial, which was kept under stirring at room temperature in an open vial. After 3 minutes there was complete consumption of **[45]**, therefore (diacetoxyiodo)benzene (1.95 g, 21.2 mmol, 1.5 equiv.) was added. The solvent was evaporated after 2 hours and the crude material was purified by column chromatography (silica gel/crude = 100:1) using n-hexane:EtOAc (8:1 till 2:1).

Yield: 63% (0.200 g, 0.28 mmol)

Appearance: orange solid

Melting point: 220.4 - 221.3°C

TLC analysis: R_f = 0.42 (n-hexane:EtOAc = 2:1)

Sum formula: $C_{39}H_{28}F_6N_4O_3$

HR-MS: $[M+H]^+$ calculated = 715.2138 Da; $[M+H]^+$ found = 715.2142 Da; difference = -2.1 mDa

^{1}H NMR (600 MHz, $CDCl_3$): δ = 1.75 – 2.00 (m, 6H, H-B + H-C + H-F), 2.06 – 2.14 (m, 1H, H-F), 2.85 – 2.93 (m, 3H, H-D + H-E), 2.98 – 3.04 (m, 1H, H-E), 3.26 (s, 1H, CH), 4.61 – 4.67 (m, 1H, H-A), 7.33 (d, J = 8.9 Hz, 2H, H-2′ or H-3′), 7.65 (d, J = 8.5 Hz, 2H, H-3), 7.67 – 7.74 (m, 4H, H-III + H-III′), 7.80 – 7.86 (m, 4H, H-II + H-II′), 7.89 (d, J = 8.6 Hz, 2H, H-2), 7.98 (d, J = 8.8 Hz, 2H, H-2′ or H-3′) ppm.

^{13}C NMR (151 MHz, $CDCl_3$): δ = 23.8 (t, C-E), 25.9 (t, C-C), 27.5 (t,C-D), 32.8 (t, C-B), 34.8 (t, C-F), 78.9 (t, C-A), 79.8 (d, C-6), 83.3 (s, C-5), 121.7 (d, 2C, C-2′ or C-3′), 123.0 (d, 2C, C-2), 124.1 (s/q, $^1J_{CF}$ = 272.4 Hz, 2C, CF_3), 124.4 (d, 2C, C-2′ or C-3′), 125.0 (s, C-4), 125.7 (d/q, $^3J_{CF}$ = 3.6 Hz, 2C, C-II or C-II′), 125.8 (d/q, $^3J_{CF}$ = 3.5 Hz, 2C, C-II or C-II′), 129.6 (d, 2C, C-III or C-III′), 129.6 (d, 2C, C-III or C-III′), 131.2 (s/q, $^2J_{CF}$ = 32.7 Hz, C-I or C-I′), 131.23 (s/q, $^2J_{CF}$ = 32.7 Hz, C-I or C-I′), 133.1 (d, 2C, C-3), 138.1 (s, C-VI or C-VI′), 138.4 (s, C-VI or C-VI′), 141.1 (s, C-IV or C-IV′), 141.1 (s, C-IV or C-IV′), 150.4 (s, C-1′ or C-4′), 152.1 (s, C-1), 152.6 (carbonyl), 153.0 (s, C-1′ or C-4′), 160.6 (s, C-V or C-V′), 160.7 (s, C-V or C-V′) ppm.

Die approbierte gedruckte Originalversion dieser Dissertation ist an der TU Wien Bibliothek verfügbar.
The approved original version of this doctoral thesis is available in print at TU Wien Bibliothek.
TU Bibliothek Your knowledge hub WIEN

E.2.4.7 1-Dodecyl-4-(4-((4-(trifluoromethyl)phenyl)diazenyl)phenyl)-1H-1,2,3-triazole [47]

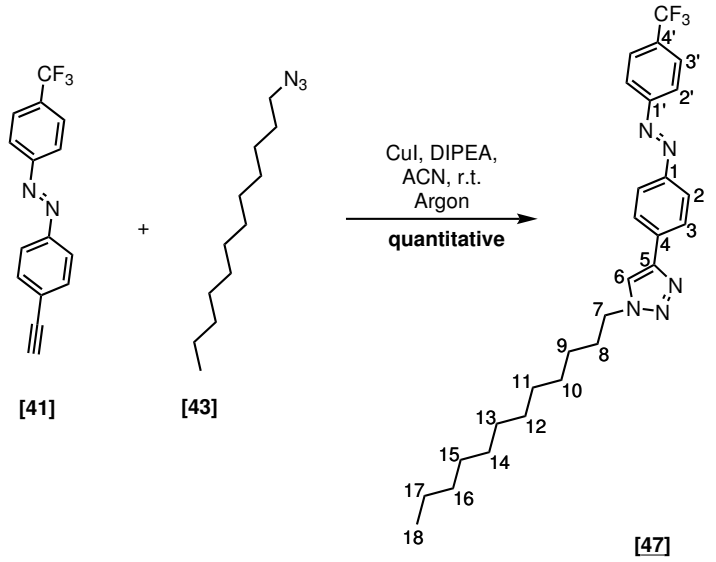

1-(4-Ethynylphenyl)-2-(4-(trifluoromethyl)phenyl)diazene **[41]** (11.1 mg, 0.04 mmol, 1 equiv.) and copper iodide (I) (1.5 mg, 0.008 mmol, 0.2 equiv.) were dissolved in 0.8 mL of acetonitrile. Then N,N'-diisopropylethylamine (14 µL, 0.08 mmol, 2 equiv.) was added followed by 1-azidododecane **[43]** (9.4 mg, 0.045 mmol, 1.1 equiv.) and the reaction mixture was placed under argon. After 3 hours the solvent was evaporated and the crude material was purified by column chromatography (silica gel/crude = 100:1) using DCM:MeOH (100:1).

Yield: quantitative (20.5 mg, 0.04 mmol)

Appearance: orange solid

Melting point: 143.2-144.8°C

TLC analysis: R_f = 0.57 (DCM:MeOH = 100:1)

Sum formula: $C_{27}H_{34}F_3N_5$

HR-MS: $[M+H]^+$ calculated = 486.2839 Da; $[M+H]^+$ found = 486.2849 Da; difference = 2.1 mDa

^{1}H NMR (400 MHz, $CDCl_3$): δ = 0.88 (t, J = 6.7, 6.7 Hz, 4H, H-18), 1.25 (s, 14H, aliphatic Hs), 1.35 – 1.39 (m, 4H, H-9 + other), 1.98 (pent., J = 6.9 Hz, 3H, H-8), 4.43 (t, J = 7.2 Hz, 2H,

Die approbierte gedruckte Originalversion dieser Dissertation ist an der TU Wien Bibliothek verfügbar.
The approved original version of this doctoral thesis is available in print at TU Wien Bibliothek.

H-7), 7.79 (d, J = 8.3 Hz, 2H, H-2 or H-2′), 7.86 (s, 1H, H-6), 8.00 – 8.04 (m, 6H, H-2 or H-2′+ H-3+ H-3′).

^{13}C NMR (101 MHz, $CDCl_3$): δ = 14.3 (q, C-18), 22.8 (t), 26.7 (t, C-9), 29.2 (t), 29.4 (t), 29.5 (t), 29.7 (t), 29.8 (t), 29.9 (t, C-8), 30.5 (t), 32.1 (t), 50.7 (t, C-7), 120.3 (d, C-6), 123.2 (d, 2C, C-2 or C-2′ or C-3), 124.0 (d, 2C, C-2 or C-2′ or C-3), 124.1 (s/q, $^1J_{CF}$ = 271.4 Hz, CF_3), 126.2 – 126.8 (d/q, $^3J_{CF}$ = 3.76 Hz, 4C, C-3′+ C-2 or C-2′), 132.3 (s/q, $^2J_{CF}$ = 32.4 Hz, C-4′), 134.2 (s, C-1 or C-1′ or C-4 or C-5), 146.9 (s, C-4 or C-5), 152.1 (s, C-1 or C-1′ or C-4 or C-5), 154.6 (s, C-1 or C-1′ or C-4 or C-5).

E.2.4.8 Equatorial cyclooct-4-en-1-yl (4-((E)-(4-(1-dodecyl-1H-1,2,3-triazol-4-yl) phenyl)diazenyl)phenyl) carbonate [48e]

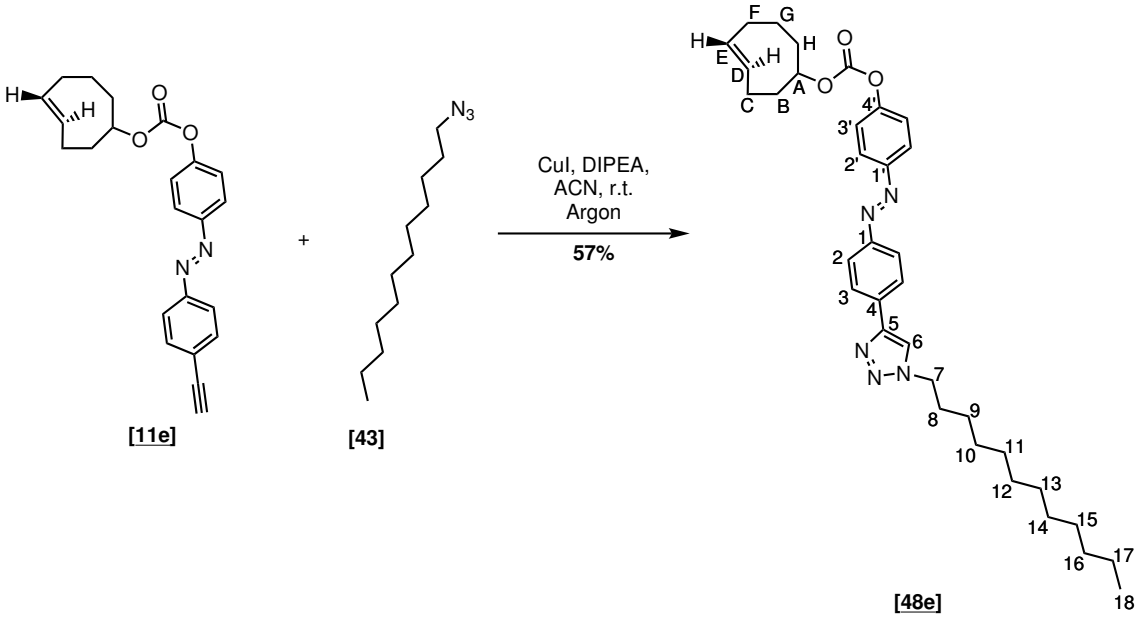

Equatorial (*E*)-cyclooct-4-en-1-yl (4-(4-ethynylphenyl)diazenyl)phenyl) carbonate **[11e]** (15 mg, 0.04 mmol, 1 equiv.) and CuI (0.7 mg, 0.008 mmol, 0.2 equiv.) were placed in 2 mL of ACN, and then the DIPEA (0.014 mL, 0.08 mmol, 2 equiv.) and 1-azidododecane **[43]** (9 mg, 0.044 mmol, 1.1 equiv.) were added. The reaction mixture was flushed with argon and stirred overnight. The solvent was evaporated and the crude material was purified by column chromatography (silica gel/crude = 100:1) using n-hexane:EtOAc (2:1) ppm.

Die approbierte gedruckte Originalversion dieser Dissertation ist an der TU Wien Bibliothek verfügbar.
The approved original version of this doctoral thesis is available in print at TU Wien Bibliothek.

Yield: 57% (13.4 mg, 0.03 mmol)

Appearance: orange solid

Melting point: 116.8 - 118.3°C

TLC analysis: R_f = 0.31 (n-hexane:EtOAc = 3:1)

Sum formula: $C_{35}H_{47}N_5O_3$

HR-MS: $[M+H]^+$ calculated = 608.3571 Da; $[M+H]^+$ found = 608.3570 Da; difference = 0.2 mDa

^{1}H NMR (400 MHz, $CDCl_3$): δ = 0.80 (s, 3H, H-18), 1.18 (s, 14H, H10 - H17), 1.27 – 1.31 (m, 4H, H-9 + H10-17), 1.57 – 1.63 (m, 3H, H-B + H-H), 1.89 – 2.15 (m, 8H, H-8 + H-C + H-G + H-F + H-B or H-H), 2.29 – 2.40 (m, 1H, H-F), 4.35 (t, J = 7.2 Hz, 2H, H-7), 4.74 – 4.81 (m, 1H, H-A), 5.55 – 5.69 (m, 2H, H-D + H-E), 7.27 (d, J = 8.9 Hz, 2H, H-3'), 7.77 (s, 1H, H-6), 7.88 – 7.93 (m, 6H, H-2 or H-3 or H-2') ppm.

^{13}C NMR (101 MHz, $CDCl_3$): δ = 14.3 (q, C-18), 22.3 (t, C-F), 22.8 (t, C-16 or C-17), 25.0 (t, C-B or C-H), 25.7 (t, C-C or C-G), 26.7 (t, C-9), 29.2 (t, C-10-C-17), 29.5 (t, C-10-C-17), 29.5 (t, C-10-C-17), 29.7 (t, C-10-C-17), 29.7 (t, C-10-C-17), 29.8 (t, C-10-C-17), 30.5 (t, C-8), 32.0 (t, C-10-C-17), 33.7 (t, C-B or C-H), 33.8 (t, C-C or C-G), 50.7 (d, C-7), 81.6 (d, C-A), 120.2 (d, C-6), 121.9 (d, 2C, C-3'), 123.7 (d, 2C, C-2, C-3 or C-2'), 124.2 (d, 2C, C-2, C-3 or C-2'), 126.4 (d, 2C, C-2, C-3 or C-2'), 129.5 (d, C-D or C-E), 130.1 (d, C-D or C-E), 133.5 (s, C-1, C-4, C-4' or C-5), 147.1 (s, C-4 or C-5), 150.4 (s, C-1'), 152.2 (s, C-1, C-4, C-4' or C-5), 152.9 (s, C-1, C-4, C-4' or C-5), 153.2 (s, carbonyl) ppm.

Die approbierte gedruckte Originalversion dieser Dissertation ist an der TU Wien Bibliothek verfügbar.
The approved original version of this doctoral thesis is available in print at TU Wien Bibliothek.

E.2.4.9 (1,4-Bis(4-(trifluoromethyl)phenyl)-5,6,7,8,9,10-hexahydrocycloocta[d] pyridazin-7-yl (4-((4-(1-dodecyl-1H-1,2,3-triazol-4-yl)phenyl)diazenyl) phenyl) carbonate [49]

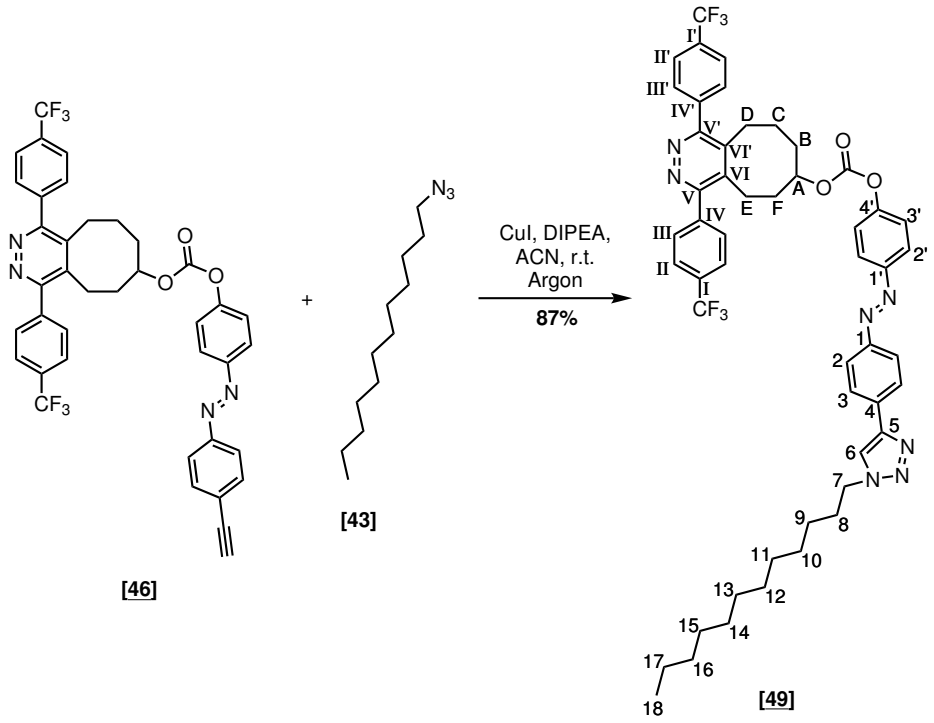

Compound **[46]** (21.3 mg, 0.03 mmol, 1 equiv.) and the CuI (1.1 mg, 0.006 mmol, 0.2 equiv.) were placed in 0.5 mL of THF and then DIPEA (0.010 mL, 0.06 mmol, 2 equiv.) and the 1-azidododecane **[43]** (6.9 mg, 0.03 mmol, 1.1 equiv.) were added. After 2 hours the solvent was evaporated and the crude material was purified by column chromatography (silica gel/crude = 100:1) using n-hexane:EtOAc (2:1).

Yield: 87% (24 mg g, 0.026 mmol)

Appearance: orange solid

Melting point: 151.3-152.8°C

TLC analysis: R_f = 0.74 (n-hexane:EtOAc = 1:1)

Sum formula: $C_{51}H_{53}F_6N_7O_3$

HR-MS: $[M+H]^+$ calculated = 926.4187 Da; $[M+H]^+$ found = 926.4185 Da; difference =

Die approbierte gedruckte Originalversion dieser Dissertation ist an der TU Wien Bibliothek verfügbar.
The approved original version of this doctoral thesis is available in print at TU Wien Bibliothek.
TU Bibliothek Your knowledge hub WIEN

0.15 mDa

^{1}H NMR (400 MHz, $CDCl_3$): δ = 0.87 (t, J = 6.7 Hz, 3H, H-18), 1.25 – 1.37 (m, 18H, H9 - H17), 1.73 – 2.02 (m, 8H, H-B + H-C + H-F+ H-8), 2.02 – 2.15 (m, 1H, H-F), 2.81 – 2.92 (m, 3H, H-D + H-E), 2.93 – 3.05 (m, 1H, H-E), 4.42 (t, J = 7.2 Hz, 2H, H-7), 4.58 – 4.68 (m, 1H, H-A), 7.30 (d, J = 8.7 Hz, 2H, H-2, H-2', H-3 or H-3'), 7.63 – 7.73 (m, 4H, H-III + H-III'), 7.76 – 7.86 (m, 5H, H-II + H-II' + H-6), 7.93 – 8.04 (m, 6H, H-2, H-2', H-3 or H-3') ppm.

^{13}C NMR (101 MHz, $CDCl_3$): δ = 14.3 (q, C-18), 22.8 (t, C-9 - C-17), 23.8 (t, C-E), 25.9 (t, C-C), 26.7 (t, C-9 - C-17), 27.5 (t, C-D), 29.2 (t, C-9 - C-17), 29.5 (t, C-9 - C-17), 29.5 (t, C-9 - C-17), 29.7 (t, C-9 - C-17), 29.7 (t, C-9 - C-17), 29.9 (t, C-9 - C-17), 30.5 (t, C-8), 32.0 (t, C-9 - C-17), 32.8 (t, C-B), 34.9 (t, C-F), 50.7 (t, C-7), 78.9 (d, C-A), 120.2 (d, C-6), 121.7 (d, 2C, C-2, C-3, C-2' or C-3'), 123.7 (d, 2C, C-2, C-3, C-2' or C-3'), 124.1 (s/q, $^1J_{CF}$ = 272.0 Hz, 2C, CF_3), 124.3 (d, 2C, C-2, C-3, C-2' or C-3'), 125.7 (d/q, $^3J_{CF}$ = 9.8 Hz, 2C, C-II or C-II'), 125.8 (d/q, $^3J_{CF}$ = 9.7 Hz, 2C, C-II or C-II'), 126.4 (d, 2C, C-2, C-3, C-2 or C-3'), 129.7 (d, 4C, C-III+C-III'), 131.24 (s/q,$^3J_{CF}$ = 32.6 Hz, 2C, C-I or C-I'), 131.3 (s/q,$^3J_{CF}$ = 32.7 Hz, 2C, C-I or C-I'), 133.6 (s, C-1, C-4, C-1' or C-4), 138.1 (s, C-VI or C-VI'), 138.4 (s, C-VI or C-VI'), 141.2 (s, 2C, C-IV + C-IV'), 147.0 (s, C-5), 150.6 (s, C-1, C-4, C-1' or C-4'), 152.1 (s, C-1, C-4, C-1' or C-4), 152.7 (s, carbonyl), 152.8 (s, C-1, C-4, C-1' or C-4), 160.6 (s, C-V or C-V'), 160.7 (s, C-V or C-V') ppm.

E.2.5 Biotin modifications

E.2.5.1 4-Azidoaniline [51]

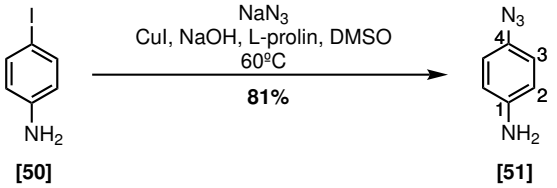

A literature protocol was used to synthetize this compound.[206] 4-Iodoaniline **[50]** (0.461 g, 2.1 mmol, 1 equiv.), CuI (0.06 g, 0.32 mmol, 0.15 equiv.), NaOH (0.02 g, 0.5 mmol, 0.24 equiv.), L-prolin (0.058 g, 0.5 mmol, 0.24 equiv.) and NaN_3 (0.286 g, 4.4 mmol, 2.1 equiv.) were dissolved in 8 mL of DMSO, flushed with argon and heated overnight at 60°C. The reaction mix-

Die approbierte gedruckte Originalversion dieser Dissertation ist an der TU Wien Bibliothek verfügbar.
The approved original version of this doctoral thesis is available in print at TU Wien Bibliothek.
TU Bibliothek Your knowledge hub WIEN

ture was diluted in EtOAc and washed with brine, the organic and water phases were separated,and the organic phase was dried over $MgSO_4$. After evaporation of the solvent, the crude material was purified by column chromatography (silica gel/crude = 100:1) with PE:EtOAc (7:3). The analytical data are in accordance with the literature.[206]

Yield: 81% (0.228 g, 1.7 mmol)

Appearance: brown crystals

Melting point: 59.8-61.3°C (Lit.:[219] 60-62°C)

TLC analysis: R_f = 0.46 (PE:EtOAc = 7:3)

Sum formula: $C_6H_6N_4$

^{1}H NMR (400 MHz, $CDCl_3$): δ = 3.65 (s, 2H, NH_2), 6.67 (d, J = 8.7 Hz, 2H, H-2), 6.84 (d, J = 8.7 Hz, 2H, H-3) ppm.

^{13}C NMR (101 MHz, $CDCl_3$): δ = 116.4 (d, 2C, C-2), 120.1 (d, 2C, C-3), 130.3 (s, C-1 or C-4), 143.8 (s, C-1 or C-4) ppm.

E.2.5.2 N-(4-Azidophenyl)-5-((3aS,4S,6aR)-2-oxohexahydro-1H-thieno[3,4-d] imidazol-4-yl)pentanamide [53]

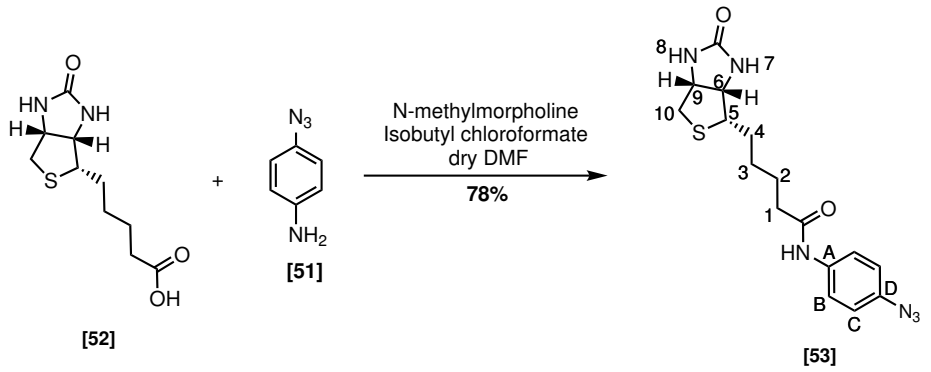

The synthesis of this compound adapted a literature protocol.[208] Biotin **[52]** (0.124 g, 0.51 mmol, 1 equiv.) was dissolved in 4 mL of dry DMF, placed under argon and cooled to 0°C. Then N-methylmorpholine (0.072 mL, 0.67 mmol, 1.3 equiv.) was added, followed by isobutyl chloroformate (0.106 mL, 0.81 mmol, 1.6 equiv.). After 30 minutes, 4-azidoaniline **[51]** (0.136 g,

Die approbierte gedruckte Originalversion dieser Dissertation ist an der TU Wien Bibliothek verfügbar.
The approved original version of this doctoral thesis is available in print at TU Wien Bibliothek.
TU Bibliothek Your knowledge hub WIEN

1.0 mmol, 2 equiv.), dissolved in 1 mL of dry DMF, was added dropwise to the reaction mixture. After 3 hours stirring at room temperature, the solvent was evaporated affording a brown glue which was triturated with cold water. The obtained solid was filtered and washed with cold methanol. The analytical data are in accordance with the literature.[220]

Yield: 78% (70.2 mg, 0.98 mmol)

Appearance: beige solid

Melting point: 200.8-201.6°C (Lit.: not reported)

TLC analysis: R_f = 0.26 (DCM:MeOH = 20:1)

Sum formula: $C_{16}H_{20}N_6O_2S$

HR-MS: $[M+H]^+$ calculated = 361.1441 Da; $[M+H]^+$ found = 361,1440; difference = 0.1 mDa

^{1}H NMR (400 MHz, DMSO-d_6): δ = 1.31 – 1.42 (m, 2H, H-3), 1.44 – 1.53 (m, 1H, H-4), 1.56 – 1.68 (m, 3H, H-2 + H-4), 2.30 (d, J = 7.4 Hz, 2H, H-1), 2.58 (d, J = 12.4 Hz, 1H, H-10), 2.82 (dd, J = 5.1 Hz, 12.4 Hz, 1H, H-10), 3.09 – 3.16 (m, 1H, H-5), 4.11 – 4.16 (m, 1H, H-6), 4.27 – 4.33 (m, 1H, H-9), 6.36 (s, 1H, H-8), 6.43 (s, 1H, H-7), 7.05 (d, J = 9.0 Hz, 2H, H-C), 7.63 (d, J = 9.0 Hz, 2H, H-B), 9.95 (s, 1H, NH amide) ppm.

^{13}C NMR (101 MHz, DMSO-d_6): δ = 25.1 (t, C-2), 28.1 (t, C-4), 28.2 (t, C-3), 36.2 (t, C-1), 39.8 (t, C-10), 55.4 (d,C-5), 59.2 (d, C-9), 61.0 (d, C-6), 119.4 (d, 2C, C-C), 120.5 (d, 2C, C-B), 133.5 (s, C-D), 136.6 (s, C-A), 162.7 (s, Carbamide), 171.1 (s, Amide) ppm.

E.2.5.3 N-(4-Iodophenyl)-5-((3aS,4S,6aR)-2-oxohexahydro-1H-thieno[3,4-d] imidazol-4-yl)pentanamide [54]

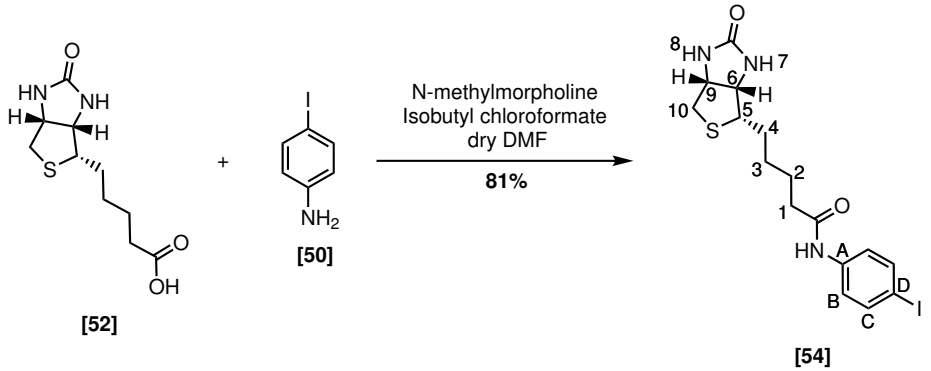

Die approbierte gedruckte Originalversion dieser Dissertation ist an der TU Wien Bibliothek verfügbar.
The approved original version of this doctoral thesis is available in print at TU Wien Bibliothek.

The synthesis of this compound adapted a literature protocol.[208] Biotin **[52]** (0.2 g, 0.82 mmol, 1 equiv.) was dissolved in 6 mL of dry DMF, placed under argon and cooled to 0°C. Then the N-methylmorpholine (0.117 mL, 1.1 mmol, 1.3 equiv.) was added, followed by the isobutyl chloroformate (0.171 mL, 1.3 mmol, 1.6 equiv.). After 30 minutes, 4-iodoaniline **[50]** (0.359 g, 1.6 mmol, 2 equiv.), dissolved in 1 mL of dry DMF, was added dropwise to the reaction mixture. After 2 hours stirring at room temperature, the solvent was evaporated, the solid was suspended in 10 mL of DCM and sonicated, filtered and washed with DCM and MeOH.The analytical data are in accordance with the literature.[221]

Yield: 81% (0.296 g, 0.66 mmol)

Appearance: colorless solid

Melting point: 255.1-255.9°C (Lit. not reported)

TLC analysis: R_f = 0.71 (DCM:MeOH = 20:1)

Sum formula: $C_{16}H_{20}IN_3O_2S$

^{1}H NMR (400 MHz, DMSO-d_6): δ = 1.29 – 1.42 (m, 2H, H-3), 1.43 – 1.55 (m, 1H, H-4), 1.55 – 1.68 (m, 3H, H-2 + H-4), 2.30 (t, J = 7.4 Hz, 2H, H-1), 2.58 (d, J = 12.4 Hz, 1H, H-10), 2.82 (dd, J = 5.1, 12.4 Hz, 1H, H-10), 3.08 – 3.14 (m, 1H, H-5), 4.11 – 4.16 (m, 1H, H-6), 4.28 – 4.33 (m, 1H, H-9), 6.36 (s, 1H, H-8), 6.43 (s, 1H, H-7), 7.43 (d, J = 8.8 Hz, 2H, H-B), 7.61 (d, J = 8.8 Hz, 2H, H-C), 9.96 (s, 1H, NH amide) ppm.

^{13}C NMR (400 MHz, DMSO-d_6): δ = 25.0 (t, C-2), 28.1 (t, C-4), 28.2 (t, C-3), 36.24 (t, C-1), 39.8 (t, C-10), 55.4 (d, C-5), 59.2 (d, C-9), 61.0 (d, C-6), 86.3 (s, C-D), 121.2 (d, 2C, C-B), 137.3 (d, 2C, C-C), 139.1 (s, C-A), 162.7 (C-carbamide), 171.3 (C-amide) ppm.

Die approbierte gedruckte Originalversion dieser Dissertation ist an der TU Wien Bibliothek verfügbar.
The approved original version of this doctoral thesis is available in print at TU Wien Bibliothek.

E.2.5.4 (*E*)-Cyclooct-4-en-1-yl 4-((4-((4-(5-((3aS,4S,6aR)-2-oxohexahydro-1H-thieno [3,4-d]imidazol-4-yl)pentanamido)phenyl)ethynyl)phenyl)diazenyl) benzoate [55]

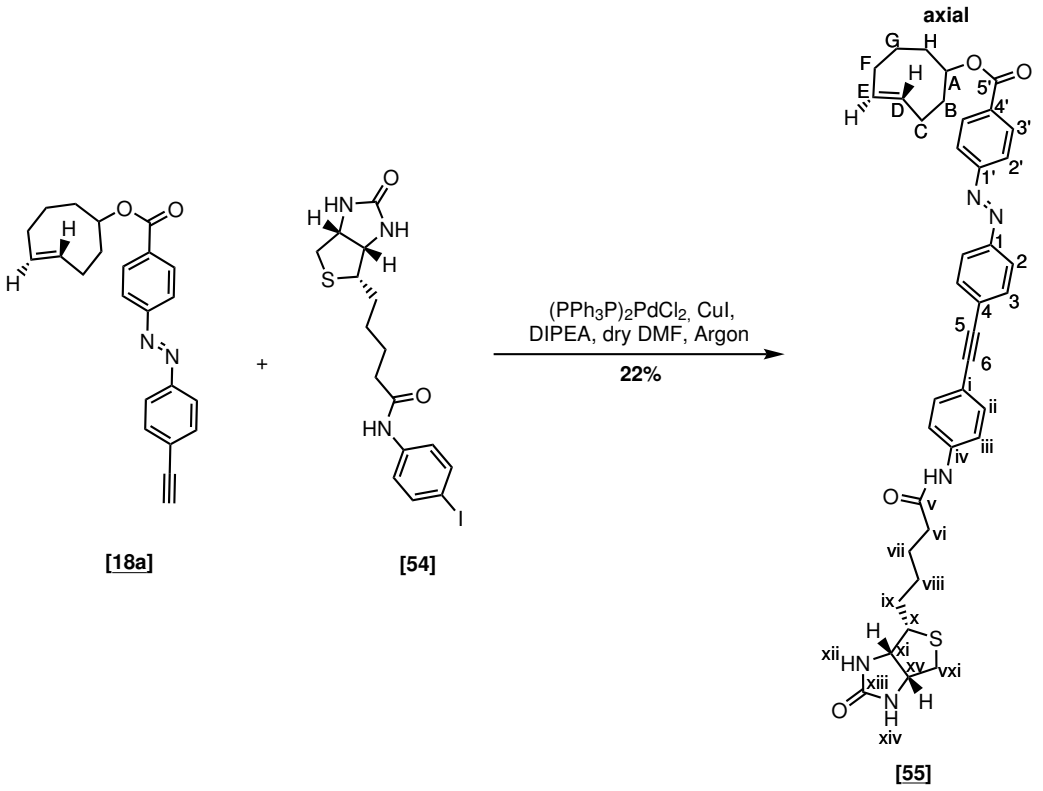

N-(4-Iodophenyl)-5-((3aS,4S,6aR)-2-oxohexahydro-1H-thieno[3,4-d] imidazol-4-yl)pentanamide **[54]** (0.101 g, 0.23 mmol, 2 equiv.), copper (I) iodide (0.8 mg, 0.004 mmol, 0.03 equiv.) and bis(triphenylphosphine)palladium(II) dichloride (2.8 mg, 0.004 mmol, 0.03 equiv.) were placed under argon, dissolved in 3.5 mL of dry DMF and DIPEA (118 µL, 0.7 mmol, 5 equiv.) was added. Axial (*E*)-cyclooct-4-en-1-yl 4-(4-ethynylphenyl) diazenyl)benzoate **[18a]** (40.7 mg, 0.14 mmol, 1 equiv.) was dissolved in 1 mL of dry DMF and added to the reaction mixture. After 1 hour, the DMF was evaporated and the crude material was purified by preparative HPLC (C18 column, MeOH/H_2O, 20 minutes method: 0.5 minutes isocratic elution with 5% MeOH, followed by 19 minutes gradient elution from 5% to 98% MeOH). After evaporation of the fractions, the solid was liophilized.

Yield: 22% (20.3 mg, 0.03 mmol)

Die approbierte gedruckte Originalversion dieser Dissertation ist an der TU Wien Bibliothek verfügbar.
The approved original version of this doctoral thesis is available in print at TU Wien Bibliothek.
TU Bibliothek Your knowledge hub WIEN

Appearance: orange solid

Melting point: 176.1-178.3°C z **TLC analysis:** R_f = 0.14 (DCM:MeOH = 20:1)

Sum formula: $C_{39}H_{41}N_5O_4S$

HR-MS: $[M+H]^+$ calculated = 676.2952 Da; $[M+H]^+$ found = 676.2983; difference = 3.1 mDa

^{1}H NMR (600 MHz, DMSO-d_6): δ = 1.30 – 1.46 (m, 3H, H-viii + H-B or H-C or H-F or H-G or H-H), 1.51 – 1.54 (m, 1H, H-ix), 1.61 – 1.67 (m, 3H, H-vii + H-ix), 1.74 – 1.91 (m, 3H, H-B or H-C or H-F or H-G or H-H), 1.91 – 2.04 (m, 2H, H-B or H-C or H-F or H-G or H-H), 2.10 – 2.22 (m, 3H, H-B or H-C or H-F or H-G or H-H), 2.30 – 2.44 (m, 3H, H-vi + H-B or H-C or H-F or H-G or H-H), 2.59 (d, J = 12.4 Hz, 1H, H-xvi), 2.83 (dd, J = 12.4, 5.2 Hz, 1H, H-xvi), 3.09 – 3.17 (m, 1H, H-x), 4.11 – 4.17 (m, 1H, H-xi), 4.28 – 4.33 (m, 1H, H-xv), 4.98 – 5.04 (m, 1H, H-A), 5.59 – 5.76 (m, 2H, H-D + H-E), 6.37 (s, 1H, H-xiv), 6.45 (s, 1H, H-xii), 7.53 (d, J = 8.5 Hz, 2H, H-ii), 7.68 – 7.71 (m, 2H, H-iii), 7.74 – 7.77 (m, 2H, H-3), 7.96 – 8.01 (m, 4H, H-2 + H-2′ or H-3′), 8.13 – 8.16 (m, 2H, H-2′ or H-3′), 10.16 (s, 1H, NH amide) ppm.

^{13}C NMR (151 MHz, DMSO-d_6): δ = 21.1 (t, C-B or C-C or C-F or C-G or C-H), 21.8 (t, C-B or C-C or C-F or C-G or C-H), 24.6 (t, C-vii), 25.2 (t, C-B or C-C or C-F or C-G or C-H), 28.1 (t, C-ix), 28.2 (t, C-viii), 33.1 (t, C-B or C-C or C-F or C-G or C-H), 33.3 (t, C-B or C-C or C-F or C-G or C-H), 36.3 (t, C-vi), 40.1 (d, C-xvi), 55.4 (d, C-x), 59.2 (d, C-xv), 61.1 (d, C-xi), 76.2 (d, C-A), 88.2 (s, C-5), 93.0 (s, C-6), 115.8 (s, C-i), 118.9 (d, 2C, C-iii), 122.8 (d, 2C, C-2′ or C-3′), 123.2 (s, C-1 or C-4), 123.3 (d, 2C, C-2), 129.6 (d, C-D or C-E), 130.5 (d, C-2′ or C-3′), 132.3 (d, 2C, C-ii), 132.5 (d, 2C, C-3), 132.8 (s, C-1′ or C-4′), 133.0 (d, C-D or C-E), 140.2 (s, C-iv), 151.0 (s, C-1 or C-4), 154.4 (s, C1′ or C-4′), 162.7 (s, C-xiii), 164.4 (s, C-5′), 171.6 (s, C-v) ppm.

Die approbierte gedruckte Originalversion dieser Dissertation ist an der TU Wien Bibliothek verfügbar.
The approved original version of this doctoral thesis is available in print at TU Wien Bibliothek.

E.2.5.5 ((6S)-1-(4-(5-((3aS,4S,6aR)-2-Oxohexahydro-1H-thieno[3,4-d]imidazol-4-yl) pentanamido)phenyl)-1,4,5,5a,6,6a,7,8-octahydrocyclopropa[5,6] cycloocta [1,2-d][1,2,3]triazol-6-yl)methyl (2-(4-((4-(((((E)-cyclooct-4-en-1-yl)oxy) carbonyl)oxy)phenyl)diazenyl)benzamido)ethyl)carbamate [56]

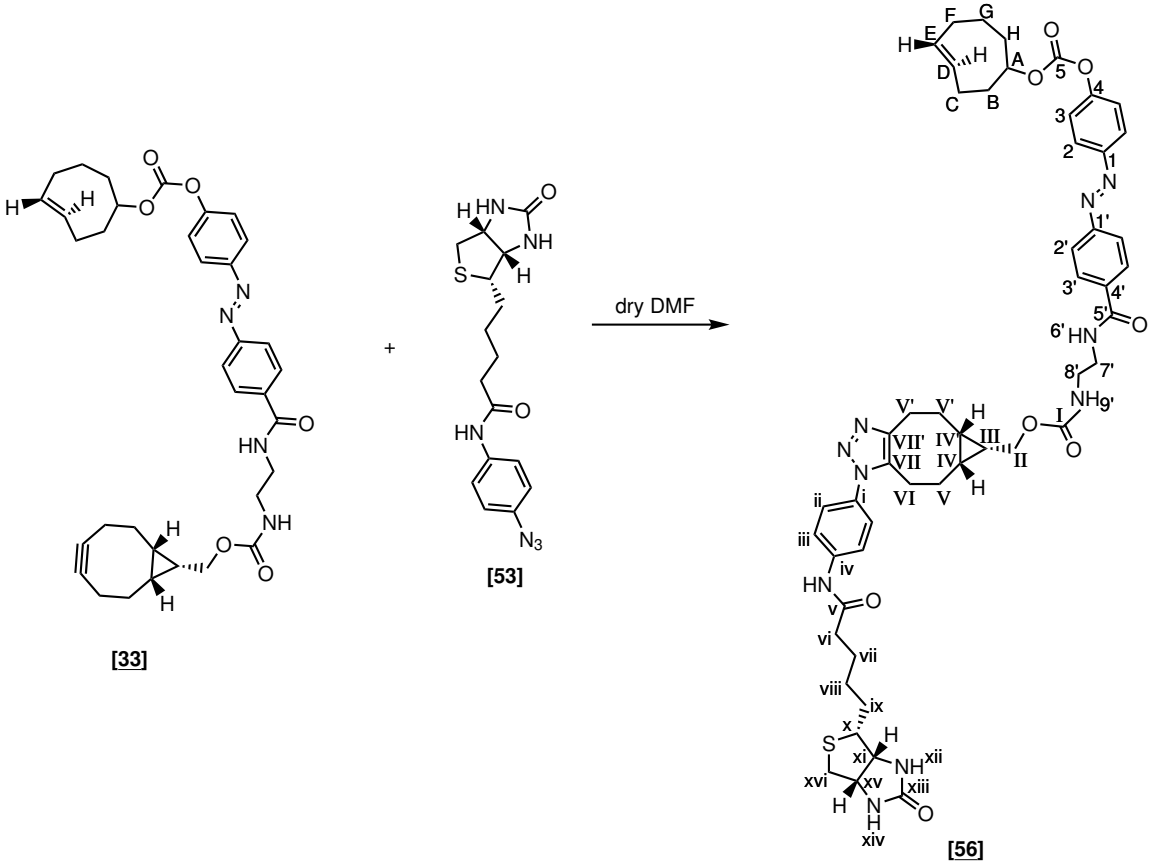

Compound **[33]** (26.0 mg, 0.042 mmol, 1.1 equiv.) and compound **[53]** (13.9 mg, 0.039 mmol, 1 equiv.) were placed in a flask and dissolved in 1.2 mL of dry DMF. After 2 hours, the DMF was evaporated and the crude material was purified by preparative HPLC (C18 column, MeOH/H_2O, 20 minutes method: 0.5 minutes isocratic elution with 5% MeOH, followed by 19 minutes gradient elution from 5% to 98% MeOH). After evaporation of the fractions, the solid was liophilized.

Yield: 65% (24.3 mg, 0.025 mmol)

Appearance: orange solid

Die approbierte gedruckte Originalversion dieser Dissertation ist an der TU Wien Bibliothek verfügbar.
The approved original version of this doctoral thesis is available in print at TU Wien Bibliothek.

Melting point: 129.0-133.4°C

TLC analysis: R_f = 0.36 (DCM:MeOH = 10:1)

Sum formula: $C_{51}H_{60}N_{10}O_8S$

HR-MS: $[M+H]^+$ calculated = 973.4389 Da; $[M+H]^+$ found = 973.4391; difference = 0.2 mDa

^{1}H NMR (600 MHz, $CDCl_3$): δ = 0.79 – 2.46 (m, 59H, H-B + H-C + H-F + H-G + H-H + H-III + H-IV + H-IV' + H-V + H-V + H-VI + H-VI' + H-vi + H-vii + H-vii + H-ix), 2.83 (s, 1H, H-xvi), 3.10 (d, *J* = 20.8 Hz, 1H, H-x), 3.43 (s, 2H, H-8'), 3.58 (s, 2H, H-7'), 4.05 – 4.17 (m, 3H, H-II+ H-xi), 4.26 (s, 1H, H-xv), 4.45 (d, J = 6.1 Hz, 1H, H-A), 5.49 (m, 1H, H-E), 5.61 (m, 1H, H-D), 5.76 (s, 1H, H-xiv), 5.90 (s, 1H, H-xii), 6.61 (s, 1H, H-6'), 7.21 (d, *J* = 8.4 Hz, 2H, H-ii or H-iii), 7.29 – 7.34 (m, 2H, H-2' or H-2 or H-3), 7.62 (s, 1H, H-9'), 7.75 (d, *J* = 9.0 Hz, 2H, H-ii or H-iii), 7.87 (d, *J* = 8.1 Hz, 2H, H-2' or H-2 or H-3), 7.94 (d, *J* = 8.6 Hz, 4H, H-3'+ H-2' or H-2 or H-3), 9.45 (s, 1H, NH amide biotin) ppm.

^{13}C NMR (151 MHz, $CDCl_3$): δ = 18.1 (d, C-III or C-IV or C-IV'), 19.2 (d, C-III or C-IV or C-IV'), 20.3 (d, C-III or C-IV or C-IV'), 22.8 (t, C-V or C-V' or C-VI or C-VI'), 23.5 (t, C-V or C-V' or C-VI or C-VI'), 25.7 (t, C-vii), 26.1 (t, C-V or C-V' or C-VI or C-VI'), 28.1 (t, C-ix), 28.3 (t, C-viii), 29.8 (t, C-V or C-V' or C-VI or C-VI'), 31.2 (t, C-G), 32.6 (t, C-C), 34.3 (t, C-F), 36.8 (t, C-vi), 38.5 (t, C-H), 40.8 (2C, C-8'+ C-xvi), 40.9 (t, C-B), 41.6 (t, -7'), 55.9 (d, C-x), 60.4 (d, C-xv), 62.0 (d, C-xi), 63.1 (t, C-II), 86.0 (t, C-A), 120.6 (d, 2C, C-ii or C-iii), 121.9 (d, 2C, C-2' or C-2 or C-3), 123.0 (d, 2C, C-2' or C-2 or C-3), 124.5 (d, 2C, C-3' or C-2' or C-2 or C-3), 126.5 (d, 2C, C-ii or C-iii), 128.3 (d, 2C, C-3' or C-2' or C-2 or C-3), 131.7 (s, C-i or C-iv), 133.2 (d, C-E), 134.9 (s, C-VII or C-VII'), 135.1 (d, C-D), 136.1 (s, C-1, C-4, C-1' or C-4'), 140.2 (s, C-i or C-iv), 145.1 (s, C-VII or C-VII'), 150.2 (s, C-1, C-4, C-1' or C-4'), 152.8 (s, C-5), 153.6 (s, C-1, C-4, C-1' or C-4'), 154.2 (s, C-1, C-4, C-1' or C-4'), 158.2 (s, C-I), 164.5 (s, C-xiii), 167.4 (s, C-5'), 172.8 (s, C-v) ppm.

Die approbierte gedruckte Originalversion dieser Dissertation ist an der TU Wien Bibliothek verfügbar.
The approved original version of this doctoral thesis is available in print at TU Wien Bibliothek.

E.2.5.6 2-((1E,3E)-5-((E)-3,3-Dimethyl-5-sulfo-1-(3-sulfopropyl)indolin-2-ylidene) penta-1,3-dien-1-yl)-3,3,4-trimethyl-1-(6-((4-(4-methyl-7-(((4-((E)-(4-((2-((((((6S)-1-(4-(5-((3aS,4S,6aR)-2-oxohexahydro-1H-thieno[3,4-d]imidazol-4-yl)pentanamido)phenyl)-1,4,5,5a,6,6a,7,8-octahydrocyclopropa[5,6] cycloocta[1,2-d][1,2,3]triazol-6-yl)methoxy)carbonyl)amino)ethyl)carbamoyl) phenyl)diazenyl)phenoxy)carbonyl)oxy)-4a,5,6,7,8,9,10,10a-octahydro cycloocta[d]pyridazin-1-yl)benzyl)amino)-6-oxohexyl)-5-vinyl-3H-pyrrol-1-ium [58]

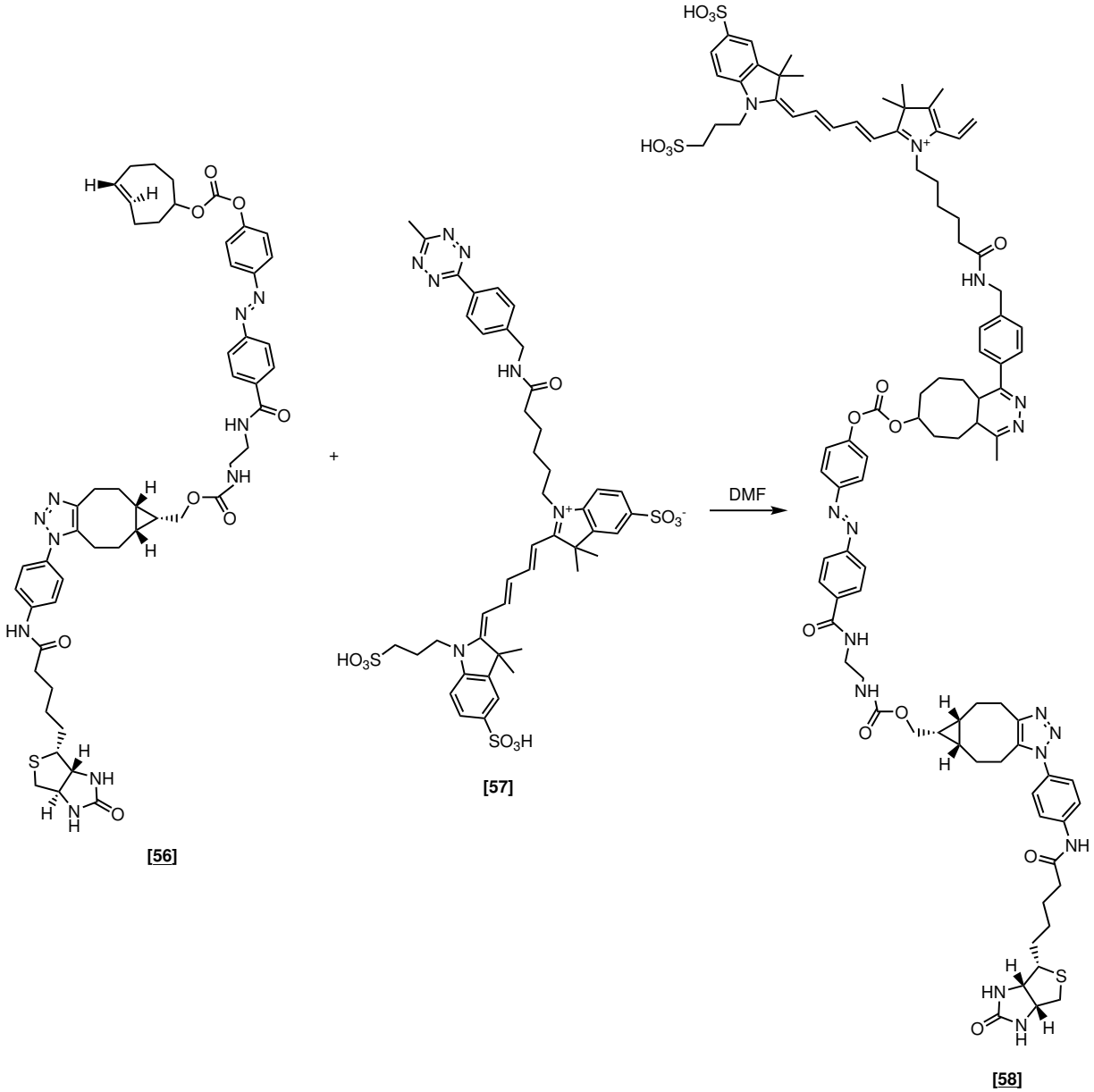

[56] [57] [58]

Die approbierte gedruckte Originalversion dieser Dissertation ist an der TU Wien Bibliothek verfügbar.
The approved original version of this doctoral thesis is available in print at TU Wien Bibliothek.
TU Bibliothek Your knowledge hub WIEN

A stock solution of azobenzene-biotin **[56]** in DMSO (5.02 mg **[56]** in 0.5 mL DMSO = 10.7 mM and of fluorophore 6-methyl-tetrazine-sulfo-Cy5 **[57]** in PBS buffer (1 mg **[57]** in 0.9 mL PBS = 11.9 mM were prepared.

Compound **[56]** (13.84 µL, 0.0014 mmol, 1 equiv.) was placed in a 2 mL eppendorf tube and fluorophore **[57]** (180 µL, 0.0021 mmol, 1.5 equiv.) was added in portions of 10 µL. Upon addition of one portion of fluorophore the tube was vortexed for 30 seconds and then the next portions was added. Afterwards, a HPLC analysis (C4 column, 5 minutes, mobile phase acetonitrile:H_2O 2:8 pH 8.5) showed complete consumption of the azobenzene **[56]** and formation of two new peaks.

Retention time (Fluorescence detector): 1.30 and 1.78 min

Retention time (Absorption detector): 1.20 and 1.70 min

[58]

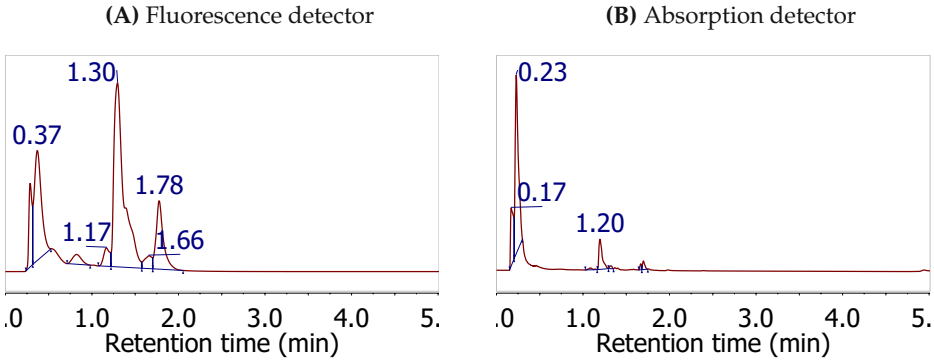

Die approbierte gedruckte Originalversion dieser Dissertation ist an der TU Wien Bibliothek verfügbar.
The approved original version of this doctoral thesis is available in print at TU Wien Bibliothek.

E.2.6 AFM click reactions

E.2.6.1 1-Ethyl-3-((5-(4-((4-ethynylphenyl)diazenyl)phenoxy)pentyl)thio) pyrrolidine-2,5-dione [59]

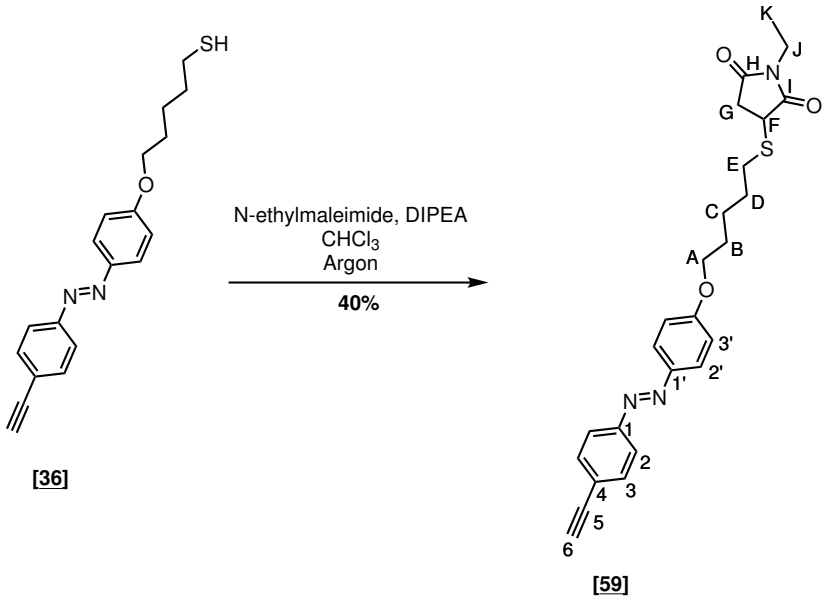

5-(4-((4-Ethynylphenyl)diazenyl)phenoxy)pentane-1-thiol **[36]** (0.314 g, 0.97 mmol, 1 equiv.) was dissolved in 3 mL of chloroform (previously purged with argon), DIPEA (5 µL, 0.03 mmol, 0.03 equiv.) was added and the reaction was placed under argon. N-Ethylmaleimide (0.162 g, 1.2 mmol, 1.2 equiv.) was dissolved in 1 mL of chloroform, also purged with argon, and added to the reaction mixture. After stirring overnight for 4 hours, the solvent was evaporated and the crude material was purified by column chromatography (silica gel/crude = 100:1) using PE:EtOAc (0-30%).

Yield: 40% (0.173 g, 0.38 mmol)

Appearance: orange solid

Melting point: 113.1-114.8°C

TLC analysis: R_f = 0.33 (n-hexane:EtOAc=5:1)

Sum formula: $C_{25}H_{27}N_3O_3S$

HR-MS: $[M+H]^+$ calculated = 450.1846 Da; $[M+H]^+$ found = 450.1852 Da; difference =

Die approbierte gedruckte Originalversion dieser Dissertation ist an der TU Wien Bibliothek verfügbar.
The approved original version of this doctoral thesis is available in print at TU Wien Bibliothek.
TU Bibliothek Your knowledge hub WIEN

0.6 mDa

^{1}H NMR (600 MHz, $CDCl_3$): δ = 1.18 (t, J = 7.2 Hz, 3H, H-K), 1.60 – 1.65 (m, 2H, H-C), 1.71 – 1.79 (m, 2H, H-D), 1.83 – 1.88 (m, 2H, H-B), 2.51 (dd, J = 18.6, 3.6 Hz, 1H, H-G), 2.81 (ddd, J = 12.5, 8.4, 6.6 Hz, 1H, H-E), 2.95 (ddd, J = 12.5, 8.2, 6.1 Hz, 1H, H-E), 3.12 (dd, J = 18.6, 9.0 Hz, 1H, H-G), 3.21 (s, 1H, H-6), 3.58 (q, J = 7.2 Hz, 2H, H-J), 3.70 (dd, J = 9.0, 3.6 Hz, 1H, H-F), 4.06 (t, J= 6.3 Hz, 2H, H-A), 7.00 (d, J = 9.0 Hz, 2H, H-3'), 7.61 (d, J = 8.6 Hz, 2H, H-3), 7.83 (d, J = 8.5 Hz, 2H, H-2), 7.91 (d, J = 8.9 Hz, 2H, H-2') ppm.

^{13}C NMR (151 MHz, $CDCl_3$): δ = 12.9 (q, C-K), 25.3 (t, C-C), 28.7 (t, C-D), 28.8 (t, C-B), 31.6 (t, C-E), 34.1 (t, C-J), 36.1 (t, C-G), 39.0 (d, C-F), 68.0 (t, C-A), 79.1 (d, C-6), 83.4 (s, C-5), 114.8 (d, 2C, C-3'), 122.5 (d, 2C, C-2), 123.9 (s, C-4), 125.0 (d, 2C, C-2'), 133.0 (d, 2C, C-3), 146.9 (s, C-1'), 152.4 (s, C-1), 161.9 (s, C-4'), 174.6 (s, C-H or C-I), 176.5 (s, C-H or C-I) ppm.

E.2.6.2 3-((5-(4-((4-(1-Dodecyl-1H-1,2,3-triazol-4-yl)phenyl)diazenyl)phenoxy) pentyl)thio)-1-ethylpyrrolidine-2,5-dione [60]

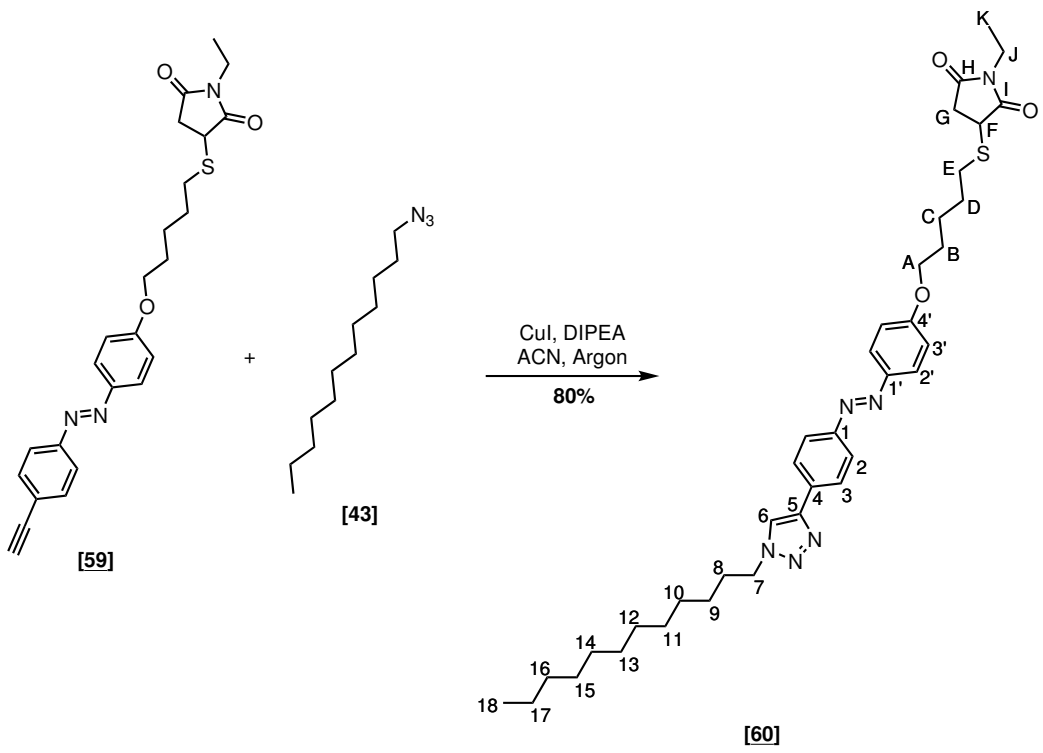

[59] + [43] → [60]

Die approbierte gedruckte Originalversion dieser Dissertation ist an der TU Wien Bibliothek verfügbar.
The approved original version of this doctoral thesis is available in print at TU Wien Bibliothek.

1-Ethyl-3-((5-(4-((4-ethynylphenyl)diazenyl)phenoxy)pentyl)thio) pyrrolidine-2,5-dione **[59]** (52.0 mg, 0.12 mmol, 1 equiv.) and copper (I) iodide (6.3 mg, 0.06 mmol, 0.5 equiv.) were dissolved in 4 mL of dry acetonitrile, the DIPEA (101 µL, 0.58 mmol, 5 equiv.) was added and the reaction mixture was flushed with argon. 1-azidododecane **[43]** (36.7 mg, 0.17 mmol, 1.5 equiv.) was dissolved in 0.5 mL of dry acetonitrile and added to the reaction mixture. After stirring overnight at room temperature, the solvent was evaporated and the crude material was purified by column chromatography (silica gel/crude = 100:1) using DCM:MeOH (0-1%).

Yield: 80% (61.4 mg, 0.093 mmol)

Melting point: 135.5-138.1°C

Appearance: orange solid

TLC analysis: R_f = 0.1 (DCM:MeOH = 99:1)

Sum formula: $C_{37}H_{52}N_6O_3S$

HR-MS: $[M+H]^+$ calculated = 661.9212 Da; $[M+H]^+$ found = 661.9223; difference = 1.1 mDa.

^{1}H NMR (600 MHz, $CDCl_3$): δ = 0.83 (t, J = 7.0 Hz, 3H, H-18), 1.14 (t, J = 7.2 Hz, 3H, H-K), 1.17 – 1.25 (m, 14H, H-10 - H-17), 1.29 – 1.34 (m, 4H, H-9 + H-10 - H-17), 1.56 – 1.61 (m, 2H, H-C), 1.65 – 1.77 (m, 2H, H-D), 1.78 – 1.85 (m, 2H, H-B), 1.92 (pent., J = 7.2 Hz, 2H, H-8), 2.47 (dd, J = 18.6, 3.5 Hz, 1H, C-G), 2.77 (ddd, J = 12.5, 8.3, 6.6 Hz, 1H, H-E), 2.91 (ddd, J = 12.4, 8.2, 6.1 Hz, 1H, H-E), 3.08 (dd, J = 18.6, 9.0 Hz, 1H, C-G), 3.54 (q, J = 7.2 Hz, 2H, H-J), 3.67 (dd, J = 9.1, 3.6 Hz, 1H, C-F), 4.02 (t, J = 6.3 Hz, 2H, H-A), 4.37 (t, J = 7.2 Hz, 2H, H-7), 6.96 (d, J = 9.0 Hz, 2H, H-3), 7.78 (s, 1H, H-6), 7.86 – 7.95 (m, 6H, H-2+H-2'+H-3') ppm.

^{13}C NMR (151 MHz, $CDCl_3$): δ = 13.0 (q, C-K), 14.2 (q, C-18), 22.8 (t, C-10-C17), 25.4 (t, C-C), 26.6 (t, C-9), 28.8 (t, C-D), 28.9 (t, C-B), 29.1 (t, C-10 - C17), 29.5 (t, C-10 - C17), 29.5 (t, C-10 - C17), 29.6 (t, C-10 - C17), 29.7 (t, C-10 - C17), 30.5 (t, C-8), 31.7 (t, C-E), 32.0 (t, C-10-C17), 34.2 (t, C-J), 36.2 (t, C-G), 39.1 (d, C-F), 50.7 (t, C-7), 68.1 (t, C-A), 114.8 (d, 2C, C-3), 120.0 (d, C-6), 123.3 (d, 2C, C-2, C2' or C-3), 124.9 (d, 2C, C-2, C2' or C-3), 126.4 (d, 2C, C-2, C2' or C-3'), 132.7 (s, C-1, C-1', C-4 or C-4' or C-5), 147.1 (s, C-4 or C-5), 147.2 (s, C-1, C-1', C-4 or C-4' or C-5), 152.4 (s, C-1, C-1', C-4 or C-4' or C-5), 161.7 (s, C-1 or C-4), 174.7 (s, C-H or C-I), 176.6 (s, C-H or C-I) ppm (2 carbons overlapping in the aliphatic region).

Die approbierte gedruckte Originalversion dieser Dissertation ist an der TU Wien Bibliothek verfügbar.
The approved original version of this doctoral thesis is available in print at TU Wien Bibliothek.
TU Bibliothek Your knowledge hub WIEN

E.3 UV-Vis spectroscopy

The UV-Vis spectroscopy was carried out using a UV-1800 spectrophotometer from Shimadzu and a quartz cuvette 6040-UV-10-531 (light path 10 mm, volume 1.4 mL) or a quartz cuvette 104-002-10-40 (light path 10 mm, volume 700 µL) from Hellma analitics.

E.3.1 Azobenzene photoswitching and thermal half-life time determination

To analyze the photoswitching, a 0.04 mM solution of the azobenzene in DMSO was prepared and a spectra between 600 and 260 nm was recorded with incremental steps of 1 nm and fast settings. Afterwards, to photoswitch the azobenzene from the *trans* to the *cis* isomer, this solution was irradiated with a 365 nm LED connected to a LX500 (Excelitas) at 100% intensity for 10 seconds and a new spectra was recorded. To confirm the reversibility of this process and switch-back to the *trans* isomer, the same solution was once again irradiated with a 460 nm LED connected to a LX500 (Excelitas) at 100% intensity for 10 seconds and a new spectra was recorded.

For the determination of the thermal half-life time, a 0.04 mM solution of the azobenzene in DMSO was prepared and irradiated with the 365 nm LED for 10 seconds. Subsequently, using the kinetic mode of the UVProbe software (instrument's software), the absorption was measured every hour for 18 hours at the maximum absorption wavelength of $\pi \rightarrow \pi^*$ band of the *trans* isomer. Finally the data were linearized (according to a first-kinetic model) using the formula $A_{linearized}$ = ln (A_{max} - A_t) and the $t_{1/2}$ was found at ln($Abs_{max}/2$).

E.3.2 HABA assay

A HABA reagent was prepared dissolving 24.2 mg of HABA in 9.9 mL of H_2O and 100 µL of 1 M NaOH. Streptavidin from *Streptomyces avidinii* (1 mg lyophilized in 50 µM NaCl) purchased from TCI was dissolved in 2 mL of PBS buffer and 60 µL of the HABA reagent were added.

A quartz cuvette of 750 µL was loaded with 450 µL of the previously prepared SA/HABA solution and a spectra between 260 and 700 nm was recorded. Afterwards the desired volume from a biotin or biotin derivative solution was added to the cuvette. In our case the solutions

Die approbierte gedruckte Originalversion dieser Dissertation ist an der TU Wien Bibliothek verfügbar.
The approved original version of this doctoral thesis is available in print at TU Wien Bibliothek.
TU Bibliothek Your knowledge hub WIEN

had a 10 mM concentration, but other concentrations can be used. The mixture was shaken and the spectra was remeasured to observe if the absorption band at 500 nm had a lower intensity.

E.4 Preparation of the silicon and aluminum samples

Silicon wafers, 1-0-0, p-type, boron-doped, 10-20 Ω cm, 500-550 µm thickness, double-sided polished were purchased from MEMC. Porous silicon was purchased from SiLiMiXT with an 20 µm oxide layer and a pore size of 15-15 nm.

Three different aluminum substrates were purchased:

- aluminum foil, 0.5mm (0.02in) thick, Puratronic(R); 99.998% (metals basis) from ABCR;
- aluminum alloy 5251 foil, Al 97.7%/ Mg 2%/ Mn 0.3%, thickness 1.5 mm, size 250x250 mm, mirror polished on both sides from Sigma-Aldrich;
- aluminum 1050 A, 99.5% Al, 0.4 mm from Conrad.

E.4.1 Cutting and cleaning of the substrates

The silicon wafers were cut into pieces of 25x18 mm with a diamond tip, which cleaved them along the crystallographic axes. The Porous silicon was cut the same way as the silicon wafers but in pieces of 12.5x18 mm. The aluminum substrates were cut into 20x20 mm pieces with an industrial guillotine from Schröder.

After cutting, a Bandelin Sonorex Super 10 P was used to sonicate the samples for 10 minutes in toluene. The sonicated samples were rinsed with toluene and dried under a stream of argon. The substrates were finally oxidized for 10 minutes on each side in a UV/Ozone chamber (Boekel UV clean model 135500).

E.4.2 Etching of silicon nanowires

The silicon etching followed a literature protocol[170]. The freshly cleaned silicon was placed in 20 mL of aqueous $AgNO_3$/HF solution ([HNO_3] = 0.005 M, [HF] = 6.2 M). After 1 minute, the samples were removed, rinsed with water and without drying placed in 20 mL of aqueous

Die approbierte gedruckte Originalversion dieser Dissertation ist an der TU Wien Bibliothek verfügbar.
The approved original version of this doctoral thesis is available in print at TU Wien Bibliothek.
TU Bibliothek Your knowledge hub WIEN

H_2O_2/HF ([H_2O_2] = 0.06 M, [HF] = 6.2 M) for 10 minutes, under the dark (aluminum foil covered beaker used to protect from light). After rinsing with water, the samples were transferred to a mixture of HNO_3:H_2O (1:1). After 5 minutes, the substrates were once again rinsed with water and transferred to piranha solution (H_2SO_4 96%: H_2O_2 36% = 1:4) for 30 minutes. Finally the samples were placed for 5 minutes in water and then in acetone, rinsed with fresh acetone and dried under a stream of argon.

E.4.3 Bohemite preparation on aluminum

A beaker was filled with 50 mL of distilled H_2O and heated till the H_2O reached boiling. Afterwards one surface was placed in the boiling H_2O for 10 or 20 minutes. Finally the surface was rinsed with water, acetone, dried under a stream of argon and placed in vacuum for 1 hour.

E.4.4 Surface modifications

E.4.4.1 Trichloro(octadecyl)silane modification

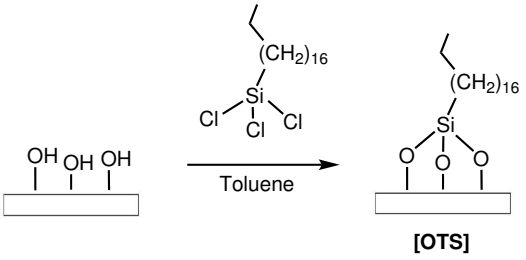

This modification was carried as described in the literature[175]. Three substrates (either silicon, silicon nanowires, porous silicon or aluminum) were placed in a beaker containing 10 mL of a 1 mM solution of trichloro(octadecyl)silane (OTS) in toluene. After 1 hour the substrates were removed, rinsed with toluene, dried under a stream of argon and placed under vacuum for 5 minutes.

Die approbierte gedruckte Originalversion dieser Dissertation ist an der TU Wien Bibliothek verfügbar.
The approved original version of this doctoral thesis is available in print at TU Wien Bibliothek.

E.4.4.2 Azide modification

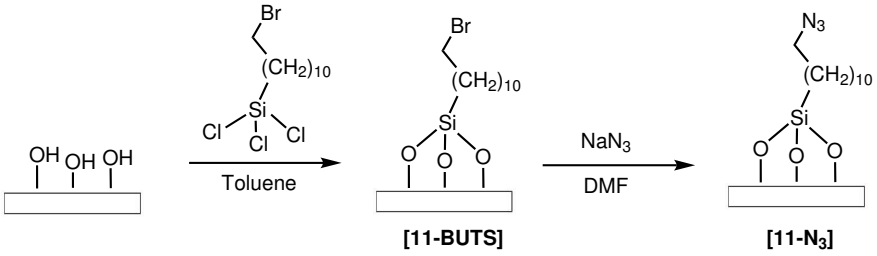

This modification was carried as described in the literature[164]. Three substrates (either silicon, silicon nanowires or aluminum) were placed in a beaker containing 10 mL of a 1 mM solution of 11-bromoundecyltrichlorosilane (BUTS) in toluene. After 4 hour the substrates were removed, rinsed with toluene, dried under a stream of argon and placed under vacuum for 5 minutes. After measuring ellipsometry (see E.4.6.1) to confirm the layer thickness, the substrates were transferred to 10 mL of a DMF saturated solution of NaN_3. After an overnight reaction the surfaces were removed from the solution, cleaned with acetone, water, acetone again, dried under a stream of argon and placed in the vacuum during 5 minutes. Finally, FTIRs (see section E.4.6.2) of the surfaces were measured.

E.4.5 Azobenene immobilization

E.4.5.1 *Trans* immobilization

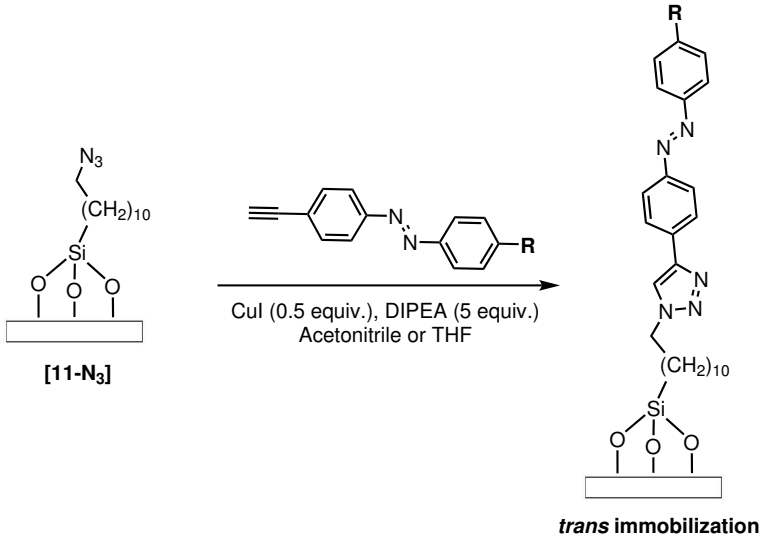

Die approbierte gedruckte Originalversion dieser Dissertation ist an der TU Wien Bibliothek verfügbar.
The approved original version of this doctoral thesis is available in print at TU Wien Bibliothek.

In the *trans* immobilization, a 0.5 mM solution of the desired azobenzene was prepared in acetonitrile or THF (11 mL) and 0.5 equivalents of CuI and 0.05 equivalents of DIPEA were added. After 5 minutes under stirring at room temperature in a round bottom vial, the azide functionalized surface 11-N_3 was added and the reaction was stirred for the desired time. The substrate was removed form the solution, rinsed with acetone, water, acetone again, dried under a stream of argon and placed under vacuum for 5 minutes.

E.4.5.2 *Cis* immobilization

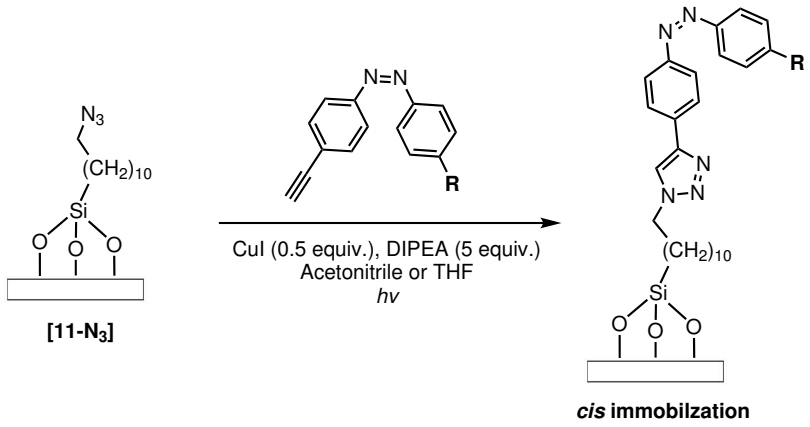

In the *cis* immobilization, a 0.5 mM solution of the desired azobenzene was prepared in acetonitrile or THF (11 mL) and 0.5 equivalents of CuI and 0.05 equivalents of DIPEA were added. The reaction mixture, in a round bottom vial covered with aluminum foil, was cooled in an ice bath and irradiated with a 365 nm LED connected to a LX500 ommnicure controller (Excelitas) from 10 cm away at 100% intensity. The LED was kept always under cooling by a fan. After 30 minutes, a 0.04 mM sample was prepared and analyzed by UV/Vis (blank containing the solvent, CuI and DIPEA). Once isomerization to the *cis* configuration was confirmed by UV/Vis, the azide functionalized silicon surface 11-N_3 was added. The reaction mixture was kept under irradiation and the temperature maintained between 10-15°C. After the desired reaction time, the substrate was removed, washed with acetone, water, acetone again, dried under a stream of argon and placed under vacuum for 5 minutes. This surface kept under the dark with aluminum foil till analysis.

Die approbierte gedruckte Originalversion dieser Dissertation ist an der TU Wien Bibliothek verfügbar.
The approved original version of this doctoral thesis is available in print at TU Wien Bibliothek.
TU Bibliothek Your knowledge hub WIEN

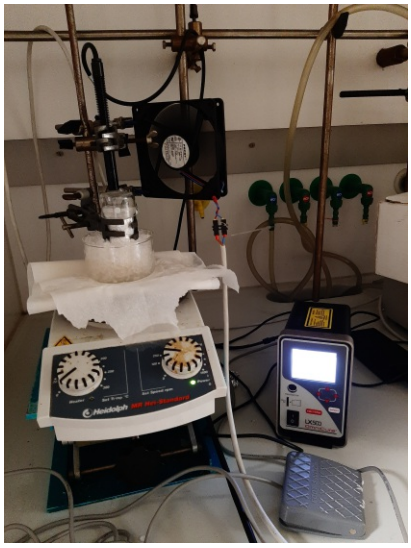

E.4.6 Surface analysis

E.4.6.1 Ellipsometry

A Sentech SE 500adv with a He-Ne laser as a light source was used to perform ellipsometry. The measurements were performed at 632.8 nm and the data analysis was carried out with the instrument software SE400advanced 2.16 with the McCracking algorithm. For the silicon surfaces the optical constants were: Si ($\eta = 3.865$, $\kappa = 0.02$), SiO_2 ($\eta = 1.465$, $\kappa = 0$), organic layer $\eta = 1.465$, $\kappa = 0$). For the aluminum the optical constants were: Al ($\eta = 1.3736$, $\kappa = 7.619$), AlO_3 ($\eta = 1.650$ $\kappa = 0$). For each surface, at least four different points of the surface were measured.

E.4.6.2 FTIR and IRRAS

The measurements were performed with a Bruker Vertex 80 FTIR using the provided OPUS 7.5 software. For silicon the FTIRs were measured with a narrow band MCT detector and a resolution of 4 cm^{-1}. For each sample 256 scans at a 40° angle of incidence were recorded. For the flat silicon surfaces an uncoated cleaned sample was used as a blank. For the silicon nanowires a spectra was always recorded after etching which was later used as its own reference. Before each measurement the chamber was purged with dry air for 2 minutes. The programs's software was used to remove the CO_2 peak.

Die approbierte gedruckte Originalversion dieser Dissertation ist an der TU Wien Bibliothek verfügbar.
The approved original version of this doctoral thesis is available in print at TU Wien Bibliothek.
TU Bibliothek Your knowledge hub WIEN

For the aluminum substrates IRRAS was performed using LN-MCT Narrow 45° COSTUM external detector and 4 cm^{-1} resolution. In total, 256 scans were measured at a 80° angle of incidence. As a reference a cleaned uncoated aluminum sample was used.

E.4.6.3 Optical goniometry and surface photoswitching

Static water contact angles were measured using a Krüss DSA 30 goniometer in combination with the provided Krüss ADVANCE 1.5.1.0 software. The surfaces were placed on the sample stage and a software-controlled equipment containing a needle placed a 7 µL water drop on the surface from 28 mm distance. The device's camera, with a resolution of 780x582, recorded a picture of the drop that was analyzed using the Young-Laplace method ($\theta > 10°$) of the instrument software. For each drop 5 different images were recorded.

For the determination of the advancing and receding water contact angles the sample stage was tilted at a rate of 30°/min. During the measurement pictures were continuously recorded until the drop rolled of the surface. The last frame which showed the still stationary drop was then used to determine the advancing and receding contact angle using the tangent method.

For the photoswitching experiments, the static WCA was measured immediately after surface preparation as previously described. Afterwards, the surface was cleaned with acetone, dried under a stream of argon, placed under vacuum for 5 minutes and irradiated with a 365 nm LED connected to a LX500 controller (4 minutes, from 5 cm distance, 100 % intensity). On the one hand, when no difference in the WCA was observed after irradiation, the surface was considered non-photoswitchablle and discarded. On the other hand, if a difference was verified the surface was cleaned with acetone, dried under a stream of Argon and irradiated with a halogen lamp Philips 7748XHP (2 hours, from 10 cm distance). A total of 6 irradiation cycles alternating between 365 nm LED and halogen lamp were performed measuring the WCA in between.

E.4.6.4 SEM

The SEM images were obtained with a FEI Quanta 200 MK2 electron microscope equipped with a Everhardt-Thornley detector. The samples were placed in the sample holder at a 8-

Die approbierte gedruckte Originalversion dieser Dissertation ist an der TU Wien Bibliothek verfügbar.
The approved original version of this doctoral thesis is available in print at TU Wien Bibliothek.
TU Bibliothek Your knowledge hub WIEN

11 mm working distance. The electron beam voltage was set at 10 KeV for the silicon and at 5 KeV for the aluminum substrates. The top-views were obtained without any further treatment. The side-views of the silicon were obtained by freshly cleaving the silicon with a diamond tip and measuring the newly exposed area.

Die approbierte gedruckte Originalversion dieser Dissertation ist an der TU Wien Bibliothek verfügbar.
The approved original version of this doctoral thesis is available in print at TU Wien Bibliothek.
TU Bibliothek Your knowledge hub WIEN

Chapter F

Bibliography

[1] M. W. Hoorens, W. Szymanski, "Reversible, Spatial and Temporal Control over Protein Activity Using Light", *Trends Biochem. Sci.* **2018**, *43*, 567 –575.

[2] W. Szymański, J. M. Beierle, H. A. V. Kistemaker, W. A. Velema, B. L. Feringa, "Reversible Photocontrol of Biological Systems by the Incorporation of Molecular Photoswitches", *Chem. Rev.* **2013**, *113*, 6114–6178.

[3] J. Broichhagen, J. A. Frank, D. Trauner, "A Roadmap to Success in Photopharmacology", *Acc. Chem. Res.* **2015**, *48*, 1947–1960.

[4] K. Hüll, J. Morstein, D. Trauner, "In Vivo Photopharmacology", *Chem. Rev.* **2018**, *118*, 10710–10747.

[5] P. Klán, T. Šolomek, C. G. Bochet, A. Blanc, R. Givens, M. Rubina, V. Popik, A. Kostikov, J. Wirz, "Photoremovable Protecting Groups in Chemistry and Biology: Reaction Mechanisms and Efficacy", *Chem. Rev.* **2013**, *113*, 119–191.

[6] H. Yu, J. Li, D. Wu, Z. Qiu, Y. Zhang, "Chemistry and biological applications of photo-labile organic molecules", *Chem. Soc. Rev.* **2010**, *39*, 464–473.

[7] M. Matsuzaki, G. C. R. Ellis-Davies, T. Nemoto, Y. Miyashita, M. Iino, H. Kasai, "Dendritic spine geometry is critical for AMPA receptor expression in hippocampal CA1 pyramidal neurons", *Nat. Neurosci.* **2001**, *4*, 1086–1092.

[8] Q. Cheng, M. G. Steinmetz, V. Jayaraman, "Photolysis of γ-(α-Carboxy-2-nitrobenzyl)-l-glutamic Acid Investigated in the Microsecond Time Scale by Time-Resolved FTIR", *J. Am. Chem. Soc.* **2002**, *124*, 7676–7677.

[9] Z. L. Pianowski, "Recent Implementations of Molecular Photoswitches into Smart Materials and Biological Systems", *Chem. Eur. J.* **2019**, *25*, 5128–5144.

[10] M. Zhu, H. Zhou, "Azobenzene-based small molecular photoswitches for protein modulation", *Org. Biomol. Chem.* **2018**, *16*, 8434–8445.

[11] A. A. Beharry, G. A. Woolley, "Azobenzene photoswitches for biomolecules", *Chem. Soc. Rev.* **2011**, *40*, 4422–4437.

[12] D. H. Waldeck, "Photoisomerization dynamics of stilbenes", *Chem. Rev.* **1991**, *91*, 415–436.

[13] S. Wiedbrauk, H. Dube, "Hemithioindigo—an emerging photoswitch", *Tetrahedron Lett.* **2015**, *56*, 4266 –4274.

[14] J. E. Zweig, T. A. Ko, J. Huang, T. R. Newhouse, "Effects of π-extension on pyrrole hemithioindigo photoswitches", *Tetrahedron* **2019**, *75*, 130466.

[15] C. Petermayer, H. Dube, "Indigoid Photoswitches: Visible Light Responsive Molecular Tools", *Acc. Chem. Res.* **2018**, *51*, 1153–1163.

[16] M. W. H. Hoorens, M. Medved', A. D. Laurent, M. Di Donato, S. Fanetti, L. Slappendel, M. Hilbers, B. L. Feringa, W. Jan Buma, W. Szymanski, "Iminothioindoxyl as a molecular photoswitch with 100 nm band separation in the visible range", *Nat. Commun.* **2019**, *10*, 2390.

[17] K. Matsuda, M. Irie, "Diarylethene as a photoswitching unit", *J. Photoch. Photobio. C* **2004**, *5*, 169 –182.

[18] M. Irie, T. Fukaminato, K. Matsuda, S. Kobatake, "Photochromism of Diarylethene Molecules and Crystals: Memories, Switches, and Actuators", *Chem. Rev.* **2014**, *114*, 12174–12277.

[19] Y. Yokoyama, "Fulgides for Memories and Switches", *Chem. Rev.* **2000**, *100*, 1717–1740.

[20] R. Klajn, "Spiropyran-based dynamic materials", *Chem. Soc. Rev.* **2014**, *43*, 148–184.

[21] B. S. Lukyanov, M. B. Lukyanova, "Spiropyrans: Synthesis, Properties, and Application. (Review)", *Chem. Heterocycl. Com.* **2005**, *41*, 281–311.

[22] M. Di Donato, M. M. Lerch, A. Lapini, A. D. Laurent, A. Iagatti, L. Bussotti, S. P. Ihrig, M. Medved', D. Jacquemin, W. Szymański, W. J. Buma, P. Foggi, B. L. Feringa, "Shedding Light on the Photoisomerization Pathway of Donor–Acceptor Stenhouse Adducts", *J. Am. Chem. Soc.* **2017**, *139*, 15596–15599.

[23] M. M. Lerch, W. Szymański, B. L. Feringa, "The (photo)chemistry of Stenhouse photoswitches: guiding principles and system design", *Chem. Soc. Rev.* **2018**, *47*, 1910–1937.

Die approbierte gedruckte Originalversion dieser Dissertation ist an der TU Wien Bibliothek verfügbar.
The approved original version of this doctoral thesis is available in print at TU Wien Bibliothek.
TU Bibliothek Your knowledge hub WIEN

[24] J. R. Hemmer, S. O. Poelma, N. Treat, Z. A. Page, N. D. Dolinski, Y. J. Diaz, W. Tomlinson, K. D. Clark, J. P. Hooper, C. Hawker, J. Read de Alaniz, "Tunable Visible and Near Infrared Photoswitches", *J. Am. Chem. Soc.* **2016**, *138*, 13960–13966.
[25] Z. Ahmed, A. Siiskonen, M. Virkki, A. Priimagi, "Controlling azobenzene photoswitching through combined ortho-fluorination and -amination", *Chem. Commun.* **2017**, *53*, 12520–12523.
[26] Y.-T. Wang, X.-Y. Liu, G. Cui, W.-H. Fang, W. Thiel, "Photoisomerization of Arylazopyrazole Photoswitches: Stereospecific Excited-State Relaxation", *Angew. Chem. Int. Ed.* **2016**, *55*, 14009–14013.
[27] M. J. Hansen, M. M. Lerch, W. Szymanski, B. L. Feringa, "Direct and Versatile Synthesis of Red-Shifted Azobenzenes", *Angew. Chem. Int. Ed.* **2016**, *55*, 13514–13518.
[28] E. Merino, "Synthesis of azobenzenes: the coloured pieces of molecular materials", *Chem. Soc. Rev.* **2011**, *40*, 3835–3853.
[29] H. M. D. Bandara, S. C. Burdette, "Photoisomerization in different classes of azobenzene", *Chem. Soc. Rev.* **2012**, *41*, 1809–1825.
[30] J. Calbo, C. E. Weston, A. J. P. White, H. S. Rzepa, J. Contreras-García, M. J. Fuchter, "Tuning Azoheteroarene Photoswitch Performance through Heteroaryl Design", *J. Am. Chem. Soc.* **2017**, *139*, 1261–1274.
[31] R. Siewertsen, H. Neumann, B. Buchheim-Stehn, R. Herges, C. Näther, F. Renth, F. Temps, "Highly Efficient Reversible Z-E Photoisomerization of a Bridged Azobenzene with Visible Light through Resolved S1(nπ*) Absorption Bands", *J. Am. Chem. Soc.* **2009**, *131*, 15594–15595.
[32] M. Hammerich, C. Schütt, C. Stähler, P. Lentes, F. Röhricht, R. Höppner, R. Herges, "Heterodiazocines: Synthesis and Photochromic Properties, Trans to Cis Switching within the Bio-optical Window", *J. Am. Chem. Soc.* **2016**, *138*, 13111–13114.
[33] S. Samanta, A. A. Beharry, O. Sadovski, T. M. McCormick, A. Babalhavaeji, V. Tropepe, G. A. Woolley, "Photoswitching Azo Compounds in Vivo with Red Light", *J. Am. Chem. Soc.* **2013**, *135*, 9777–9784.
[34] O. Sadovski, A. Beharry, F. Zhang, G. Woolley, "Spectral Tuning of Azobenzene Photoswitches for Biological Applications", *Angew. Chem. Int. Ed.* **2009**, *48*, 1484–1486.
[35] A. A. Beharry, O. Sadovski, G. A. Woolley, "Azobenzene Photoswitching without Ultraviolet Light", *J. Am. Chem. Soc.* **2011**, *133*, 19684–19687.
[36] C. Knie, M. Utecht, F. Zhao, H. Kulla, S. Kovalenko, A. M. Brouwer, P. Saalfrank, S. Hecht, D. Bléger, "ortho-Fluoroazobenzenes: Visible Light Switches with Very Long-Lived Z Isomers", *Chem. Eur. J.* **2014**, *20*, 16492–16501.
[37] M. Dong, A. Babalhavaeji, C. V. Collins, K. Jarrah, O. Sadovski, Q. Dai, G. A. Woolley, "Near-Infrared Photoswitching of Azobenzenes under Physiological Conditions", *J. Am. Chem. Soc.* **2017**, *139*, 13483–13486.
[38] Y. Yang, R. P. Hughes, I. Aprahamian, "Near-Infrared Light Activated Azo-BF2 Switches", *J. Am. Chem. Soc.* **2014**, *136*, 13190–13193.
[39] Y. Li, B. O. Patrick, D. Dolphin, "Near-Infrared Absorbing Azo Dyes: Synthesis and X-ray Crystallographic and Spectral Characterization of Monoazopyrroles, Bisazopyrroles, and a Boron-Azopyrrole Complex", *J. Org. Chem.* **2009**, *74*, 5237–5243.
[40] C. E. Weston, R. D. Richardson, P. R. Haycock, A. J. P. White, M. J. Fuchter, "Arylazopyrazoles: Azoheteroarene Photoswitches Offering Quantitative Isomerization and Long Thermal Half-Lives", *J. Am. Chem. Soc.* **2014**, *136*, 11878–11881.
[41] T. Wendler, C. Schütt, C. Näther, R. Herges, "Photoswitchable Azoheterocycles via Coupling of Lithiated Imidazoles with Benzenediazonium Salts", *J. Org. Chem.* **2012**, *77*, 3284–3287.
[42] J. Otsuki, K. Suwa, K. Narutaki, C. Sinha, I. Yoshikawa, K. Araki, "Photochromism of 2-(Phenylazo)imidazoles", *J. Phys. Chem. A* **2005**, *109*, 8064–8069.
[43] P. Kumar, A. Srivastava, C. Sah, S. Devi, S. Venkataramani, "Arylazo-3,5-dimethylisoxazoles: Azoheteroarene Photoswitches Exhibiting High Z-Isomer Stability, Solid-State Photochromism, and Reversible Light-Induced Phase Transition", *Chem. Eur. J.* **2019**, *25*, 11924–11932.
[44] W. A. Velema, W. Szymanski, B. L. Feringa, "Photopharmacology: Beyond Proof of Principle", *J. Am. Chem. Soc.* **2014**, *136*, PMID: 24456115, 2178–2191.
[45] M. J. Fuchter, "On the Promise of Photopharmacology Using Photoswitches: A Medicinal Chemist's Perspective", *J. Med. Chem.* **2020**, *63*, PMID: 32511922, 11436–11447.
[46] M. M. Lerch, M. J. Hansen, G. M. van Dam, W. Szymanski, B. L. Feringa, "Emerging Targets in Photopharmacology", *Angew. Chem. Int. Ed.* **2016**, *55*, 10978–10999.
[47] M. Banghart, K. Borges, E. Isacoff, D. Trauner, R. H. Kramer, "Light-activated ion channels for remote control of neuronal firing", *Nat. Neurosci.* **2004**, *7*, 1381–1386.
[48] H. Asanuma, T. Takarada, T. Yoshida, D. Tamaru, X. Liang, M. Komiyama, "Enantioselective Incorporation of Azobenzenes into Oligodeoxyribonucleotide for Effective Photoregulation of Duplex Formation", *Angew. Chem. Int. Ed.* **2001**, *40*, 2671–2673.
[49] Y. Kamiya, T. Takagi, H. Ooi, H. Ito, X. Liang, H. Asanuma, "Synthetic Gene Involving Azobenzene-Tethered T7 Promoter for the Photocontrol of Gene Expression by Visible Light", *ACS Synth. Biol.* **2015**, *4*, 365–370.
[50] L. Albert, J. Xu, R. Wan, V. Srinivasan, Y. Dou, O. Vázquez, "Controlled inhibition of methyltransferases using photoswitchable peptidomimetics: towards an epigenetic regulation of leukemia", *Chem. Sci.* **2017**, *8*, 4612–4618.

Die approbierte gedruckte Originalversion dieser Dissertation ist an der TU Wien Bibliothek verfügbar.
The approved original version of this doctoral thesis is available in print at TU Wien Bibliothek.
TU Bibliothek Your knowledge hub WIEN

[51] L. Guerrero, O. S. Smart, G. A. Woolley, R. K. Allemann, "Photocontrol of DNA Binding Specificity of a Miniature Engrailed Homeodomain", *J. Am. Chem. Soc.* **2005**, *127*, 15624–15629.
[52] P. Wysoczanski, R. J. Mart, E. J. Loveridge, C. Williams, S. B.-M. Whittaker, M. P. Crump, R. K. Allemann, "NMR Solution Structure of a Photoswitchable Apoptosis Activating Bak Peptide Bound to Bcl-xL", *J. Am. Chem. Soc.* **2012**, *134*, 7644–7647.
[53] R. Mogaki, K. Okuro, T. Aida, "Adhesive Photoswitch: Selective Photochemical Modulation of Enzymes under Physiological Conditions", *J. Am. Chem. Soc.* **2017**, *139*, 10072–10078.
[54] T. Weber, V. Chandrasekaran, I. Stamer, M. B. Thygesen, A. Terfort, T. K. Lindhorst, "Switching of Bacterial Adhesion to a Glycosylated Surface by Reversible Reorientation of the Carbohydrate Ligand", *Angew. Chem. Int. Ed.* **2014**, *53*, 14583–14586.
[55] P. D. Bregestovski, G. V. Maleeva, "Photopharmacology: A Brief Review Using the Control of Potassium Channels as an Example", *Neurosci. Behav. Physi.* **2019**, *49*, 184–191.
[56] A. Mourot, M. A. Kienzler, M. R. Banghart, T. Fehrentz, F. M. E. Huber, M. Stein, R. H. Kramer, D. Trauner, "Tuning Photochromic Ion Channel Blockers", *ACS Chem. Neurosci.* **2011**, *2*, 536–543.
[57] M. Wegener, M. J. Hansen, A. J. M. Driessen, W. Szymanski, B. L. Feringa, "Photocontrol of Antibacterial Activity: Shifting from UV to Red Light Activation", *J. Am. Chem. Soc.* **2017**, *139*, 17979–17986.
[58] W. A. Velema, J. P. van der Berg, M. J. Hansen, W. Szymanski, A. J. M. Driessen, B. L. Feringa, "Optical control of antibacterial activity", *Nat. Chem.* **2013**, *5*, 924–928.
[59] J. A. Frank, D. A. Yushchenko, D. J. Hodson, N. Lipstein, J. Nagpal, G. A. Rutter, J.-S. Rhee, A. Gottschalk, N. Brose, C. Schultz, D. Trauner, "Photoswitchable diacylglycerols enable optical control of protein kinase C", *Nat. Chem. Bio.* **2016**, *12*, 755–762.
[60] M. Borowiak, W. Nahaboo, M. Reynders, K. Nekolla, P. Jalinot, J. Hasserodt, M. Rehberg, M. Delattre, S. Zahler, A. Vollmar, D. Trauner, O. Thorn-Seshold, "Photoswitchable Inhibitors of Microtubule Dynamics Optically Control Mitosis and Cell Death", *Cell* **2015**, *162*, 403 –411.
[61] M. Schönberger, D. Trauner, "A Photochromic Agonist for μ-Opioid Receptors", *Angew. Chem. Int. Ed.* **2014**, *53*, 3264–3267.
[62] Y. Hao, H. Cui, J. Meng, S. Wang, "Photo-responsive smart surfaces with controllable cell adhesion", *J. Photoch. Photobiol. A* **2018**, *355*, 202 –211.
[63] J. Zhang, W. Ma, X.-P. He, H. Tian, "Taking Orders from Light: Photo-Switchable Working/Inactive Smart Surfaces for Protein and Cell Adhesion", *ACS Appl. Mater. Interfaces* **2017**, *9*, 8498–8507.
[64] L. F. Kadem, M. Holz, K. G. Suana, Q. Li, C. Lamprecht, R. Herges, C. Selhuber-Unkel, "Rapid Reversible Photoswitching of Integrin-Mediated Adhesion at the Single-Cell Level", *Adv. Mater.* **2016**, *28*, 1799–1802.
[65] D. Liu, Y. Xie, H. Shao, X. Jiang, "Using Azobenzene-Embedded Self-Assembled Monolayers To Photochemically Control Cell Adhesion Reversibly", *Angew. Chem. Int. Ed.* **2009**, *48*, 4406–4408.
[66] A. Goulet-Hanssens, K. Lai Wing Sun, T. E. Kennedy, C. J. Barrett, "Photoreversible Surfaces to Regulate Cell Adhesion", *Biomacromolecules* **2012**, *13*, 2958–2963.
[67] E. Vaselli, C. Fedele, S. Cavalli, P. A. Netti, ""On–Off" RGD Signaling Using Azobenzene Photoswitch-Modified Surfaces", *ChemPlusChem* **2015**, *80*, 1547–1555.
[68] Q. Bian, W. Wang, G. Han, Y. Chen, S. Wang, G. Wang, "Photoswitched Cell Adhesion on Azobenzene-Containing Self-Assembled Films", *ChemPhysChem* **2016**, *17*, 2503–2508.
[69] J. Auernheimer, C. Dahmen, U. Hersel, A. Bausch, H. Kessler, "Photoswitched Cell Adhesion on Surfaces with RGD Peptides", *J. Am. Chem. Soc.* **2005**, *127*, 16107–16110.
[70] G. Despras, L. Möckl, A. Heitmann, I. Stamer, C. Bräuchle, T. K. Lindhorst, "A Photoswitchable Trivalent Cluster Mannoside to Probe the Effects of Ligand Orientation in Bacterial Adhesion", *ChemBioChem* **2019**, *20*, 2373–2382.
[71] T. Wei, W. Zhan, Q. Yu, H. Chen, "Smart Biointerface with Photoswitched Functions between Bactericidal Activity and Bacteria-Releasing Ability", *ACS Appl. Mater. Interfaces* **2017**, *9*, 25767–25774.
[72] Y.-H. Gong, C. Li, J. Yang, H.-Y. Wang, R.-X. Zhuo, X.-Z. Zhang, "Photoresponsive "Smart Template" via Host–Guest Interaction for Reversible Cell Adhesion", *Macromolecules* **2011**, *44*, 7499–7502.
[73] Q. Bian, W. Wang, S. Wang, G. Wang, "Light-Triggered Specific Cancer Cell Release from Cyclodextrin/Azobenzene and Aptamer-Modified Substrate", *ACS Appl. Mater. Interfaces* **2016**, *8*, 27360–27367.
[74] W. Zhan, T. Wei, L. Cao, C. Hu, Y. Qu, Q. Yu, H. Chen, "Supramolecular Platform with Switchable Multivalent Affinity: Photo-Reversible Capture and Release of Bacteria", *ACS Appl. Mater. Interfaces* **2017**, *9*, 3505–3513.
[75] T. Wei, W. Zhan, L. Cao, C. Hu, Y. Qu, Q. Yu, H. Chen, "Multifunctional and Regenerable Antibacterial Surfaces Fabricated by a Universal Strategy", *ACS Appl. Mater. Interfaces* **2016**, *8*, PMID: 27759376, 30048–30057.
[76] L. A. T. W. Asri, M. Crismaru, S. Roest, Y. Chen, O. Ivashenko, P. Rudolf, J. C. Tiller, H. C. van der Mei, T. J. A. Loontjens, H. J. Busscher, "A Shape-Adaptive, Antibacterial-Coating of Immobilized Quaternary-Ammonium Compounds Tethered on Hyperbranched Polyurea and its Mechanism of Action", *Adv. Funct. Mater.* **2014**, *24*, 346–355.
[77] D. Pearson, A. J. Downard, A. Muscroft-Taylor, A. D. Abell, "Reversible Photoregulation of Binding of α-Chymotrypsin to a Gold Surface", *J. Am. Chem. Soc.* **2007**, *129*, 14862–14863.

Die approbierte gedruckte Originalversion dieser Dissertation ist an der TU Wien Bibliothek verfügbar.
The approved original version of this doctoral thesis is available in print at TU Wien Bibliothek.
TU Bibliothek Your knowledge hub WIEN

[78] D. Pearson, A. Abell, "Structural Optimization of Photoswitch Ligands for Surface Attachment of α-Chymotrypsin and Regulation of Its Surface Binding", *Chem. Eur. J.* **2010**, *16*, 6983–6992.
[79] P. Wan, Y. Xing, Y. Chen, L. Chi, X. Zhang, "Host–guest chemistry at interface for photoswitchable bioelectrocatalysis", *Chem. Commun.* **2011**, *47*, 5994–5996.
[80] G. B. Demirel, N. Dilsiz, M. A. Ergün, M. Çakmak, T. Çaykara, "Photocontrollable DNA hybridization on reversibly photoresponsive surfaces", *J. Mater. Chem.* **2011**, *21*, 10415–10420.
[81] G. Hayashi, M. Hagihara, C. Dohno, K. Nakatani, "Photoregulation of a Peptide-RNA Interaction on a Gold Surface", *J. Am. Chem. Soc.* **2007**, *129*, 8678–8679.
[82] F. L. Callari, S. Sortino, ""Catch-and-release" of porphyrins by photoswitchable self-assembled monolayers", *J. Mater. Chem.* **2007**, *17*, 4184–4188.
[83] P. Xu, J. Quan, W. Chen, J. Zhang, H. Yan, Y. Liu, S. Tan, X. Zeng, H. Li, G. Yang, "A Chirality/Light Dual-Responsive Calixarene-Functionalized Gold Surface for the Separation of Naproxen Enantiomers", *ChemPlusChem* **2019**, *84*, 907–912.
[84] N. L. Weineisen, C. A. Hommersom, J. Voskuhl, S. Sankaran, A. M. A. Depauw, N. Katsonis, P. Jonkheijm, J. J. L. M. Cornelissen, "Photoresponsive, reversible immobilization of virus particles on supramolecular platforms", *Chem. Commun.* **2017**, *53*, 1896–1899.
[85] J. Deng, X. Liu, W. Shi, C. Cheng, C. He, C. Zhao, "Light-Triggered Switching of Reversible and Alterable Biofunctionality via β-Cyclodextrin/Azobenzene-Based Host–Guest Interaction", *ACS Macro Lett.* **2014**, *3*, 1130–1133.
[86] H. S. Lim, J. T. Han, D. Kwak, M. Jin, K. Cho, "Photoreversibly Switchable Superhydrophobic Surface with Erasable and Rewritable Pattern", *J. Am. Chem. Soc.* **2006**, *128*, 14458–14459.
[87] J. Huang, Y. Huang, C. He, Y. Gao, "Synthesis and characterization of photoresponsive POSS-based polymers and their switchable water and oil wettability on cotton fabric", *RSC Adv.* **2015**, *5*, 100339–100346.
[88] A. B. D. Cassie, S. Baxter, "Wettability of porous surfaces", *Trans. Faraday Soc.* **1944**, *40*, 546–551.
[89] K.-Y. Law, H. Zhao, Surface wetting: characterization, contact angle, and fundamentals, Springer International Publishing, **2016**.
[90] Q. Gao, L. He, Y. Li, X. Ran, L. Guo, "Controllable wettability and adhesion of superhydrophobic self-assembled surfaces based on a novel azobenzene derivative", *RSC Adv.* **2017**, *7*, 50403–50409.
[91] M. Chen, F. Besenbacher, "Light-Driven Wettability Changes on a Photoresponsive Electrospun Mat", *ACS Nano* **2011**, *5*, 1549–1555.
[92] S. Pan, R. Guo, W. Xu, "Photoresponsive superhydrophobic surfaces for effective wetting control", *Soft Matter* **2014**, *10*, 9187–9192.
[93] W. Jiang, G. Wang, Y. He, X. Wang, Y. An, Y. Song, L. Jiang, "Photo-switched wettability on an electrostatic self-assembly azobenzene monolayer", *Chem. Commun.* **2005**, 3550–3552.
[94] C. Jin, R. Yan, J. Huang, "Cellulose substance with reversible photo-responsive wettability by surface modification", *J. Mater. Chem.* **2011**, *21*, 17519–17525.
[95] H. C. Kolb, M. G. Finn, K. B. Sharpless, "Click Chemistry: Diverse Chemical Function from a Few Good Reactions", *Angew. Chem. Int. Ed.* **2001**, *40*, 2004–2021.
[96] J. E. Moses, A. D. Moorhouse, "The growing applications of click chemistry", *Chem. Soc. Rev.* **2007**, *36*, 1249–1262.
[97] R. Huisgen, "Proceedings of the Chemical Society. October 1961", *Proc. Chem. Soc.* **1961**, 357–396.
[98] V. V. Rostovtsev, L. G. Green, V. V. Fokin, K. B. Sharpless, "A Stepwise Huisgen Cycloaddition Process: Copper(I)-Catalyzed Regioselective "Ligation" of Azides and Terminal Alkynes", *Angew. Chem. Int. Ed.* **2002**, *41*, 2596–2599.
[99] C. W. Tornøe, C. Christensen, M. Meldal, "Peptidotriazoles on Solid Phase: [1,2,3]-Triazoles by Regiospecific Copper(I)-Catalyzed 1,3-Dipolar Cycloadditions of Terminal Alkynes to Azides", *J. Org. Chem.* **2002**, *67*, 3057–3064.
[100] M. Meldal, C. W. Tornøe, "Cu-Catalyzed Azide-Alkyne Cycloaddition", *Chem. Rev.* **2008**, *108*, 2952–3015.
[101] S. Neumann, M. Biewend, S. Rana, W. H. Binder, "The CuAAC: Principles, Homogeneous and Heterogeneous Catalysts, and Novel Developments and Applications", *Macromol. Rapid Commun.* **2020**, *41*, 1900359.
[102] D. Döhler, P. Michael, W. H. Binder, "CuAAC-Based Click Chemistry in Self-Healing Polymers", *Acc. Chem. Res* **2017**, *50*, 2610–2620.
[103] M. Meldal, "Polymer "Clicking" by CuAAC Reactions", *Macromol. Rapid Commun.* **2008**, *29*, 1016–1051.
[104] P. Thirumurugan, D. Matosiuk, K. Jozwiak, "Click Chemistry for Drug Development and Diverse Chemical–Biology Applications", *Chem. Rev.* **2013**, *113*, 4905–4979.
[105] K. Holland-Nell, M. Meldal, "Maintaining Biological Activity by Using Triazoles as Disufide Bond Mimetics", *Angew. Chem. Int. Ed.* **2011**, *50*, 5204–5206.
[106] M. Yang, J. Li, P. R. Chen, "Transition metal-mediated bioorthogonal protein chemistry in living cells", *Chem. Soc. Rev.* **2014**, *43*, 6511–6526.
[107] N. Moini, M. Zohuriaan-Mehr, K. Kabiri, H. Khonakdar, ""Click" on SAP: Superabsorbent polymer surface modification via CuAAC reaction toward antibacterial activity and improved swollen gel strength", *Appl. Surf. Sci.* **2019**, *487*, 1131 –1144.

Die approbierte gedruckte Originalversion dieser Dissertation ist an der TU Wien Bibliothek verfügbar.
The approved original version of this doctoral thesis is available in print at TU Wien Bibliothek.
TU Bibliothek Your knowledge hub WIEN

[108] A. Marrocchi, A. Facchetti, D. Lanari, S. Santoro, L. Vaccaro, "Click-chemistry approaches to π-conjugated polymers for organic electronics applications", *Chem. Sci.* **2016**, *7*, 6298–6308.
[109] D. Svatunek, G. Eilenberger, C. Denk, D. Lumpi, C. Hametner, G. Allmaier, H. Mikula, "Live Monitoring of Strain-Promoted Azide Alkyne Cycloadditions in Complex Reaction Environments by Inline ATR-IR Spectroscopy", *Chem. Eur.* **2020**, *n/a*, DOI 10.1002/chem.201905478.
[110] E. Lallana, E. Fernandez-Megia, R. Riguera, "Surpassing the Use of Copper in the Click Functionalization of Polymeric Nanostructures: A Strain-Promoted Approach", *J. Am. Chem. Soc.* **2009**, *131*, 5748–5750.
[111] J. Dommerholt, S. Schmidt, R. Temming, L. J. A. Hendriks, F. P. J. T. Rutjes, J. C. M. van Hest, D. J. Lefeber, P. Friedl, F. L. van Delft, "Readily Accessible Bicyclononynes for Bioorthogonal Labeling and Three Dimensional Imaging of Living Cells", *Angew. Chem. Int. Ed.* **2010**, *49*, 9422–9425.
[112] N. K. Devaraj, "The Future of Bioorthogonal Chemistry", *ACS Cent. Sci.* **2018**, *4*, 952–959.
[113] E. Kim, H. Koo, "Biomedical applications of copper-free click chemistry: in vitro, in vivo, and ex vivo", *Chem. Sci.* **2019**, *10*, 7835–7851.
[114] C. R. Bertozzi, L. L. Kiessling, "Chemical Glycobiology", *Science* **2001**, *291*, 2357–2364.
[115] M. Köhn, R. Breinbauer, "The Staudinger Ligation-A Gift to Chemical Biology", *Angew. Chem. Int. Ed.* **2004**, *43*, 3106–3116.
[116] F. L. Lin, H. M. Hoyt, H. van Halbeek, R. G. Bergman, C. R. Bertozzi, "Mechanistic Investigation of the Staudinger Ligation", *J. Am. Chem. Soc.* **2005**, *127*, 2686–2695.
[117] Q. Zhang, A. Gimeno, D. Santana, Z. Wang, Y. Valdés-Balbin, L. M. Rodríguez-Noda, T. Hansen, L. Kong, M. Shen, H. S. Overkleeft, V. Vérez-Bencomo, G. A. van der Marel, J. Jiménez-Barbero, F. Chiodo, J. D. C. Codée, "Synthetic, Zwitterionic Sp1 Oligosaccharides Adopt a Helical Structure Crucial for Antibody Interaction", *ACS Cent. Sci.* **2019**, *5*, 1407–1416.
[118] E. Saxon, S. J. Luchansky, H. C. Hang, C. Yu, S. C. Lee, C. R. Bertozzi, "Investigating Cellular Metabolism of Synthetic Azidosugars with the Staudinger Ligation", *J. Am. Chem. Soc.* **2002**, *124*, 14893–14902.
[119] C. C.-Y. Wang, T. S. Seo, Z. Li, H. Ruparel, J. Ju, "Site-Specific Fluorescent Labeling of DNA Using Staudinger Ligation", *Bioconjug. Chem.* **2003**, *14*, 697–701.
[120] B. L. Nilsson, R. J. Hondal, M. B. Soellner, R. T. Raines, "Protein Assembly by Orthogonal Chemical Ligation Methods", *J. Am. Chem. Soc.* **2003**, *125*, 5268–5269.
[121] B. L. Oliveira, Z. Guo, G. J. L. Bernardes, "Inverse electron demand Diels–Alder reactions in chemical biology", *Chem. Soc. Rev.* **2017**, *46*, 4895–4950.
[122] C. R. Bertozzi, "A Decade of Bioorthogonal Chemistry", *Acc. Chem. Res.* **2011**, *44*, 651–653.
[123] G. Wittig, A. Krebs, "Zur Existenz niedergliedriger Cycloalkine, I", *Chem. Ber.* **1961**, *94*, 3260–3275.
[124] N. J. Agard, J. A. Prescher, C. R. Bertozzi, "A Strain-Promoted [3 + 2] Azide-Alkyne Cycloaddition for Covalent Modification of Biomolecules in Living Systems", *J. Am. Chem. Soc.* **2004**, *126*, PMID: 15547999, 15046–15047.
[125] D. Svatunek, N. Houszka, T. A. Hamlin, F. M. Bickelhaupt, H. Mikula, "Chemoselectivity of Tertiary Azides in Strain-Promoted Alkyne-Azide Cycloadditions", *Chem. Eur.* **2019**, *25*, 754–758.
[126] N. K. Devaraj, R. Weissleder, S. A. Hilderbrand, "Tetrazine-Based Cycloadditions: Application to Pretargeted Live Cell Imaging", *Bioconjug. Chem.* **2008**, *19*, 2297–2299.
[127] M. L. Blackman, M. Royzen, J. M. Fox, "Tetrazine Ligation: Fast Bioconjugation Based on Inverse-Electron-Demand Diels-Alder Reactivity", *J. Am. Chem. Soc.* **2008**, *130*, 13518–13519.
[128] A.-C. Knall, C. Slugovc, "Inverse electron demand Diels–Alder (iEDDA)-initiated conjugation: a (high) potential click chemistry scheme", *Chem. Soc. Rev.* **2013**, *42*, 5131–5142.
[129] N. Devaraj, S. Hilderbrand, R. Upadhyay, R. Mazitschek, R. Weissleder, "Bioorthogonal Turn-On Probes for Imaging Small Molecules inside Living Cells", *Angew. Chem. Int. Ed.* **2010**, *49*, 2869–2872.
[130] Y.-R. Kim, Y. H. Kim, S. W. Kim, Y. J. Lee, D.-E. Chae, K.-A. Kim, Z.-W. Lee, N. D. Kim, J.-S. Choi, I. S. Choi, K.-B. Lee, "A bioorthogonal approach for imaging the binding between Dasatinib and its target proteins inside living cells", *Chem. Commun.* **2016**, *52*, 11764–11767.
[131] A. Rutkowska, D. W. Thomson, J. Vappiani, T. Werner, K. M. Mueller, L. Dittus, J. Krause, M. Muelbaier, G. Bergamini, M. Bantscheff, "A Modular Probe Strategy for Drug Localization, Target Identification and Target Occupancy Measurement on Single Cell Level", *ACS Chem. Biol.* **2016**, *11*, 2541–2550.
[132] R. Xie, L. Dong, Y. Du, Y. Zhu, R. Hua, C. Zhang, X. Chen, "In vivo metabolic labeling of sialoglycans in the mouse brain by using a liposome-assisted bioorthogonal reporter strategy", *PNAS* **2016**, *113*, 5173–5178.
[133] A. Zlitni, N. Janzen, F. S. Foster, J. F. Valliant, "Catching Bubbles: Targeting Ultrasound Microbubbles Using Bioorthogonal Inverse-Electron-Demand Diels–Alder Reactions", *Angew. Chem. Int. Ed.* **2014**, *53*, 6459–6463.
[134] H. Shao, J. Chung, L. Balaj, A. Charest, D. D. Bigner, B. S. Carter, F. H. Hochberg, X. O. Breakefield, R. Weissleder, H. Lee, "Protein typing of circulating microvesicles allows real-time monitoring of glioblastoma therapy", *Nat. Med.* **2012**, *18*, 1835–1840.
[135] L. Taemaitree, A. Shivalingam, A. H. El-Sagheer, T. Brown, "An artificial triazole backbone linkage provides a split-and-click strategy to bioactive chemically modified CRISPR sgRNA", *Nat. Commun.* **2019**, *10*, 1610.

Die approbierte gedruckte Originalversion dieser Dissertation ist an der TU Wien Bibliothek verfügbar.
The approved original version of this doctoral thesis is available in print at TU Wien Bibliothek.
TU Bibliothek Your knowledge hub WIEN

[136] Y. Liu, W. Hou, H. Sun, C. Cui, L. Zhang, Y. Jiang, Y. Wu, Y. Wang, J. Li, B. S. Sumerlin, Q. Liu, W. Tan, "Thiol–ene click chemistry: a biocompatible way for orthogonal bioconjugation of colloidal nanoparticles", *Chem. Sci.* **2017**, *8*, 6182–6187.
[137] N. B. Cramer, C. N. Bowman in Chemoselective and Bioorthogonal Ligation Reactions, John Wiley & Sons, Ltd, **2017**, Chapter 5, pp. 117–145.
[138] J. C. Grim, T. E. Brown, B. A. Aguado, D. A. Chapnick, A. L. Viert, X. Liu, K. S. Anseth, "A Reversible and Repeatable Thiol-Ene Bioconjugation for Dynamic Patterning of Signaling Proteins in Hydrogels", *ACS Cent. Sci* **2018**, *4*, 909–916.
[139] Q.-F. Li, Y. Yang, A. Maleckis, G. Otting, X.-C. Su, "Thiol–ene reaction: a versatile tool in site-specific labelling of proteins with chemically inert tags for paramagnetic NMR", *Chem. Commun.* **2012**, *48*, 2704–2706.
[140] D. P. Nair, M. Podgórski, S. Chatani, T. Gong, W. Xi, C. R. Fenoli, C. N. Bowman, "The Thiol-Michael Addition Click Reaction: A Powerful and Widely Used Tool in Materials Chemistry", *Chem. Mater.* **2014**, *26*, 724–744.
[141] A. B. Lowe, "Thiol–ene "click" reactions and recent applications in polymer and materials synthesis: a first update", *Polym. Chem.* **2014**, *5*, 4820–4870.
[142] Y. Sun, H. Liu, L. Cheng, S. Zhu, C. Cai, T. Yang, L. Yang, P. Ding, "Thiol Michael addition reaction: a facile tool for introducing peptides into polymer-based gene delivery systems", *Polym. Int.* **2018**, *67*, 25–31.
[143] K. Hüll, T. Benster, M. B. Manookin, D. Trauner, R. N. Van Gelder, L. Laprell, "Photopharmacologic Vision Restoration Reduces Pathological Rhythmic Field Potentials in Blind Mouse Retina", *Scientific Reports* **2019**, *9*, 13561.
[144] D. Svatunek, C. Denk, V. Rosecker, B. Sohr, C. Hametner, G. Allmaier, J. Fröhlich, H. Mikula, "Efficient low-cost preparation of trans-cyclooctenes using a simplified flow setup for photoisomerization", *Monatsh. Chem.* **2016**, *147*, 579–585.
[145] A. Blencowe, G. G. Qiao, "Ring-Opening Metathesis Polymerization with the Second Generation Hoveyda–Grubbs Catalyst: An Efficient Approach toward High-Purity Functionalized Macrocyclic Oligo(cyclooctene)s", *J. Am. Chem. Soc.* **2013**, *135*, 5717–5725.
[146] N. K. Devaraj, R. Upadhyay, J. B. Haun, S. A. Hilderbrand, R. Weissleder, "Fast and Sensitive Pretargeted Labeling of Cancer Cells through a Tetrazine/trans-Cyclooctene Cycloaddition", *Angew. Chem. Int. Ed.* **2009**, *121*, 7147–7150.
[147] R. M. Versteegen, W. ten Hoeve, R. Rossin, M. A. R. de Geus, H. M. Janssen, M. S. Robillard, "Click-to-Release from trans-Cyclooctenes: Mechanistic Insights and Expansion of Scope from Established Carbamate to Remarkable Ether Cleavage", *Angew. Chem. Int. Ed.* **2018**, *57*, 10494–10499.
[148] F. Zhang, S. Guang, F. Ke, J. Li, H. Xu, "Facile preparation and properties of multifunctional polyacetylene via highly efficient click chemistry", *RSC Adv.* **2016**, *6*, 448–455.
[149] D. Takamatsu, K.-i. Fukui, S. Aroua, Y. Yamakoshi, "Photoswitching tripodal single molecular tip for non-contact AFM measurements: synthesis, immobilization, and reversible configurational change on gold surface", *Org. Biomol. Chem.* **2010**, *8*, 3655–3664.
[150] J. Dommerholt, F. P. J. T. Rutjes, F. L. van Delft, "Strain-Promoted 1,3-Dipolar Cycloaddition of Cycloalkynes and Organic Azides", *Top. Curr. Chem. (Z)* **2016**, *374*, 16.
[151] M. T. Taylor, M. L. Blackman, O. Dmitrenko, J. M. Fox, "Design and Synthesis of Highly Reactive Dienophiles for the Tetrazine–trans-Cyclooctene Ligation", *J. Am. Chem. Soc.* **2011**, *133*, 9646–9649.
[152] T. Fiala, J. Wang, M. Dunn, P. Šebej, S. J. Choi, E. C. Nwadibia, E. Fialova, D. M. Martinez, C. E. Cheetham, K. J. Fogle, M. J. Palladino, Z. Freyberg, D. Sulzer, D. Sames, "Chemical Targeting of Voltage Sensitive Dyes to Specific Cells and Molecules in the Brain", *J. Am. Chem. Soc.* **2020**, *142*, PMID: 32395989, 9285–9301.
[153] N. Stuhr-Hansen, C.-D. Vagianou, O. Blixt, "Synthesis of BODIPY-Labeled Cholesterylated Glycopeptides by Tandem Click Chemistry for Glycocalyxification of Giant Unilamellar Vesicles (GUVs)", *Chem. Eur. J.* **2017**, *23*, 9472–9476.
[154] D. A. Roberts, B. S. Pilgrim, G. Sirvinskaite, T. K. Ronson, J. R. Nitschke, "Covalent Post-assembly Modification Triggers Multiple Structural Transformations of a Tetrazine-Edged Fe4L6 Tetrahedron", *J. Am. Chem. Soc.* **2018**, *140*, PMID: 29983061, 9616–9623.
[155] J. Meinecke, U. Koert, "Copper-Free Click Reaction Sequence: A Chemoselective Layer-by-Layer Approach", *Org. Lett.* **2019**, *21*, PMID: 31487194, 7609–7612.
[156] J. Garcia-Hartjes, J. Dommerholt, T. Wennekes, F. L. van Delft, H. Zuilhof, "Electronic Effects versus Distortion Energies During Strain-Promoted Alkyne-Azide Cycloadditions: A Theoretical Tool to Predict Reaction Kinetics", *Eur. J. Org. Chem.* **2013**, *2013*, 3712–3720.
[157] F. Vera, J. Barberá, P. Romero, J. Serrano, M. Ros, T. Sierra, "Orthogonal Action of Noncovalent Interactions for Photoresponsive Chiral Columnar Assemblies", *Angew. Chem. Int. Ed.* **2010**, *49*, 4910–4914.
[158] C. L. Folcia, I. Alonso, J. Ortega, J. Etxebarria, I. Pintre, M. B. Ros, "Achiral Bent-Core Liquid Crystals with Azo and Azoxy Linkages: Structural and Nonlinear Optical Properties and Photoisomerization", *Chem. Mater.* **2006**, *18*, 4617–4626.
[159] T. H. Poole, J. A. Reisz, W. Zhao, L. B. Poole, C. M. Furdui, S. B. King, "Strained Cycloalkynes as New Protein Sulfenic Acid Traps", *J. Am. Chem. Soc.* **2014**, *136*, 6167–6170.

Die approbierte gedruckte Originalversion dieser Dissertation ist an der TU Wien Bibliothek verfügbar.
The approved original version of this doctoral thesis is available in print at TU Wien Bibliothek.
TU Bibliothek Your knowledge hub WIEN

[160] Y.-T. Chang, S. H. Alamudi, R. Satapathy, D. Su, *pat.*, WO2017078623, **2017**.
[161] H. Wolf, H. Ringsdorf, E. Delamarche, T. Takami, H. Kang, B. Michel, C. Gerber, M. Jaschke, H. J. Butt, E. Bamberg, "End-Group-Dominated Molecular Order in Self-Assembled Monolayers", *J. Phys. Chem.* **1995**, *99*, 7102–7107.
[162] D. Bléger, J. Schwarz, A. M. Brouwer, S. Hecht, "o-Fluoroazobenzenes as Readily Synthesized Photoswitches Offering Nearly Quantitative Two-Way Isomerization with Visible Light", *J. Am. Chem. Soc.* **2012**, *134*, 20597–20600.
[163] D. Dreier, PhD thesis, Institute of Applied Synthetic Chemistry, TU Wien, **2018**.
[164] T. Lummerstorfer, H. Hoffmann, "Click Chemistry on Surfaces: 1,3-Dipolar Cycloaddition Reactions of Azide-Terminated Monolayers on Silica", *J. Phys. Chem. B* **2004**, *108*, 3963–3966.
[165] R. Rossin, S. M. J. van Duijnhoven, W. ten Hoeve, H. M. Janssen, L. H. J. Kleijn, F. J. M. Hoeben, R. M. Versteegen, M. S. Robillard, "Triggered Drug Release from an Antibody–Drug Conjugate Using Fast "Click-to-Release" Chemistry in Mice", *Bioconjug. Chem.* **2016**, *27*, 1697–1706.
[166] S. A. Albu, S. A. Al-Karmi, A. Vito, J. P. K. Dzandzi, A. Zlitni, D. Beckford-Vera, M. Blacker, N. Janzen, R. M. Patel, A. Capretta, J. F. Valliant, "125I-Tetrazines and Inverse-Electron-Demand Diels–Alder Chemistry: A Convenient Radioiodination Strategy for Biomolecule Labeling, Screening, and Biodistribution Studies", *Bioconjug. Chem.* **2016**, *27*, 207–216.
[167] R. Jurok, J. Hodačová, V. Eigner, H. Dvořáková, V. Setnička, R. Cibulka, "Planar Chiral Flavinium Salts: Synthesis and Evaluation of the Effect of Substituents on the Catalytic Efficiency in Enantioselective Sulfoxidation Reactions", *Eur. J. Org. Chem.* **2013**, *2013*, 7724–7738.
[168] Z. Miao, Y. Zhang, Y. Zhao, Z. Wang, D. Wang, "Asymmetrical Azobenzene Liquid Crystals with High Birefringence Prepared via Click Chemistry", *Mol. Cryst. Liq. Cryst.* **2014**, *591*, 10–18.
[169] M. Juríček, P. H. J. Kouwer, J. Rehák, J. Sly, A. E. Rowan, "A Novel Modular Approach to Triazole-Functionalized Phthalocyanines Using Click Chemistry", *J. Org. Chem.* **2009**, *74*, 21–25.
[170] R. Bittner, PhD thesis, Institute of Applied Synthetic Chemistry, TU Wien, Vienna, Austria, **2017**.
[171] R. Selvaraj, J. M. Fox, "An efficient and mild oxidant for the synthesis of s-tetrazines", *Tetrahedron Lett.* **2014**, *55*, 4795–4797.
[172] B. Schulze, U. S. Schubert, "Beyond click chemistry - supramolecular interactions of 1,2,3-triazoles", *Chem. Soc. Rev.* **2014**, *43*, 2522–2571.
[173] Z. Zhou, C. J. Fahrni, "A Fluorogenic Probe for the Copper(I)-Catalyzed Azide-Alkyne Ligation Reaction: Modulation of the Fluorescence Emission via 3 (n,π*)-(π,π*) Inversion", *J. Am. Chem. Soc.* **2004**, *126*, 8862–8863.
[174] Y. He, C. Fan, S.-T. Lee, "Silicon nanostructures for bioapplications", *Nano Today* **2010**, *5*, 282 –295.
[175] H. Hoffmann, U. Mayer, A. Krischanitz, "Structure of Alkylsiloxane Monolayers on Silicon Surfaces Investigated by External Reflection Infrared Spectroscopy", *Langmuir* **1995**, *11*, 1304–1312.
[176] T. Moldt, D. Brete, D. Przyrembel, S. Das, J. R. Goldman, P. K. Kundu, C. Gahl, R. Klajn, M. Weinelt, "Tailoring the Properties of Surface-Immobilized Azobenzenes by Monolayer Dilution and Surface Curvature", *Langmuir* **2015**, *31*, 1048–1057.
[177] T. Moldt, D. Przyrembel, M. Schulze, W. Bronsch, L. Boie, D. Brete, C. Gahl, R. Klajn, P. Tegeder, M. Weinelt, "Differing Isomerization Kinetics of Azobenzene-Functionalized Self-Assembled Monolayers in Ambient Air and in Vacuum", *Langmuir* **2016**, *32*, 10795–10801.
[178] L. Xu, J. Farrell, R. G. Karunakaran, A. Honglawan, S. Yang, "Synthesis of dual-functional copolymer with orthogonally photosensitive groups", *J. Polym. Sci. Part A: Polym. Chem.* **2013**, *51*, 1215–1222.
[179] Z. Huang, N. Geyer, P. Werner, J. de Boor, U. Gösele, "Metal-Assisted Chemical Etching of Silicon: A Review", *Adv. Mater.* **2011**, *23*, 285–308.
[180] M.-L. Zhang, K.-Q. Peng, X. Fan, J.-S. Jie, R.-Q. Zhang, S.-T. Lee, N.-B. Wong, "Preparation of Large-Area Uniform Silicon Nanowires Arrays through Metal-Assisted Chemical Etching", *J. Phys. Chem. C* **2008**, *112*, 4444–4450.
[181] N. A. Patankar, "Hysteresis with Regard to Cassie and Wenzel States on Superhydrophobic Surfaces", *Langmuir* **2010**, *26*, 7498–7503.
[182] F. Wang, K. Zhao, J. Cheng, J. Zhang, "Conciliating surface superhydrophobicities and mechanical strength of porous silicon films", *Appl. Surf. Sci.* **2011**, *257*, 2752 –2755.
[183] M. He, X. Zhou, X. Zeng, D. Cui, Q. Zhang, J. Chen, H. Li, J. Wang, Z. Cao, Y. Song, L. Jiang, "Hierarchically structured porous aluminum surfaces for high-efficient removal of condensed water", *Soft Matter* **2012**, *8*, 6680–6683.
[184] P. Kim, M. J. Kreder, J. Alvarenga, J. Aizenberg, "Hierarchical or Not? Effect of the Length Scale and Hierarchy of the Surface Roughness on Omniphobicity of Lubricant-Infused Substrates", *Nano Lett.* **2013**, *13*, 1793–1799.
[185] J. Yang, Z. Zhang, X. Xu, X. Men, X. Zhu, X. Zhou, "Superoleophobic textured aluminum surfaces", *New J. Chem.* **2011**, *35*, 2422–2426.
[186] R. Ngongang, E. Marceau, X. Carrier, C.-M. Pradier, C. Methivier, J.-L. Blanc, M. Carre, "Surface passivation of aluminum alloy 6061 with gaseous trichlorosilane: A surface investigation", *Appl. Surf. Sci.* **2014**, *292*, 165 –173.

Die approbierte gedruckte Originalversion dieser Dissertation ist an der TU Wien Bibliothek verfügbar.
The approved original version of this doctoral thesis is available in print at TU Wien Bibliothek.
TU Bibliothek Your knowledge hub WIEN

[187] L. Feng, Y. Che, Y. Liu, X. Qiang, Y. Wang, "Fabrication of superhydrophobic aluminium alloy surface with excellent corrosion resistance by a facile and environment-friendly method", *Appl. Surf. Chem.* **2013**, *283*, 367 –374.
[188] H. Wang, D. Dai, X. Wu, "Fabrication of superhydrophobic surfaces on aluminum", *Appl. Surf. Sci.* **2008**, *254*, 5599 –5601.
[189] X.-W. Li, Q.-X. Zhang, Z. Guo, J.-G. Yu, M.-K. Tang, X.-J. Huang, "Low-cost and large-scale fabrication of a superhydrophobic 5052 aluminum alloy surface with enhanced corrosion resistance", *RSC Adv.* **2015**, *5*, 29639–29646.
[190] N. Saadi, L. Hassan, T. Karaback, "Metal oxide nanostructures by a simple hot water treatment", *Sci. Rep.* **2017**, *7*, 7158–7165.
[191] J. Lee, J. Bong, Y.-G. Ha, S. Park, S. Ju, "Durability of self-assembled monolayers on aluminum oxide surface for determining surface wettability", *Appl. Surf. Sci.* **2015**, *330*, 445 –448.
[192] J. A. Owen, S. A. Stranford, J. Punt, Kuby Immunology, (Ed.: L. Schultz), W. H. Freeman, **2009**.
[193] J. B. Huppa, M. M. Davis in, (Ed.: F. W. Alt), Advances in Immunology, Academic Press, **2013**, pp. 1 –50.
[194] J. E. Smith-Garvin, G. A. Koretzky, M. S. Jordan, "T Cell Activation", *Annu. Rev. Immunol.* **2009**, *27*, PMID: 19132916, 591–619.
[195] K. Guram, S. S. Kim, V. Wu, P. D. Sanders, S. Patel, S. P. Schoenberger, E. E. W. Cohen, S.-Y. Chen, A. B. Sharabi, "A Threshold Model for T-Cell Activation in the Era of Checkpoint Blockade Immunotherapy", *Front. immunol.* **2019**, *10*, 491.
[196] F. Hong, F. Zhang, Y. Liu, H. Yan, "DNA Origami: Scaffolds for Creating Higher Order Structures", *Chem. Rev.* **2017**, *117*, 12584–12640.
[197] A. R. Chandrasekaran, N. Anderson, M. Kizer, K. Halvorsen, X. Wang, "Beyond the Fold: Emerging Biological Applications of DNA Origami", *ChemBioChem* **2016**, *17*, 1081–1089.
[198] P. Wang, T. A. Meyer, V. Pan, P. K. Dutta, Y. Ke, "The Beauty and Utility of DNA Origami", *Chem* **2017**, *2*, 359 –382.
[199] P. W. K. Rothemund, "Folding DNA to create nanoscale shapes and patterns", *Nature* **2006**, *440*, 297–302.
[200] V. Motsch, J. Hellmeier, G. J. Schütz, E. Sevcsik, "DNA Origami as a Nanoscale Platform for T-Cell Activation", *Biophys. J.* **2018**, *114*, 201a.
[201] C. M. Dundas, D. Demonte, S. Park, "Streptavidin–biotin technology: improvements and innovations in chemical and biological applications", *Appl. Microbiol. Biotechnol.* **2013**, *97*, 9343–9353.
[202] O. H. Laitinen, H. R. Nordlund, V. P. Hytönen, M. S. Kulomaa, "Brave new (strept)avidins in biotechnology", *Trends Biotechnol* **2007**, *25*, 269–277.
[203] M. Wilchek, E. A. Bayer, "The avidin-biotin complex in bioanalytical applications", *Anal. Biochem* **1988**, *171*, 1–32.
[204] Y. Eisenberg-Domovich, Y. Pazy, O. Nir, B. Raboy, E. A. Bayer, M. Wilchek, O. Livnah, "Structural elements responsible for conversion of streptavidin to a pseudoenzyme", *PNAS* **2004**, *101*, 5916–5921.
[205] M. Hestericová, T. Heinisch, L. Alonso-Cotchico, J.-D. Maréchal, P. Vidossich, T. R. Ward, "Directed Evolution of an Artificial Imine Reductase", *Angew. Chem. Int. Ed.* **2018**, *57*, 1863–1868.
[206] R. Eychenne, S. Guizani, J.-H. Wang, C. Picard, N. Malek, P.-L. Fabre, M. Wolff, B. Machura, N. Saffon, N. Lepareur, E. Benoist, "Rhenium Complexes Based on an N2O Tridentate Click Scaffold: From Synthesis, Structural and Theoretical Characterization to a Radiolabelling Study", *Eur. J. Inorg. Chem.* **2017**, *2017*, 69–81.
[207] W. Zhu, D. Ma, "Synthesis of aryl azides and vinyl azides via proline-promoted CuI-catalyzed coupling reactions", *Chem. Commun.* **2004**, 888–889.
[208] C. Bourget, E. Trévisiol, I. Bridon, M. Kotera, J. Lhomme, A. Laayoun, "Biotin-phenyldiazomethane conjugates as labeling reagents at phosphate in mono and polynucleotides", *Bioorg. Med. Chem.* **2005**, *13*, 1453 –1461.
[209] N. Green in Vitamins and Coenzymes, Methods in Enzymology, Academic Press, **1970**, pp. 418 –424.
[210] N. M. Green in, (Eds.: C. Anfinsen, J. T. Edsall, F. M. Richards), Advances in Protein Chemistry, Academic Press, **1975**, pp. 85 –133.
[211] N. B. Holland, T. Hugel, G. Neuert, A. Cattani-Scholz, C. Renner, D. Oesterhelt, L. Moroder, M. Seitz, H. E. Gaub, "Single Molecule Force Spectroscopy of Azobenzene Polymers: Switching Elasticity of Single Photochromic Macromolecules", *Macromolecules* **2003**, *36*, 2015–2023.
[212] G. Neuert, T. Hugel, R. R. Netz, H. E. Gaub, "Elasticity of Poly(azobenzene-peptides)", *Macromolecules* **2006**, *39*, 789–797.
[213] A. Ebner, L. Wildling, H. J. Gruber in Atomic Force Microscopy: Methods and Protocols, (Eds.: N. C. Santos, F. A. Carvalho), Springer New York, New York, NY, **2019**, pp. 117–151.
[214] D. S. Liu, A. Tangpeerachaikul, R. Selvaraj, M. T. Taylor, J. M. Fox, A. Y. Ting, "Diels–Alder Cycloaddition for Fluorophore Targeting to Specific Proteins inside Living Cells", *J. Am. Chem. Soc* **2012**, *134*, PMID: 22176354, 792–795.
[215] T. Plass, S. Milles, C. Koehler, J. Szymański, R. Mueller, M. Wießler, C. Schultz, E. A. Lemke, "Amino Acids for Diels–Alder Reactions in Living Cells", *Angew. Chem. Int. Ed.* **2012**, *51*, 4166–4170.

Die approbierte gedruckte Originalversion dieser Dissertation ist an der TU Wien Bibliothek verfügbar.
The approved original version of this doctoral thesis is available in print at TU Wien Bibliothek.
TU Bibliothek Your knowledge hub WIEN

[216] S. N. A. Shomali, H. Valizadeh, "New Generation of Nitrile Functionalized Star-like Polyvinyl Imidazolium Compound: Application as a Nitrsonium Source and Three Dimensional Nanocatalyst for the Synthesis of Azo Dyes", *Lett. Org. Chem.* **2017**, *14*, 409–418.
[217] A. Defoin, "Simple Preparation of Nitroso Benzenes and Nitro Benzenes by Oxidation of Anilines with H2O2 Catalysed with Molybdenum Salts", *Synthesis* **2004**, *2004*, 706–710.
[218] B.-C. Yu, Y. Shirai, J. M. Tour, "Syntheses of new functionalized azobenzenes for potential molecular electronic devices", *Tetrahedron* **2006**, *62*, 10303–10310.
[219] Y. Chen, Z.-J. Zhuo, D.-M. Cui, C. Zhang, "Copper catalyzed synthesis of 1-aryl-1,2,3-triazoles from aryl iodides, alkynes, and sodium azide", *J. Organomet. Chem.* **2014**, *749*, 215–218.
[220] M.-A. Kasper, M. Glanz, A. Stengl, M. Penkert, S. Klenk, T. Sauer, D. Schumacher, J. Helma, E. Krause, M. C. Cardoso, H. Leonhardt, C. P. R. Hackenberger, "Cysteine-Selective Phosphonamidate Electrophiles for Modular Protein Bioconjugations", *Angew. Chem. Int. Ed.* **2019**, *58*, 11625–11630.
[221] M. S. Messina, J. M. Stauber, M. A. Waddington, A. L. Rheingold, H. D. Maynard, A. M. Spokoyny, "Organometallic Gold(III) Reagents for Cysteine Arylation", *J. Am. Chem. Soc.* **2018**, *140*, PMID: 29790740, 7065–7069.

Die approbierte gedruckte Originalversion dieser Dissertation ist an der TU Wien Bibliothek verfügbar.
The approved original version of this doctoral thesis is available in print at TU Wien Bibliothek.
TU Bibliothek Your knowledge hub WIEN

Chapter G

Appendix

G.1 Half-life time calculations - linear regressions

(A) Compound [11a]

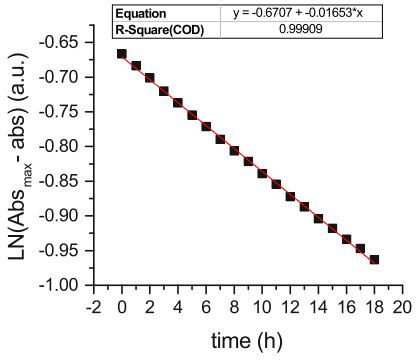

Time	LN(Abs max - abs)
0	-0.6667
1	-0.68379
2	-0.70098
3	-0.7199
4	-0.7371
5	-0.75438
6	-0.77111
7	-0.78966
8	-0.80609
9	-0.82166
10	-0.8391
11	-0.85426
12	-0.87203
13	-0.88722
14	-0.90387
15	-0.91804
16	-0.93369
17	-0.94701
18	-0.96312

(B) Compound [11e]

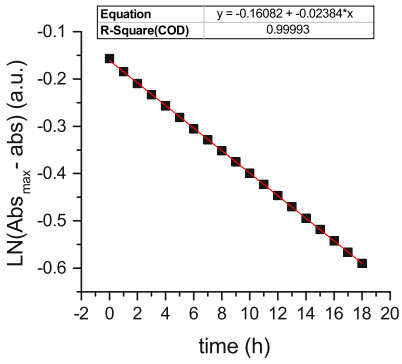

Time	LN(Abs max - abs)
0	-0.157
1	-0.1844
2	-0.20949
3	-0.23319
4	-0.25722
5	-0.28104
6	-0.30544
7	-0.3285
8	-0.35183
9	-0.37557
10	-0.39869
11	-0.42297
12	-0.44629
13	-0.47
14	-0.49413
15	-0.51819
16	-0.54232
17	-0.56634
18	-0.58987

(C) Compound [18a]

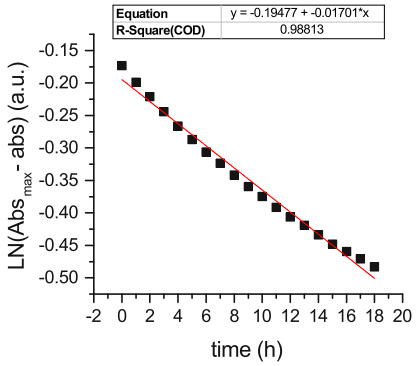

Time	LN(Abs max - abs)
0	-0.1734
1	-0.19882
2	-0.22127
3	-0.24398
4	-0.26618
5	-0.28688
6	-0.30612
7	-0.32365
8	-0.34193
9	-0.35954
10	-0.37469
11	-0.39127
12	-0.40617
13	-0.41916
14	-0.43386
15	-0.44816
16	-0.45966
17	-0.4708
18	-0.48321

(D) Compound [18e]

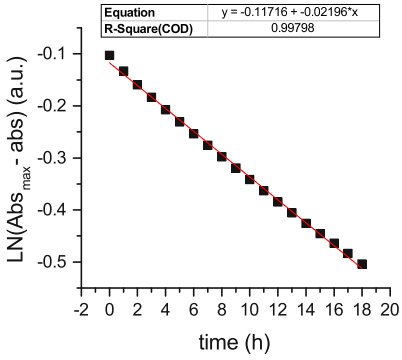

Time	LN(Abs max - abs)
0	-0.10281
1	-0.13319
2	-0.15958
3	-0.18368
4	-0.20764
5	-0.23067
6	-0.2536
7	-0.27562
8	-0.29773
9	-0.31952
10	-0.3415
11	-0.36284
12	-0.38449
13	-0.40527
14	-0.42572
15	-0.44551
16	-0.4641
17	-0.48386
18	-0.50385

Die approbierte gedruckte Originalversion dieser Dissertation ist an der TU Wien Bibliothek verfügbar.
The approved original version of this doctoral thesis is available in print at TU Wien Bibliothek.
TU Bibliothek Your knowledge hub WIEN

(E) Compound [33]

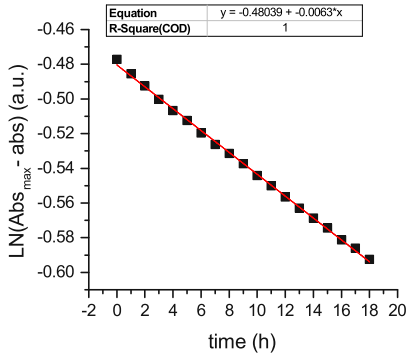

Time	LN(Abs$_{max}$ - abs)
0	-0.47707
1	-0.48548
2	-0.49249
3	-0.50022
4	-0.50667
5	-0.51233
6	-0.51953
7	-0.52628
8	-0.53137
9	-0.53734
10	-0.54421
11	-0.55009
12	-0.55652
13	-0.563
14	-0.56863
15	-0.57448
16	-0.58125
17	-0.58609
18	-0.5924

(F) Compound [36]

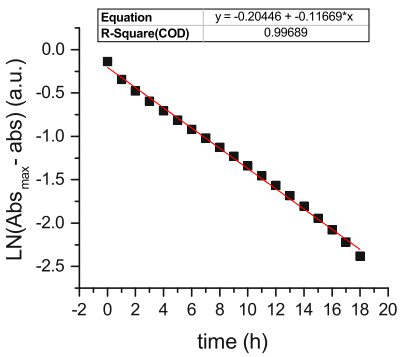

Time	LN(Abs$_{max}$ - abs)
0	-0.13754
1	-0.34461
2	-0.47787
3	-0.59584
4	-0.70623
5	-0.81148
6	-0.91804
7	-1.01777
8	-1.12547
9	-1.22929
10	-1.34017
11	-1.45415
12	-1.5659
13	-1.68524
14	-1.80667
15	-1.94421
16	-2.07704
17	-2.21916
18	-2.38271

(G) Compound [41]

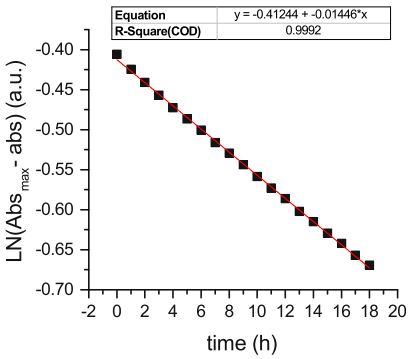

Time	LN(Abs$_{max}$ - abs)
0	-0.40572
1	-0.42465
2	-0.44099
3	-0.45713
4	-0.47257
5	-0.48646
6	-0.50071
7	-0.51601
8	-0.52933
9	-0.54352
10	-0.55862
11	-0.5727
12	-0.58627
13	-0.60203
14	-0.61471
15	-0.62942
16	-0.64188
17	-0.65682
18	-0.66924

(H) Compound [46]

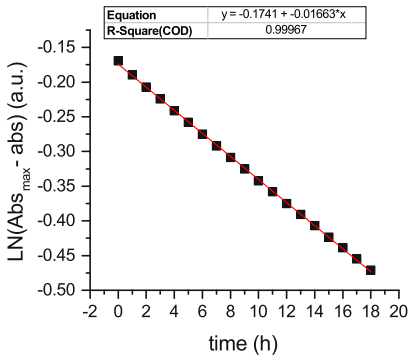

Time	LN(Abs$_{max}$ - abs)
0	-0.16937
1	-0.18971
2	-0.20702
3	-0.22414
4	-0.24131
5	-0.25799
6	-0.27509
7	-0.29196
8	-0.30857
9	-0.32518
10	-0.34221
11	-0.3581
12	-0.37513
13	-0.39082
14	-0.40692
15	-0.42343
16	-0.43882
17	-0.45476
18	-0.47096

(I) Compound [47]

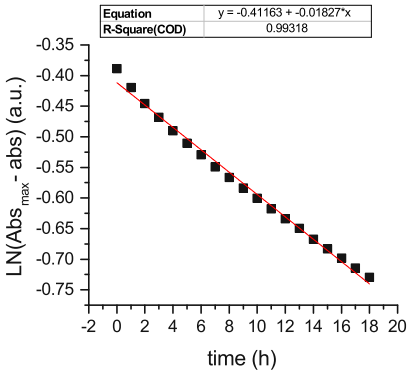

Time	LN(Abs$_{max}$ - abs)
0	-0.38876
1	-0.41946
2	-0.44551
3	-0.46793
4	-0.49021
5	-0.51049
6	-0.5295
7	-0.54922
8	-0.56634
9	-0.58358
10	-0.6002
11	-0.61748
12	-0.63394
13	-0.6497
14	-0.66709
15	-0.683
16	-0.69816
17	-0.71458
18	-0.7296

(J) Compound [48e]

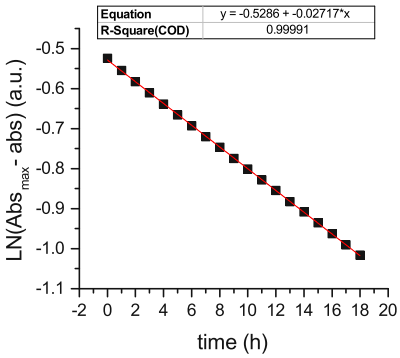

Time	LN(Abs$_{max}$ - abs)
0	-0.52408
1	-0.55443
2	-0.58286
3	-0.61083
4	-0.63847
5	-0.66592
6	-0.69275
7	-0.72052
8	-0.74676
9	-0.77479
10	-0.80073
11	-0.82828
12	-0.85473
13	-0.88237
14	-0.90807
15	-0.93547
16	-0.96233
17	-0.99021
18	-1.01611

Die approbierte gedruckte Originalversion dieser Dissertation ist an der TU Wien Bibliothek verfügbar.
The approved original version of this doctoral thesis is available in print at TU Wien Bibliothek.

(K) Compound [49]

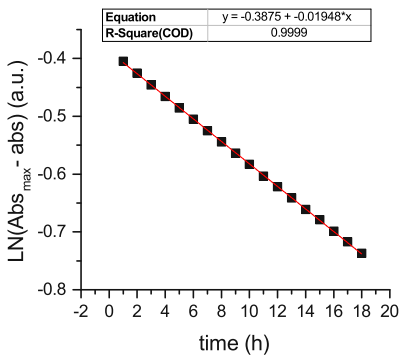

Time	LN(Abs max - abs)
1	-0.40467
2	-0.42511
3	-0.44582
4	-0.46553
5	-0.48565
6	-0.50517
7	-0.52476
8	-0.54421
9	-0.56352
10	-0.58304
11	-0.60331
12	-0.62194
13	-0.64093
14	-0.66126
15	-0.67885
16	-0.69896
17	-0.71723
18	-0.73689

(L) Compound [56]

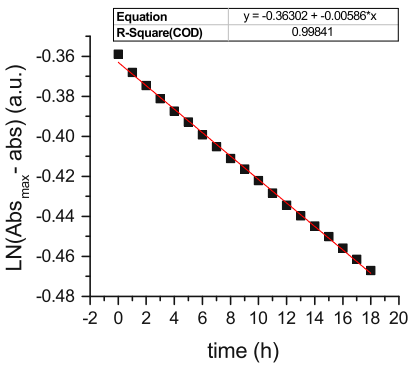

Time	LN(Abs max - abs)
0	-0.35896
1	-0.36802
2	-0.37469
3	-0.38111
4	-0.38743
5	-0.39289
6	-0.39928
7	-0.40512
8	-0.41113
9	-0.41642
10	-0.42205
11	-0.42832
12	-0.43448
13	-0.43975
14	-0.44488
15	-0.45004
16	-0.45586
17	-0.4614
18	-0.46697

(M) Compound [59]

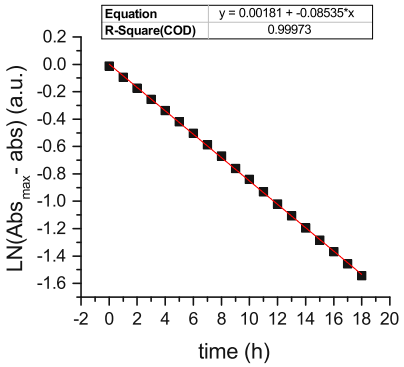

Time	LN(Abs max - abs)
0	-0.01339
1	-0.09508
2	-0.17423
3	-0.25554
4	-0.33659
5	-0.41977
6	-0.50319
7	-0.58663
8	-0.67021
9	-0.75971
10	-0.84026
11	-0.93191
12	-1.01915
13	-1.10654
14	-1.19534
15	-1.28302
16	-1.36924
17	-1.45758
18	-1.54365

(N) Compound [60]

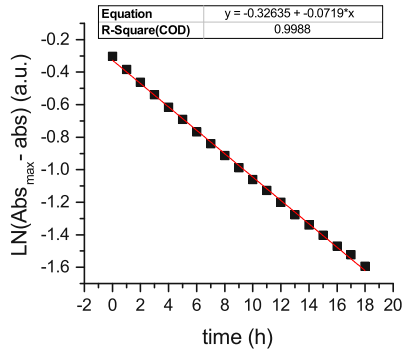

Time	LN(Abs max - abs)
0	-0.30313
1	-0.38287
2	-0.4614
3	-0.53871
4	-0.61508
5	-0.69075
6	-0.76744
7	-0.83979
8	-0.91354
9	-0.98725
10	-1.05958
11	-1.12701
12	-1.20065
13	-1.27619
14	-1.34056
15	-1.40324
16	-1.47055
17	-1.52372
18	-1.59356

Die approbierte gedruckte Originalversion dieser Dissertation ist an der TU Wien Bibliothek verfügbar.
The approved original version of this doctoral thesis is available in print at TU Wien Bibliothek.

G.2 WCA photoswitchable surfaces - raw data

G.2.1 *Trans* immobilization

G.2.1.1 Surface [SiF-41*trans*]

Cycle	7 min		15 min		30 min	
	WCA	Error	WCA	Error	WCA	Error
0	90.8	0.51	85.3	0.88	87.1	0.20
1	86.9	0.58	80.4	0.56	82.4	0.37
2	89.4	0.20	87.5	0.19	85.1	0.53
3	86.7	0.43	81.2	0.63	80.6	0.22
4	91.5	0.78	87.2	0.11	84.7	0.92
5	86.8	0.11	78.6	0.92	80.7	0.20
6	88.9	0.29	86.9	0.32	85.0	0.41

G.2.1.2 Surface [SiF-46*trans*] and [SiF-11e*trans*]

Cycle	[SiF-46*trans*]		[SiF-11e*trans*]	
	WCA	Error	WCA	Error
0	65.8	0.15	64.5	0.19
1	61.1	0.35	61.5	0.04
2	64.7	1.45	64.4	0.17
3	60.5	0.16	60.2	0.07
4	66.0	0.23	65.1	0.21
5	63.5	0.45	61.9	0.18
6	67.7	0.36	64.6	0.11

Die approbierte gedruckte Originalversion dieser Dissertation ist an der TU Wien Bibliothek verfügbar.
The approved original version of this doctoral thesis is available in print at TU Wien Bibliothek.

G.2.2 *Cis* immobilization

Cycle	[SiF-41*cis*]		[[SiF-46*cis*]		[SiF-18e*cis*]	
	WCA	**Error**	**WCA**	**Error**	**WCA**	**Error**
0	79.5	0.35	58.3	0.17	56.3	0.23
1	89.2	0.86	60.7	0.13	59.2	0.19
2	78.8	1.11	56.2	0.21	54.9	0.20
3	88.1	0.11	61.1	0.31	57.6	0.09
4	77.8	0.28	56.5	0.17	52.6	0.17
5	86.8	0.79	61.7	0.50	56.5	0.19
6	77.90	0.45	57.7	0.26	54.2	0.15

Die approbierte gedruckte Originalversion dieser Dissertation ist an der TU Wien Bibliothek verfügbar.
The approved original version of this doctoral thesis is available in print at TU Wien Bibliothek.
TU Bibliothek Your knowledge hub WIEN

G.3 Publications and conference activities resulting from this thesis

Journal articles

R.C.O Conceição, H. Hoffmann, M.D. Mihovilovic: "Azobenzene *cis* immobilization: a practical approach to obtain azobenzene light-responsive surfaces while avoiding overcrowding"; in preparation.

Poster presentations

R.C.O. Conceição, H. Hoffmann, M.D. Mihovilovic: "Azobenzene *Cis* Immobilization: A New Practical Approach To Obtain Azobenzene Light Responsive Surfaces"; 14^{th} international conference on material chemistry; Birmingham, England, UK, July 2019.

R.C.O. Conceição, M.D. Mihovilovic: "Synthesis Of Double-Click Azobenzenes For An Easy Functionalization Of Biomolecules", 21^{st} Symposium on Organic Chemistry; Vienna, Austria, July 2019

R.C.O. Conceição, H. Hoffmann, M.D. Mihovilovic: "Silicon Nanowires As An Alternative For The Development Of Light Responsive Smart Surfaces"; 27^{th} PhotoIUPAC; Dublin, Ireland, July 2018.

Die approbierte gedruckte Originalversion dieser Dissertation ist an der TU Wien Bibliothek verfügbar.
The approved original version of this doctoral thesis is available in print at TU Wien Bibliothek.
TU Bibliothek Your knowledge hub WIEN

Die approbierte gedruckte Originalversion dieser Dissertation ist an der TU Wien Bibliothek verfügbar.
The approved original version of this doctoral thesis is available in print at TU Wien Bibliothek.

G.4 List of abbreviations

λ_{max}	maximum absorption wavelength	MeOH	methanol
AFM	atom force microscopy	MHC	major histocompability complex
Al	aluminum	OTS	octadecyltrichlorosilane
APC	antigen-presenting cell	PBS	phosphate buffered saline
BUTS	11-bromoundecyl trichlorosilane	PE	petroleum ether
CuAAC	copper-catalyzed alkyne-azide cycloaddition	$PhI(OAc)_2$	(diacetoxyiodo)benzene
DCM	dicloromethane	RGD	arginylglyculaspartic acid
DIPEA	N,N-diisopropylehtylamine	r.t	room temperature
DMF	dimethyl formamide	SA	streptadivin
ΔWCA	difference in the WCA	SAM	self-assembled monolayer
equiv.	equivalent(s)	SEM	scanning electron microscopy
EtOAc	ethyl acetate	SiF	silicon flat
EtOH	ethanol	SiNW	silicon nanowires
FAD	flavin adenine nucleotide	SPAAC	strain-promoted alkyne-azide cycloaddition
FTIR	Fourier-transform infrared spectroscopy	$t_{1/2}$	thermal relaxation half-life time
HABA	4-hydroxyazobenzene-2′-carboxylic acid	TCR	T-cell receptor
HPLC	high-performance liquid chromatography	THF	tetrahydrofuran
iEDDA	inverse electron-demand Diels-Alder	TMS	trimethylsilane
IRRAS	Infra-Red Reflection Absorption Spectroscopy	UV/Vis	ultraviolet/visible spectroscopy
LED	light-emitting diode	WCA	water contact angle

Die approbierte gedruckte Originalversion dieser Dissertation ist an der TU Wien Bibliothek verfügbar.
The approved original version of this doctoral thesis is available in print at TU Wien Bibliothek.
TU Bibliothek Your knowledge hub WIEN

G.5 Reference list of compounds

[2]	RC058	**[30endo]**	RC195
[3]	RC068	**[32endo]**	RC198
[4a] and **[4e]**	RC084	**[33]**	RC199
[6e]	RC085	**[34]**	RC173
[6a]	RC086	**[35]**	RC174
[8]	RC043	**[36]**	RC175
[9]	RC047	**[38]**	RC028
[10]	RC061	**[40]**	RC052
[11e]	RC091	**[41]**	RC056
[11a]	RC096	**[43]**	RC095
[13]	RC151	**[45]**	RC073
[15]	RC152	**[46]**	RC098
[16]	RC153	**[47]**	RC103
[17]	RC154	**[48e]**	RC115
[18a]	RC187	**[49]**	RC121
[18e]	RC167	**[51]**	RC126
[19exo] and **[19endo]**	JER001	**[53]**	JER008
[20endo]	JER004	**[54]**	RC181
[21endo]	JER005	**[55]**	RC188
[22endo]	JER006	**[56]**	RC200
[24]	JER002	**[58]**	RC201
[25]	JER003	**[59]**	RC189
[26]	JER007	**[60]**	RC190
[28]	RC192		

Die approbierte gedruckte Originalversion dieser Dissertation ist an der TU Wien Bibliothek verfügbar.
The approved original version of this doctoral thesis is available in print at TU Wien Bibliothek.
TU Bibliothek Your knowledge hub WIEN

G.6 Curriculum vitae

Name: Rafaela Conceição

Phone: 067763402656

E-mail: rafaela.carinaoc@gmail.com

Address: Veronikagasse 29, top 2, 1170 Vienna, Austria

LinkedIn: https://www.linkedin.com/in/rafaela-conceição-a3213766/

Date and place of birth: 16.12.1991, Santa Maria da Feira, Portugal

Relevant work experience

12/2020-present — Material Engineer at Cubicure GmbH

- Member of the Research and Development Team
- Synthesis of new monomers for application in 3D printing
- Study of the properties of newly synthesized photopolymers

02/2017-11/2020 — University Assistant, TU Wien, Institute of Applied Synthetic Chemistry

- Development of photoswitchable surfaces
- Synthesis of photoswitches and determination of their photophysical properties
- Teaching of undegraduate students
- NMR, preparative HPLC, photometer, ellipsometer and goniometer operator

06/2016-12/2016 — Researcher for a joint project between University of Minho and Fibromade (wood veneer manufacturer, http://www.fibromade.com)

- Development of chemical treatments to control the natural color of oak wood during the production process of wood veneers
- Scale-up of the process from lab scale to industrial scale

Education

02/2017-present — PhD in Technical chemistry at TU Wien

- Research field of organic synthesis, photopharmacology and photoswitchable surfaces
- 3 poster presentations in international conferences and 1 paper currently in preparation

Die approbierte gedruckte Originalversion dieser Dissertation ist an der TU Wien Bibliothek verfügbar.
The approved original version of this doctoral thesis is available in print at TU Wien Bibliothek.

02/2017-03/2019	Member of the BioInterface Doctoral program • Regular presentations in seminars • Collaboration in interdisciplinary projects • Organization and participation in scientific retreats
2012-2015	Master's degree, Medicinal Chemistry, University of Minho • final grade of 18 out of 20 • master thesis focused on the photocontrolled release of bioactive molecules from coumarin conjugates. This work resulted in one publication is one peer reviewed journal and in 4 poster presentations • in addition to the master thesis work, 2 internships in different research groups were performed
2009-2012	Bachelor's degree, Biochemistry, University of Minho • final grade of 15 out of 20 • bachelor thesis focused on the synthesis of purine derivatives for screening on *Mycobacterium tuberculosis*

Complementary formation

June 2015	Formation in Cell Culture, The Faculty of Medicine of OPorto, OPorto, 17 out of 20.
September 2017	Advances in drug discovery, Prague Summer School, Czech Republic

Language skills

Portuguese	Mother tongue	
English	C2	*International English Language Testing System from Cambridge (8 out of 9)*
German	B2.2	*Certificate from the Sprachen Zentrum Universität Wien (17 out of 20)*

Additional skills

Software skills:

- Microsoft office (word, excel, powerpoint)
- latex
- Chemistry software (Chemdraw, MestreNova, Chemsketch)

Driving licence class B

Die approbierte gedruckte Originalversion dieser Dissertation ist an der TU Wien Bibliothek verfügbar.
The approved original version of this doctoral thesis is available in print at TU Wien Bibliothek.
TU Bibliothek Your knowledge hub WIEN

Interests

Piano and Flute	Studied from young age both instruments and latter taught both as a part-time job. Nowadays still play as a hobby
Workout	
Reading	A fan of specially the thriller genre

Die approbierte gedruckte Originalversion dieser Dissertation ist an der TU Wien Bibliothek verfügbar.
The approved original version of this doctoral thesis is available in print at TU Wien Bibliothek.
TU Bibliothek Your knowledge hub WIEN